Title	New reaction model for revealing deuteron inside nuclei
Author(s)	茶園, 亮樹
Citation	大阪大学, 2022, 博士論文
Version Type	VoR
URL	https://doi.org/10.18910/87811
rights	
Note	

OSAKA UNIVERSITY
GRADUATE SCHOOL OF SCIENCE

DOCTORAL THESIS

New reaction model for revealing deuteron inside nuclei

Yoshiki Chazono

Research Center for Nuclear Physics (RCNP), Osaka University
Ibaraki 567-0047, Osaka, Japan

Defended on Feubruary 9th, 2022

Supervisor:	Kazuyuki Ogata	RCNP
Chief Examiner:	Atsushi Hosaka	RCNP
Examiners:	Takahiro Kawabata	Osaka University
	Nori Aoi	RCNP
	Tatsushi Shima	RCNP

Abstract

The proton (p) induced nucleon (N) knockout reaction (p, pN) is a nuclear reaction in which the incident proton interacts with the target nucleus, and one proton and one nucleon are detected. This process is the most dominant reaction between 200 MeV and 1000 MeV. Because of this high energy nature, this reaction can be regarded as essentially a scattering of the incident proton and a nucleon in the target nucleus. Thanks to this intuitive picture, the nucleon knockout reaction is employed as a probe of the single-particle structure of nuclei. A natural extension of this reaction would be the cluster knockout reaction, in which a cluster, a composite particle consisting of nucleons, is knocked out instead of a nucleon, and is also expected to be a good probe of the cluster structure of nuclei. The proton-induced α knockout reaction $(p, p\alpha)$, in which the α cluster (^{4}He nucleus, a typical cluster) is knocked out, has been studied theoretically, and corresponding experiments are being conducted aiming at demonstrating the α cluster structure from light to heavy nuclei.

There are a few studies of the proton-induced deuteron (d) knockout reaction (p, pd). In the experiment performed 40 years ago at the University of Maryland, it was reported that the cross section of the ^{16}O$(p, pd)^{14}$N reaction is almost half of that of the ^{16}O$(p, 2p)^{15}$N. It is known that the number of proton that behaves like an independent particle in nuclei is about 60–65 % of the total proton number. Therefore, if we naively interpret the experimental result of (p, pd) about 30 % of proton forms deuterons with neutrons in the ground state of ^{16}O, which is surprisingly large. The deuteron is, however, a weakly bound system with a binding energy of about 1 MeV per nucleon, and in this respect, the deuteron knockout reaction is definitely different from the proton knockout and α knockout reactions. Because of its fragility, the deuteron can be broken up by the incident proton in the elementary process of the (p, pd) reaction. In addition, the deuteron knocked out of the nucleus is expected to have a transition between bound and breakup states by the Final-State Interactions (FSIs). Furthermore, the deuteron that is once broken up in the elementary process can reform a deuteron by the FSIs. These processes are not taken into account in the Distorted Wave Impulse Approximation (DWIA) framework, which is the standard reaction model describing the knockout reactions. Therefore, even if measurement results of deuteron knockout reactions are obtained, it is not possible to conclude clearly whether or not deuterons exist in nuclei by analyzing the results with the DWIA framework.

The purpose of this doctoral thesis is to construct a new reaction model that adequately describes the deuteron knockout reaction to reveal the deuteron inside nuclei. To achieve this, (a) microscopic description of the deuteron inside nuclei, (b) deuteron breakup in the elementary process, and (c) transition between bound and breakup states of the proton-neutron system by FSIs are essentially important. In the present work, the (p, pd) reaction has been described with these three ingredients for the first time, and the role of each in the reaction has been clarified.

First, the isoscalar proton-neutron (pn) pair wave function in ^{16}O obtained by the nuclear Energy-Density Functional (EDF) method, which describes the nuclear structure microscopically, is used for the DWIA calculation of the (p, pd) reaction. Three different strengths of the pairing interaction between protons and neutrons are employed in the nuclear EDF calculation. It is found that the cross section of the reaction reflects the paring strength, and thus, the existence of the isoscalar pn pairs in ^{16}O. On the other hand, the calculated cross sections underestimate the experimental data by two orders of magnitude. The reason for this discrepancy is mainly due to the mean-field approach to the wave function of the pair.

Second, a framework describing the elastic scattering and breakup reactions of the proton and deuteron system using a nucleon-nucleon effective interaction is constructed and tested for the reliability. It is shown that the framework reproduces the experimental data of elastic scattering well in the energy and angular ranges that contribute to the kinematics of the deuteron knockout reaction discussed in this thesis. For the deuteron breakup reaction, no comparison is possible due to the absence of experimental data, but the present framework can describe the processes in which the deuteron remains in the ground state and is excited to a breakup state on the same footing. It is, therefore, expected that this framework can safely be employed to describe the elementary processes of the (p, pd) reaction.

Third, the transition of the proton-neutron system in the final state is treated by the Continuum-Discretized Coupled-Channel method (CDCC). It is found that the *back coupling* process, in which the knocked-out deuteron

goes to breakup channels and comes back to the elastic channel due to the FSIs, reduces the cross section of the (p, pd) reaction. The impact of this process is large at low energies in particular. It is also shown that the deuteron reformation of the knocked-out proton-neutron pair also reduces the cross section.

In this thesis, a new reaction model to reliably describe the deuteron knockout reaction is developed. In this model, the above-mentioned ingredients (a), (b), and (c) are taken into account. It is shown to be important to treat each ingredient properly to reveal the deuteron inside nuclei by deuteron knockout reactions.

Acknowledgements

First of all, I would like to express my utmost gratitude to Prof. Kazuyuki Ogata for leading me to the researches on nuclear reaction theory and for his patient guidance. I would also like to extend my sincere thanks to Dr. Kazuki Yoshida for many discussions and his comments on my research. All the contents in this thesis would not have been accomplished without their great help. I am deeply grateful to Dr. Kenichi Yoshida for the quite fruitful collaboration research.

I sincerely appreciate Prof. Atsushi Hosaka and Prof. Noriyoshi Ishii for their advice and suggestions on my research from a wide range of perspectives, from nuclear physics to hadron physics. I would also like to thank Dr. Kosho Minomo for giving me fundamental knowledge about nuclear physics. I would like to express my thanks to Mr. Tomoatsu Edagawa, Mr. Hibiki Nakada, and Mr. Takuto Okinaga for their *primitive* questions on nuclear physics; they let me realize my ambiguous understanding of it. I am very grateful to all staff members of the Research Center for Nuclear Physics (RCNP), especially to our secretary Ms. Sachiko Karasuyama for providing me with a comfortable environment for smooth researches. Even though I had few opportunities to discuss or chat with the member of the theory group face-to-face in these two years due to COVID-19, I was very glad to have discussions on physics or chats via the internet.

I thank my brother, Michiya, for discussing physics in general. Finally, I would like to offer my special thanks to my parents, Kohki and Keiko, for their support in my daily life.

Yoshiki Chazono

Contents

List of Figures

Chapter 1

Introduction

1.1 Picture of atomic nucleus

Although the nucleus is a system composed of only two types of Fermi particle, proton (p) and neutron (n), it has a variety of aspects. The liquid drop model [1, 2], which appeared in the early days of nuclear physics, is a structure model that describes the nucleus as a system of strongly correlated nucleons (N). The liquid drop model is based on the fact that the nuclear force is a strong short-range interaction. In other words, this model focuses on the motion of the nucleus as a whole, not on that of each nucleon inside the nucleus. The liquid drop model reproduces well the gross properties of stable nuclei, such as the dependence of mass on the nucleon number and the energy spectrum of surface oscillations of nuclei. The Bethe-Weizsäcker semi-empirical mass formula is one of the most well-known outcomes of this model. It also gives an intuitive understanding of fission, in which the liquid drop is deformed to form a neck and then the Coulomb repulsion tears off the neck.

A counterpart of the liquid drop model is the independent particle model. In this model, correlations among nucleons are assumed to be weak, and each nucleon is regarded as having a single particle motion independently of other nucleons in the nucleus. The shell model [3–7] is one of the highly successful independent particle models, in which protons and neutrons are moving in orbits specified by several quantum numbers (principal quantum number n, orbital angular momentum ℓ, and total angular momentum j) just as electrons in an atom. The shell model reproduces the magic number of stable nuclei very well, which could not be explained by the liquid drop model. Nuclear spectroscopy based on the shell model is one of the major subjects in nuclear physics.

As mentioned above, the nucleus has two different aspects. The unified model (or collective model) makes it possible to understand these aspects in a unified manner [8–11]. The basic idea of this model is that the nucleons in the nucleus move on the orbits described above in a slowly (adiabatically) varying mean-field potential. The mean-field potential is a simple one-body potential that is obtained as the sum of the complex nuclear forces (interactions between nucleons). The mean-field potential that governs the nucleon motion, and the nucleon motion that determines the potential are calculated in a self-consistent manner. In other words, in the unified model, particle motion and collective motion couples each other. When the mean-field potential can be regarded as spherical and only the nucleon motion needs to be considered, the nucleus shows the aspect of a weakly correlated system. When the mean-field potential oscillates in a nearly spherical shape, or it oscillates and rotates around an equilibrium point with large deformation, the nucleus shows an aspect of a strongly correlated system. In addition, the residual interaction, the nuclear force that could not be fully incorporated into the mean-field potential, leads to various correlations between a small number of nucleons.

From the analysis of many experimental data, it has been found that the wave functions of the ground and low-lying excited states of stable nuclei have independent particle components accounting for about 65 $\%$ [12, 13]. This indicates that the remaining 35 $\%$ of the wave function is understood as a result of some correlations between nucleons, which cannot be included in the single-particle potential. An example of nucleon correlations is an isovector and spin-singlet pairing correlation of two protons or neutrons [14, 15], in which two nucleons of the same species form just like a Cooper pair in condensed matter physics. The pairing correlation has been intensively studied for many years and found to play an important role in explaining properties such as deformation and moment of inertia of nuclei. A short-range tensor correlation is another example of nucleon correlations, which are thought to introduce a high-momentum component to the relative motion of proton-neutron pairs in nuclei [16–21].

1.2 Cluster structure of nucleus and deuteron inside nuclei

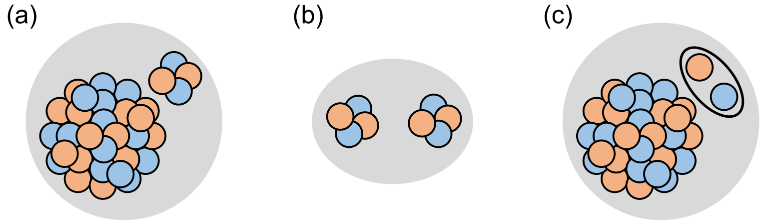

FIGURE 1.1: (a) Concept of the α cluster structure of nuclei. (b) Cluster structure of ^{8}Be. (c) Concept of a deuteron inside nuclei. It should be noted that the picture shown in panel (c) has not been established.

The correlations listed above are momentum and angular momentum correlations. Another type of nucleon correlation is a spatial one. The cluster structure of an atomic nucleus is known as an example of spatial nucleon correlations. A cluster is a composite particle inside a nucleus, which is spatially localized and weakly interacts with other nucleons and clusters. Because an α particle (^{4}He nucleus) is a strongly bound system consisting of two protons and two neutrons, it is known as a typical cluster. The concept of the α cluster is shown in Figure 1.1(a). Many efforts to describe nuclei with a cluster picture have been devoted since the early days of nuclear physics. These were mainly motivated by the existence of nuclei that undergo α decay. In particular, it is known that α cluster structures appear in light nuclei [22] when the energy of the nucleus is near the threshold energy to break up into a few parts including alphas, such as the ground state of ^{8}Be (see Fig. 1.1(b)) and the 0_2^+ excited state of ^{12}C [23]. Today, with great progress in both nuclear structure theory and experimental technique, it has been experimentally confirmed that even in the ground state of heavy nuclei such as tin, α cluster structures develop on their surfaces [24].

Apart from the α particle, the deuteron (d) is considered to be a candidate for the cluster. The deuteron is an isoscalar and spin-triplet particle consisting of a proton and a neutron, and as is well known, it is the only two-nucleon bound system in free space. This indicates that the nuclear force is particularly strong in the component that makes protons and neutrons form spin-triplet pairs, that is, the $^3S_1$ channel component. It has also been found that the $^3S_1$ channel component of a pairing interaction is strong in a nuclear matter [25–27]. Therefore, we can expect that protons and neutrons form isoscalar pairs in nuclei, just as in free space. Fig. 1.1(c) shows a schematic picture of a deuteron inside nuclei. In addition, from the viewpoint of the existence of isovector and spin-singlet pairing correlations (pp and nn pairings) and the isospin symmetry, it is natural to consider the existence of a deuteron-like proton-neutron (pn) pairing. It should be noted that the pp and nn pairings are known to have a correlation range equal to a diameter of a nucleus, whereas the pn pair is expected to be spatially compact. The pn pair is thought to be formed in the $N \approx Z$ nuclei because the shell structures of protons and neutrons are close to each other around the Fermi surface and the overlap of wave functions is large [28, 29]. It has been suggested by the nuclear Energy-Density Functional (EDF) approach an isoscalar pn pairing vibrational mode possibly emerges in $N = Z$ nuclei [30, 31]. The Cluster Orbital Shell Model (COSM) approach in which ^{18}F ($N = Z = 9$) is treated as a three-body system of $^{16}\mathrm{O} + p + n$ also suggests the formation of deuteron-like pn pair [32]. The understanding of this pn pair is getting more important since the invention of the unstable beams, which has provided more opportunities to study $N \approx Z$ nuclei in medium- and heavy-mass regions. However, analysis of experimental data in the past has not provided clear evidence for the existence of deuteron-like pn pair [29]. To overcome this situation, we need a "new" experimental approach and nuclear reaction theory.

Two nuclear reactions that may probe deuteron-like pn pairs are briefly mentioned. The first is the transfer reaction, in which a part of the incident particle is stripped by the target nucleus or vice versa. Here, we consider the pn-pair transfer reaction, in which a proton and a neutron are transferred from the incident particle (Fig. 1.2). Taking a naive view of this reaction, if there is a correlation between the proton and neutron, they are transferred from the incident particle to the target nucleus simultaneously with high probability. On the other hand, however, it is also possible that the proton and neutron are individually transferred in two steps. Although it depends on the reaction system and energy which of these two processes is dominant, the theoretical calculation based on the Distorted Wave Born Approximation (DWBA) has shown that the two-step process is more dominant than the simultaneous process in ^{12}C(^{14}N,^{12}C)^{14}N reactions at 79 and 155 MeV [33]. When the two-step process is dominant, the question arises

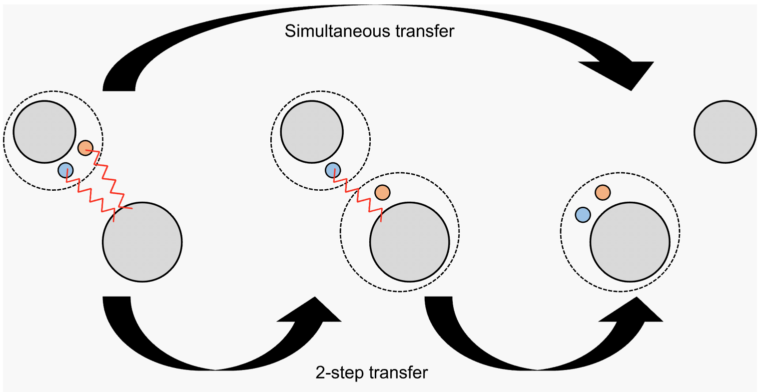

FIGURE 1.2: Proton-neutron pair transfer reaction.

whether the analysis can indicate the existence of deuteron-like pn pairs in the nucleus. In other words, it is difficult to theoretically exclude the possibility that the proton and neutron, which do not correlate, are accidentally transferred. In addition, in the second-order DWBA, there are two representations of the transition matrix describing each of the first and second nucleon transfer, that is, the prior- and post-form; in total, four representations exist. It is found in Ref. [34] that the results of theoretical calculations depend on which representation is taken. Therefore, it can be said that the pn pair transfer reaction is difficult to adopt in the study of deuteron-like pn pairs because of its large uncertainty.

The second is the photonuclear reaction (or photodisintegration). This is a reaction in which an incident high-energy photon excites the nucleus and the emission of particles follows. In the measurements reported in Refs. [35–37], the emission of protons with high momentum was observed, but the model assuming the absorption of photons by the entire nucleus could not explain this process. The quasi-deuteron model was then introduced [38, 39]. In this model, a deuteron-like pn pair is assumed to exist in the nucleus, which absorbs photons and is excited. If the spatial distance between the proton and neutron is close, the Heisenberg uncertainty relation allows the proton in the quasi-deuteron to have a high-momentum component. The basic idea of the quasi-deuteron model is that these protons fly out of the nucleus with high momentum. Therefore, this model focuses on the high-momentum component of the pn pair and is considered to be useful as a model to verify the short-range tensor correlations mentioned above. However, the pn pair that interested in this thesis is more similar to the deuteron in free space, and for the empirical study, it is better to focus on the low-momentum component as the first step. In this sense, the photonuclear reaction and the quasi-deuteron model are beyond the scope of this thesis. It should be note that in the deuteron knockout reaction mentioned in the next section, the high-momentum component of a proton-neutron pair can be probed with a kinetics in which the deuteron emitted in a forward angle and proton emitted in a backward angle are observed, that is, the neutron pick-up process is dominant in the elementary process [40].

1.3 Knockout reaction as probe for particle inside nuclei

1.3.1 Proton-induced nucleon and α knockout reaction

In the previous section, we mentioned two reactions that might be a probe for deuteron-like pn pairs and briefly described their "problems." In this section, we will review the knockout reaction, which is simpler than those reactions and has been used in nuclear spectroscopy based on the shell model and in studies of alpha cluster structures.

The proton-induced nucleon knockout reaction (p, pN) is a nuclear reaction in which the incident proton interacts with the target nucleus, and one proton and one nucleon are detected. This process is the most dominant reaction between 200 MeV and 1000 MeV. Because of this high energy nature, this reaction can be regarded as essentially a scattering of the incident proton and a nucleon in the target nucleus [12]. Thanks to this intuitive picture, the nucleon knockout reaction is employed as a probe of the single-particle structure of nuclei [41–51]. A natural extension of this reaction would be the cluster knockout reaction, in which a cluster is knocked out instead of a nucleon, and is also expected to be a good probe of the cluster structure of nuclei. The proton-induced α knockout reaction $(p, p\alpha)$, in which the α cluster is knocked out, has been studied theoretically [52–54], and corresponding experiments are being conducted aiming at demonstrating the α cluster structure from light to heavy nuclei [24, 55–61].

1.3.2 Proton-induced deuteron knockout reaction

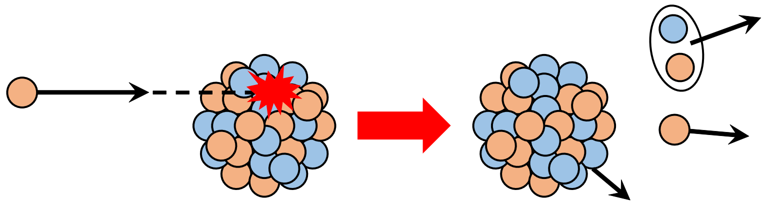

FIGURE 1.3: Proton-induced deuteron knockout reaction.

There are a few studies of the proton-induced deuteron knockout reaction (p, pd). The naive picture of (p, pd) reaction is shown in Fig. 1.3. In the experiment performed 40 years ago at the University of Maryland, it was reported that the cross section of the ^{16}O$(p, pd)^{14}$N reaction [62] is almost half of that of the ^{16}O$(p, 2p)^{15}$N [46]. It is known that the number of proton that behaves like an independent particle in nuclei is about 60–65 % of the total proton number. Therefore, if we naively interpret the experimental result of (p, pd) about 30 % of proton forms deuterons with neutrons in the ground state of ^{16}O, which is surprisingly large. The deuteron is, however, a weakly bound system with a binding energy of about 1 MeV per nucleon, and in this respect, the deuteron knockout reaction is definitely different from the proton knockout and α knockout reactions. Because of its fragility, the deuteron can be broken up by the incident proton in the elementary process of the (p, pd) reaction. In addition, the deuteron knocked out of the nucleus is expected to transition between bound and breakup states by the Final-State Interactions (FSIs). Furthermore, the deuteron that is once broken up in the elementary process can reform a deuteron by the FSIs. These processes are not taken into account in the Distorted Wave Impulse Approximation (DWIA) framework, which is the standard reaction model describing the knockout reactions. Therefore, even if measurement results of deuteron knockout reactions are obtained, it is not possible to conclude clearly whether or not deuterons exist in nuclei by analyzing the results with the DWIA framework.

1.4 Purpose and construction of this thesis

The purpose of this doctoral thesis is to construct a new reaction model that adequately describes the deuteron knockout reaction to reveal the deuteron inside nuclei. To achieve this, three ingredients:

- microscopic description of the deuteron inside nuclei,
- deuteron breakup in the elementary process,
- transition between bound and breakup states of the proton-neutron system by FSIs,

are essentially important. In the following chapters, the (p, pd) reaction is described with these three ingredients for the first time, and each contribution to the reaction is clarified.

The construction of this doctoral thesis is as follows. In Chapter 2, the framework of the DWIA is explained. A new reaction model named *CDCCIA* is introduced for a more adequate description of deuteron knockout reactions. In the CDCCIA framework, the deuteron breakup in the elementary process and the transition of the emitted deuteron due to FSIs are considered. In addition, a framework is developed to describe the proton-deuteron elastic scattering and deuteron breakup reactions $d(p, p)pn$ in the elementary process of the (p, pd) reaction by a single-scattering of the incident proton off each nucleon inside deuteron by a nucleon-nucleon effective interaction. In Chapter 3, the cross section of the ^{16}O$(p, pd)^{14}$N* reaction, in which ^{14}N is in the 1_2^+ excited state, is calculated within the DWIA framework with a microscopic wave function of deuteron inside ^{16}O obtained by the nuclear EDF framework. The strength of the pairing interaction between proton and neutron is varied in the nuclear EDF calculation, and how the difference appears in the cross section of the reaction is investigated. In Chapter 4, the reliability of the framework for the p-d scattering and the $d(p,p)pn$ reaction is tested. In Chapter 5, the cross section of the ^{16}O$(p,pd)^{14}$N* reaction is calculated within the CDCCIA framework. How the *back coupling* process, in which the knocked-out deuteron goes to breakup channels and comes back to the elastic channel due to the FSIs, affects the cross section is investigated. The impact of the deuteron reformation of the knocked-out proton-neutron pair on the cross section is also studied. Finally, the summary of this thesis is given in Chapter 6.

Chapter 2

Formulation

2.1 Distorted wave impulse approximation formalism

In this section, I introduce the Distorted Wave Impulse Approximation (DWIA) formalism, which is employed widely to describe and analyze knockout reactions in both theoretical and experimental studies. The DWIA has been successful, especially in the nucleon knockout [41–51] and α-particle knockout [52, 55–61] reactions.

In the following formulation, the proton (p) induced deuteron (d) knockout reaction (p, pd) in normal kinematics is described within the DWIA framework, similarly as shown in the recent review article [12] of the proton-induced nucleon (N) knockout reaction (p, pN). A three-body reaction model, in which a deuteron is treated not as a two-nucleon system but a single particle, is adopted. The incident and emitted protons are labeled as particles 0 and 1, and the knocked-out deuteron is referred to as particle 2. The target (residual) nucleus is labeled as A (B), whose mass number is A (B), and the deuteron bound in the target as particle x. All quantities are evaluated in the center-of-mass (c.m.) frame of the three-body system (the G frame for short), and we attach a certain superscript to those in another frame. The spin-orbit component in each optical potential is ignored. The Coulomb interaction is not discussed explicitly because of its complexity due to the long-range property. It should be noted, however, that all the numerical results shown except in Chapter 4 are calculated by taking into account the Coulomb interaction in a conventional way. The Madison convention, in which the momentum of the incident proton is taken to be parallel to the z-axis, is employed. The reaction is assumed to be coplanar, that is, all the momenta of the particles are on the same plane.

2.1.1 Transition matrix based on DWIA

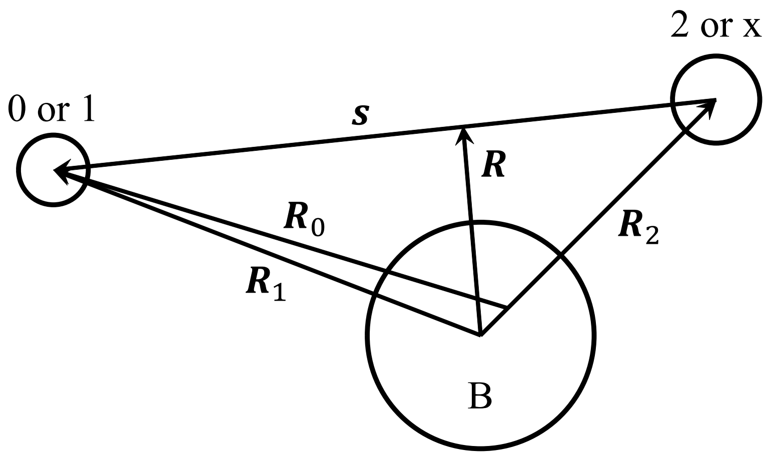

FIGURE 2.1: Coordinates of the A(p, pd)B reaction system.

The coordinates to describe the A(p, pd)B reaction are shown in Fig. 2.1, and we take $\boldsymbol{R}_0$ and $\boldsymbol{R}_2$ as the independent coordinates. The transition matrix of the (p, pd) reaction is given in the post form by

$$T_{\mu_1\mu_2\mu_\mathrm{B}\mu_0\mu_\mathrm{A}} = \left\langle \Psi^{\mathrm{free}}_{12\mathrm{B}} \middle| V_f \Omega^{(+)}_0 \middle| \Psi^{\mathrm{free}}_{0\mathrm{A}} \right\rangle , \tag{2.1}$$

$$\left|\Psi_{0\mathrm{A}}^{\mathrm{free}}\right\rangle = \left|\phi_{\boldsymbol{K}_0}(\boldsymbol{R}_0)\eta_{\frac{1}{2}\mu_0}^{(0)}\zeta_{\frac{1}{2}\nu_0}^{(0)}\Phi_{I_\mathrm{A}\mu_\mathrm{A}}^{t_\mathrm{A}\nu_\mathrm{A}}(\epsilon_\mathrm{A},\xi_\mathrm{A})\right\rangle, \tag{2.2}$$

$$\left\langle\Psi_{12\mathrm{B}}^{\mathrm{free}}\right| = \left\langle\phi_{\boldsymbol{K}_1}(\boldsymbol{R}_0)\eta_{\frac{1}{2}\mu_1}^{(1)}\zeta_{\frac{1}{2}\nu_1}^{(1)}\phi_{\boldsymbol{K}_{2\mathrm{B}}}(\boldsymbol{R}_2)\Phi_{I_2\mu_2}^{t_2\nu_2}(\epsilon_2,\xi_2)\Phi_{I_\mathrm{B}\mu_\mathrm{B}}^{t_\mathrm{B}\nu_\mathrm{B}}(\epsilon_\mathrm{B},\xi_\mathrm{B})\right|, \tag{2.3}$$

in which $\phi_{\boldsymbol{K}_0}(\phi_{\boldsymbol{K}_1})$ is the plane wave between particle 0 and A (particle 1 and B), and $\phi_{\boldsymbol{K}_{2\mathrm{B}}}$ between particle 2 and B. $\boldsymbol{K}_i$ is the momentum (in the unit of $\hbar$) of particle i $(= 0, 1,\ \text{and}\ 2)$ in the asymptotic region in the G frame, and $\boldsymbol{K}_{2\mathrm{B}}$ is the relative momentum between particle 2 and B. The spin and isospin functions of particles 0 and 1 are denoted by $\eta_{\frac{1}{2}\mu_i}^{(i)}$ and $\zeta_{\frac{1}{2}\nu_i}^{(i)}$, in which μ_i and ν_i mean the third components of the spin and isospin, respectively. The internal wave function of particle j $(= 2, \mathrm{A},\ \text{and B})$ is represented by $\Phi_{I_j\mu_j}^{t_j\nu_j}(\epsilon_j,\xi_j)$, in which I_j, t_j, ϵ_j, and ξ_j are, respectively, the spin, isospin, eigenenergy, and internal coordinate.

$\Omega_0^{(+)}$ in Eq. (2.1), which is called the Møller operator, makes the plane wave $\phi_{\boldsymbol{K}_0}$ distorted by A as

$$\Omega_0^{(+)}\left|\Psi_{0\mathrm{A}}^{\mathrm{free}}\right\rangle = \left|\chi_{0,\boldsymbol{K}_0}^{(+)}(\boldsymbol{R}_0)\eta_{\frac{1}{2}\mu_0}^{(0)}\zeta_{\frac{1}{2}\nu_0}^{(0)}\Phi_{I_\mathrm{A}\mu_\mathrm{A}}^{t_\mathrm{A}\nu_\mathrm{A}}(\epsilon_\mathrm{A},\xi_\mathrm{A})\right\rangle, \tag{2.4}$$

in which $\chi_{0,\boldsymbol{K}_0}^{(+)}$ is the distorted wave of particle 0. This distorted wave is obtained as the solution of the Schrödinger equation:

$$\left[T_{\boldsymbol{R}_0} + U_{0\mathrm{A}}(R_0) - \frac{\hbar^2}{2\mu_{0\mathrm{A}}}K_0^2\right]\chi_{0,\boldsymbol{K}_0}^{(+)}(\boldsymbol{R}_0) = 0, \tag{2.5}$$

in which $\mu_{0\mathrm{A}}$ is the reduced mass of particle 0 and A. $T_{\boldsymbol{R}_0}$ is the kinetic energy operator regarding $\boldsymbol{R}_0$, and $U_{0\mathrm{A}}$ is an optical model potential between particle 0 and A. The superscript $(+)$ means that $\chi_{0,\boldsymbol{K}_0}^{(+)}$ satisfies the outgoing boundary condition:

$$\chi_{0,\boldsymbol{K}_0}^{(+)}(\boldsymbol{R}_0) \to \mathrm{e}^{iK_0z} + f_{0\mathrm{A}}(\Omega_0)\frac{\mathrm{e}^{iK_0R_0}}{R_0} \quad (R_0 \to \infty), \tag{2.6}$$

in which $f_{0\mathrm{A}}$ is the scattering amplitude, and Ω_0 is the solid angle of particle 0.

The transition interaction V_f is given by the sum of all the two-body interactions in the final state:

$$V_f = U_{1\mathrm{B}} + U_{2\mathrm{B}} + \tau_{12}, \tag{2.7}$$

in which $U_{1\mathrm{B}}$ $(U_{2\mathrm{B}})$ is an optical potential between particle 1 (2) and B, and τ_{12} is an effective interaction between particles 1 and 2. In the DWIA framework, the impulse approximation, which replaces τ_{12} with an effective interaction between paritcles 1 and 2 in free space, t_{12}, is employed.

For smooth discussion, we rewrite the product of the plane waves in Eq. (2.3) as

$$\begin{aligned}
\phi_{\boldsymbol{K}_1}(\boldsymbol{R}_0)\phi_{\boldsymbol{K}_{2\mathrm{B}}}(\boldsymbol{R}_2) &= \frac{1}{(2\pi)^{3/2}}\exp(i\boldsymbol{K}_1\cdot\boldsymbol{R}_0)\cdot\frac{1}{(2\pi)^{3/2}}\exp(i\boldsymbol{K}_{2\mathrm{B}}\cdot\boldsymbol{R}_2)\\
&= \frac{1}{(2\pi)^3}\exp\left[i\boldsymbol{K}_1\cdot\left(\boldsymbol{R}_1 - \frac{m_2}{m_2+m_\mathrm{B}}\boldsymbol{R}_2\right)\right]\exp\left[i\left(\frac{m_2}{m_2+m_\mathrm{B}}\boldsymbol{K}_1+\boldsymbol{K}_2\right)\cdot\boldsymbol{R}_2\right]\\
&= \frac{1}{(2\pi)^{3/2}}\exp(i\boldsymbol{K}_1\cdot\boldsymbol{R}_1)\cdot\frac{1}{(2\pi)^{3/2}}\exp(i\boldsymbol{K}_2\cdot\boldsymbol{R}_2)\\
&= \phi_{\boldsymbol{K}_1}(\boldsymbol{R}_1)\phi_{\boldsymbol{K}_2}(\boldsymbol{R}_2)
\end{aligned} \tag{2.8}$$

because $U_{1\mathrm{B}}$ and $U_{2\mathrm{B}}$ are the functions of $\boldsymbol{R}_1$ and $\boldsymbol{R}_2$, respectively. Here, the momentum conservation in the G frame:

$$\boldsymbol{K}_1 + \boldsymbol{K}_2 + \boldsymbol{K}_\mathrm{B} = \boldsymbol{K}_0 + \boldsymbol{K}_\mathrm{A} = 0, \tag{2.9}$$

in which $\boldsymbol{K}_{\rm A}$ and $\boldsymbol{K}_{\rm B}$ are the momentum of the target and residue, respectively, has been used to express $\boldsymbol{K}_{2\rm B}$ by $\boldsymbol{K}_1$ and $\boldsymbol{K}_2$ as

$$\boldsymbol{K}_{2\rm B} = \frac{m_{\rm B}}{m_2 + m_{\rm B}}\boldsymbol{K}_2 - \frac{m_2}{m_2 + m_{\rm B}}\boldsymbol{K}_{\rm B} = \frac{m_2}{m_2 + m_{\rm B}}\boldsymbol{K}_1 + \boldsymbol{K}_2, \tag{2.10}$$

with m_2 and $m_{\rm B}$ being the masses of particle 2 and B, respectively.

Applying the Gell-Mann-Goldberger transformation (see Appendix A) to the transition matrix (2.1), the optical potentials distort the plane waves in the final state as

$$\begin{aligned} T_{\mu_1\mu_2\mu_{\rm B}\mu_0\mu_{\rm A}} = \Bigg\langle \Psi^{(-)}_{\boldsymbol{K}_1,\boldsymbol{K}_2}(\boldsymbol{R}_1,\boldsymbol{R}_2)\eta^{(1)}_{\frac{1}{2}\mu_1}\zeta^{(1)}_{\frac{1}{2}\nu_1}\Phi^{t_2\nu_2}_{I_2\mu_2}(\epsilon_2,\xi_2)\Phi^{t_{\rm B}\nu_{\rm B}}_{I_{\rm B}\mu_{\rm B}}(\epsilon_{\rm B},\xi_{\rm B})\Bigg| \\ \times\, t_{12}(\boldsymbol{s})\Bigg|\chi^{(+)}_{0,\boldsymbol{K}_0}(\boldsymbol{R}_0)\eta^{(0)}_{\frac{1}{2}\mu_0}\zeta^{(0)}_{\frac{1}{2}\nu_0}\Phi^{t_{\rm A}\nu_{\rm A}}_{I_{\rm A}\mu_{\rm A}}(\epsilon_{\rm A},\xi_{\rm A})\Bigg\rangle, \end{aligned} \tag{2.11}$$

in which $\Psi^{(-)}_{\boldsymbol{K}_1,\boldsymbol{K}_2}$ is the three-body scattering wave satisfying the Schrödinger equation:

$$\left[\hat{T}_f + U^*_{1\rm B}(R_1) + U^*_{2\rm B}(R_2) - T_f\right]\Psi^{(-)}_{\boldsymbol{K}_1,\boldsymbol{K}_2}(\boldsymbol{R}_1,\boldsymbol{R}_2) = 0. \tag{2.12}$$

$\hat{T}_f$ and T_f are the kinetic energy operator and the scattering energy in the final state given by

$$\hat{T}_f = -\frac{\hbar^2}{2m_1}\nabla^2_{\boldsymbol{r}_1} - \frac{\hbar^2}{2m_2}\nabla^2_{\boldsymbol{r}_2} - \frac{\hbar^2}{2m_{\rm B}}\nabla^2_{\boldsymbol{r}_{\rm B}} + \frac{\hbar^2}{2m_{\rm tot}}\nabla^2_{\boldsymbol{r}_{\rm c.m.}}, \tag{2.13}$$

$$T_f = \frac{\hbar^2}{2m_1}K_1^2 + \frac{\hbar^2}{2m_2}K_2^2 + \frac{\hbar^2}{2m_{\rm B}}K_{\rm B}^2, \tag{2.14}$$

in which m_1 is the mass of particle 1, and $m_{\rm tot} \equiv m_1 + m_2 + m_{\rm B}$ (the total mass of the system in the final state). $\boldsymbol{r}_i$ is the position vector of particle i $(= 1, 2,$ and B), and we can find

$$\boldsymbol{R}_1 = \boldsymbol{r}_1 - \boldsymbol{r}_{\rm B}, \quad \boldsymbol{R}_2 = \boldsymbol{r}_2 - \boldsymbol{r}_{\rm B}, \quad \boldsymbol{R}_{\rm c.m.} = \frac{m_1\boldsymbol{r}_1 + m_2\boldsymbol{r}_2 + m_{\rm B}\boldsymbol{r}_{\rm B}}{m_{\rm tot}}. \tag{2.15}$$

These lead to (see Appendix B)

$$\nabla_{\boldsymbol{r}_1} = \nabla_{\boldsymbol{R}_1} + \frac{m_1}{m_{\rm tot}}\nabla_{\boldsymbol{R}_{\rm c.m.}}, \quad \nabla_{\boldsymbol{r}_2} = \nabla_{\boldsymbol{R}_2} + \frac{m_2}{m_{\rm tot}}\nabla_{\boldsymbol{R}_{\rm c.m.}}, \quad \nabla_{\boldsymbol{r}_{\rm B}} = -\nabla_{\boldsymbol{R}_1} - \nabla_{\boldsymbol{R}_2} + \frac{m_{\rm B}}{m_{\rm tot}}\nabla_{\boldsymbol{R}_{\rm c.m.}}, \tag{2.16}$$

and then $\hat{T}_f$ becomes

$$\hat{T}_f = -\frac{\hbar^2}{2\mu_{1\rm B}}\nabla^2_{\boldsymbol{R}_1} - \frac{\hbar^2}{2\mu_{2\rm B}}\nabla^2_{\boldsymbol{R}_2} - \frac{\hbar^2}{m_{\rm B}}\nabla_{\boldsymbol{R}_1}\cdot\nabla_{\boldsymbol{R}_2}, \tag{2.17}$$

in which $\mu_{1\rm B}$ and $\mu_{2\rm B}$ are the reduced masses of the 1-B and 2-B systems. Using Eq. (2.9), T_f also becomes

$$T_f = \frac{\hbar^2}{2\mu_{1\rm B}}K_1^2 + \frac{\hbar^2}{2\mu_{2\rm B}}K_2^2 + \frac{\hbar^2}{m_{\rm B}}\boldsymbol{K}_1\cdot\boldsymbol{K}_2. \tag{2.18}$$

Although it is possible to solve the Schrödinger equation (2.12) within the three-body Faddeev(-Alt-Grassberger-Sandhas) theory [63–65], the semiclassical approximation [66], which replaces the third term in the right-hand-side of Eq. (2.17) as

$$-\frac{\hbar^2}{m_{\rm B}}\nabla_{\boldsymbol{R}_1}\cdot\nabla_{\boldsymbol{R}_2} \approx \frac{\hbar^2}{m_{\rm B}}\boldsymbol{K}_1\cdot\boldsymbol{K}_2, \tag{2.19}$$

is employed to solve the equation effectively. This approximation is commonly adopted in the study of the (p, pN) reaction, e.g., in Ref. [44], and the order of the uncertainty coming from it is $\mathcal{O}(m_2/m_{\rm B})$. Then we can factorize the three-body wave function $\Psi^{(-)}_{\boldsymbol{K}_1,\boldsymbol{K}_2}$ as

$$\Psi^{(-)}_{\boldsymbol{K}_1,\boldsymbol{K}_2}(\boldsymbol{R}_1,\boldsymbol{R}_2) \approx \chi^{(-)}_{1,\boldsymbol{K}_1}(\boldsymbol{R}_1)\chi^{(-)}_{2,\boldsymbol{K}_2}(\boldsymbol{R}_2) \tag{2.20}$$

and Eq. (2.12) becomes decoupled into

$$\left[\hat{T}_{\boldsymbol{R}_1} + U^*_{1\mathrm{B}}(R_1) - \frac{\hbar^2}{2\mu_{1\mathrm{B}}}K_1^2\right]\chi^{(-)}_{1,\boldsymbol{K}_1}(\boldsymbol{R}_1) = 0, \tag{2.21}$$

$$\left[\hat{T}_{\boldsymbol{R}_2} + U^*_{2\mathrm{B}}(R_2) - \frac{\hbar^2}{2\mu_{2\mathrm{B}}}K_2^2\right]\chi^{(-)}_{2,\boldsymbol{K}_2}(\boldsymbol{R}_2) = 0, \tag{2.22}$$

in which $\chi^{(-)}_{i,\boldsymbol{K}_i}$ is the distorted wave of particle i ($=$ 1 and 2), and the superscript $(-)$ means that the incoming boundary condition:

$$\chi^{(-)}_{i,\boldsymbol{K}_i}(\boldsymbol{R}_i) \to \mathrm{e}^{iK_i z} + f^*_{i\mathrm{B}}(\Omega_i)\frac{e^{-iK_iR_i}}{R_i} \quad (R_i \to \infty) \tag{2.23}$$

is satisfied with Ω_i being the solid angle of particle i.

Now the transition matrix (2.11) becomes

$$\begin{aligned} T_{\mu_1\mu_2\mu_\mathrm{B}\mu_0\mu_\mathrm{A}} = &\left\langle \chi^{(-)}_{1,\boldsymbol{K}_1}(\boldsymbol{R}_1)\eta^{(1)}_{\frac{1}{2}\mu_1}\zeta^{(1)}_{\frac{1}{2}\nu_1}\chi^{(-)}_{2,\boldsymbol{K}_2}(\boldsymbol{R}_2)\Phi^{t_2\nu_2}_{I_2\mu_2}(\epsilon_2,\xi_2)\Phi^{t_\mathrm{B}\nu_\mathrm{B}}_{I_\mathrm{B}\mu_\mathrm{B}}(\epsilon_\mathrm{B},\xi_\mathrm{B})\right| \\ &\times t_{12}(\boldsymbol{s})\left|\chi^{(+)}_{0,\boldsymbol{K}_0}(\boldsymbol{R}_0)\eta^{(0)}_{\frac{1}{2}\mu_0}\zeta^{(0)}_{\frac{1}{2}\nu_0}\Phi^{t_\mathrm{A}\nu_\mathrm{A}}_{I_\mathrm{A}\mu_\mathrm{A}}(\epsilon_\mathrm{A},\xi_\mathrm{A})\right\rangle. \end{aligned} \tag{2.24}$$

Making the assumption that residue B is inert and a spectator during the reaction, Eq. (2.24) is reduced to

$$\begin{aligned} T_{\mu_1\mu_2\mu_\mathrm{B}\mu_0\mu_\mathrm{A}} = &\left\langle \chi^{(-)}_{1,\boldsymbol{K}_1}(\boldsymbol{R}_1)\eta^{(1)}_{\frac{1}{2}\mu_1}\zeta^{(1)}_{\frac{1}{2}\nu_1}\chi^{(-)}_{2,\boldsymbol{K}_2}(\boldsymbol{R}_2)\Phi^{t_2\nu_2}_{I_2\mu_2}(\epsilon_2,\xi_2)\right| \\ &\times t_{12}(\boldsymbol{s})\left|\chi^{(+)}_{0,\boldsymbol{K}_0}(\boldsymbol{R}_0)\eta^{(0)}_{\frac{1}{2}\mu_0}\zeta^{(0)}_{\frac{1}{2}\nu_0}\psi^{t_\mathrm{B}\nu_\mathrm{B}:t_\mathrm{A}\nu_\mathrm{A}}_{I_\mathrm{B}\mu_\mathrm{B}:I_\mathrm{A}\mu_\mathrm{A}}(\epsilon_\mathrm{x},\xi_\mathrm{x},\boldsymbol{R}_2)\right\rangle, \end{aligned} \tag{2.25}$$

in which $\psi^{t_\mathrm{B}\nu_\mathrm{B}:t_\mathrm{A}\nu_\mathrm{A}}_{I_\mathrm{B}\mu_\mathrm{B}:I_\mathrm{A}\mu_\mathrm{A}}$ is the overlap function between the target A and the (x + B) system defined by

$$\psi^{t_\mathrm{B}\nu_\mathrm{B}:t_\mathrm{A}\nu_\mathrm{A}}_{I_\mathrm{B}\mu_\mathrm{B}:I_\mathrm{A}\mu_\mathrm{A}}(\epsilon_\mathrm{x},\xi_\mathrm{x},\boldsymbol{R}_2) \equiv \left\langle \Phi^{t_\mathrm{B}\nu_\mathrm{B}}_{I_\mathrm{B}\mu_\mathrm{B}}(\epsilon_\mathrm{B},\xi_\mathrm{B})\middle|\Phi^{t_\mathrm{A}\nu_\mathrm{A}}_{I_\mathrm{A}\mu_\mathrm{A}}(\epsilon_\mathrm{A},\xi_\mathrm{A})\right\rangle. \tag{2.26}$$

In general, we can expand $\Phi^{t_\mathrm{A}\nu_\mathrm{A}}_{I_\mathrm{A}\mu_\mathrm{A}}$ by the sets of the eigenstates of particle x and B as

$$\begin{aligned} \Phi^{t_\mathrm{A}\nu_\mathrm{A}}_{I_\mathrm{A}\mu_\mathrm{A}}(\epsilon_\mathrm{A},\xi_\mathrm{A}) = &\sum\!\!\!\!\!\!\int_{\epsilon'_\mathrm{B}}\sum_{t'_\mathrm{B}\nu'_\mathrm{B}}(t_\mathrm{x}\nu_\mathrm{x}t'_\mathrm{B}\nu'_\mathrm{B}|t_\mathrm{A}\nu_\mathrm{A})\sum_{I'_\mathrm{B}\mu'_\mathrm{B}}\sum_{\ell j\mu_j}\theta^{n\ell j\nu_x}_{I'_\mathrm{B}t'_\mathrm{B}\nu'_\mathrm{B}:I_\mathrm{A}t_\mathrm{A}\nu_\mathrm{A}}(j\mu_jI'_\mathrm{B}\mu'_\mathrm{B}|I_\mathrm{A}\mu_\mathrm{A}) \\ &\times\varphi_{n\ell j}(R_2)\left[Y_\ell\left(\hat{\boldsymbol{R}}_2\right)\otimes\Phi^{t_\mathrm{x}\nu_\mathrm{x}}_{I_\mathrm{x}}(\epsilon_\mathrm{x},\xi_\mathrm{x})\right]_{j\mu_j}\Phi^{t'_\mathrm{B}\nu'_\mathrm{B}}_{I'_\mathrm{B}\mu'_\mathrm{B}}(\epsilon'_\mathrm{B},\xi_\mathrm{B}), \end{aligned} \tag{2.27}$$

in which $(abcd|ef)$ is the Clebsch-Gordan coefficient and

$$\left[Y_\ell\left(\hat{\boldsymbol{R}}_2\right)\otimes\Phi^{t_\mathrm{x}\nu_\mathrm{x}}_{I_\mathrm{x}}(\epsilon_\mathrm{x},\xi_\mathrm{x})\right]_{j\mu_j} \equiv \sum_{m\mu_\mathrm{x}}(\ell mI_\mathrm{x}\mu_\mathrm{x}|j\mu_j)Y_{\ell m}\left(\hat{\boldsymbol{R}}_2\right)\Phi^{t_\mathrm{x}\nu_\mathrm{x}}_{I_\mathrm{x}\mu_\mathrm{x}}(\epsilon_\mathrm{x},\xi_\mathrm{x}) \tag{2.28}$$

with $Y_{\ell m}$ being the spherical harmonics. $\theta^{n\ell j\nu_x}_{I'_\mathrm{B}t'_\mathrm{B}\nu'_\mathrm{B}:I_\mathrm{A}t_\mathrm{A}\nu_\mathrm{A}}$ is the expansion coefficient related to the "deuteron spectroscopic factor" defined below. The cluster state of particle x inside A, their relative wave function in fact, is specified by the principal quantum number n, the orbital angular momentum $\boldsymbol{\ell}$, the total angular momentum $\boldsymbol{j}$ ($\equiv \boldsymbol{\ell} + \boldsymbol{I}_\mathrm{x}$), and its third component μ_j. Inserting Eq. (2.27) into Eq. (2.26), we obtain

$$\psi^{t_{\mathrm{B}}\nu_{\mathrm{B}}:t_{\mathrm{A}}\nu_{\mathrm{A}}}_{I_{\mathrm{B}}\mu_{\mathrm{B}}:I_{\mathrm{A}}\mu_{\mathrm{A}}}(\epsilon_{\mathrm{x}},\xi_{\mathrm{x}},\boldsymbol{R}_2)=\sum_{\ell j\mu_j}S^{1/2}_{n\ell j\nu_{\mathrm{x}}}(j\mu_j I_{\mathrm{B}}\mu_{\mathrm{B}}|I_{\mathrm{A}}\mu_{\mathrm{A}})\varphi_{n\ell j}(R_2)\left[Y_\ell\left(\hat{\boldsymbol{R}}_2\right)\otimes\Phi^{t_{\mathrm{x}}\nu_{\mathrm{x}}}_{I_{\mathrm{x}}}(\epsilon_{\mathrm{x}},\xi_{\mathrm{x}})\right]_{j\mu_j} \tag{2.29}$$

with the use of the orthonormality of $\Phi^{t_{\mathrm{B}}\nu_{\mathrm{B}}}_{I_{\mathrm{B}}\mu_{\mathrm{B}}}$. $S^{1/2}_{n\ell j\nu_{\mathrm{x}}}$ is the "deuteron spectroscopic amplitude" given by

$$S^{1/2}_{n\ell j\nu_{\mathrm{x}}}\equiv(t_{\mathrm{x}}\nu_{\mathrm{x}}t_{\mathrm{B}}\nu_{\mathrm{B}}|t_{\mathrm{A}}\nu_{\mathrm{A}})\theta^{n\ell j\nu_x}_{I_{\mathrm{B}}t_{\mathrm{B}}\nu_{\mathrm{B}}:I_{\mathrm{A}}t_{\mathrm{A}}\nu_{\mathrm{A}}}, \tag{2.30}$$

and its squared absolute value is called the "deuteron spectroscopic factor." The transition matrix (2.25) is, therefore, rewritten as

$$\begin{aligned}T_{\mu_1\mu_2\mu_{\mathrm{B}}\mu_0\mu_{\mathrm{A}}}=\Bigg\langle&\chi^{(-)}_{1,\boldsymbol{K}_1}(\boldsymbol{R}_1)\eta^{(1)}_{\frac{1}{2}\mu_1}\zeta^{(1)}_{\frac{1}{2}\nu_1}\chi^{(-)}_{2,\boldsymbol{K}_2}(\boldsymbol{R}_2)\Phi^{t_2\nu_2}_{I_2\mu_2}(\epsilon_2,\xi_2)\Bigg|t_{12}(\boldsymbol{s})\Bigg|\chi^{(+)}_{0,\boldsymbol{K}_0}(\boldsymbol{R}_0)\eta^{(0)}_{\frac{1}{2}\mu_0}\zeta^{(0)}_{\frac{1}{2}\nu_0}\\&\times\sum_{\ell j\mu_j}S^{1/2}_{n\ell j\nu_{\mathrm{x}}}(j\mu_j I_{\mathrm{B}}\mu_{\mathrm{B}}|I_{\mathrm{A}}\mu_{\mathrm{A}})\varphi_{n\ell j}(R_2)\left[Y_\ell\left(\hat{\boldsymbol{R}}_2\right)\otimes\Phi^{t_{\mathrm{x}}\nu_{\mathrm{x}}}_{I_{\mathrm{x}}}(\epsilon_{\mathrm{x}},\xi_{\mathrm{x}})\right]_{j\mu_j}\Bigg\rangle.\end{aligned} \tag{2.31}$$

2.1.2 Asymptotic momentum approximation

To express all the coordinates relevant to the transition matrix (2.31) by $\boldsymbol{R}$ and $\boldsymbol{s}$, which are the c.m. and relative coordinates of the 1-x system (see Fig. 2.1), we employ the Asymptotic Momentum Approximation (AMA) [52], which has been widely applyed to the DWIA analysis. In this approximation, the propagation of each distorted wave from a point $\boldsymbol{x}$ to another point $\boldsymbol{x}+\Delta\boldsymbol{x}$ is expressed by the plane wave with the asymptotic momentum, that is,

$$\chi_{\boldsymbol{K}}(\boldsymbol{x}+\Delta\boldsymbol{x})\approx\chi_{\boldsymbol{K}}(\boldsymbol{x})\mathrm{e}^{i\boldsymbol{K}\cdot\Delta\boldsymbol{x}}. \tag{2.32}$$

It should be noted that in the plane wave limit:

$$\chi_{\boldsymbol{K}}(\boldsymbol{x})\to\mathrm{e}^{i\boldsymbol{K}\cdot\boldsymbol{x}},\quad\chi_{\boldsymbol{K}}(\boldsymbol{x}+\Delta\boldsymbol{x})\to\mathrm{e}^{i\boldsymbol{K}\cdot(\boldsymbol{x}+\Delta\boldsymbol{x})}, \tag{2.33}$$

Eq. (2.32) holds not approximatelly but exactly, and it suggests that the AMA is good in the case of weak distortion by an optical potential. This approximation is also expected to be good with $\Delta\boldsymbol{x}$ being small (about 0.5 fm) from the analogy with the local semiclassical approximation [67–69], in which each asymptotic momentum is replaced with the momentum determined by the local energy conservation and the local flux of the distorted wave.

The coordinates $\boldsymbol{R}_0$, $\boldsymbol{R}_1$, and $\boldsymbol{R}_2$ can be expressed in terms of $\boldsymbol{R}$ and $\boldsymbol{s}$ as

$$\boldsymbol{R}_0=\boldsymbol{R}-\alpha_R\boldsymbol{R}+\alpha_{0s}\boldsymbol{s},\quad\boldsymbol{R}_1=\boldsymbol{R}+\alpha_{1s}\boldsymbol{s},\quad\boldsymbol{R}_2=\boldsymbol{R}-\alpha_{2s}\boldsymbol{s}, \tag{2.34}$$

in which

$$\alpha_R\equiv\frac{m_2}{m_{\mathrm{A}}},\quad\alpha_{0s}\equiv\frac{m_2}{m_1+m_2}\frac{m_1+m_{\mathrm{A}}}{m_{\mathrm{A}}},\quad\alpha_{1s}\equiv\frac{m_2}{m_1+m_2},\quad\alpha_{2s}\equiv\frac{m_1}{m_1+m_2}. \tag{2.35}$$

Applying the AMA to the distorted waves in Eq. (2.31), they become

$$\chi^{(+)}_{0,\boldsymbol{K}_0}(\boldsymbol{R}_0)\approx\chi^{(+)}_{0,\boldsymbol{K}_0}(\boldsymbol{R})\mathrm{e}^{-i\alpha_R\boldsymbol{K}_0\cdot\boldsymbol{R}}\mathrm{e}^{i\alpha_{0s}\boldsymbol{K}_0\cdot\boldsymbol{s}}, \tag{2.36}$$

$$\chi^{(-)}_{1,\boldsymbol{K}_1}(\boldsymbol{R}_1)\approx\chi^{(-)}_{1,\boldsymbol{K}_1}(\boldsymbol{R})\mathrm{e}^{i\alpha_{1s}\boldsymbol{K}_1\cdot\boldsymbol{s}},\quad\chi^{(-)}_{2,\boldsymbol{K}_2}(\boldsymbol{R}_2)\approx\chi^{(-)}_{2,\boldsymbol{K}_2}(\boldsymbol{R})\mathrm{e}^{-i\alpha_{2s}\boldsymbol{K}_2\cdot\boldsymbol{s}}. \tag{2.37}$$

Inserting Eqs. (2.36) and (2.37) and the Fourier transform of the bound state wave function of particle x:

$$\varphi_{n\ell jm}(\boldsymbol{R}_2)\equiv\varphi_{n\ell j}(R_2)Y_{\ell m}\left(\hat{\boldsymbol{R}}_2\right)$$

$$
\begin{aligned}
&= \frac{1}{(2\pi)^{3/2}} \int \mathrm{d}\boldsymbol{K}_{\mathrm{x}}\, \tilde{\varphi}_{n\ell jm}(\boldsymbol{K}_{\mathrm{x}}) \mathrm{e}^{i\boldsymbol{K}_{\mathrm{x}}\cdot\boldsymbol{R}_2} \\
&= \frac{1}{(2\pi)^{3/2}} \int \mathrm{d}\boldsymbol{K}_{\mathrm{x}}\, \tilde{\varphi}_{n\ell jm}(\boldsymbol{K}_{\mathrm{x}}) \mathrm{e}^{i\boldsymbol{K}_{\mathrm{x}}\cdot\boldsymbol{R}} \mathrm{e}^{-i\alpha_{2s}\boldsymbol{K}_{\mathrm{x}}\cdot\boldsymbol{s}}
\end{aligned}
\tag{2.38}
$$

into the transition matrix (2.31), we obtain

$$
\begin{aligned}
T_{\mu_1\mu_2\mu_{\mathrm{B}}\mu_0\mu_{\mathrm{A}}} = {}& \frac{1}{(2\pi)^{3/2}} \int \mathrm{d}\boldsymbol{R}\, \chi^{(-)*}_{1,\boldsymbol{K}_1}(\boldsymbol{R}) \chi^{(-)*}_{2,\boldsymbol{K}_2}(\boldsymbol{R}) \chi^{(+)}_{0,\boldsymbol{K}_0}(\boldsymbol{R}) \mathrm{e}^{-i\alpha_R \boldsymbol{K}_0\cdot\boldsymbol{R}} \\
&\times \sum_{\ell j \mu_j} \sum_{m\mu_{\mathrm{x}}} S^{1/2}_{n\ell j\nu_{\mathrm{x}}} (j\mu_j I_{\mathrm{B}}\mu_{\mathrm{B}} | I_{\mathrm{A}}\mu_{\mathrm{A}}) (\ell m I_{\mathrm{x}}\mu_{\mathrm{x}} | j\mu_j) \int \mathrm{d}\boldsymbol{K}_{\mathrm{x}}\, \tilde{\varphi}_{n\ell jm}(\boldsymbol{K}_{\mathrm{x}}) \mathrm{e}^{i\boldsymbol{K}_{\mathrm{x}}\cdot\boldsymbol{R}} \\
&\times \tilde{t}_{12}(\boldsymbol{\kappa}', \mu_1\nu_1\mu_2\nu_2; \boldsymbol{\kappa}, \mu_0\nu_0\mu_{\mathrm{x}}\nu_{\mathrm{x}}),
\end{aligned}
\tag{2.39}
$$

in which $\tilde{t}_{12}$ is the transition matrix of the elementary process of the (p, pd) reaction defined by

$$
\tilde{t}_{12}(\boldsymbol{\kappa}', \mu_1\nu_1\mu_2\nu_2; \boldsymbol{\kappa}, \mu_0\nu_0\mu_{\mathrm{x}}\nu_{\mathrm{x}}) \equiv \left\langle \mathrm{e}^{i\boldsymbol{\kappa}'\cdot\boldsymbol{s}} \eta^{(1)}_{\frac{1}{2}\mu_1} \zeta^{(1)}_{\frac{1}{2}\nu_1} \Phi^{t_2\nu_2}_{I_2\mu_2}(\epsilon_2, \xi_2) \middle| t_{12}(\boldsymbol{s}) \middle| \mathrm{e}^{i\boldsymbol{\kappa}\cdot\boldsymbol{s}} \eta^{(0)}_{\frac{1}{2}\mu_0} \zeta^{(0)}_{\frac{1}{2}\nu_0} \Phi^{t_{\mathrm{x}}\nu_{\mathrm{x}}}_{I_{\mathrm{x}}\mu_{\mathrm{x}}}(\epsilon_{\mathrm{x}}, \xi_{\mathrm{x}}) \right\rangle . \tag{2.40}
$$

$\boldsymbol{\kappa}$ ($\boldsymbol{\kappa}'$) is the relative momentum between paricles 0 and x (particles 1 and 2) in the initial (final) state given by

$$
\boldsymbol{\kappa} \equiv \alpha_{0s}\boldsymbol{K}_0 - \alpha_{2s}\boldsymbol{K}_{\mathrm{x}}, \quad \boldsymbol{\kappa}' \equiv \alpha_{1s}\boldsymbol{K}_1 - \alpha_{2s}\boldsymbol{K}_2. \tag{2.41}
$$

Supposing the momentum conservation of the two colliding particles in the elementary process holds, that is,

$$
\frac{m_1 + m_{\mathrm{A}}}{m_{\mathrm{A}}} \boldsymbol{K}_0 + \boldsymbol{K}_{\mathrm{x}} \approx \boldsymbol{K}_1 + \boldsymbol{K}_2, \tag{2.42}
$$

$\boldsymbol{\kappa}$ is determined by

$$
\boldsymbol{\kappa} = \frac{m_1 + m_{\mathrm{A}}}{m_{\mathrm{A}}} \boldsymbol{K}_0 - \alpha_{2s}(\boldsymbol{K}_1 + \boldsymbol{K}_2) \equiv \boldsymbol{\kappa}_0 \tag{2.43}
$$

and the $\boldsymbol{K}_{\mathrm{x}}$ dependence is removed from $\tilde{t}_{12}$. Then, with the inverse Fourier transformation, we obtain

$$
\begin{aligned}
T_{\mu_1\mu_2\mu_{\mathrm{B}}\mu_0\mu_{\mathrm{A}}} = {}& \sum_{\mu_{\mathrm{x}}} \tilde{t}_{12}(\boldsymbol{\kappa}', \mu_1\nu_1\mu_2\nu_2; \boldsymbol{\kappa}_0, \mu_0\nu_0\mu_{\mathrm{x}}\nu_{\mathrm{x}}) \\
&\times \int \mathrm{d}\boldsymbol{R}\, \chi^{(-)*}_{1,\boldsymbol{K}_1}(\boldsymbol{R}) \chi^{(-)*}_{2,\boldsymbol{K}_2}(\boldsymbol{R}) \chi^{(+)}_{0,\boldsymbol{K}_0}(\boldsymbol{R}) \mathrm{e}^{-i\alpha_R \boldsymbol{K}_0\cdot\boldsymbol{R}} \\
&\times \sum_{\ell m j \mu_j} S^{1/2}_{n\ell j\nu_{\mathrm{x}}} (j\mu_j I_{\mathrm{B}}\mu_{\mathrm{B}} | I_{\mathrm{A}}\mu_{\mathrm{A}}) (\ell m I_{\mathrm{x}}\mu_{\mathrm{x}} | j\mu_j) \varphi_{n\ell jm}(\boldsymbol{R}).
\end{aligned}
\tag{2.44}
$$

The effective interaction t_{12} and its matrix element $\tilde{t}_{12}$ are usually defined in the c.m. frame of the 0-x (or 1-2) system (the t frame for short). So we need to multiply $\tilde{t}_{12}$ by the so-called Møller factor:

$$
f_{\text{Møller}} \equiv \left(\frac{E^{\mathrm{t}}_1 E^{\mathrm{t}}_2 E^{\mathrm{t}}_0 E^{\mathrm{t}}_{\mathrm{x}}}{E_1 E_2 E_0 E_{\mathrm{x}}} \right)^{1/2}, \tag{2.45}
$$

in which E^{t}_j and E_j are the relativistic energies of particle j $(= 0, 1, 2,$ and $x)$ in the t and G frame, to take into account the Lorentz invariance of the reaction probability of the elementary process.

2.1.3 Triple differential cross section

We start the derivation of the Triple Differential CROSS section (TDX), which is the most explicit quantity of the knockout reaction, with the infinitesimal cross section of a three-body emission channel:

$$\mathrm{d}\sigma = \frac{(2\pi)^4}{\hbar v_i}\,\mathrm{d}\boldsymbol{K}_1\,\mathrm{d}\boldsymbol{K}_2\,\mathrm{d}\boldsymbol{K}_\mathrm{B}\,\delta(E_f - E_i)\delta(\boldsymbol{K}_f - \boldsymbol{K}_i)\frac{1}{2I_0+1}\frac{1}{2I_\mathrm{A}+1}\sum_{\mu_1\mu_2\mu_\mathrm{B}\mu_0\mu_\mathrm{A}}\left|T_{\mu_1\mu_2\mu_\mathrm{B}\mu_0\mu_\mathrm{A}}\right|^2, \tag{2.46}$$

in which $T_{\mu_1\mu_2\mu_\mathrm{B}\mu_0\mu_\mathrm{A}}$ is the transition matrix discussed in the previous subsection. The two Dirac's delta functions $\delta(E_f - E_i)$ and $\delta(\boldsymbol{K}_f - \boldsymbol{K}_i)$ guarantee the energy and momentum conservations through the reaction, respectively. I_0 $(= 1/2)$ is the spin of particle 0. v_i is the magnitude of the relative velocity between particle 0 and A given by

$$v_i \equiv c^2\frac{\hbar K_0^\mathrm{L}}{E_0^\mathrm{L}}, \tag{2.47}$$

in which the quantities with the superscript L are evaluated in the laboratory (L) frame. Utilizing the four-momentum delta function, v_i and $\hbar\,\mathrm{d}\boldsymbol{K}_j/E_j$ of particle j $(= 1, 2,$ and B$)$ are Lorentz invariant,

$$\begin{aligned}\mathrm{d}\sigma = \frac{(2\pi)^4}{\hbar v_i}\frac{E_1E_2E_\mathrm{B}}{E_1^\mathrm{L}E_2^\mathrm{L}E_\mathrm{B}^\mathrm{L}}\,\mathrm{d}\boldsymbol{K}_1^\mathrm{L}\,\mathrm{d}\boldsymbol{K}_2^\mathrm{L}\,\mathrm{d}\boldsymbol{K}_\mathrm{B}^\mathrm{L}\,\delta\big(E_f^\mathrm{L} - E_i^\mathrm{L}\big)\\ \times\,\delta\big(\boldsymbol{K}_f^\mathrm{L} - \boldsymbol{K}_i^\mathrm{L}\big)\frac{1}{2I_0+1}\frac{1}{2I_\mathrm{A}+1}\sum_{\mu_1\mu_2\mu_\mathrm{B}\mu_0\mu_\mathrm{A}}\left|T_{\mu_1\mu_2\mu_\mathrm{B}\mu_0\mu_\mathrm{A}}\right|^2\end{aligned} \tag{2.48}$$

is obtained. In what follows, the TDX in the L frame of the form:

$$\frac{\mathrm{d}^3\sigma}{\mathrm{d}E_1^\mathrm{L}\,\mathrm{d}\Omega_1^\mathrm{L}\,\mathrm{d}\Omega_2^\mathrm{L}}, \tag{2.49}$$

which indicates we does not observe the residual nucleus B in experiments explicitly, is derived from Eq. (2.48).

We can evaluate $\boldsymbol{K}_\mathrm{B}^\mathrm{L}$ as

$$\boldsymbol{K}_\mathrm{B}^\mathrm{L} = \boldsymbol{K}_0^\mathrm{L} + \boldsymbol{K}_\mathrm{A}^\mathrm{L} - \boldsymbol{K}_1^\mathrm{L} - \boldsymbol{K}_2^\mathrm{L} = \boldsymbol{X}^\mathrm{L} - \boldsymbol{K}_2^\mathrm{L} \quad \big(\boldsymbol{X}^\mathrm{L} \equiv \boldsymbol{K}_0^\mathrm{L} + \boldsymbol{K}_\mathrm{A}^\mathrm{L} - \boldsymbol{K}_1^\mathrm{L}\big) \tag{2.50}$$

from the δ function for the momentum conservation, and remove the variable from the expression of Eq. (2.48) by integrating it. In addition, from the relativistic energy-momentum relation:

$$E_i^\mathrm{L} = \sqrt{(m_ic^2)^2 + \big(\hbar cK_i^\mathrm{L}\big)^2}, \tag{2.51}$$

we can calculate the total derivative of E_i^L as

$$\mathrm{d}E_i^\mathrm{L} = \mathrm{d}\left[\sqrt{(m_ic^2)^2 + \big(\hbar cK_i^\mathrm{L}\big)^2}\right] = \frac{\hbar^2c^2K_i^\mathrm{L}}{E_i^\mathrm{L}}\,\mathrm{d}K_i^\mathrm{L}, \tag{2.52}$$

and it gives

$$\mathrm{d}\boldsymbol{K}_i^\mathrm{L} = \big(K_i^\mathrm{L}\big)^2\,\mathrm{d}K_i^\mathrm{L}\,\mathrm{d}\Omega_i^\mathrm{L} = \frac{E_i^\mathrm{L}K_i^\mathrm{L}}{\hbar^2c^2}\,\mathrm{d}E_i^\mathrm{L}\,\mathrm{d}\Omega_i^\mathrm{L}. \tag{2.53}$$

As a result,

$$\begin{aligned}\mathrm{d}\sigma = \frac{(2\pi)^4}{\hbar v_i}\frac{E_1E_2E_\mathrm{B}}{E_1^\mathrm{L}E_2^\mathrm{L}E_\mathrm{B}^\mathrm{L}}\frac{E_1^\mathrm{L}K_1^\mathrm{L}}{\hbar^2c^2}\,\mathrm{d}E_1^\mathrm{L}\,\mathrm{d}\Omega_1^\mathrm{L}\,\big(K_2^\mathrm{L}\big)^2\,\mathrm{d}K_2^\mathrm{L}\,\mathrm{d}\Omega_2^\mathrm{L}\,\delta\big(E_f^\mathrm{L} - E_i^\mathrm{L}\big)\\ \times\,\frac{1}{2I_0+1}\frac{1}{2I_\mathrm{A}+1}\sum_{\mu_1\mu_2\mu_\mathrm{B}\mu_0\mu_\mathrm{A}}\left|T_{\mu_1\mu_2\mu_\mathrm{B}\mu_0\mu_\mathrm{A}}\right|^2\end{aligned} \tag{2.54}$$

is obtained. Because the argument of the δ function for the energy conservation is

$$E_f^{\mathrm{L}} - E_i^{\mathrm{L}} = \sqrt{(m_1c^2)^2 + \left(\hbar c K_1^{\mathrm{L}}\right)^2} + \sqrt{(m_2c^2)^2 + \left(\hbar c K_2^{\mathrm{L}}\right)^2} + \sqrt{(m_{\mathrm{B}}c^2)^2 + \left(\hbar c K_{\mathrm{B}}^{\mathrm{L}}\right)^2} - \sqrt{(m_0c^2)^2 + \left(\hbar c K_0^{\mathrm{L}}\right)^2} - \sqrt{(m_{\mathrm{A}}c^2)^2 + \left(\hbar c K_{\mathrm{A}}^{\mathrm{L}}\right)^2}, \tag{2.55}$$

in which $K_{\mathrm{B}}^{\mathrm{L}}$ has already been determined by Eq. (2.50) as

$$K_{\mathrm{B}}^{\mathrm{L}} = \sqrt{(X^{\mathrm{L}})^2 + \left(K_2^{\mathrm{L}}\right)^2 - 2X^{\mathrm{L}}K_2^{\mathrm{L}}\cos\theta_{\mathrm{X}2}^{\mathrm{L}}} \quad \left(\cos\theta_{\mathrm{X}2}^{\mathrm{L}} \equiv \boldsymbol{X}^{\mathrm{L}} \cdot \boldsymbol{K}_2^{\mathrm{L}}\right), \tag{2.56}$$

we get

$$\frac{\partial(E_f^{\mathrm{L}} - E_i^{\mathrm{L}})}{\partial K_2^{\mathrm{L}}} = \frac{\hbar^2c^2K_2^{\mathrm{L}}}{E_2^{\mathrm{L}}} + \frac{\hbar^2c^2K_{\mathrm{B}}^{\mathrm{L}}}{E_{\mathrm{B}}^{\mathrm{L}}}\frac{K_2^{\mathrm{L}} - X^{\mathrm{L}}\cos\theta_{\mathrm{X}2}^{\mathrm{L}}}{K_{\mathrm{B}}^{\mathrm{L}}}, \tag{2.57}$$

and then the phase volume F_{kin}:

$$\begin{aligned} F_{\mathrm{kin}} &\equiv \frac{E_1^{\mathrm{L}}K_1^{\mathrm{L}}\left(K_2^{\mathrm{L}}\right)^2}{\hbar^2c^2}\left[\frac{\hbar^2c^2K_2^{\mathrm{L}}}{E_2^{\mathrm{L}}} + \frac{\hbar^2c^2K_{\mathrm{B}}^{\mathrm{L}}}{E_{\mathrm{B}}^{\mathrm{L}}}\frac{K_2^{\mathrm{L}} - X^{\mathrm{L}}\cos\theta_{\mathrm{X}2}^{\mathrm{L}}}{K_{\mathrm{B}}^{\mathrm{L}}}\right]^{-1} \\ &= \frac{E_1^{\mathrm{L}}K_1^{\mathrm{L}}E_2^{\mathrm{L}}K_2^{\mathrm{L}}}{\hbar^4c^4}\left[1 + \frac{E_2^{\mathrm{L}}}{E_{\mathrm{B}}^{\mathrm{L}}} + \frac{E_2^{\mathrm{L}}}{E_{\mathrm{B}}^{\mathrm{L}}}\frac{\left(\boldsymbol{K}_1^{\mathrm{L}} - \boldsymbol{K}_0^{\mathrm{L}} - \boldsymbol{K}_{\mathrm{A}}^{\mathrm{L}}\right)\cdot\boldsymbol{K}_2^{\mathrm{L}}}{\left(K_2^{\mathrm{L}}\right)^2}\right]^{-1}. \end{aligned} \tag{2.58}$$

It should be noted that K_2^{L} has already been specified by the energy conservation.

It is found that the dependence of the transition matrix (2.44) on μ_1 and μ_2 appears only in the Clebsch-Gordan coefficient. So unless these are specified experimentally, the summation over μ_1 and μ_2 is calculated as

$$\sum_{\mu_{\mathrm{B}}\mu_{\mathrm{A}}}\sum_{j'\mu_j'}\sum_{j\mu_j}(j'\mu_j'I_{\mathrm{B}}\mu_{\mathrm{B}}|I_{\mathrm{A}}\mu_{\mathrm{A}})(j\mu_jI_{\mathrm{B}}\mu_{\mathrm{B}}|I_{\mathrm{A}}\mu_{\mathrm{A}}) = \sum_{j'\mu_j'}\sum_{j\mu_j}\frac{2I_{\mathrm{A}}+1}{2j+1}\delta_{j'j}\delta_{\mu_j'\mu_j} = \sum_{j\mu_j}\frac{2I_{\mathrm{A}}+1}{2j+1}. \tag{2.59}$$

Here, we employ an averaging prescription on μ_{x}:

$$\begin{aligned} &\tilde{t}_{12}^*(\boldsymbol{\kappa}', \mu_1\nu_1\mu_2\nu_2 : \boldsymbol{\kappa}_0, \mu_0\nu_0\mu_{\mathrm{x}}'\nu_{\mathrm{x}})\tilde{t}_{12}(\boldsymbol{\kappa}', \mu_1\nu_1\mu_2\nu_2; \boldsymbol{\kappa}_0, \mu_0\nu_0\mu_{\mathrm{x}}\nu_{\mathrm{x}}) \\ &\approx \frac{1}{2I_{\mathrm{x}}+1}\sum_{\bar{\mu}_{\mathrm{x}}}\left|\tilde{t}_{12}(\boldsymbol{\kappa}', \mu_1\nu_1\mu_2\nu_2; \boldsymbol{\kappa}_0, \mu_0\nu_0\bar{\mu}_{\mathrm{x}}\nu_{\mathrm{x}})\right|^2\delta_{\mu_{\mathrm{x}}'\mu_{\mathrm{x}}} \end{aligned} \tag{2.60}$$

in the calculation of the squared norm in Eq. (2.54). Then this prescription leads to

$$\begin{aligned} &\sum_{\mu_j}\sum_{\mu_{\mathrm{x}}'\mu_{\mathrm{x}}}\sum_{\ell'm'}\sum_{\ell m}(\ell'm'I_{\mathrm{x}}\mu_{\mathrm{x}}'|j\mu_j)(\ell mI_{\mathrm{x}}\mu_{\mathrm{x}}|j\mu_j)\delta_{\mu_{\mathrm{x}}'\mu_{\mathrm{x}}} \\ &= \sum_{\mu_j}\sum_{\mu_{\mathrm{x}}}\sum_{\ell'm'}\sum_{\ell m}(\ell'm'I_{\mathrm{x}}\mu_{\mathrm{x}}|j\mu_j)(\ell mI_{\mathrm{x}}\mu_{\mathrm{x}}|j\mu_j) \\ &= \sum_{\ell'm'}\sum_{\ell m}\frac{2j+1}{2\ell+1}\delta_{\ell'\ell}\delta_{m'm} \\ &= \sum_{\ell m}\frac{2j+1}{2\ell+1}. \end{aligned} \tag{2.61}$$

In addition, $\tilde{t}_{12}$ is related to the differential cross section of p-d elastic scattering $\mathrm{d}\sigma_{12}\,/\,\mathrm{d}\Omega_{12}$ as

$$\frac{\mathrm{d}\sigma_{12}}{\mathrm{d}\Omega_{12}}(T_{12}, \theta_{12}) = \left(\frac{\mu_{12}}{2\pi\hbar^2}\right)^2\frac{1}{2I_0+1}\frac{1}{2I_{\mathrm{x}}+1}\sum_{\mu_1\mu_2\mu_0\bar{\mu}_{\mathrm{x}}}\left|\tilde{t}_{12}(\boldsymbol{\kappa}', \mu_1\nu_1\mu_2\nu_2; \boldsymbol{\kappa}_0, \mu_0\nu_0\bar{\mu}_{\mathrm{x}}\nu_{\mathrm{x}})\right|^2, \tag{2.62}$$

in which T_{12} and θ_{12} are the scattering energy and angle of the elementary process, respectively, given by

$$E_{12} = \frac{\hbar^2}{2\mu_{12}}\left(\kappa'\right)^2, \quad \cos\theta_{12} = \frac{\boldsymbol{\kappa}'\cdot\boldsymbol{\kappa}_0}{\kappa'\kappa_0}. \tag{2.63}$$

μ_{12} is the reduced mass between paricles 1 and 2. Finally, we obtain the expression of the TDX of the (p, pd) reaction in the L frame:

$$\begin{aligned}\frac{\mathrm{d}^3\sigma}{\mathrm{d}E_1^{\mathrm{L}}\,\mathrm{d}\Omega_1^{\mathrm{L}}\,\mathrm{d}\Omega_2^{\mathrm{L}}} &= \frac{(2\pi)^4}{\hbar v_i}\frac{E_1E_2E_{\mathrm{B}}}{E_1^{\mathrm{L}}E_2^{\mathrm{L}}E_{\mathrm{B}}^{\mathrm{L}}}F_{\mathrm{kin}}\frac{1}{2I_0+1}\left(\frac{2\pi\hbar^2}{\mu_{12}}\right)^2\frac{\mathrm{d}\sigma_{12}}{\mathrm{d}\Omega_{12}}(T_{12},\theta_{12})\sum_{\ell j}\frac{2I_0+1}{2\ell+1}S_{n\ell j\nu_{\mathrm{x}}}\\ &\times\sum_m\left|\int \mathrm{d}\boldsymbol{R}\,\chi^{(-)*}_{1,\boldsymbol{K}_1}(\boldsymbol{R})\chi^{(-)*}_{2,\boldsymbol{K}_2}(\boldsymbol{R})\chi^{(+)}_{0,\boldsymbol{K}_0}(\boldsymbol{R})\mathrm{e}^{-i\alpha_R\boldsymbol{K}_0\cdot\boldsymbol{R}}\varphi_{n\ell jm}(\boldsymbol{R})\right|^2.\end{aligned} \tag{2.64}$$

2.1.4 Plane wave impulse approximation

For intuitively understanding the meaning of the knockout reaction observables, let us consider the plane wave limit of the DWIA framework, which is called the Plane Wave Impulse Approximation (PWIA). In the PWIA framework, each distorted wave in Eq. (2.64) is replaced with the plane wave with its asymptotic momentum as shown in Eq. (2.33):

$$\begin{aligned}\frac{\mathrm{d}^3\sigma^{\mathrm{PW}}}{\mathrm{d}E_1^{\mathrm{L}}\,\mathrm{d}\Omega_1^{\mathrm{L}}\,\mathrm{d}\Omega_2^{\mathrm{L}}} &= \frac{(2\pi)^4}{\hbar v_i}\frac{E_1E_2E_{\mathrm{B}}}{E_1^{\mathrm{L}}E_2^{\mathrm{L}}E_{\mathrm{B}}^{\mathrm{L}}}F_{\mathrm{kin}}\frac{1}{2I_0+1}\left(\frac{2\pi\hbar^2}{\mu_{12}}\right)^2\frac{\mathrm{d}\sigma_{12}}{\mathrm{d}\Omega_{12}}(T_{12},\theta_{12})\sum_{\ell j}\frac{2I_0+1}{2\ell+1}S_{n\ell j\nu_{\mathrm{x}}}\\ &\times\sum_m\left|\tilde{\varphi}_{n\ell jm}(\boldsymbol{K}_{\mathrm{ms}})\right|^2,\end{aligned} \tag{2.65}$$

in which $\tilde{\varphi}_{n\ell jm}$ is the Fourier transform of $\varphi_{n\ell jm}$:

$$\tilde{\varphi}_{n\ell jm}(\boldsymbol{K}_{\mathrm{ms}}) = \int \mathrm{d}\boldsymbol{R}\,\mathrm{e}^{i\boldsymbol{K}_{\mathrm{ms}}}\varphi_{n\ell jm}(\boldsymbol{R}) = \int \mathrm{d}\boldsymbol{R}\,\mathrm{e}^{i\boldsymbol{K}_{\mathrm{ms}}}\varphi_{n\ell j}(R)Y_{\ell m}\left(\hat{\boldsymbol{R}}\right). \tag{2.66}$$

$\boldsymbol{K}_{\mathrm{ms}}$ is the so-called missing momentum given by

$$\boldsymbol{K}_{\mathrm{ms}} \equiv (1-\alpha_R)\boldsymbol{K}_0 - \boldsymbol{K}_1 - \boldsymbol{K}_2, \tag{2.67}$$

which is known to correspond to the momentum of the residual nucleus B in the L frame, $\boldsymbol{K}_{\mathrm{B}}^{\mathrm{L}}$. By assuming B is a spectator in the knockout reaction, in addition, we can interpret $-\boldsymbol{K}_{\mathrm{ms}}$ as the momentum of the c.m. of the pn pair, $\boldsymbol{K}_{pn}^{\mathrm{L}}$, because the target nucleus A is at rest in the L frame. Thus, we can say that in the PWIA limit, the TDX of the knockout reaction is a "snapshot" of the motion of the particle in the target. This is why the knockout reaction has been regarded as an appropriate tool to investigate the single-particle and cluster state inside nuclei in both theoretical and experimental studies.

2.2 *CDCCIA* formalism

Although deuteron is a weakly bound system consisting of a proton and a neutron, whose binding energy is about 1.1 MeV per nucleon, we have treated it as a single particle in the previous section. In this section, I present the new framework, which describes the (p, pd) reaction with taking into account the deuteron breakup in the elementary process and the contributions of the Final-State Interactions (FSIs). The framework is called *CDCCIA*, which comes from the combination of the Continuum-Discretized Coupled-Channels method (CDCC) [70–72] explained briefly below and the Impulse Approximation (IA). The notation in the following formulation is the same as in the previous section.

2.2.1 Transition matrix based on CDCCIA

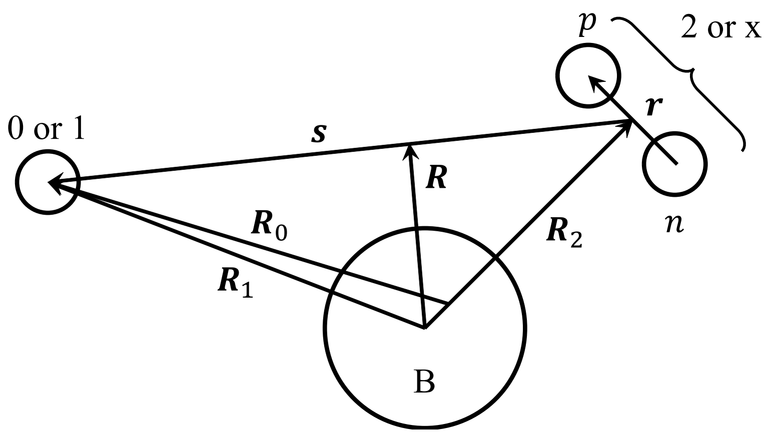

FIGURE 2.2: Coordinates of the A(p, pd)B reaction system with treating the deuteron as a two-nucleon system.

The coordinates to describe the A(p, pd)B reaction within the CDCCIA framework are shown in Fig. 2.2, and we take $\boldsymbol{R}_0$, $\boldsymbol{R}_2$, and $\boldsymbol{r}$ as the independent coordinates. The transition matrix in the post form is the same as Eqs. (2.1)-(2.3). It should be noted that the internal coordinates $\xi_{\rm A}$ and ξ_2 include $\boldsymbol{r}$.

The transition interaction V_f is given by the sum of the two-body interactions in the final state:

$$V_f = U_{1\rm B} + U_{p\rm B} + U_{n\rm B} + \tau_{1p} + \tau_{1n}, \tag{2.68}$$

in which τ_{1p} (τ_{1n}) is an effective interaction between particle 1 and the proton (neutron) in particle 2. The employment of these interactions makes the difference between CDCCIA and the DWIA. In the latter, τ_{12} has been employed as shown in Eq. (2.7), and it assumes that the deuteron breakup in the elementary process can be ignored. On the other hand, in the CDCCIA framework, the elementary process is described by the summation of the collisions of particle 1 and nucleons in particle 2, in which the breakup can happen. As in the DWIA, the IA is adopted, that is,

$$\tau_{1p} \approx t_{1p}, \quad \tau_{1n} \approx t_{1n}, \tag{2.69}$$

in which t_{1p} and t_{1p} are effective interactions in free space. By making the use of Eq. (2.8) and the Gell-Mann-Goldberger transformation, the transition matrix becomes

$$\begin{aligned} T_{\mu_1\mu_2\mu_{\rm B}\mu_0\mu_{\rm A}} = \Big\langle \Psi^{(-)}_{\boldsymbol{K}_1,\boldsymbol{K}_2}(\boldsymbol{R}_1,\boldsymbol{R}_2,\xi_2)\eta^{(1)}_{\frac{1}{2}\mu_1}\zeta^{(1)}_{\frac{1}{2}\nu_1}\Phi^{t_{\rm B}\nu_{\rm B}}_{I_{\rm B}\mu_{\rm B}}(\epsilon_{\rm B},\xi_{\rm B}) \Big| \\ \times \left[t_{1p}(\boldsymbol{s}_{1p}) + t_{1n}(\boldsymbol{s}_{1n})\right] \Big| \chi^{(+)}_{0,\boldsymbol{K}_0}(\boldsymbol{R}_0)\eta^{(0)}_{\frac{1}{2}\mu_0}\zeta^{(0)}_{\frac{1}{2}\nu_0}\Phi^{t_{\rm A}\nu_{\rm A}}_{I_{\rm A}\mu_{\rm A}}(\epsilon_{\rm A},\xi_{\rm A}) \Big\rangle \end{aligned} \tag{2.70}$$

with

$$\boldsymbol{s}_{1p} \equiv \boldsymbol{s} + \frac{1}{2}\boldsymbol{r}, \quad \boldsymbol{s}_{1n} \equiv \boldsymbol{s} - \frac{1}{2}\boldsymbol{r}. \tag{2.71}$$

It is worth pointing out that the same formalism has been employed in the studies of the electron (e) induced deuteron knockout reaction $(e, e'd)$ [73]. As a remarkable advantage of the present research over the preceding one, we take into account the transition of the knocked-out deuteron by the FSIs. $\Psi^{(-)}_{\boldsymbol{K}_1,\boldsymbol{K}_2}$ is the scattering wave of the $1 + (p + n) + \rm B$ four-body system satisfying the Schrödinger equation:

$$\left[\hat{T}_f + U^*_{1\rm B}(R_1) + U^*_{p\rm B}(R_{p\rm B}) + U^*_{n\rm B}(R_{n\rm B}) + h_{pn} - T_f\right]\Psi^{(-)}_{\boldsymbol{K}_1,\boldsymbol{K}_2}(\boldsymbol{R}_1,\boldsymbol{R}_2,\xi_2) = 0, \tag{2.72}$$

in which $\hat{T}_f$ is defined by Eq. (2.17) and T_f is the scattering energy given by

$$T_f = \frac{\hbar^2}{2\mu_{1\mathrm{B}}}K_1^2 + \frac{\hbar^2}{2\mu_{2\mathrm{B}}}K_2^2 + \frac{\hbar^2}{m_{\mathrm{B}}}\boldsymbol{K}_1 \cdot \boldsymbol{K}_2 + \epsilon_{2,c}. \tag{2.73}$$

It should be noted that we have used the momentum conservation (2.9) in the final state. h_{pn} is the internal Hamiltonian of the proton-neutron system. Applying the semiclassical approximation (2.19) to the third term on the right-hand-side of Eq. (2.73), we can rewrite Eq. (2.72) as

$$\left[H_{1\mathrm{B}} + H_{2\mathrm{B}} - \frac{\hbar^2}{2\mu_{1\mathrm{B}}}K_1^2 - \frac{\hbar^2}{2\mu_{2\mathrm{B}}}K_2^2 - \epsilon_{2,c}\right]\Psi^{(-)}_{\boldsymbol{K}_1,\boldsymbol{K}_2}(\boldsymbol{R}_1, \boldsymbol{R}_2, \xi_2) = 0, \tag{2.74}$$

$$H_{1\mathrm{B}} \equiv \hat{T}_{\boldsymbol{R}_1} + U^*_{1\mathrm{B}}(R_1), \quad H_{2\mathrm{B}} \equiv \hat{T}_{\boldsymbol{R}_2} + U^*_{p\mathrm{B}}(R_{p\mathrm{B}}) + U^*_{n\mathrm{B}}(R_{n\mathrm{B}}) + h_{pn}, \tag{2.75}$$

and then Eq. (2.74) is separated into the Schrödinger equations (2.21) and

$$\left[\hat{T}_{\boldsymbol{R}_2} + U^*_{p\mathrm{B}}(R_{p\mathrm{B}}) + U^*_{n\mathrm{B}}(R_{n\mathrm{B}}) + h_{pn} - \frac{\hbar^2}{2\mu_{2\mathrm{B}}}K_2^2 - \epsilon_{2,c}\right]\Xi^{(-)}_{pn\mathrm{B},\boldsymbol{K}_2}(\boldsymbol{R}_2, \xi_2) = 0 \tag{2.76}$$

with the separation of variables:

$$\Psi^{(-)}_{\boldsymbol{K}_1,\boldsymbol{K}_2}(\boldsymbol{R}_1, \boldsymbol{R}_2, \xi_2) \approx \chi^{(-)}_{1,\boldsymbol{K}_1}(\boldsymbol{R}_1)\Xi^{(-)}_{pn\mathrm{B},\boldsymbol{K}_2}(\boldsymbol{R}_2, \xi_2). \tag{2.77}$$

$\Xi^{(-)}_{pn\mathrm{B},\boldsymbol{K}_2}$ is the scattering wave of the three-body system $(p+n)+\mathrm{B}$. We adopt CDCC to obtain it:

$$\Xi^{(-)}_{pn\mathrm{B},\boldsymbol{K}_2}(\boldsymbol{R}_2, \xi_2) \approx \sum_c \chi^{(0c)(-)}_{2,\boldsymbol{K}_2}(\boldsymbol{R}_2)\Phi^{t_2\nu_2}_{I_2\mu_2,c}(\epsilon_{2,c}, \xi_2), \tag{2.78}$$

in which $\Phi^{t_2\mu_2}_{I_2\nu_2,c}$ is the deuteron bound-state wave function for $c = 0$ and the discretized-continuum states of the proton-neutron system for $c \neq 0$. This wave function satisfies the eigenvalue equation:

$$h_{pn}\Phi^{t_2\nu_2}_{I_2\mu_2,c}(\epsilon_{2,c}, \xi_2) = \epsilon_{2,c}\Phi^{t_2\nu_2}_{I_2\mu_2,c}(\epsilon_{2,c}, \xi_2) \tag{2.79}$$

with $\epsilon_{2,c}$ being the eigenenergy of the p-n system in the cth channel. Eq. (2.78) means that the three-body wave function is expanded in terms of the set of the eigenstates of h_{pn}, which is assumed to form a complete set in the model space relevant to the physics observables of interests. The expansion "coefficients" $\chi^{(0c)(-)}_{2,\boldsymbol{K}_2}$ represent the distorted waves between the c.m. of the p-n system in the cth state and the reaction residue B. In addition, $\Xi^{(-)}_{pn\mathrm{B},\boldsymbol{K}_2}$ satisfies the incoming boundary condition:

$$\begin{aligned}\Xi^{(-)}_{pn\mathrm{B},\boldsymbol{K}_2}(\boldsymbol{R}_2, \xi_2) \to &\left[\mathrm{e}^{iK_2z} + f^*_{2\mathrm{B}}(\Omega_2)\frac{\mathrm{e}^{-iK_2R_2}}{R_2}\right]\Phi^{t_2\nu_2*}_{I_2\mu_2,0}(\epsilon^0_2, \xi_2) \\ &+ \sum_c f^*_{2\mathrm{B},c}(\Omega_2)\frac{\mathrm{e}^{-iK_{2,c}R_2}}{R_2}\Phi^{t_2\nu_2*}_{I_2\mu_2,c}(\epsilon^c_2, \xi_2) \quad (R_2 \to \infty),\end{aligned} \tag{2.80}$$

in which $\boldsymbol{K}_{2,c}$ is the momentum of particle 2 in the cth chnnel.

Now the transition matrix (2.70) becomes

$$\begin{aligned}T_{\mu_1\mu_2\mu_\mathrm{B}\mu_0\mu_\mathrm{A}} = &\left\langle \chi^{(-)}_{1,\boldsymbol{K}_1}(\boldsymbol{R}_1)\eta^{(1)}_{\frac{1}{2}\mu_1}\zeta^{(1)}_{\frac{1}{2}\nu_1}\Xi^{(-)}_{pn\mathrm{B},\boldsymbol{K}_2}(\boldsymbol{R}_2, \xi_2)\Phi^{t_\mathrm{B}\nu_\mathrm{B}}_{I_\mathrm{B}\mu_\mathrm{B}}(\epsilon_\mathrm{B}, \xi_\mathrm{B})\right| \\ &\times [t_{1p}(\boldsymbol{s}_{1p}) + t_{1n}(\boldsymbol{s}_{1n})]\left|\chi^{(+)}_{0,\boldsymbol{K}_0}(\boldsymbol{R}_0)\eta^{(0)}_{\frac{1}{2}\mu_0}\zeta^{(0)}_{\frac{1}{2}\nu_0}\Phi^{t_\mathrm{A}\nu_\mathrm{A}}_{I_\mathrm{A}\mu_\mathrm{A}}(\epsilon_\mathrm{A}, \xi_\mathrm{A})\right\rangle.\end{aligned} \tag{2.81}$$

As in the DWIA framework, the assumption that B is inert and a spectator reduces Eq. (2.81) to

$$T_{\mu_1\mu_2\mu_\mathrm{B}\mu_0\mu_\mathrm{A}} = \left\langle \chi^{(-)}_{1,\boldsymbol{K}_1}(\boldsymbol{R}_1)\eta^{(1)}_{\frac{1}{2}\mu_1}\zeta^{(1)}_{\frac{1}{2}\nu_1}\chi^{(-)}_{2,\boldsymbol{K}_2}(\boldsymbol{R}_2)\Xi^{(-)}_{pn\mathrm{B},\boldsymbol{K}_2}(\boldsymbol{R}_2,\xi_2)\right| \times \left[t_{1p}(\boldsymbol{s}_{1p})+t_{1n}(\boldsymbol{s}_{1n})\right]\left|\chi^{(+)}_{0,\boldsymbol{K}_0}(\boldsymbol{R}_0)\eta^{(0)}_{\frac{1}{2}\mu_0}\zeta^{(0)}_{\frac{1}{2}\nu_0}\psi^{t_\mathrm{B}\nu_\mathrm{B}:t_\mathrm{A}\nu_\mathrm{A}}_{I_\mathrm{B}\mu_\mathrm{B}:I_\mathrm{A}\mu_\mathrm{A}}(\epsilon_\mathrm{x},\xi_\mathrm{x},\boldsymbol{R}_2)\right\rangle, \tag{2.82}$$

in which $\psi^{t_\mathrm{B}\nu_\mathrm{B}:t_\mathrm{A}\nu_\mathrm{A}}_{I_\mathrm{B}\mu_\mathrm{B}:I_\mathrm{A}\mu_\mathrm{A}}$ is given by Eq. (2.29). Then we obtain

$$\begin{aligned} &T_{\mu_1\mu_2\mu_\mathrm{B}\mu_0\mu_\mathrm{A}} \\ &= \left\langle \chi^{(-)}_{1,\boldsymbol{K}_1}(\boldsymbol{R}_1)\eta^{(1)}_{\frac{1}{2}\mu_1}\zeta^{(1)}_{\frac{1}{2}\nu_1}\sum_c \chi^{(0c)(-)}_{2,\boldsymbol{K}_2}(\boldsymbol{R}_2)\Phi^{t_2\nu_2}_{I_2\mu_2,c}(\epsilon_{2,c},\xi_2)\right| \left[t_{1p}(\boldsymbol{s}_{1p})+t_{1n}(\boldsymbol{s}_{1n})\right] \\ &\quad \times \left|\chi^{(+)}_{0,\boldsymbol{K}_0}(\boldsymbol{R}_0)\eta^{(0)}_{\frac{1}{2}\mu_0}\zeta^{(0)}_{\frac{1}{2}\nu_0}\sum_{\ell j\mu_j} S^{1/2}_{n\ell j\nu_\mathrm{x}}(j\mu_j I_\mathrm{B}\mu_\mathrm{B}|I_\mathrm{A}\mu_\mathrm{A})\varphi_{n\ell j}(R_2)\left[Y_\ell\left(\hat{\boldsymbol{R}}_2\right)\otimes\Phi^{t_\mathrm{x}\nu_\mathrm{x}}_{I_\mathrm{x}}(\epsilon_\mathrm{x},\xi_\mathrm{x})\right]_{j\mu_j}\right\rangle. \end{aligned} \tag{2.83}$$

The transition matrix of Eq. (2.83) includes the deuteron breakup in the elementary process and the transition of the knocked-out deuteron or pn pair due to the FSIs.

To discuss these processes separately, we define

$$\begin{aligned} &T^{(\mathrm{EL})}_{\mu_1\mu_2\mu_\mathrm{B}\mu_0\mu_\mathrm{A}} \\ &= \left\langle \chi^{(-)}_{1,\boldsymbol{K}_1}(\boldsymbol{R}_1)\eta^{(1)}_{\frac{1}{2}\mu_1}\zeta^{(1)}_{\frac{1}{2}\nu_1}\chi^{(00)(-)}_{2,\boldsymbol{K}_2}(\boldsymbol{R}_2)\Phi^{t_2\nu_2}_{I_2\mu_2,0}(\epsilon_{2,0},\xi_2)\right| \left[t_{1p}(\boldsymbol{s}_{1p})+t_{1n}(\boldsymbol{s}_{1n})\right] \\ &\quad \times \left|\chi^{(+)}_{0,\boldsymbol{K}_0}(\boldsymbol{R}_0)\eta^{(0)}_{\frac{1}{2}\mu_0}\zeta^{(0)}_{\frac{1}{2}\nu_0}\sum_{\ell j\mu_j} S^{1/2}_{n\ell j\nu_\mathrm{x}}(j\mu_j I_\mathrm{B}\mu_\mathrm{B}|I_\mathrm{A}\mu_\mathrm{A})\varphi_{n\ell j}(R_2)\left[Y_\ell\left(\hat{\boldsymbol{R}}_2\right)\otimes\Phi^{t_\mathrm{x}\nu_\mathrm{x}}_{I_\mathrm{x}}(\epsilon_\mathrm{x},\xi_\mathrm{x})\right]_{j\mu_j}\right\rangle, \end{aligned} \tag{2.84}$$

in which the elementary process is assumed to be the proton-deuteron elastic scattering. It should be noted that $\chi^{(00)(-)}_{2,\boldsymbol{K}_2}$ is a solution of CDCC and the *back coupling* process, in which the knocked-out deuteron goes to breakup channels and comes back to the elastic channel due to the FSIs, is included. The p-d elastic scattering is described by the effective interaction t_{12} between proton and deuteron. Eq. (2.84) is reduced to

$$\begin{aligned} T^{(\mathrm{EL})}_{\mu_1\mu_2\mu_\mathrm{B}\mu_0\mu_\mathrm{A}} = &\left\langle \chi^{(-)}_{1,\boldsymbol{K}_1}(\boldsymbol{R}_1)\eta^{(1)}_{\frac{1}{2}\mu_1}\zeta^{(1)}_{\frac{1}{2}\nu_1}\chi^{(00)(-)}_{2,\boldsymbol{K}_2}(\boldsymbol{R}_2)\Phi^{t_2\nu_2}_{I_2\mu_2,0}(\epsilon_{2,0},\xi_2)\right| t_{12}(\boldsymbol{s}) \left|\chi^{(+)}_{0,\boldsymbol{K}_0}(\boldsymbol{R}_0)\eta^{(0)}_{\frac{1}{2}\mu_0}\zeta^{(0)}_{\frac{1}{2}\nu_0}\right. \\ &\left. \times \sum_{\ell j\mu_j} S^{1/2}_{n\ell j\nu_\mathrm{x}}(j\mu_j I_\mathrm{B}\mu_\mathrm{B}|I_\mathrm{A}\mu_\mathrm{A})\varphi_{n\ell j}(R_2)\left[Y_\ell\left(\hat{\boldsymbol{R}}_2\right)\otimes\Phi^{t_\mathrm{x}\nu_\mathrm{x}}_{I_\mathrm{x}}(\epsilon_\mathrm{x},\xi_\mathrm{x})\right]_{j\mu_j}\right\rangle. \end{aligned} \tag{2.85}$$

We once again remark that the $c = 0$ solution of the three-body Schrödinger equation (2.76) within CDCC is used as the distorted wave of particle 2 in Eq. (2.85), whereas the solution of Eq. (2.22) is used in the DWIA transition matrix (2.31). Because there is no guarantee that the two scattering wave functions of particle 2 are the same, the TDX calculated with Eq. (2.85) can be different from that of the DWIA framework.

If we further approximate the scattering wave of particle 2 with a solution of a one-body optical model calculation, that is,

$$\Xi^{(-)}_{pn\mathrm{B},\boldsymbol{K}_2}(\boldsymbol{R}_2,\xi_2) \to \chi^{(\mathrm{NB})(-)}_{2,\boldsymbol{K}_2}(\boldsymbol{R}_2)\Phi^{t_2\nu_2}_{I_2\mu_2,0}(\epsilon_{2,0},\xi_2), \tag{2.86}$$

any deuteron breakup due to the FSIs is not included. To emphasize this, we put the superscript (NB), the abbreviation of "No Breakup" on the distorted wave. It should be noted that $\chi^{(\mathrm{NB})(-)}_{2,\boldsymbol{K}_2}$ is a solution of the Schrödinger equation (2.76) with the sum of optical potentials $U_{p\mathrm{B}}$ and $U_{n\mathrm{B}}$ for nucleons, not with $U_{d\mathrm{B}}$ for deuteron, and would be different from the distorted wave of particle 2 used in the DWIA framework. The transition matrix (2.85) is then rewritten by

$$T^{(\mathrm{NB})}_{\mu_1\mu_2\mu_\mathrm{B}\mu_0\mu_\mathrm{A}} = \left\langle \chi^{(-)}_{1,\boldsymbol{K}_1}(\boldsymbol{R}_1)\eta^{(1)}_{\frac{1}{2}\mu_1}\zeta^{(1)}_{\frac{1}{2}\nu_1}\chi^{(\mathrm{NB})(-)}_{2,\boldsymbol{K}_2}(\boldsymbol{R}_2)\Phi^{t_2\nu_2}_{I_2\mu_2,0}(\epsilon_{2,0},\xi_2)\right| t_{12}(\boldsymbol{s}) \left|\chi^{(+)}_{0,\boldsymbol{K}_0}(\boldsymbol{R}_0)\eta^{(0)}_{\frac{1}{2}\mu_0}\zeta^{(0)}_{\frac{1}{2}\nu_0}\right.$$
$$\left.\times \sum_{\ell j\mu_j} S^{1/2}_{n\ell j\nu_\mathrm{x}}(j\mu_j I_\mathrm{B}\mu_\mathrm{B}|I_\mathrm{A}\mu_\mathrm{A})\varphi_{n\ell j}(R_2)\left[Y_\ell\left(\hat{\boldsymbol{R}}_2\right)\otimes\Phi^{t_\mathrm{x}\nu_\mathrm{x}}_{I_\mathrm{x}}(\epsilon_\mathrm{x},\xi_\mathrm{x})\right]_{j\mu_j}\right\rangle. \tag{2.87}$$

2.2.2 Application of AMA to CDCCIA transition matrix

To express all coordinates relevant to the transition matrix (2.83) by $\boldsymbol{R}$ and $\boldsymbol{s}$, we employ the AMA. The calculation process is the same as presented in Subsection 2.1.2, and Eq. (2.83) becomes

$$T_{\mu_1\mu_2\mu_\mathrm{B}\mu_0\mu_\mathrm{A}} = \sum_c\sum_{\mu_\mathrm{x}}\tilde{t}^c_{12}(\boldsymbol{\kappa}'_c,\mu_1\nu_1\mu_2\nu_2;\boldsymbol{\kappa}_{0,c},\mu_0\nu_0\mu_\mathrm{x}\nu_\mathrm{x})$$
$$\times\int \mathrm{d}\boldsymbol{R}\,\chi^{(-)*}_{1,\boldsymbol{K}_1}(\boldsymbol{R})\chi^{(0c)(-)*}_{2,\boldsymbol{K}_2}(\boldsymbol{R})\chi^{(+)}_{0,\boldsymbol{K}_0}(\boldsymbol{R})\mathrm{e}^{-i\alpha_R\boldsymbol{K}_0\cdot\boldsymbol{R}}$$
$$\times\sum_{\ell mj\mu_j} S^{1/2}_{n\ell j\nu_\mathrm{x}}(j\mu_j I_\mathrm{B}\mu_\mathrm{B}|I_\mathrm{A}\mu_\mathrm{A})(\ell m I_\mathrm{x}\mu_\mathrm{x}|j\mu_j)\varphi_{n\ell jm}(\boldsymbol{R}), \tag{2.88}$$

$$\tilde{t}^c_{12}(\boldsymbol{\kappa}'_c,\mu_1\nu_1\mu_2\nu_2;\boldsymbol{\kappa}_{0,c},\mu_0\nu_0\mu_\mathrm{x}\nu_\mathrm{x})$$
$$\equiv\left\langle \mathrm{e}^{i\boldsymbol{\kappa}'_c\cdot\boldsymbol{s}}\eta^{(1)}_{\frac{1}{2}\mu_1}\zeta^{(1)}_{\frac{1}{2}\nu_1}\Phi^{t_2\nu_2}_{I_2\mu_2,c}(\epsilon_{2,c},\xi_2)\right| t_{1p}(\boldsymbol{s}_{1p})+t_{1n}(\boldsymbol{s}_{1n})\left|\mathrm{e}^{i\boldsymbol{\kappa}_{0,c}\cdot\boldsymbol{s}}\eta^{(0)}_{\frac{1}{2}\mu_0}\zeta^{(0)}_{\frac{1}{2}\nu_0}\Phi^{t_\mathrm{x}\nu_\mathrm{x}}_{I_\mathrm{x}\mu_\mathrm{x}}(\epsilon_\mathrm{x},\xi_\mathrm{x})\right\rangle, \tag{2.89}$$

$$\boldsymbol{\kappa}_{0,c}\equiv\frac{m_1+m_\mathrm{A}}{m_\mathrm{A}}\boldsymbol{K}_0-\alpha_{2s}(\boldsymbol{K}_1+\boldsymbol{K}_{2,c}),\quad \boldsymbol{\kappa}'_c\equiv\alpha_{1s}\boldsymbol{K}_1-\alpha_{2s}\boldsymbol{K}_{2,c}, \tag{2.90}$$

in which $\boldsymbol{K}_{2,c}$ is determined by

$$\frac{\hbar^2}{2\mu_{2\mathrm{B}}}K^2_{2,c}+\epsilon_{2,c}=\frac{\hbar^2}{2\mu_{2\mathrm{B}}}K^2_{2,0}+\epsilon_{2,0}. \tag{2.91}$$

It should be noted that $\boldsymbol{K}_{2,c}$ is the momentum of particle 2 in the asymptotic region after scattered by B, and can be different from that inside A. Although we can evaluate it from the local energy conservation, that is, the LSCA, the asymptotic momentum by Eq. (2.91) is employed in this study. $\tilde{t}^c_{12}$ is the transition matrix of the p-d elastic scattering for $c=0$ and breakup reaction for $c\neq 0$. How to calculate it is presented in Section 2.3 and Appendix C.

2.2.3 TDX with CDCCIA

We finally obtain the TDX of the (p,pd) reaction:

$$\frac{\mathrm{d}^3\sigma}{\mathrm{d}E^\mathrm{L}_1\,\mathrm{d}\Omega^\mathrm{L}_1\,\mathrm{d}\Omega^\mathrm{L}_2}=\frac{(2\pi)^4}{\hbar v_i}\frac{E_1E_2E_\mathrm{B}}{E^\mathrm{L}_1E^\mathrm{L}_2E^\mathrm{L}_\mathrm{B}}F_\mathrm{kin}\frac{1}{2I_0+1}\frac{1}{2I_\mathrm{A}+1}\sum_j\sum_{\mu_1\mu_2\mu_0\mu_j}\frac{2I_A+1}{2j+1}$$
$$\times\left|\sum_c\sum_{\mu_\mathrm{x}}\sum_{\ell m}\tilde{t}^c_{12}(\boldsymbol{\kappa}'_c,\mu_1\nu_1\mu_2\nu_2;\boldsymbol{\kappa}_{0,c},\mu_0\nu_0\mu_\mathrm{x}\nu_\mathrm{x})S^{1/2}_{n\ell j}(\ell m I_\mathrm{x}\mu_\mathrm{x}|j\mu_j)\tilde{T}^c_{n\ell jm}\right|^2, \tag{2.92}$$

$$\tilde{T}^c_{n\ell jm}\equiv\int\mathrm{d}\boldsymbol{R}\,\chi^{(-)*}_{1,\boldsymbol{K}_1}(\boldsymbol{R})\chi^{(0c)(-)*}_{2,\boldsymbol{K}_2}(\boldsymbol{R})\chi^{(+)}_{0,\boldsymbol{K}_0}(\boldsymbol{R})\mathrm{e}^{-i\alpha_R\boldsymbol{K}_0\cdot\boldsymbol{R}}\varphi_{n\ell jm}(\boldsymbol{R}) \tag{2.93}$$

from the infinitesimal cross section (2.46). It is the important difference between CDCCIA and the DWIA that the summation over label c appears in the squared norm of Eq. (2.92). It causes interference between distorted waves in each channel, and changes the TDX from that calculated taking into accout only the elastic channel ($c = 0$).

2.3 Proton-deuteron elastic scattering and breakup reaction with nucleon-nucleon effective interactions

As shown in Eq. (2.64), the differential cross section of the p-d elastic scattering has been factorized with using the approximation (2.60). We can evaluate $\mathrm{d}\sigma_{12} / \mathrm{d}\Omega_{12}$ at arbitrary energy and scattering angle by using the experimental data of the p-d scattering with the Lagrange interpolation. On the other hand, the matrix element of the elementary process has not been factorized in Eq. (2.92) and then we need to calculate it theoretically. In this section, I briefly present the calculation framework, which has been adopted to describe the elastic scattering of the two nucleons and is known to work well [74–76].

In the following formulation, the isospin representation, in which proton and neutron are regarded as identical fermions whose third components of isospin have opposite signs ($-1/2$ for proton and $+1/2$ for neutron), is employed. Each nucleon is labeled as particle N_j ($j = 1, 2,$ and 3), and the two-nucleon system is particle x. In quantum mechanics, it is impossible to identify each event

- that particle N_1 behaves a single nucleon and particle x consists of particles N_2 and N_3,
- that particle N_2 behaves a single nucleon and particle x consists of particles N_1 and N_3,
- that particle N_3 behaves a single nucleon and particle x consists of particles N_2 and N_3,

experimentally, and these are orthogonal each other. In practice, therefore, it is allowed that we calculate the cross section considering only one case and multiply it by the number of events listed above $N_\mathrm{f} = 3$. The Coulomb interaction between protons and three-body interactions are ignored for simplicity.

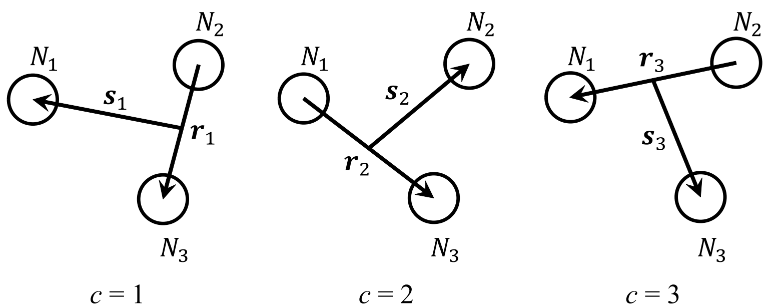

FIGURE 2.3: Coordinates for reactions between a nucleon and two-nucleon system.

For a while, the first case in the above list is treated. The coordinates to describe the reactions including both the elastic scattering and breakup reaction are shown in Fig. 2.3. The differential cross section is given by

$$\frac{\mathrm{d}\sigma_{1\mathrm{x}}}{\mathrm{d}\Omega_{1\mathrm{x}}} = \left(\frac{\mu_{1\mathrm{x}}}{2\pi\hbar^2}\right)^2 \frac{1}{2I_1+1}\frac{1}{2I_\mathrm{x}+1} \sum_{\mu_1'\mu_\mathrm{x}'\mu_1\mu_\mathrm{x}} \left| T^{I_\mathrm{x}t_\mathrm{x}}(\boldsymbol{\kappa}', \mu_1'\nu_1'\mu_\mathrm{x}'\nu_\mathrm{x}'|\boldsymbol{\kappa}, \mu_1\nu_1\mu_\mathrm{x}\nu_\mathrm{x})\right|^2, \tag{2.94}$$

in which $\mu_{1\mathrm{x}}$ is the reduced mass and I_1 (I_x) is the spin of particle N_1 (x). $T^{I_\mathrm{x}t_\mathrm{x}}(\boldsymbol{\kappa}', \mu_1'\nu_1'\mu_\mathrm{x}'\nu_\mathrm{x}'|\boldsymbol{\kappa}, \mu_1\nu_1\mu_\mathrm{x}\nu_\mathrm{x})$ is the transition matrix defined by

$$T^{I_\mathrm{x}t_\mathrm{x}}(\boldsymbol{\kappa}', \mu_1'\nu_1'\mu_\mathrm{x}'\nu_\mathrm{x}'|\boldsymbol{\kappa}, \mu_1\nu_1\mu_\mathrm{x}\nu_\mathrm{x}) \equiv \left\langle \Phi^{I_\mathrm{x}t_\mathrm{x}(\mathrm{f})}_{\boldsymbol{\kappa}',\mu_1'\nu_1'\mu_\mathrm{x}'\nu_\mathrm{x}'} \middle| V_{12} + V_{13} \middle| \Phi^{I_\mathrm{x}t_\mathrm{x}(\mathrm{i})}_{\boldsymbol{\kappa},\mu_1\nu_1\mu_\mathrm{x}\nu_\mathrm{x}} \right\rangle, \tag{2.95}$$

$$\left|\Phi^{I_\mathrm{x}t_\mathrm{x}(\mathrm{i})}_{\boldsymbol{\kappa},\mu_1\nu_1\mu_\mathrm{x}\nu_\mathrm{x}}\right\rangle \equiv \hat{\mathcal{A}}\left|\phi_\mathrm{x}(\boldsymbol{r}_1)\mathrm{e}^{i\boldsymbol{\kappa}\cdot\boldsymbol{s}_1}\eta^{(1)}_{\frac{1}{2}\mu_1}\left[\eta^{(2)}_{\frac{1}{2}}\otimes\eta^{(3)}_{\frac{1}{2}}\right]_{I_\mathrm{x}\mu_\mathrm{x}}\zeta^{(1)}_{\frac{1}{2}\nu_1}\left[\zeta^{(2)}_{\frac{1}{2}}\otimes\zeta^{(3)}_{\frac{1}{2}}\right]_{t_\mathrm{x}\nu_\mathrm{x}}\right\rangle, \tag{2.96}$$

$$\left\langle\Phi^{I_\mathrm{x}t_\mathrm{x}(\mathrm{f})}_{\boldsymbol{\kappa}',\mu_1'\nu_1'\mu_\mathrm{x}'\nu_\mathrm{x}'}\right| \equiv \left\langle\phi_\mathrm{x}'(\boldsymbol{r}_1)\mathrm{e}^{i\boldsymbol{\kappa}'\cdot\boldsymbol{s}_1}\eta^{(1)}_{\frac{1}{2}\mu_1'}\left[\eta^{(2)}_{\frac{1}{2}}\otimes\eta^{(3)}_{\frac{1}{2}}\right]_{I_\mathrm{x}\mu_\mathrm{x}'}\zeta^{(1)}_{\frac{1}{2}\nu_1'}\left[\zeta^{(2)}_{\frac{1}{2}}\otimes\zeta^{(3)}_{\frac{1}{2}}\right]_{t_\mathrm{x}\nu_\mathrm{x}'}\right|, \tag{2.97}$$

in which $\boldsymbol{\kappa}$ is the relative momentum (in the unit of $\hbar$) between particles N_1 and x in the center-of-mass (c.m.) frame of the N_1-x system. μ_j and ν_j are the third components of the spin and isospin of particle N_j, respectively. ϕ_x is the spacial component of the antisymmetrized wave function of particle x. These quantities without (with) the prime are evaluated in the initial (final) state of the reactions. In the case of $\phi_\mathrm{x}' = \phi_\mathrm{x}$, Eqs. (2.94) and (2.95) are the cross section and the transition matrix of the elastic scattering; otherwise those of the breakup reaction. $\eta^{(j)}$ and $\zeta^{(j)}$ are the spin and isospin functions of particle N_j, respectively, and the subscripts of them represent the spin or isospin and its third component. Although I_x and t_x can have the different values in the final state from those in the initial state, we consider only the case I_x and t_x do not change through the reactions in this study. V_{12} (V_{13}) is an interaction between particles N_1 and N_2 (N_3), and the impulse approximation, which replaces the interaction with the effective one in free space t_{12} (t_{13}), is adopted. It should be noted that t_{12} and t_{13} are the same in the isospin representation. We consider that t_{12} and t_{13} are constructed by

$$t_{1j} = \sum_{S_{1j}T_{1j}} t^{S_{1j}T_{1j}}_{1j}\hat{P}^{S_{1j}T_{1j}}_{1j}, \tag{2.98}$$

$$t^{S_{12}T_{12}}_{12} = t^{S_{12}T_{12}(\mathrm{C})}_{12}(r_3) + t^{S_{12}T_{12}(\mathrm{LS})}_{12}(r_3)\hat{\boldsymbol{\ell}}_{12}\cdot\boldsymbol{S}_{12} + t^{S_{12}T_{12}(\mathrm{T})}_{12}(r_3)\hat{S}^\mathrm{T}_{12}, \tag{2.99}$$

$$t^{S_{13}T_{13}}_{13} = t^{S_{13}T_{13}(\mathrm{C})}_{13}(r_2) + t^{S_{13}T_{13}(\mathrm{LS})}_{13}(r_2)\hat{\boldsymbol{\ell}}_{13}\cdot\boldsymbol{S}_{13} + t^{S_{13}T_{13}(\mathrm{T})}_{13}(r_2)\hat{S}^\mathrm{T}_{13}, \tag{2.100}$$

in which S_{1j} and T_{1j} are the total spin and isospin of the N_1-N_j system. $\hat{P}^{S_{1j}T_{1j}}_{1j}$ in Eq. (2.98) is the projection operator on the channel with S_{1j} and T_{1j}. $\hat{\boldsymbol{\ell}}_{1j}$ is the operator of the angular momentum between particles N_1 and N_j. $\hat{S}^\mathrm{T}_{1j}$ is the tensor operator defined by

$$\hat{S}^\mathrm{T}_{12} = \frac{3(\boldsymbol{\sigma}_1\cdot\boldsymbol{r}_3)(\boldsymbol{\sigma}_2\cdot\boldsymbol{r}_3)}{r_3^2} - (\boldsymbol{\sigma}_1\cdot\boldsymbol{\sigma}_2), \quad \hat{S}^\mathrm{T}_{13} = \frac{3(\boldsymbol{\sigma}_1\cdot\boldsymbol{r}_2)(\boldsymbol{\sigma}_3\cdot\boldsymbol{r}_2)}{r_2^2} - (\boldsymbol{\sigma}_1\cdot\boldsymbol{\sigma}_3), \tag{2.101}$$

in which σ_j is the Pauli matrix. The first, second, and third terms on the right-hand-sides of Eqs. (2.99) and (2.100) represent the central, spin-orbit, and tensor parts of t_{12} and t_{13}, respectively. $\hat{\mathcal{A}}$ in Eq. (2.96) is the antisymmetrization operator on the initial state given by

$$\hat{\mathcal{A}} = \frac{1}{\sqrt{3}}\left[1 - \hat{P}^{(\mathrm{ex})}_{12} - \hat{P}^{(\mathrm{ex})}_{13}\right], \tag{2.102}$$

in which $\hat{P}^{(\mathrm{ex})}_{1j}$ is the operator which exchanges particles N_1 and N_j, and the initial state becomes

$$\left|\Phi^{I_\mathrm{x}t_\mathrm{x}(\mathrm{i})}_{\boldsymbol{\kappa},\mu_1\nu_1\mu_\mathrm{x}\nu_\mathrm{x}}\right\rangle = \frac{1}{\sqrt{3}}\left[\left|\Phi^{I_\mathrm{x}t_\mathrm{x}(123)}_{\boldsymbol{\kappa},\mu_1\nu_1\mu_\mathrm{x}\nu_\mathrm{x}}\right\rangle - \left|\Phi^{I_\mathrm{x}t_\mathrm{x}(213)}_{\boldsymbol{\kappa},\mu_1\nu_1\mu_\mathrm{x}\nu_\mathrm{x}}\right\rangle - \left|\Phi^{I_\mathrm{x}t_\mathrm{x}(321)}_{\boldsymbol{\kappa},\mu_1\nu_1\mu_\mathrm{x}\nu_\mathrm{x}}\right\rangle\right], \tag{2.103}$$

$$\left|\Phi^{I_\mathrm{x}t_\mathrm{x}(123)}_{\boldsymbol{\kappa},\mu_1\nu_1\mu_\mathrm{x}\nu_\mathrm{x}}\right\rangle \equiv \left|\phi_\mathrm{x}(\boldsymbol{r}_1)\mathrm{e}^{i\boldsymbol{\kappa}\cdot\boldsymbol{s}_1}\eta^{(1)}_{\frac{1}{2}\mu_1}\left[\eta^{(2)}_{\frac{1}{2}}\otimes\eta^{(3)}_{\frac{1}{2}}\right]_{I_\mathrm{x}\mu_\mathrm{x}}\zeta^{(1)}_{\frac{1}{2}\nu_1}\left[\zeta^{(2)}_{\frac{1}{2}}\otimes\zeta^{(3)}_{\frac{1}{2}}\right]_{t_\mathrm{x}\nu_\mathrm{x}}\right\rangle, \tag{2.104}$$

$$\left|\Phi^{I_\mathrm{x}t_\mathrm{x}(213)}_{\boldsymbol{\kappa},\mu_1\nu_1\mu_\mathrm{x}\nu_\mathrm{x}}\right\rangle \equiv \hat{P}^{(\mathrm{ex})}_{12}\left|\Phi^{I_\mathrm{x}t_\mathrm{x}(123)}_{\boldsymbol{\kappa},\mu_1\nu_1\mu_\mathrm{x}\nu_\mathrm{x}}\right\rangle = \left|\phi_\mathrm{x}(\boldsymbol{r}_2)\mathrm{e}^{i\boldsymbol{\kappa}\cdot\boldsymbol{s}_2}\eta^{(2)}_{\frac{1}{2}\mu_1}\left[\eta^{(1)}_{\frac{1}{2}}\otimes\eta^{(3)}_{\frac{1}{2}}\right]_{I_\mathrm{x}\mu_\mathrm{x}}\zeta^{(2)}_{\frac{1}{2}\nu_1}\left[\zeta^{(1)}_{\frac{1}{2}}\otimes\zeta^{(3)}_{\frac{1}{2}}\right]_{t_\mathrm{x}\nu_\mathrm{x}}\right\rangle, \tag{2.105}$$

$$\left|\Phi^{I_{\mathrm{x}}t_{\mathrm{x}}(321)}_{\boldsymbol{\kappa},\mu_1\nu_1\mu_{\mathrm{x}}\nu_{\mathrm{x}}}\right\rangle \equiv \hat{P}^{(\mathrm{ex})}_{13}\left|\Phi^{I_{\mathrm{x}}t_{\mathrm{x}}(123)}_{\boldsymbol{\kappa},\mu_1\nu_1\mu_{\mathrm{x}}\nu_{\mathrm{x}}}\right\rangle = \left|\phi_{\mathrm{x}}(\boldsymbol{r}_3)\mathrm{e}^{i\boldsymbol{\kappa}\cdot\boldsymbol{s}_3}\eta^{(3)}_{\frac{1}{2}\mu_1}\left[\eta^{(2)}_{\frac{1}{2}}\otimes\eta^{(1)}_{\frac{1}{2}}\right]_{I_{\mathrm{x}}\mu_{\mathrm{x}}}\zeta^{(3)}_{\frac{1}{2}\nu_1}\left[\zeta^{(2)}_{\frac{1}{2}}\otimes\zeta^{(1)}_{\frac{1}{2}}\right]_{t_{\mathrm{x}}\nu_{\mathrm{x}}}\right\rangle. \tag{2.106}$$

Therefore, the the matrix elements we calculate in the following sections are here:

$$\begin{aligned} &T^{I_{\mathrm{x}}t_{\mathrm{x}}}(\boldsymbol{\kappa}',\mu_1'\nu_1'\mu_{\mathrm{x}}'\nu_{\mathrm{x}}'|\boldsymbol{\kappa},\mu_1\nu_1\mu_{\mathrm{x}}\nu_{\mathrm{x}}) \\ &= \frac{1}{\sqrt{3}}\Big[\bar{T}^{I_{\mathrm{x}}t_{\mathrm{x}}}_{12}(\boldsymbol{\kappa}',\mu_1'\nu_1'\mu_{\mathrm{x}}'\nu_{\mathrm{x}}'|\boldsymbol{\kappa},\mu_1\nu_1\mu_{\mathrm{x}}\nu_{\mathrm{x}}) + \bar{T}^{I_{\mathrm{x}}t_{\mathrm{x}}}_{13}(\boldsymbol{\kappa}',\mu_1'\nu_1'\mu_{\mathrm{x}}'\nu_{\mathrm{x}}'|\boldsymbol{\kappa},\mu_1\nu_1\mu_{\mathrm{x}}\nu_{\mathrm{x}})\Big], \end{aligned} \tag{2.107}$$

$$\begin{aligned} &\bar{T}^{I_{\mathrm{x}}t_{\mathrm{x}}}_{1j}(\boldsymbol{\kappa}',\mu_1'\nu_1'\mu_{\mathrm{x}}'\nu_{\mathrm{x}}'|\boldsymbol{\kappa},\mu_1\nu_1\mu_{\mathrm{x}}\nu_{\mathrm{x}}) \\ &\equiv \bar{T}^{I_{\mathrm{x}}t_{\mathrm{x}}}_{1j:123}(\boldsymbol{\kappa}',\mu_1'\nu_1'\mu_{\mathrm{x}}'\nu_{\mathrm{x}}'|\boldsymbol{\kappa},\mu_1\nu_1\mu_{\mathrm{x}}\nu_{\mathrm{x}}) \\ &\quad - \bar{T}^{I_{\mathrm{x}}t_{\mathrm{x}}}_{1j:213}(\boldsymbol{\kappa}',\mu_1'\nu_1'\mu_{\mathrm{x}}'\nu_{\mathrm{x}}'|\boldsymbol{\kappa},\mu_1\nu_1\mu_{\mathrm{x}}\nu_{\mathrm{x}}) \\ &\qquad - \bar{T}^{I_{\mathrm{x}}t_{\mathrm{x}}}_{1j:321}(\boldsymbol{\kappa}',\mu_1'\nu_1'\mu_{\mathrm{x}}'\nu_{\mathrm{x}}'|\boldsymbol{\kappa},\mu_1\nu_1\mu_{\mathrm{x}}\nu_{\mathrm{x}}), \end{aligned} \tag{2.108}$$

$$\begin{aligned} &\bar{T}^{I_{\mathrm{x}}t_{\mathrm{x}}}_{1j:123}(\boldsymbol{\kappa}',\mu_1'\nu_1'\mu_{\mathrm{x}}'\nu_{\mathrm{x}}'|\boldsymbol{\kappa},\mu_1\nu_1\mu_{\mathrm{x}}\nu_{\mathrm{x}}) \\ &\equiv \left\langle\Phi^{I_{\mathrm{x}}t_{\mathrm{x}}(\mathrm{f})}_{\boldsymbol{\kappa}',\mu_1'\nu_1'\mu_{\mathrm{x}}'\nu_{\mathrm{x}}'}\right|t_{1j}\left|\Phi^{I_{\mathrm{x}}t_{\mathrm{x}}(123)}_{\boldsymbol{\kappa},\mu_1\nu_1\mu_{\mathrm{x}}\nu_{\mathrm{x}}}\right\rangle \\ &= \left\langle\phi_{\mathrm{x}}'(\boldsymbol{r}_1)\mathrm{e}^{i\boldsymbol{\kappa}'\cdot\boldsymbol{s}_1}\eta^{(1)}_{\frac{1}{2}\mu_1'}\left[\eta^{(2)}_{\frac{1}{2}}\otimes\eta^{(3)}_{\frac{1}{2}}\right]_{I_{\mathrm{x}}\mu_{\mathrm{x}}'}\zeta^{(1)}_{\frac{1}{2}\nu_1'}\left[\zeta^{(2)}_{\frac{1}{2}}\otimes\zeta^{(3)}_{\frac{1}{2}}\right]_{t_{\mathrm{x}}\nu_{\mathrm{x}}'}\right| \\ &\qquad \times t_{1j}\left|\phi_{\mathrm{x}}(\boldsymbol{r}_1)\mathrm{e}^{i\boldsymbol{\kappa}\cdot\boldsymbol{s}_1}\eta^{(1)}_{\frac{1}{2}\mu_1}\left[\eta^{(2)}_{\frac{1}{2}}\otimes\eta^{(3)}_{\frac{1}{2}}\right]_{I_{\mathrm{x}}\mu_{\mathrm{x}}}\zeta^{(1)}_{\frac{1}{2}\nu_1}\left[\zeta^{(2)}_{\frac{1}{2}}\otimes\zeta^{(3)}_{\frac{1}{2}}\right]_{t_{\mathrm{x}}\nu_{\mathrm{x}}}\right\rangle, \end{aligned} \tag{2.109}$$

$$\begin{aligned} &\bar{T}^{I_{\mathrm{x}}t_{\mathrm{x}}}_{1j:213}(\boldsymbol{\kappa}',\mu_1'\nu_1'\mu_{\mathrm{x}}'\nu_{\mathrm{x}}'|\boldsymbol{\kappa},\mu_1\nu_1\mu_{\mathrm{x}}\nu_{\mathrm{x}}) \\ &\equiv \left\langle\Phi^{I_{\mathrm{x}}t_{\mathrm{x}}(\mathrm{f})}_{\boldsymbol{\kappa}',\mu_1'\nu_1'\mu_{\mathrm{x}}'\nu_{\mathrm{x}}'}\right|t_{1j}\left|\Phi^{I_{\mathrm{x}}t_{\mathrm{x}}(213)}_{\boldsymbol{\kappa},\mu_1\nu_1\mu_{\mathrm{x}}\nu_{\mathrm{x}}}\right\rangle \\ &= \left\langle\phi_{\mathrm{x}}'(\boldsymbol{r}_1)\mathrm{e}^{i\boldsymbol{\kappa}'\cdot\boldsymbol{s}_1}\eta^{(1)}_{\frac{1}{2}\mu_1'}\left[\eta^{(2)}_{\frac{1}{2}}\otimes\eta^{(3)}_{\frac{1}{2}}\right]_{I_{\mathrm{x}}\mu_{\mathrm{x}}'}\zeta^{(1)}_{\frac{1}{2}\nu_1'}\left[\zeta^{(2)}_{\frac{1}{2}}\otimes\zeta^{(3)}_{\frac{1}{2}}\right]_{t_{\mathrm{x}}\nu_{\mathrm{x}}'}\right| \\ &\qquad \times t_{1j}\left|\phi_{\mathrm{x}}(\boldsymbol{r}_2)\mathrm{e}^{i\boldsymbol{\kappa}\cdot\boldsymbol{s}_2}\eta^{(2)}_{\frac{1}{2}\mu_1}\left[\eta^{(1)}_{\frac{1}{2}}\otimes\eta^{(3)}_{\frac{1}{2}}\right]_{I_{\mathrm{x}}\mu_{\mathrm{x}}}\zeta^{(2)}_{\frac{1}{2}\nu_1}\left[\zeta^{(1)}_{\frac{1}{2}}\otimes\zeta^{(3)}_{\frac{1}{2}}\right]_{t_{\mathrm{x}}\nu_{\mathrm{x}}}\right\rangle, \end{aligned} \tag{2.110}$$

$$\begin{aligned} &\bar{T}^{I_{\mathrm{x}}t_{\mathrm{x}}}_{1j:321}(\boldsymbol{\kappa}',\mu_1'\nu_1'\mu_{\mathrm{x}}'\nu_{\mathrm{x}}'|\boldsymbol{\kappa},\mu_1\nu_1\mu_{\mathrm{x}}\nu_{\mathrm{x}}) \\ &\equiv \left\langle\Phi^{I_{\mathrm{x}}t_{\mathrm{x}}(\mathrm{f})}_{\boldsymbol{\kappa}',\mu_1'\nu_1'\mu_{\mathrm{x}}'\nu_{\mathrm{x}}'}\right|t_{1j}\left|\Phi^{I_{\mathrm{x}}t_{\mathrm{x}}(321)}_{\boldsymbol{\kappa},\mu_1\nu_1\mu_{\mathrm{x}}\nu_{\mathrm{x}}}\right\rangle \\ &= \left\langle\phi_{\mathrm{x}}'(\boldsymbol{r}_1)\mathrm{e}^{i\boldsymbol{\kappa}'\cdot\boldsymbol{s}_1}\eta^{(1)}_{\frac{1}{2}\mu_1'}\left[\eta^{(2)}_{\frac{1}{2}}\otimes\eta^{(3)}_{\frac{1}{2}}\right]_{I_{\mathrm{x}}\mu_{\mathrm{x}}'}\zeta^{(1)}_{\frac{1}{2}\nu_1'}\left[\zeta^{(2)}_{\frac{1}{2}}\otimes\zeta^{(3)}_{\frac{1}{2}}\right]_{t_{\mathrm{x}}\nu_{\mathrm{x}}'}\right| \\ &\qquad \times t_{1j}\left|\phi_{\mathrm{x}}(\boldsymbol{r}_3)\mathrm{e}^{i\boldsymbol{\kappa}\cdot\boldsymbol{s}_3}\eta^{(3)}_{\frac{1}{2}\mu_1}\left[\eta^{(2)}_{\frac{1}{2}}\otimes\eta^{(1)}_{\frac{1}{2}}\right]_{I_{\mathrm{x}}\mu_{\mathrm{x}}}\zeta^{(3)}_{\frac{1}{2}\nu_1}\left[\zeta^{(2)}_{\frac{1}{2}}\otimes\zeta^{(1)}_{\frac{1}{2}}\right]_{t_{\mathrm{x}}\nu_{\mathrm{x}}}\right\rangle. \end{aligned} \tag{2.111}$$

Equation (2.109) is called the direct term of Eq. (2.108), and Eqs. (2.110) and (2.111) are the exchange terms. By substituting 2 or 3 for j in these matrices, we can find the correspodence:

$$\bar{T}^{I_{\mathrm{x}}t_{\mathrm{x}}}_{12:123}(\boldsymbol{\kappa}',\mu_1'\nu_1'\mu_{\mathrm{x}}'\nu_{\mathrm{x}}'|\boldsymbol{\kappa},\mu_1\nu_1\mu_{\mathrm{x}}\nu_{\mathrm{x}}) \leftrightarrow \bar{T}^{I_{\mathrm{x}}t_{\mathrm{x}}}_{13:123}(\boldsymbol{\kappa}',\mu_1'\nu_1'\mu_{\mathrm{x}}'\nu_{\mathrm{x}}'|\boldsymbol{\kappa},\mu_1\nu_1\mu_{\mathrm{x}}\nu_{\mathrm{x}}), \tag{2.112}$$

$$\bar{T}^{I_{\mathrm{x}}t_{\mathrm{x}}}_{12:213}(\boldsymbol{\kappa}',\mu_1'\nu_1'\mu_{\mathrm{x}}'\nu_{\mathrm{x}}'|\boldsymbol{\kappa},\mu_1\nu_1\mu_{\mathrm{x}}\nu_{\mathrm{x}}) \leftrightarrow \bar{T}^{I_{\mathrm{x}}t_{\mathrm{x}}}_{13:321}(\boldsymbol{\kappa}',\mu_1'\nu_1'\mu_{\mathrm{x}}'\nu_{\mathrm{x}}'|\boldsymbol{\kappa},\mu_1\nu_1\mu_{\mathrm{x}}\nu_{\mathrm{x}}), \tag{2.113}$$

$$\bar{T}^{I_\mathrm{x}t_\mathrm{x}}_{12:321}\left(\boldsymbol{\kappa}', \mu_1'\nu_1'\mu_\mathrm{x}'\nu_\mathrm{x}'|\boldsymbol{\kappa}, \mu_1\nu_1\mu_\mathrm{x}\nu_\mathrm{x}\right) \leftrightarrow \bar{T}^{I_\mathrm{x}t_\mathrm{x}}_{13:213}\left(\boldsymbol{\kappa}', \mu_1'\nu_1'\mu_\mathrm{x}'\nu_\mathrm{x}'|\boldsymbol{\kappa}, \mu_1\nu_1\mu_\mathrm{x}\nu_\mathrm{x}\right). \tag{2.114}$$

The concrete calculation of these matrices, that is, the spin-isospin-rearrangement and the components of the central, spin-orbit, and tensor interactions are given in Appendix C. Comparing Eqs. (2.95)-(2.97) with Eq. (2.89), we can find

$$\tilde{t}^c_{12}(\boldsymbol{\kappa}_c', \mu_1\nu_1\mu_2\nu_2; \boldsymbol{\kappa}_{0,c}, \mu_0\nu_0\mu_\mathrm{x}\nu_\mathrm{x}) \leftrightarrow T^{I_\mathrm{x}t_\mathrm{x}}\left(\boldsymbol{\kappa}', \mu_1'\nu_1'\mu_\mathrm{x}'\nu_\mathrm{x}'|\boldsymbol{\kappa}, \mu_1\nu_1\mu_\mathrm{x}\nu_\mathrm{x}\right), \tag{2.115}$$

$$\Phi^{t_\mathrm{x}\nu_\mathrm{x}}_{I_\mathrm{x}\mu_\mathrm{x}}(\epsilon_\mathrm{x}, \xi_\mathrm{x}) \leftrightarrow \phi_\mathrm{x}(\boldsymbol{r}_1)\left[\eta^{(2)}_{\frac{1}{2}} \otimes \eta^{(3)}_{\frac{1}{2}}\right]_{I_\mathrm{x}\mu_\mathrm{x}}\left[\zeta^{(2)}_{\frac{1}{2}} \otimes \zeta^{(3)}_{\frac{1}{2}}\right]_{t_\mathrm{x}\nu_\mathrm{x}}, \tag{2.116}$$

$$\Phi^{t_2\nu_2}_{I_2\mu_2,c}(\epsilon_{2,c}, \xi_2) \leftrightarrow \phi_\mathrm{x}'(\boldsymbol{r}_1)\left[\eta^{(2)}_{\frac{1}{2}} \otimes \eta^{(3)}_{\frac{1}{2}}\right]_{I_\mathrm{x}\mu_\mathrm{x}'}\left[\zeta^{(2)}_{\frac{1}{2}} \otimes \zeta^{(3)}_{\frac{1}{2}}\right]_{t_\mathrm{x}\nu_\mathrm{x}'}, \tag{2.117}$$

$$t_{1p}(\boldsymbol{s}_{1p}) + t_{1n}(\boldsymbol{s}_{1n}) \leftrightarrow t_{12} + t_{13}. \tag{2.118}$$

and so on.

The same calculation shown above can be applied to the second and third cases listed at the beginning of this section. So the differential cross section taking into account them is

$$\frac{\mathrm{d}\sigma}{\mathrm{d}\Omega} = C_\mathrm{corr} \cdot N_\mathrm{f}\frac{\mathrm{d}\sigma_{1\mathrm{x}}}{\mathrm{d}\Omega_{1\mathrm{x}}} = C_\mathrm{corr} \cdot 3\frac{\mathrm{d}\sigma_{1\mathrm{x}}}{\mathrm{d}\Omega_{1\mathrm{x}}}, \tag{2.119}$$

in which the correction factor C_corr is introduced. It should be noted that because nucleon-nucleon interactions are parametrized to reproduce the nucleon-nucleon scattering data, there is no guarantee for the interactions to reproduce the experimental data of the reactions between a nucleon and a two-nucleon system. The correction factor is expected to take care of a modification of the nucleon-nucleon interaction. In the case of proton-deuteron reactions, we can determine C_corr to reproduce the forward-angle data of p-d elastic scatterings and use it also in the calculation of the breakup reaction. When we need a transformation matrix, the square root of C_corr is included in Eq. (2.95).

Chapter 3

Proton-induced deuteron knockout reaction with an isoscalar *pn* pair inside nuclei

3.1 Introduction

As mentioned in Section 1.2, the nuclear force has a particularly strong attractive behavior in the $^3S_1$ channel component. In addition, the pairing correlations between identical nucleons (N) play an important role in understanding nuclei, and there is isospin symmetry between protons (p) and neutrons (n). It is, therefore, natural to think that isoscalar and spin-triplet proton-neutron (pn) pair correlations can appear in nuclei. Especially in $N = Z$ nuclei, in which N (Z) is the nucleon (proton) number, the possibility of the existence of the isoscalar pn pair has been theoretically suggested with the nuclear Energy-Density Functional (EDF) [30, 31] and Cluster Orbital Shell Model (COSM) [32] approaches because the shell structures of protons and neutrons near the Fermi surface are similar to each other in such nuclei. However, the analysis of past experimental data has not provided clear evidence for the existence of this deuteron-like pn pair [29], and a different experimental approach is needed. Here, we consider proton-induced deuteron knockout reactions (p, pd) as a possible probe of the pn pair inside nuclei.

As mentioned in Section 1.3, knockout reactions are regarded as good probes of nucleons and clusters in nuclei, and there are a few experimental results of deuteron knockout reactions. In an experiment conducted 40 years ago, it was reported that the cross section of the ^{16}O$(p, pd)^{14}$N reaction at 101.3 MeV [62] was almost half of that of the ^{16}O$(p, 2p)^{15}$N reaction at the same incident energy [46]. However, it has not been clarified what the origin of the deuteron observed in the experiment is. Therefore, it is important to investigate whether the deuteron-like pn pair can be the origin of the deuteron observed in the deuteron knockout experiment, in order to motivate the use of this reaction as a probe for proton-neutron pairs.

In this chapter, we describe the study of the (p, pd) reaction employing the Distorted Wave Impulse Approximation (DWIA) explained in Section 2.1. As a remarkable feature of this study, the nuclear EDF method is employed to describe the isoscalar ($t_\mathrm{x} = 0$) and spin-triplet ($I_\mathrm{x} = 1$) pn pair in the target nucleus. Both the shape and height of the radial wave function of the pair are microscopically evaluated. All nuclear EDF calculations shown below are done by Dr. Kenichi Yoshida (Kyoto University). It should be noted, however, that only the DWIA evaluation is not sufficient for an accurate understanding of this pair, and the CDCCIA framework introduced in Section 2.2 is essential. For reference, the studies in this chapter can be found in Ref. [77].

3.2 Theoretical preparation

3.2.1 Microscopic description of an isoscalar *pn* pair in nuclei

In this subsection, I give a brief explanation of the nuclear EDF method, which describes the wave function of an isoscalar proton-neutron pair microscopically. In the nuclear EDF framework, the pn-pair-removal excited states in the core nucleus B are described in the proton-neutron hole-hole random-phase approximation (pn-hhRPA) [30] regarding the ground state of the target A as an RPA vacuum, that is,

$$\left|\Phi^{t_\mathrm{B}\nu_\mathrm{B}}_{I_\mathrm{B}\mu_\mathrm{B}}(\epsilon_\mathrm{B}, \xi_\mathrm{B})\right\rangle = \hat{\Gamma}^\dagger \left|\Phi^{t_\mathrm{A}\nu_\mathrm{A}}_{I_\mathrm{A}\mu_\mathrm{A}}(\epsilon_\mathrm{A}, \xi_\mathrm{A})\right\rangle, \tag{3.1}$$

in which $\hat{\Gamma}^\dagger$ is the RPA phonon operator defined by

$$\hat{\Gamma}^\dagger \equiv \sum_{ii'} X_{ii'} \hat{b}^\dagger_{p,i} \hat{b}^\dagger_{n,i'} - \sum_{mm'} Y_{m'm} \hat{b}^\dagger_{n,m'} \hat{b}^\dagger_{p,m}. \tag{3.2}$$

Here, $\hat{b}^\dagger_{p,i}$ ($\hat{b}^\dagger_{n,i'}$) is the creation operator of proton (neutron) hole in the single-particle state i (i') below the Fermi level. That for the proton (neutron) single-particle state m (m') above the Fermi level is represented by $\hat{b}^\dagger_{p,m}$ ($\hat{b}^\dagger_{n,m'}$). It should be noted that the backward-going amplitudes $Y_{m'm}$ vanish if we neglect the ground-state correlation in A.

The spin-triplet pn-pair-removal transition density is given by

$$\begin{aligned}\delta\bar{\rho}_\mu(\boldsymbol{r}_n, \boldsymbol{r}_p) = \frac{1}{2}\sum_{\sigma\sigma'} (-2\sigma') \left\langle \sigma' \middle| \sigma_\mu \middle| \sigma \right\rangle \Big\langle \Phi^{t_\mathrm{B}\nu_\mathrm{B}}_{I_\mathrm{B}\mu_\mathrm{B}}(\epsilon_\mathrm{B}, \xi_\mathrm{B}) \Big| \hat{\psi}_n(\boldsymbol{r}_n, -\sigma')\hat{\psi}_p(\boldsymbol{r}_p, \sigma) \\ - \hat{\psi}_p(\boldsymbol{r}_p, -\sigma')\hat{\psi}_n(\boldsymbol{r}_n, \sigma) \Big| \Phi^{t_\mathrm{A}\nu_\mathrm{A}}_{I_\mathrm{A}\mu_\mathrm{A}}(\epsilon_\mathrm{A}, \xi_\mathrm{A}) \Big\rangle,\end{aligned} \tag{3.3}$$

in which $\sigma_\mu = (\sigma_{-1}, \sigma_0, \sigma_{+1})$ are the spherical components of the Pauli matrices. $\hat{\psi}_q(\boldsymbol{r}_q, \sigma)$ is the nucleon annihilation operator at the position $\boldsymbol{r}_q$ with the spin direction $\sigma = \pm 1/2$ expanded in the single-particle basis with q being p (proton) or n (neutron). It should be noted that $\delta\bar{\rho}_\mu$ is spherical in spin space and hence we need to consider only one component of μ; we take $\mu = 0$.

Combining Eqs. (2.26), (2.28), (2.29), and (3.3), we can regard the transition density $\delta\bar{\rho}_0$ as

$$\delta\bar{\rho}_0(\boldsymbol{R}_2, \boldsymbol{r}) \approx \sum_{\ell j \mu_j} (j\mu_j I_\mathrm{B}\mu_\mathrm{B}|I_\mathrm{A}\mu_\mathrm{A}) \left[\varphi^{pn}_{\ell jm}(\boldsymbol{R}_2) \otimes \Phi^{00}_{10}(\epsilon_\mathrm{x}, \bar{\xi}_\mathrm{x}, \boldsymbol{r})\right]_{j\mu_j}, \tag{3.4}$$

in which we show the spatial coordinate $\boldsymbol{r}$ explicitly and the other internal coordinates of particle x by $\bar{\xi}_\mathrm{x}$ in the argument of Φ^{00}_{10}. The spectroscopic amplitude is set to unity. The left-hand-side of the equation is the transition density represented by $\boldsymbol{R}_2 = (\boldsymbol{r}_n + \boldsymbol{r}_p)/2$ and $\boldsymbol{r} = \boldsymbol{r}_p - \boldsymbol{r}_n$. This approximate treatment means that the transition density is factorized into the two wave functions for the relative motion of the pn pair with respect to the core B and internal motion of the pair, which are represented by $\varphi^{pn}_{\ell jm}$ and Φ^{00}_{10}, respectively. Assuming that the pn pair is bound in the S-wave state inside A, we can simplify Eq. (3.4) as

$$\begin{aligned}\delta\bar{\rho}_0(\boldsymbol{R}_2, \boldsymbol{r}) &\approx \sum_{j\mu_j} (j\mu_j I_\mathrm{B}\mu_\mathrm{B}|I_\mathrm{A}\mu_\mathrm{A}) \left[\varphi^{pn}_{0j0}(\boldsymbol{R}_2) \otimes \Phi^{00}_{10}(\epsilon_\mathrm{x}, \bar{\xi}_\mathrm{x}, \boldsymbol{r})\right]_{j\mu_j} \\ &= \frac{1}{\sqrt{4\pi}} (10 I_\mathrm{B}\mu_\mathrm{B}|I_\mathrm{A}\mu_\mathrm{A}) \varphi^{pn}_{01}(R_2) \Phi^{00}_{10}(\epsilon_\mathrm{x}, \bar{\xi}_\mathrm{x}, \boldsymbol{r}),\end{aligned} \tag{3.5}$$

in which φ^{pn}_{01} is the radial wave function between the c.m. of the pn pair and B evaluated by

$$\varphi^{pn}_{01}(R_2) \equiv \frac{\delta\bar{\rho}_0(R_2, 0)}{\Phi^{00}_{10}(\epsilon_\mathrm{x}, \bar{\xi}_\mathrm{x}, 0)}, \tag{3.6}$$

that is, we consider the pn pair is S wave and a point particle with $\boldsymbol{r} = 0$. The use of Eqs. (3.4)-(3.6) means that the component of the wave function of A containing a deuteron is selected out. This treatment is consistent with the DWIA framework. It should be noted that φ^{pn}_{01} becomes the function of R after the application of the AMA introduced in Subsection 2.1.2. Using this transition density, the pn-pair-removal transition strength is given by

$$I_\mathrm{rem} \equiv 3\left|4\pi \int_0^\infty \mathrm{d}R\, R^2 \varphi^{pn}_{01}(R) \Phi^{00}_{10}(\epsilon_\mathrm{x}, \bar{\xi}_\mathrm{x}, 0)\right|^2, \tag{3.7}$$

in which the factor three comes from the sum of the components of $\mu = -1$, 0, and $+1$.

3.2.2 In the PWIA limit

Taking into account the discussion in the previous subsection, we can rewrite Eq. (2.65) as

$$\frac{\mathrm{d}^3\sigma^{\mathrm{PW}}}{\mathrm{d}E_1^{\mathrm{L}}\,\mathrm{d}\Omega_1^{\mathrm{L}}\,\mathrm{d}\Omega_2^{\mathrm{L}}} = \frac{(2\pi)^4}{\hbar v_i}\frac{E_1 E_2 E_{\mathrm{B}}}{E_1^{\mathrm{L}} E_2^{\mathrm{L}} E_{\mathrm{B}}^{\mathrm{L}}} F_{\mathrm{kin}} \left(\frac{2\pi\hbar^2}{\mu_{12}}\right)^2 \frac{\mathrm{d}\sigma_{12}}{\mathrm{d}\Omega_{12}}(T_{12},\theta_{12}) |\tilde{\varphi}_{010}^{pn}(\boldsymbol{K}_{\mathrm{ms}})|^2 \tag{3.8}$$

with

$$\tilde{\varphi}_{010}^{pn}(\boldsymbol{K}_{\mathrm{ms}}) = \int \mathrm{d}\boldsymbol{R}\,\mathrm{e}^{i\boldsymbol{K}_{\mathrm{ms}}\cdot\boldsymbol{R}} \varphi_{01}^{pn}(R) Y_{00}\left(\hat{\boldsymbol{R}}\right) = \frac{1}{\sqrt{4\pi}} \int \mathrm{d}\boldsymbol{R}\,\mathrm{e}^{i\boldsymbol{K}_{\mathrm{ms}}\cdot\boldsymbol{R}} \varphi_{01}^{pn}(R). \tag{3.9}$$

The spectroscopic factor is set to unity. In the recoilless condition, which is characterized by $\boldsymbol{K}_{\mathrm{ms}} = 0$, Eq. (3.9) becomes

$$\tilde{\varphi}_{010}^{pn}(0) = \sqrt{4\pi} \int_0^\infty \mathrm{d}R\, R^2 \varphi_{01}^{pn}(R), \tag{3.10}$$

and this means that the TDX in the recoilless condition contains the direct information about the total amplitude of the pn pair.

3.3 Result and discussion

3.3.1 Numerical inputs

We consider the ${}^{16}\mathrm{O}(p,pd){}^{14}\mathrm{N}^*$ at 101.3 MeV in normal kinematics; ^{14}N is in the 1_2^+ excited state. For the distorting potentials of the incident and outgoing protons, the EDAD1 parameter set of the Dirac phenomenology [78–80] is used, and we employed the global optical potential by An and Cai [81] for the emitted deuteron. The Coulomb potential in each distorting potential is constructed by assuming to be a uniformly charged sphere whose radius is $r_0 C^{1/3}$ ($C = A$ or B) with r_0 being 1.41 fm. The nonlocality correction to the distorted wave of deuteron is considered by multiplying it by the Perey factor [82] with the range of nonlocality of 0.54 fm, and that for proton is made by including the Darwin factor [78, 83]. We take the experimental data of the proton-deuteron elastic scattering from Refs. [84–93] and apply the Lagrange interpolation to them concerning the scattering energy and angle for the cross section in Eq. (2.64). The emission angle of particle 1 is fixed at $(\theta_1^{\mathrm{L}}, \phi_1^{\mathrm{L}}) = (40.1^\circ, 0^\circ)$ and that for particle 2 at $(\theta_2^{\mathrm{L}}, \phi_2^{\mathrm{L}}) = (40.0^\circ, 180^\circ)$, in which θ_i^{L} and ϕ_i^{L} are the polar and azimuthal angles of particle i evaluated in the L frame, respectively.

To obtain the single-particle basis used in the pn-hhRPA calculation, the Skyrme-Hartree-Fock equation is solved in the cylindrical coordinate $\boldsymbol{r} = (r, z, \phi)$ with a box boundary condition at $(r_{\mathrm{max}}, z_{\mathrm{max}}) = (14.7, 14.4)$ fm. A mesh size employed in the calculation is $\Delta r = \Delta z = 0.6$ fm. The axial and reflection symmetries are assumed in the ground state of ^{14}N, and the ground state of ^{16}O is calculated to be spherical. The detailed scheme of the calculation is given in Ref. [94, 95]. The SGII interaction [96] is employed for the particle-hole channel, whereas the density-dependent contact interaction defined by

$$v_{\mathrm{pp}}\left(\boldsymbol{r},\sigma,\tau;\boldsymbol{r}',\sigma',\tau'\right) \equiv V_0 \frac{1+P_\sigma}{2}\frac{1-P_\tau}{2}\left[1-\frac{\rho(\boldsymbol{r})}{\rho_0}\right]\delta\left(\boldsymbol{r}'-\boldsymbol{r}\right) \tag{3.11}$$

is adopted for the particle-particle channel. τ is the isospin of the nucleon, and P_σ (P_τ) is the exchange operator for the spin (isospin) of the two particles. ρ_0 is 0.16 fm^{-3} and $\rho(\boldsymbol{r}) = \rho_n(\boldsymbol{r}) + \rho_p(\boldsymbol{r})$. V_0 is a parameter which determines the pairing strength; we take $V_0 = -100$, -490, and -600 MeV fm^3 here.

3.3.2 Structure of the low-lying 1^+ state in ^{14}N

Before discussing the TDX of the knockout reaction, a brief discussion on the structure of low-lying states in ^{14}N calculated within the present framework is given in this subsection. Figure 3.1 shows the spin-triplet pn-pair-removal

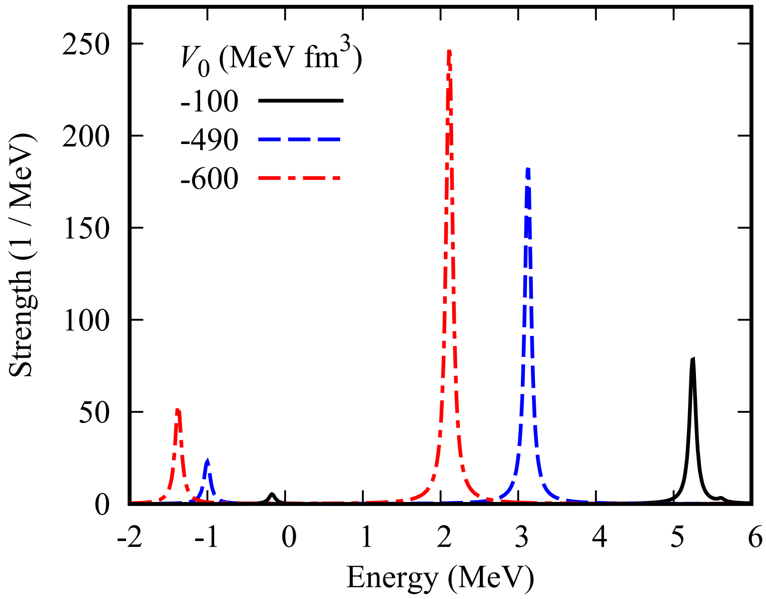

FIGURE 3.1: Spin-triplet pn-pair-removal transition strengths as functions of the excitation energy, which is defined with that for the unperturbed $(p_{1/2})^{-2}$ configuration being zero. The solid, dashed, and dot-dashed lines are the calculation results of $V_0 = -100$, -490 and -600 MeV fm^3, respectively.

transition-strength distributions. The horizontal axis means the excitation energy, which is defined so that the excitation energy of the simplest configuration of $(p_{1/2})^{-2}$ coupled to $I_{\rm x} = 1$ and $t_{\rm x} = 0$ inside ^{16}O is zero. The lowest state for each pairing strength V_0 is the 1_1^+ ground state of ^{14}N, which is constructed by mainly the $(\nu p_{1/2})^{-1}(\pi p_{1/2})^{-1}$ configuration. On the other hand, the second-lowest one for each V_0 is the 1_2^+state of our interest, which is described by the superposition of the $(\nu p_{1/2})^{-1}(\pi p_{3/2})^{-1}$ and $(\nu p_{3/2})^{-1}(\pi p_{1/2})^{-1}$ configurations. The labels ν and π indicate neutron and proton, respectively. With the increase of the pairing strength, the excitation energies become lower, and the transition strengths are enhanced for both states. For $V_0 = -600$ MeV fm^3, the $(p_{3/2})^{-2}$ configuration has a non-negligible contribution to the enhancement of the transition strength to the 1_2^+ state. It means that the collectivity of the state becomes stronger as the pairing strength increases.

Let us look at the enegy difference between the 1_1^+ and 1_2^+ states defined by

$$\Delta E \equiv E_{1_2^+} - E_{1_1^+}. \tag{3.12}$$

In the theoretical calculation, the obtained ΔE are 5.41 MeV for $V_0 = -100$ MeV fm^3, 4.12 MeV for $V_0 = -490$ MeV fm^3, and 3.48 MeV for $V_0 = -600$ MeV fm^3. According to the experimental value of $\Delta E = 3.95$ MeV, reported in Ref. [62], one can see that $V_0 = -490$ describes the low-lying states of 14N rather well.

Next, we discuss the behavior of φ_{01}^{pn}. In Fig. 3.2, the wave functions calculated with $V_0 = -100$, -490, and -600 MeV fm^3 are represented by the solid, dashed, and dot-dashed lines, respectively. It should be noted that each line is multiplied by R^2. We can clealy find that the amplitude of $R^2\varphi_{01}^{pn}$ becomes larger as the pairing strength increases. The enhancement of the amplitude reflects the collectivity of the pn pair, and it is consistent with the result in Fig. 3.1. It is worth mentioning that the independent-particle picture is realized in ^{16}O in the limit of $V_0 \to 0$; then the peak of $R^2\varphi_{01}^{pn}$ will almost vanish.

3.3.3 TDX of ^{16}O(*p,pd*)^{14}N* reaction at 101.3 MeV

In this subsection, we discuss the behavior of the TDX of the ^{16}O$(p,pd)^{14}$N* reaction at 101.3 MeV. Figure 3.3 shows the TDX of the knockout reaction as a function of $T_1^{\rm L}$, the kinetic energy of particle 1 in the L frame. The results using φ_{01}^{pn} of $V_0 = -100$, -490, and -600 MeV fm^3 are represented by the solid, dashed, and dot-dashed lines, respectively. The recoilless consition is almost realized at $T_1^{\rm L} \approx 52$ MeV. The scattering energy and angel of the

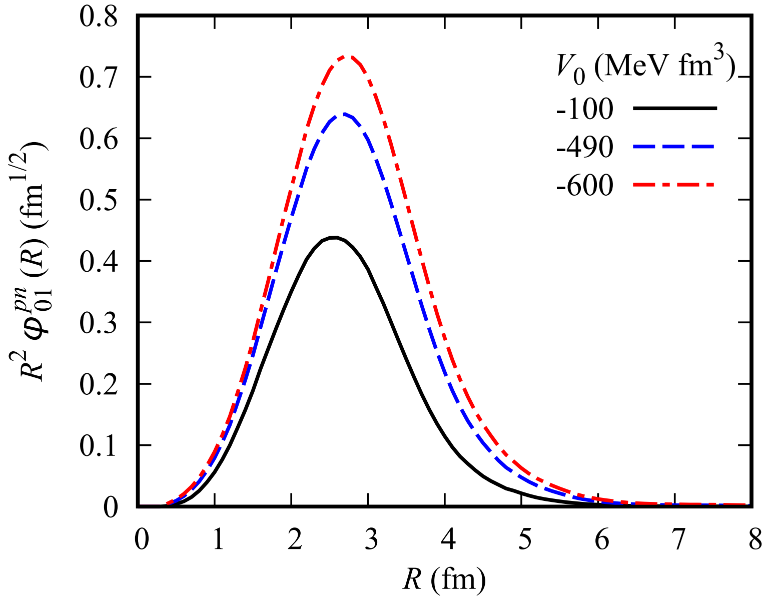

FIGURE 3.2: The radial wave function of the pn pair, φ_{01}^{pn}. The solid, dashed, and dot-dashed lines correspond to the calculation with $V_0 = -100$, -490, and -600 MeV fm^3, respectively. Each line is multiplied by R^2.

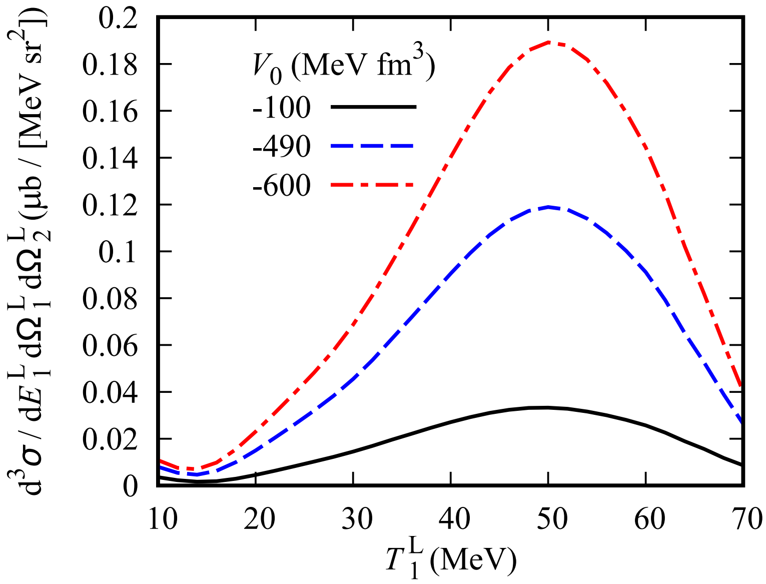

FIGURE 3.3: TDX of ^{16}O$(p, pd)^{14}$N* reaction with the incident energy being 101.3 MeV. The solid, dashed, and dot-dashed lines are the results calculated with φ_{01}^{pn} represented by the same type of line in Fig. 3.2.

p-d scattering correspond to the recoilless condition are $T_{12} \approx 56$ MeV and $\theta \approx 68^\circ$, respectively. As we see, there exists a clear correspondence between V_0 and the TDX; the magnitude of the TDX becomes larger when the pairing strength increases. Thus, we can say that the TDX reflects the collectivity of the isoscalar pn pair inside ^{16}O. It should be noted, however, that even in the case of $V_0 = -600$ MeV fm^3, the TDX is samll by about two orders of magnitude compared with that observed in the experiment [62]. A similar underestimation was reported in the study of the $(p, p\alpha)$ reaction [97]. In that study, the authors calculated the TDX of the ^{48}Ti$(p, p\alpha)^{44}$Ca reaction using the α-particle wave function obtained with a mean-field approximation and compared it with the experimental data [58]. As a result of the comparison, the calculated TDX was found to be smaller than the data by three orders of magnitude. Therefore, one may infer that it is difficult for the existing mean-field approach of the nuclear structure theory including the nuclear EDF to describe the wave function of a composite particle (cluster) inside nuclei reproducing the TDX of the knockout reaction. Furthermore, the approximate treatment of φ_{01}^{pn} in Eq. (3.6) can also be responsible for the undershooting issue; the TDX of knockout reactions is known to be quite sensitive to the radial distribution of the wave function of the particle to be knocked out, which may be affected by the approximation. At this stage, therefore, it must be too early to quantitatively compare the result presented above with the experimental data. Nevertheless, we can safely discuss the V_0 dependence of the TDX, which is the primary purpose of this chapter.

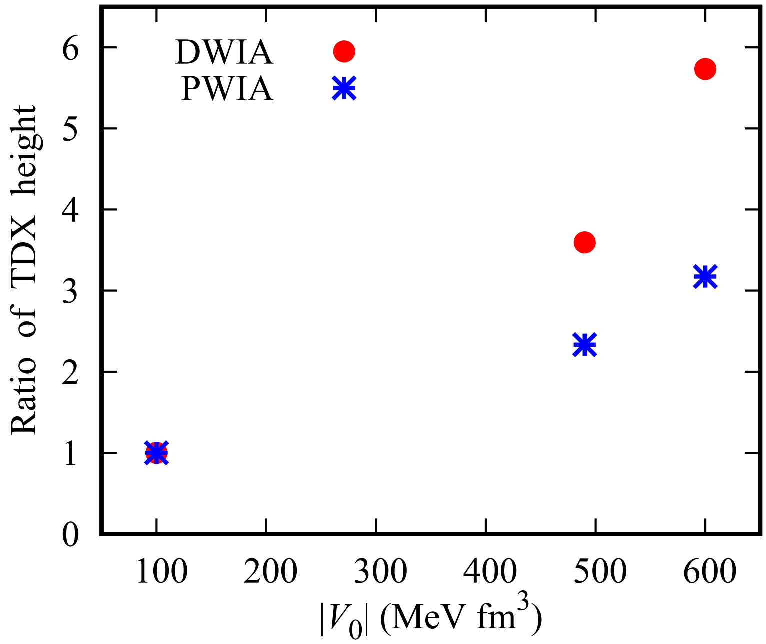

FIGURE 3.4: Ratio of the TDX height to that calculated with $V_0 = -100$ MeV fm^3. The circles (asterisks) are the results obtained with the DWIA (PWIA) calculations.

To see the V_0-TDX correspondence more clealy, the values of the TDX in the recoilless condition, which is called the TDX height here, in ratio to the value obtained with $V_0 = -100$ MeV fm^3 are shown in Fig. 3.4. The results calculated within the DWIA and PWIA frameworks are represented by the circles and asterisks, respectively. As one sees from Eqs. (3.8) and (3.10), the asterisks show the V_0 dependence which is consistent with that of φ_{01}^{pn} shown in Fig. 3.2. When the distortion for each particle is included, the ratio is more emphasized as shown by the circles. This result indicates that the TDX height observed in the ^{16}O$(p, pd)^{14}$N* reaction at 101.3 MeV is more sensitive to the amplitude of the pn pair than naively expected in the PWIA limit. For quantitative extraction of the collectivity, however, we need a more accurate description of the (p, pd) reaction, which is mentioned in Chapter 1 and discussed in Chapter 5.

Finally, the Transition Matrix Density (TMD) $\delta(R)$, which was originally introduced as a weighting function for the mean density of the $(p, 2p)$ reaction in Ref. [98], is shown in Fig. 3.5. The definition of $\delta(R)$ is given by

$$\delta(R) \equiv T^* I(R), \tag{3.13}$$

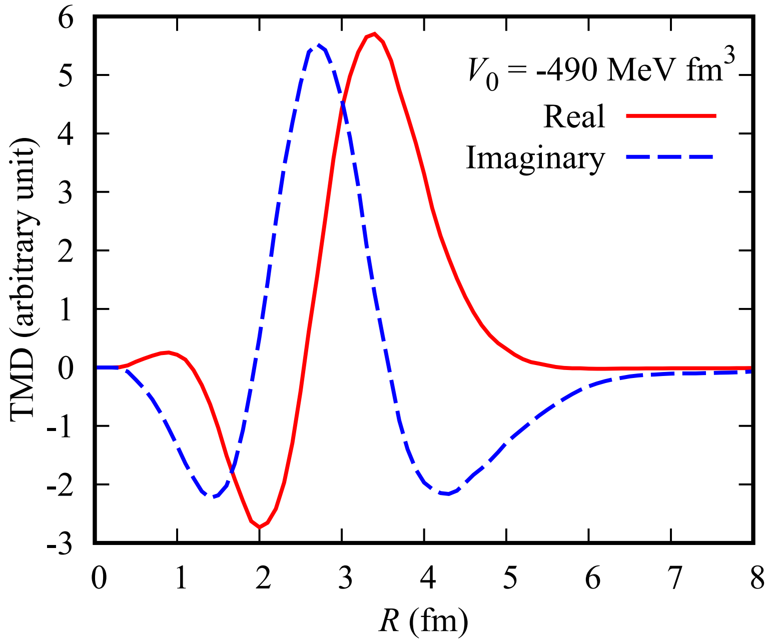

FIGURE 3.5: TMD corresponding the TDX calculated with $V_0 = -490$ MeV fm^3 at $T_1^{\mathrm{L}} = 52$ MeV. The solid and dashed lines denote the real and imaginary part of the TMD.

in which I is the complex radial distribution of the transition matrix of Eq. (2.1) satisfying the following relation:

$$T = \int_0^{\infty} \mathrm{d}R\, I(R). \tag{3.14}$$

It should be noted that the subscripts of the transition matrix are dropped in Eqs. (3.13) and (3.14) for simplicity. The solid line represents the real part of the TMD, which can be interpreted as the radial distribution of the TDX in Refs. [12, 98]. There are two conditions, however, for the interpretation making sense. One is that the real part of the TMD should not have a large negative value. The other is that the imaginary part represented by the dashed line nearly equals zero in the entire range of R. As seen from Fig. 3.5, neither of the two conditions is satisfied. This indicates that we cannot ignore the interference between amplitudes at different position. In addition, the TMD has a finite value even at small R, which means that the absorption is not enough to mask the interior region of the target in the evaluation of the transition matrix. These features are completely different from for $(p, p\alpha)$ reactions discussed in Refs. [53, 54], in which the strong absorption is realized even in the interior region of light nuclei, e.g., ^{20}Ne. In other words, the distortion effect in the (p, pd) reaction investigated above is found to be more complicated than in the $(p, p\alpha)$ reaction, and the mechanism for the increase in the relative TDX height due to the distortion is still unclear.

3.4 Summary

We have investigated the ^{16}O$(p, pd)^{14}$N* reaction at 101.3 MeV theoretically within the DWIA framework combined with a bound state wave function described microscopically by the nuclear EDF method. The correspondence between the pairing strength V_0 and the TDX of the reaction has been shown clearly. It indicates that the (p, pd) reaction will be a promising probe for the isoscalar pn pair inside $N \approx Z$ nuclei.

It is found that the distortion effect enhances the V_0 dependence of the TDX. The mechanism of this enhancement, however, has not been clarified at this stage because the region probed by the (p, pd) process is not clear. This situation is different from the α knockout reaction, in which only the nuclear surface is selectively probed.

It should be noted that the calculated TDX does not reproduce the experimental data reported in Ref. [62]; it is underestimated by two orders of magnitude. This result is mainly because of the mean-field approach to the wave function of the pn pair bound in the target nucleus. It is difficult, therefore, to make a quantitative comparison with the data at this stage. For a quantitative discussion to interpret the experimental data, progress in both nuclear structure and reaction theories is desirable. On the latter, we discuss the elementary process of the (p, pd) reaction in Chapter 4 and the transition of the knocked out deuteron due to the FSIs in Chapter 5, respectively.

Chapter 4

Proton-deuteron elastic scattering and breakup reaction

4.1 Introduction

As discussed in Chapter 2, in the Triple Differential CROSS section (TDX) of the Distorted Wave Impulse Approximation (DWIA) (2.64), the cross section of the elementary process appears outside the absolute value squared under some approximations. Therefore, if there is a sufficient number of experimental data of the elementary process in the range of energies and angles required to describe a knockout reaction, the values of the elementary-process cross section at arbitrary energies and angles can be obtained by interpolating between the data points. In the case of proton-induced nucleon knockout reactions, this method is often used thanks to plenty of data on nucleon-nucleon elastic scattering. It should be, however, noted that this prescription is allowed when the spin-orbit term is not included (or can be neglected) in the distortion potential for each particle, otherwise it is necessary to evaluate the transition matrix of the elementary process instead of the cross section. The reason for this is that the summation over the spin-projections of distorted waves appears in the squared absolute value. The matrix elements are generally complex numbers and can have different phases for each index of spin-projection. Therefore, a simple interpolation of the cross section for each index cannot properly evaluate the interference between different indices because of the lack of phase information. Similarly, in the TDX of CDCCIA (2.92), the cross section of the elementary process does not appear explicitly but is included in the squared norm in the form of matrix elements with the summation of channels. These matrix elements can also have different phases for each channel. Therefore, to properly evaluate the interference between channels, it is necessary to describe the transition matrix for the elementary processes theoretically, even if the spin-orbit term is not included in the distorting potentials.

In the case of proton-induced deuteron knockout reactions (p, pd), the elementary processes are the proton-deuteron elastic scattering and deuteron breakup reactions $d(p, p)pn$. It should be noted that a deuteron consists of a proton and a neutron and that the proton and neutron have almost the same properties except charge. Thus, these reactions can be regarded as a three-nucleon scattering problem. For three-body problems, there are theories that give the exact solution, that is, the Faddeev theory [63, 64] or the Faddeev-Alt-Grassberger-Sandhas (FAGS) theory [65]. In this respect, it is possible to say that the issue mentioned in the previous paragraph has already been solved. However, due to its strictness, the calculations based on the FAGS theory are difficult and are difficult to adapt flexibly to the physical system being treated. Considering the purpose of this doctoral thesis, a rigorous description of the p-d reactions is not necessary, and it is sufficient if the experimental data can be described effectively with enough accuracy to quantitatively describe the deuteron knockout reaction. In Section 2.3, to achieve this, we developed a framework to describe the elastic scattering and breakup reactions of protons and deuterons using a nucleon-nucleon effective interaction as a single-scattering of the incident proton off each nucleon in the deuteron. The same framework has also been applied to the description of nucleon-nucleon scattering, which reproduces the experimental data well [74–76]. In this chapter, we test this framework. We also confirm the energy dependence of the newly introduced correction factor C_{corr}. In the following discussion, all numerical results are obtained with this framework.

4.2 Result and discussion

4.2.1 Numerical inputs

We consider the p-d scattering and the $d(p,p)pn$ reaction at the incident energy T_p^{L}, the kinetic energy of the proton in the L frame; we take $T_p^{\mathrm{L}} = 120$, 135, 155, 170, 190, and 250 MeV. The Franey-Love parameter set [76] is employed for the nucleon-nucleon effective interactions in Eqs. (2.99) and (2.100). The Coulomb interaction between two protons is ignored for simplicity. Only the S wave is included in the bound and breakup states of the deuteron in the present calculation. The breakup state is discretized within the pseudostate method [99], in which the wave functions of the discretized breakup states are obtained by diagonalizing the internal Hamiltonian h_{pn} of the pn system. The potential between the proton and neutron in h_{pn} is assumed to have a one-range Gaussian form:

$$v_{pn}(r) = v_0 \exp\left[-\left(\frac{r}{r_0}\right)^2\right], \tag{4.1}$$

in which $v_0 = -72.15$ MeV and $r_0 = 1.484$ fm are used to reproduce the binding energy and radius of deuteron. The discretized breakup states are included up to their eigenenergies of 20 MeV in the calculation of the breakup cross sections. The correction factor introduced in Eq. (2.119) at each incident energy is determined to reproduce the elastic scattering data up to $60°$.

4.2.2 Cross sections and correction factor C_{corr}

Figure 4.1 shows the differential cross sections of the p-d elastic scattering and $d(p,p)pn$ reaction as functions of the scattering angle in the t frame. Panels (a), (b), (c), (d), (e), and (f) correspond to 120, 135, 155, 170, 190, and 250 MeV, respectively. In each panel, the solid and dashed lines represent the calculated results of the elastic scattering and breakup reaction. We take the experimental data of the p-d scattering denoted by the dots from Ref. [88] (120, 135, 170, and 190 MeV), Ref. [89] (155 MeV), and Ref. [90] (250 MeV).

TABLE 4.1: Correction factor C_{corr}

T_p^{L} (MeV)	120	135	155	170	190	250
C_{corr}	0.70	0.70	0.71	0.68	0.69	0.68

One sees that the solid line reproduces the forward-angle data in each panel. The obtained correction factors are shown in Table 4.1; it is found that the energy dependence of C_{corr} is small enough to be regarded as a constant in the range between 120 MeV and 250 MeV. Then, we use the average value of C_{corr}, 0.69, in the calculation shown in Chapter 5.

The solid lines describe the data quite well at backward angles ($> 150°$), though some undershooting is found at 250 MeV. It is known that the pickup process, in which the incident proton picks up the neutron inside the deuteron and forms a deuteron, plays a dominant role in the backward scattering. In the present framework, the transition matrices (2.114) correspond to this process. When the incident energy increases, the neutron needs to have a high momentum inside the deuteron to be picked up by the high energy proton; this is called the momentum matching condition. The potential (4.1) cannot generate such a high-momentum component, and the lack of it becomes visible in Fig. 4.1(f). We will need to improve the framework to be applied to the study of the (p,pd) reaction with the backward emission of the proton such as in Ref. [40]; the use of a realistic pn interaction will be necessary. However, it is beyond the scope of this thesis because the kinematics employed in Ref. [40] are completely different from those in Chapters 3 and 5.

From $90°$ to $150°$, one finds that the calculations underestimate the data. It is well known that three-body interactions, which are not included in the present calculation, are essential to reproduce the observables of the nucleon-deuteron elastic scattering in the angle region [87, 88, 100–103].

It should be noted that the p-d scattering at forward angles between $65°$ and $80°$ mainly contributes to the (p,pd) process with the kinematics condition adopted in this study. Thus, we can safely use the present framework to achieve

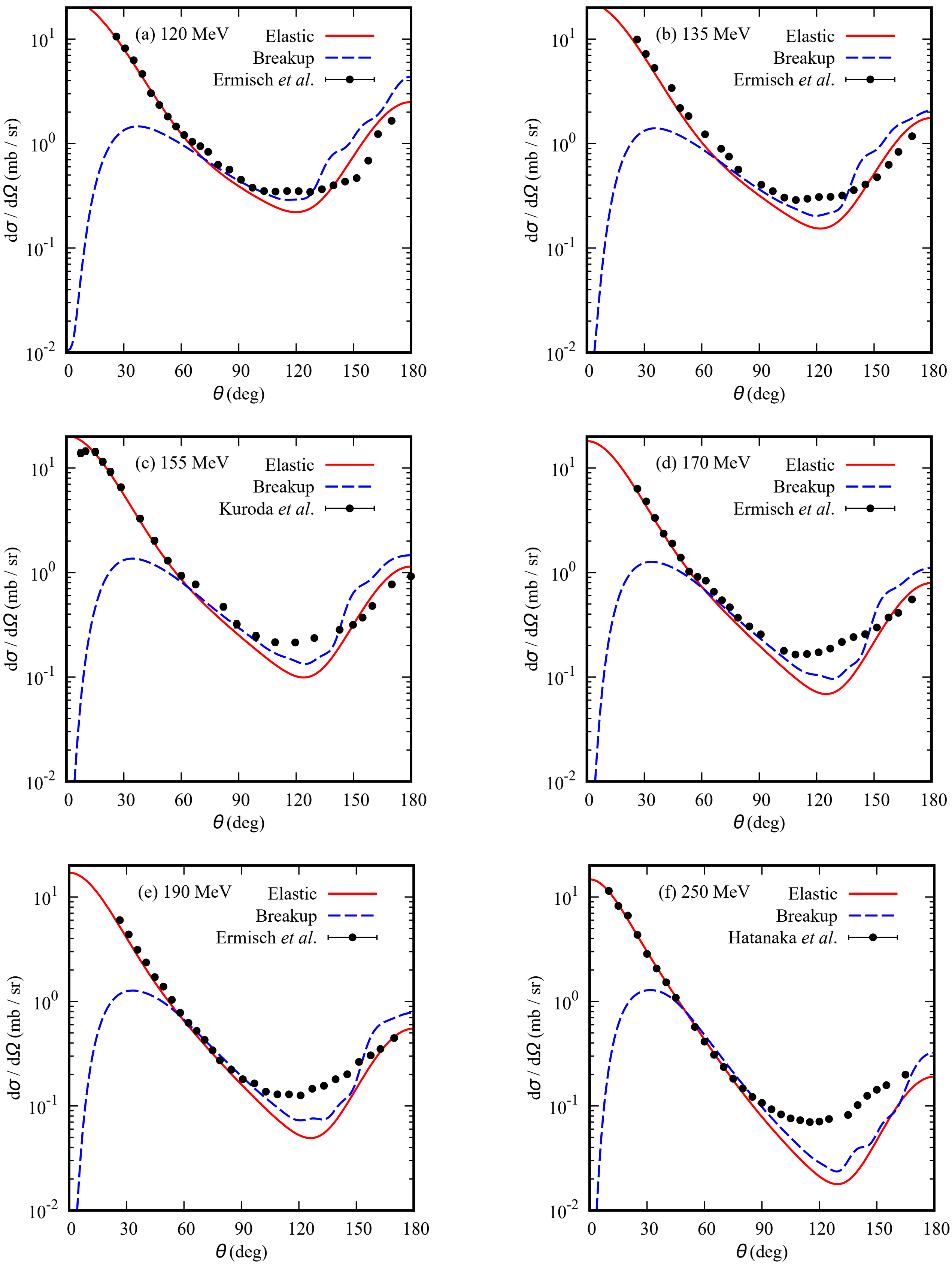

FIGURE 4.1: Differential cross sections of the p-d elastic scattering and the $d(p,p)pn$ reaction at $T_p^{\mathrm{L}} =$ (a) 120, (b) 135, (c) 155, (d) 170, (e) 190, and (f) 250 MeV. The horizontal axis of each panel is the scattering angle in the t frame. The solid (dashed) line shows the numerical result of elastic scattering (breakup reaction) in each panel. The dots are the experimental data of the p-d scattering taken from Ref. [88] (120, 135, 170, and 190 MeV), Ref. [89] (155 MeV), and Ref. [90] (250 MeV).

one of the purposes of this thesis, that is, evaluating the contribution of the deuteron breakup in the elementary process to the TDX of the (p, pd) reaction theoretically.

The dashed lines drop to zero at $\theta = 0^\circ$ because of the orthonormality of the internal wave functions ϕ_{x} of deuteron. Unfortunately, no experimental data of the breakup reaction cross section exists that is comparable with the present calculation. It is, therefore, difficult to discuss the breakup cross section in more detail; experimental studies of the $d(p, p)pn$ reaction are desirable for the quantitative evaluation of the present framework. It is, however, expected that the picture of the single-scattering by the nucleon-nucleon effective interaction can be reliable regardless of whether the pn system is in the bound state (deuteron) or the breakup one.

It is worth mentioning that the framework can describe the inverse process of the deuteron breakup reaction, that is, $pn(p, p)d$ reaction with regarding ϕ_{x} and ϕ'_{x} in Eqs. (2.109)-(2.111) as the wave functions of the breakup and bound states of deuteron, respectively. We need this process to consider the (p, pd) reaction in which the pn pair inside nuclei is described within the nuclear EDF method because the wave function of the pair is allowed to have different components from that of deuteron; the pn pair can form a deuteron when it interacts with the incident proton. Investigation of the role of such processes will be interesting and important to identify the origin of the detected deuteron in (p, pd) reactions, though it is beyond the scope of this thesis mainly because of the lack of reliable nuclear structure calculations (see Chapter 3).

4.3 Summary

We have discussed the elastic scattering and breakup reaction of the proton-deuteron system at 120, 135, 155, 170, 190, and 250 MeV. All the theoretical cross sections have been calculated with the framework in Section 2.3; the reaction process is described by a single-scattering of the incident proton off each nucleon inside deuteron by a nucleon-nucleon effective interaction. We found that the framework works well to reproduce the experimental data of the p-d scattering at forward angles. In addition, the correction factor C_{corr} is found to be almost energy-independent; the average value of C_{corr} of 0.69 is used in Chapter 5. The backward-angle data are also reproduced by the calculated cross sections except at 250 MeV, whereas some undershooting was found at middle angles. We need to improve the framework to be applied to (p, pd) reactions to which the p-d process at middle scattering angles are relevant. We can, however, safely use the framework combined with the CDCCIA framework (see Section 2.2) without considering such issues because in this thesis we discuss only the (p, pd) reaction with the kinematics in which the framework works well.

Although the deuteron breakup cross sections have also been calculated, there exists no experimental data for making a comparison. Experimental studies of the $d(p, p)pn$ reaction are desirable for the quantitative evaluation of the framework.

Chapter 5

Role of fragility of deuteron in proton-induced deuteron knockout reactions

5.1 Introduction

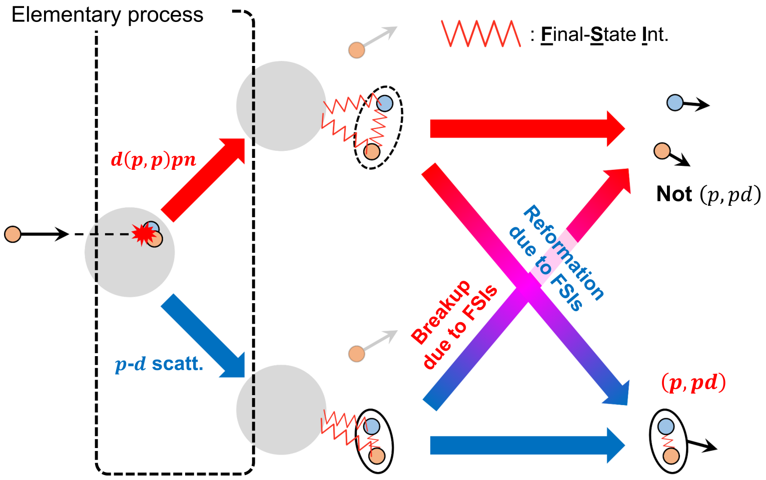

FIGURE 5.1: Processes included in the CDCCIA framework.

As mentioned in Section 1.3, the deuteron is a weakly bound system with a binding energy of about 1 MeV per nucleon and can be easily broken up by external interactions. In the case of proton-induced deuteron knockout reactions (p, pd), which is the central subject of this doctoral thesis, there is a possibility of deuteron breakup due to the interaction with incident protons in the elementary process. Deuterons knocked out of the nucleus without breakup in the elementary process may also undergo a transition between bound and breakup states due to the Final-State Interactions (FSIs). In addition, the ease of decomposition is also the ease of binding, and the knocked-out proton-neutron (pn) pair must also be considered to be bound again by the FSIs. These processes are illustrated in Fig. 5.1. The reaction model that describes the deuteron knockout reaction including these processes is the CDCCIA introduced in Section 2.2.

In this chapter, the CDCCIA is used to calculate the Triple Differential CROSS section (TDX) of the (p, pd) reaction. The description of the elementary processes is based on the framework constructed in Section 2.3 and tested in Chapter 4. In the following, we clarify how the *back coupling* process, in which the knocked-out deuteron goes to breakup channels and comes back to the elastic channel due to the FSIs, and the reformation of the deuteron by the FSIs contribute to TDX, respectively.

5.2 Result and discussion

5.2.1 Numerical inputs

We consider the ^{16}O$(p,pd)^{14}$N* reaction in normal kinematics; ^{14}N is in the 1_2^+ excited state. The incident energy T_0^{L} is set to 101.3, 250, and 400 MeV. The emission angle of the proton (deuteron) in the final state is fixed at 40.1° (40.0°) for 101.3 MeV, 47.1° (48.8°) for 250 MeV, and 46.6° (49.5°) for 400 MeV; the asymptotic momenta of particles 0, 1, and 2 are kept on the same plane.

In the initial state of the reaction, we assume that the deuteron to be knocked-out inside target A is bound in the $1S$ orbit having one node in a central Woods-Saxon potential:

$$V(R) = -V_0 \frac{1}{1+\exp[(R-R_0)/a_0]} \tag{5.1}$$

with the radial parameter $R_0 = 1.41 \times B^{1/3}$ fm and the diffuseness parameter $a_0 = 0.65$ fm; these parameters are taken from Ref. [62]. The depth V_0 of the potential is determined to reproduce the separation energy of the d-B system of 24.68 MeV. The Coulomb part is constructed by assuming a uniformly charged sphere with the radius R_C being $1.41 \times B^{1/3}$ fm.

We adopt the EDAD1 parameter set of the Dirac phenomenology [78–80] for the distorting potentials of the p-A, p-B, and n-B systems. The Coulomb potential in each potential is constructed in the same way as in the previous paragraph with $R_C = 1.2 \times C^{1/3}$ fm ($C = A$ or B).

In the CDCC calculation, the breakup state of deuteron is discretized with the pseudostate method [99] as in Chapter 4. The pn continuum states of $\ell = 0, 2, 4,$ and 6 are included with $k_{\max} = 2.1$ fm^{-1}, in which ℓ is the orbital angular momentum between p and n, and $k_{\max}$ is the maximum p-n linear momentum (in unit of $\hbar$). For 250 and 400 MeV, those of $\ell = 0, 2,$ and 4 are considered with the same $k_{\max}$. The CDCC equations are integrated up to $R = 20$ fm with the increment of 0.1 fm. The Coulomb breakup is ignored in the present study; the essence of the following discussion will not be affected with this treatment.

According to the discussion in Chapter 4, it is expected that the framework for the proton-deuteron elastic scattering and breakup reaction works well in the range of elementary process energies from 120 to 250 MeV. Thus, the TDX of the CDCCIA framework is calculated only for the (p,pd) reaction at $T_0^{\mathrm{L}} = 250$ MeV, in which the energy of the elementary process falls well within the above range, because of the reliability of the framework discussed in Chapter 4. We treat only the S wave bound and discretized-breakup states in the CDCCIA calculation; the breakup states are included up to their eigenenergies of 20 MeV, which corresponds to the momentum of 0.75 fm^{-1}. We calculate the TDX of the DWIA framework in the same manner as in Chapter 3 except for the bound wave function $\varphi_{n\ell j}$ of the deuteron to be knocked-out inside A. The nonlocality to the distorted waves of the incoming and outgoing ptorons are taken into account by including the Darwin factor [78, 83], meanwhile that for deuteron is not considered because it is difficult to treat it in the CDCCIA and DWIA calculations in a consistent way. We refer to the TDXs obtained from the transition matrices (2.85) and (2.87) as those of the *EL-CDCCIA* and *NB-CDCCIA* frameworks, respectively. Comparing the TDX of the EL-CDCCIA or DWIA frameworks with that of the NB-CDCCIA, we can evaluate contributions of the back coupling in the (p,pd) reaction.

5.2.2 Back coupling in the ^{16}O$(p,pd)^{14}$N* reaction

The TDX of the ^{16}O$(p,pd)^{14}$N* reaction at $T_0^{\mathrm{L}} = 101.3$ MeV is shown in Fig. 5.2(a). The horizontal axis means the kinetic energy of the outgoing proton. The recoilless condition is almost realized at $T_1^{\mathrm{L}} \approx 52$ MeV. The result of the EL-CDCCIA (DWIA) framework is denoted by the solid (dashed) line, and that of the NB-CDCCIA by dot-dashed line. One finds that the solid line is smaller than the dot-dashed one in the whole region of T_1^{L}; at around the peak, the former has only one-third of the latter in magnitude. These results indicate that the back coupling of the emitted deuteron due to the FSIs drastically reduces the TDX of the (p,pd) reaction at this incident energy. The dashed line also shows a somewhat large reduction from the dash-dotted line, though not so significant compared with the solid line. In general, CDCC can treat the transition of the deuteron in the d-B scattering problem more appropriately than in potential model calculation, in which the transition is effectively considered by the imaginary part of an optical

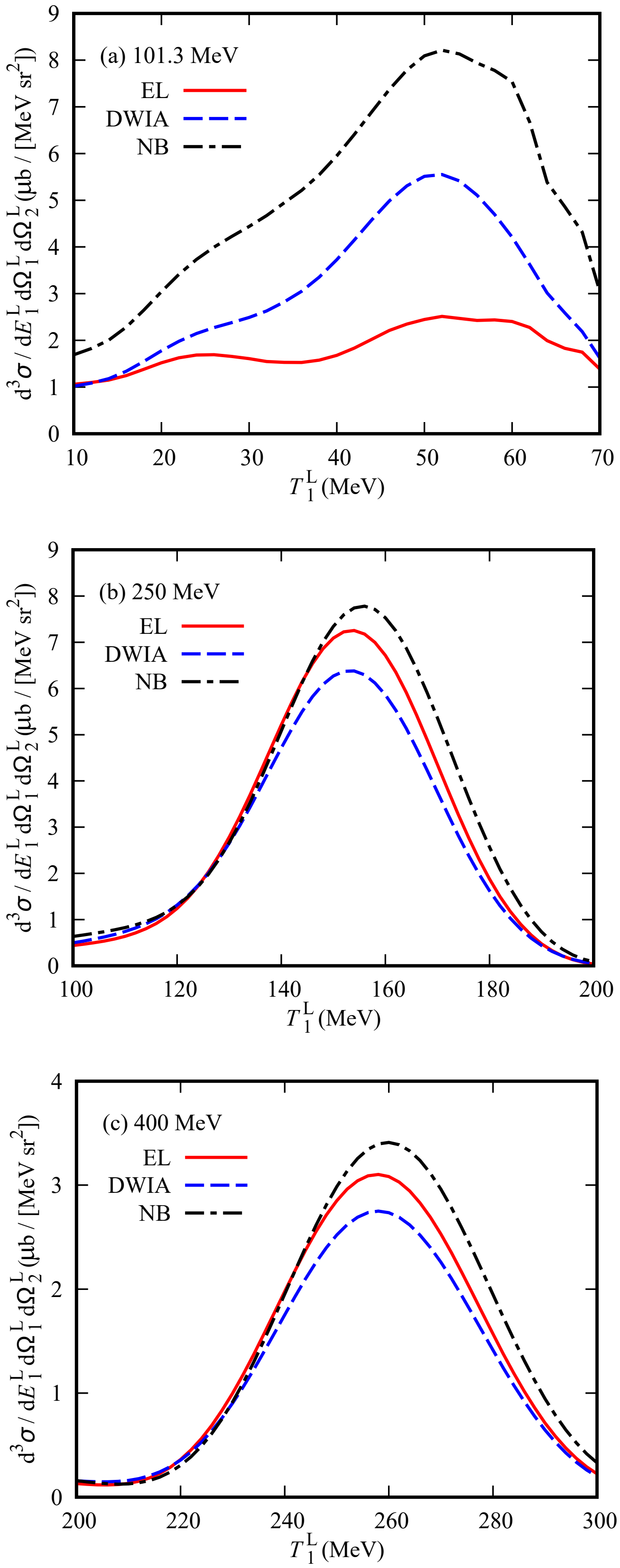

FIGURE 5.2: TDXs of the $^{16}O(p, pd)^{14}N^*$ reaction at (a) 101.3, (b) 250, and (c) 400 MeV as functions of the kinetic energy T_1^L of the outgoing proton. In each panel, the solid, dashed, and dot-dashed lines represent the results of the EL-CDCCIA, DWIA, and NB-CDCCIA frameworks, respectively.

potential. Thus, the difference between the solid and dashed lines shows that the back coupling is underestimated in the DWIA framework compared with that in the EL-CDCCIA one.

Figures 5.2(b) and 5.2(c) are the same as Fig. 5.2(a) but at $T_0^{\mathrm{L}} = 250$ and 400 MeV, respectively. The recoilless condition is satisfied at $T_1^{\mathrm{L}} \approx 150$ and 250 MeV in panels (b) and (c), respectively. As at 101.3 MeV, the back coupling reduces the TDXs around their peaks at both energies; the TDX of the EL-CDCCIA framework is smaller than that of the NB-CDCCIA one by about 7 (10) $\%$ at 250 (400) MeV. It should be noted that the solid line is above the dashed line around the recoilless point in Figs. 5.2(b) and 5.2(c). It means that the DWIA framework overestimates the back coupling than the EL-CDCCIA framework at these energies.

A clear conclusion from Fig. 5.2 is that the back coupling considerably reduces the theoretical TDX of the (p, pd) reaction. This fact indicates that the calculation without taking into account the back coupling may underestimate the amount of deuteron in nuclei, at relatively low energy in particular. Furthermore, it is expected that the process in which the pn pair reforms the deuteron also plays an important role in the (p, pd) reaction because the FSIs will cause both the back coupling and reformation. Since the contributions of the back coupling are comparable in the results at 250 and 400 MeV, below we will discuss the difference in the back coupling at 101.3 and 250 MeV.

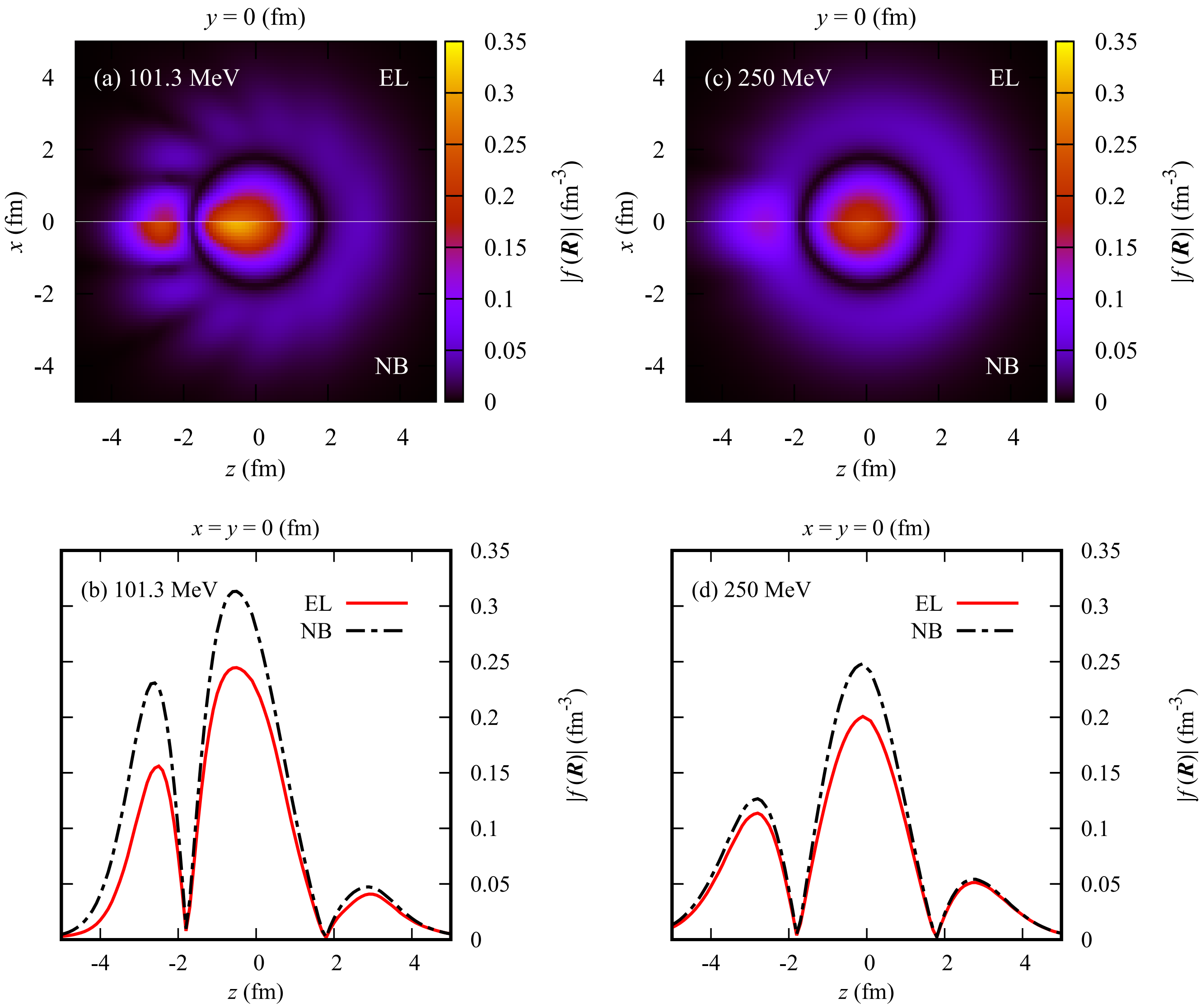

FIGURE 5.3: (a) Norm of $f(\boldsymbol{R})$ defined by Eq. (5.2) at the recoilless condition, $T_1^{\mathrm{L}} = 52$ MeV, for $T_0^{\mathrm{L}} = 101.3$ MeV on the z-x plane with $y = 0$ fm; the direction of the outgoing deuteron is taken to be parallel to the z-axis. The upper and lower halves show the results of the EL- and NB-CDCCIA frameworks. (b) Slice of panel (a) along to the z-axis with $x = 0$ fm. The results of the EL- and NB-CDCCIA frameworks are denoted by the solid and dot-dashed lines. (c)(d) Same as (a)(b) but for $T_0^{\mathrm{L}} = 250$ MeV with $T_1^{\mathrm{L}} = 150$ MeV.

Here, we define the product of the wave function φ_{101} of the deuteron bound to ^{14}N* and the distorted wave of the outgoing deuteron by

$$f(\boldsymbol{R}) \equiv \frac{1}{\sqrt{4\pi}}\varphi_{101}(R)\chi^{(\mathrm{XX})(-)}_{2,\boldsymbol{K}_2}(\boldsymbol{R}), \tag{5.2}$$

in which the coefficient $1/\sqrt{4\pi}$ comes from the spherical harmonics Y_{00} and XX = EL or NB. Figure 5.3(a) shows the norm of $f(\boldsymbol{R})$ at the recoilless condition for 101.3 MeV on the z-x plane with $y = 0$ fm. The direction of the knocked-out deuteron to be parallel is taken to the z-axis. The results obtained within the EL- and NB-CDCCIA frameworks are shown in the upper and lower halves, respectively. It should be noted that each $|f(\boldsymbol{R})|$ is symmetrical about the azimuth angle. One sees that there is a focus around $z = 2.5$ fm and $x = 0$ fm, and the upper is obscurer than the lower. From the slice of Fig. 5.3(a) along to the z axis with $x = 0$ fm presented in Fig. 5.3(b), it is found more clearly that the back coupling reduces the amplitude of $|f(\boldsymbol{R})|$ at the focus. In addition similar reduction is seen in the internal region of the target nucleus.

Although it is difficult to explain the clear reason for the reduction because of the complexity of the coupled-channel effect, we can interpret it qualitatively in terms of the flux. As mentioned in the previous section, no deuteron breakup occurs within the NB-CDCCIA framework. When we include the breakup channel in the CDCC calculation as in Eq. (2.78), the flux of the elastic channel will be distributed to breakup channels and then decreases based on the conservation of the probability. Part of the flux returns to the elastic channel, while some remain in the breakup channels. As a result, $|f(\boldsymbol{R})|$ of the EL-CDCCIA framework becomes small compared with that of the NB-CDCCIA one; it causes the reduction of the TDX. The above process is considered in an optical potential for deuteron effectively, though its accuracy for describing the scattering wave function is not guaranteed as discussed above.

Figures 5.3(c) and 5.3(d) are the same as Figs. 5.3(a) and 5.3(b), respectively, but for $T_0^{\mathrm{L}} = 250$ MeV with $T_1^{\mathrm{L}} = 150$ MeV. Compared with the result at 101.3 MeV, the focus becomes unclear and shows almost the same behavior in each framework, whereas the difference in the interior of the target remains at this energy. Thus, the difference between the TDXs in Fig. 5.2(b) mainly comes from the interior.

5.2.3 TDX of ^{16}O(*p,pd*)^{14}N* reaction at 250 MeV

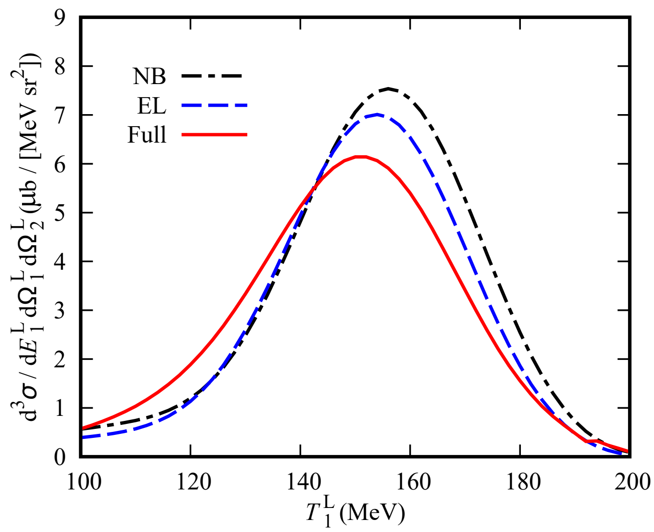

FIGURE 5.4: TDX of ^{16}O$(p,pd)^{14}$N* at 250 MeV. The solid line is the result calculated within the CDCCIA framework, and the dashed and dot-dashed lines are those of the EL- and NB-CDCCIA frameworks. The elementary process, that is, the p-d scattering and the $d(p,p)pn$ reaction, is described with the framework discussed in Chapter 4.

We show the TDX of the ^{16}O$(p,pd)^{14}$N* at 250 MeV in Fig. 5.4 as a function of T_1^{L}, in which the numerical result obtained with the CDCCIA is represented by the solid line, and those of the EL- and NB-CDCCIA by the dashed and dot-dashed lines, respectively. The elementary process of the (p,pd) reaction, that is, the elastic scattering and the breakup reaction of the proton-deuteron system, is described by the framework discussed in Chapter 4. The height and shape of the dashed (dot-dashed) line in this figure is almost the same as those of the solid (dot-dashed) line in Fig. 5.2(b); this means the framework used in Chapter 4 is successfully incorporated into the CDCCIA frameworks. By comparing the solid line with the dashed one, one finds that the reformation of deuteron also reduces the TDX of the (p, pd) reaction as the back coupling. Although this resutl seems counterintuitive, it should be noted that the elastic and discretized breakup components of the transition matrix are summed coherently as shown in Eq. (2.92). Figure 5.4 indicates that the interference between the different channels has a destructive contribution to the TDX. The solid line is smaller than the dashed (dot-dashed) line around the peak by about 13 (20) $\%$.

It is worth pointing out that the position of the peak of the TDX is shifted to the lower side of T_1^{L}; that of the solid line is nearest to the recoilless point, $T_1^{\mathrm{L}} = 150$ MeV. As mentioned in Subsection 3.2.2, the TDX in the recoilless condition contains the direct information about the total amplitude of the deuteron inside nuclei, and it is important to measure the TDX of knockout reaction including the recoilless condition in experiments. The CDCCIA result, therefore, will predict the appropriate kinematics condition of the (p, pd) reaction for measurements.

5.3 Summary

The ^{16}O$(p, pd)^{14}$N* reactions at 101.3, 250, and 400 MeV have been investigated in view of the deuteron breakup in the elementary process and the transition of the knocked-out deuteron or pn pair due to the FSIs. It has been found that the back coupling, in which the deuteron knocked out by the incident proton is once broken up by the FSIs and comes back to deuteron also due to the FSIs, reduces the magnitude of TDX around the peak. This process has a large contribution at relatively low incident energies in particular. We can interpret the reduction qualitatively in terms of the conservation of the flux.

At 250 MeV, we have calculated the TDX of the (p, pd) reaction within the "full" CDCCIA framework, in which deuteron breakup in the elementary process and the reformation of deuteron due to the FSIs in addition to the back coupling are taken into account. It is found that the reformation reduces the TDX as the back coupling, indicating the destructive interference between different channels. The shift of the peak of the TDX is also obtained; the recoilless condition is satisfied at the peak of the TDX as a result of the present calculation.

Chapter 6

Summary

In this doctoral thesis, a theoretical study of the proton (p) induced deuteron (d) knockout reaction (p, pd) has been presented. In Chapter 2, the framework of the Distorted Wave Impulse Approximation (DWIA), which is a reaction model adopted widely to describe knockout reactions, is explained. Then, a new reaction model, *CDCCIA*, is introduced for a more adequate description of deuteron knockout reactions. This model takes into account the deuteron breakup in the elementary process and the transition of the emitted deuteron due to Final-State Interactions (FSIs). In addition, a framework is developed to describe the elastic scattering and breakup reactions of protons and deuterons in the elementary process of the (p, pd) reaction by a single-scattering between the incident proton and each nucleon in the deuteron, using an effective interaction between nucleons. Since there is no guarantee that a nucleon-nucleon effective interaction can describe proton-deuteron reactions well, a correction factor C_{corr} is introduced.

In Chapter 3, the ^{16}O$(p, pd)^{14}$N* reaction at 101.3 MeV has been investigated theoretically within the DWIA framework combined with a bound state wave function described microscopically by the nuclear EDF method. The correspondence between the pairing strength V_0 and the Triple Differential CROSS section (TDX) of the reaction is shown clearly. It indicates that the (p, pd) reaction will be a promising probe for the isoscalar pn pair inside $N \approx Z$ nuclei. It is found that the distortion effect enhances the V_0 dependence of the TDX. Because the region probed by the (p, pd) process is unclear, however, the mechanism of this enhancement is not clarified at this stage. This situation is different from the α-particle knockout reaction, in which only the nuclear surface is selectively probed. It should be noted that the calculated TDX does not reproduce the experimental data reported in Ref. [62]; it is underestimated by two orders of magnitude. This result is mainly because of the mean-field approach to the wave function of the pn pair bound in the target nucleus. It is difficult, therefore, to make a quantitative comparison with the data at this stage. For a quantitative discussion to interpret the experimental data, progress in both nuclear structure and reaction theories is desirable.

In Chapter 4, the proton-deuteron elastic scattering and breakup reactions at 120, 135, 155, 170, 190, and 250 MeV have been discussed. All the numerical cross sections are calculated with the framework constructed in Chapter 2. It is found that the framework reproduces the experimental data of the p-d scattering well at forward angles. In addition, the correction factor C_{corr} is found to be almost energy-independent; the average value of C_{corr} of 0.69 is used in Chapter 5. The backward-angle data are also reproduced by the calculated cross sections except at 250 MeV, whereas some undershooting is found at middle angles. The improvement of the framework is needed to be applied to (p, pd) reactions to which the p-d process at middle scattering angles are relevant. We can, however, safely use the framework combined with the CDCCIA framework without considering such issues because in this thesis only the (p, pd) reaction with the kinematics in which the framework works well is discussed. Although the deuteron breakup cross sections are also calculated, there exists no experimental data for making a comparison. Experimental studies of the $d(p, p)pn$ reaction are desirable for the quantitative evaluation of the framework.

In Chapter 5, the ^{16}O$(p, pd)^{14}$N* reactions at 101.3, 250, and 400 MeV have been investigated in view of the deuteron breakup in the elementary process and the transition of the knocked-out deuteron or pn pair due to the FSIs. It has been found that the back coupling, in which the deuteron knocked out by the incident proton is once broken up by the FSIs and comes back to deuteron also due to the FSIs, reduces the magnitude of TDX around the peak. This process has a large contribution at relatively low incident energies in particular. We can interpret the reduction qualitatively in terms of the conservation of the flux. At 250 MeV, the TDX of the (p, pd) reaction has been calculated within the "full" CDCCIA framework, in which deuteron breakup in the elementary process and the reformation of deuteron due to the FSIs in addition to the back coupling are taken into account. It is found that the reformation reduces the TDX as the back coupling, indicating the destructive interference between different channels. The shift of the peak of the TDX is also obtained; the recoilless condition is satisfied at the peak of the TDX as a result of the present calculation.

From these results, we can conclude that it is important to treat each element properly to reveal the deuteron inside nuclei by deuteron knockout reactions.

Appendix A

Gell-Mann-Goldberger transformation

In this appendix, the Hamiltonian of the total system in channel $j\ (= c_1, c_2, \cdots)$ is defined by

$$H = T_{c_1} + V_{c_1} + h_{c_1} = T_{c_2} + V_{c_2} + h_{c_2} = \cdots, \tag{A.1}$$

in which T_j is the kinetic energy operator, V_j is the interaction, and h_j is the internal Hamiltonian, respectively. The goal of this appendix is to show that the post-form transition matrix from the initial channel i to the final channel f given by

$$T_{fi} = \left\langle \phi_f \middle| V_f \middle| \Psi_i^{(+)} \right\rangle \tag{A.2}$$

is transformed to

$$T_{fi} = \left\langle \phi_f \middle| U_f \middle| \chi_i^{(+)} \right\rangle \delta_{fi} + \left\langle \chi_f^{(-)} \middle| V_f - U_f \middle| \Psi_i^{(+)} \right\rangle, \tag{A.3}$$

in which U_j is an auxiliary interaction like an optical potential whose property we know well. ϕ_j and χ_j are the plane and distorted wave functions which satisfy the Schrödinger equations

$$[E - T_j - h_j]\phi_j = 0 \tag{A.4}$$

and

$$[E - T_j - U_j - h_j]\chi_j = 0, \tag{A.5}$$

respectively, and Ψ_j is the wave function of the total system which is the solution of

$$[E - T_j - V_j - h_j]\Psi_j = 0. \tag{A.6}$$

The superscripts $(+)$ and $(-)$ show that the Schrödinger equations are integrated with the outgoing and incoming boundary conditions, respectively. It should be noted that the eigenstate of h_j is included in ϕ_j, χ_j, and Ψ_j in this appendix.

The formal solution of Equation (A.6) with the outgoing boundary condition is obtained as

$$\Psi_i^{(+)} = \phi_i + \frac{1}{E - T_i - h_i + i\eta} V_i \Psi_i^{(+)} = \left(1 + \frac{1}{E - H + i\eta} V_i\right)\phi_i, \tag{A.7}$$

which is called the Lippmann-Schwinger equation. We can transform this equation as

$$\begin{aligned}
\Psi_i^{(+)} &= \left[1 + \frac{1}{E - H + i\eta}(V_i - U_i + U_i)\right]\phi_i \\
&= \left[1 + \frac{1}{E - H + i\eta}(V_i - U_i)\right]\phi_i + \frac{1}{E - H + i\eta} U_i \phi_i \\
&= \left[1 + \frac{1}{E - H + i\eta}(V_i - U_i)\right]\phi_i + \frac{1}{E - T_i - U_i - h_i + i\eta - (V_i - U_i)} U_i \phi_i.
\end{aligned} \tag{A.8}$$

Applying the Gell-Mann-Goldberger identity

$$\frac{1}{a-b} = \frac{1}{a}\left(1 + b\frac{1}{a-b}\right) = \left(1 + \frac{1}{a-b}b\right)\frac{1}{a} \tag{A.9}$$

to the second term of Eq. (A.8) with

$$a = E - T_i - U_i - h_i + i\eta \quad \text{and} \quad b = V_i - U_i, \tag{A.10}$$

we obtain

$$\begin{aligned}\Psi_i^{(+)} &= \left[1 + \frac{1}{E-H+i\eta}(V_i - U_i)\right]\phi_i + \left[1 + \frac{1}{E-H+i\eta}(V_i - U_i)\right]\frac{1}{E-T_i-U_i-h_i+i\eta}U_i\phi_i \\ &= \left[1 + \frac{1}{E-H+i\eta}(V_i - U_i)\right]\left(1 + \frac{1}{E-T_i-U_i-h_i+i\eta}U_i\right)\phi_i.\end{aligned} \tag{A.11}$$

Similar to Eq (A.7), the formal solution of Eq. (A.5) is given by

$$\chi_i^{(+)} = \phi_i + \frac{1}{E-T_i-h_i+i\eta}U_i\chi_i^{(+)} = \left(1 + \frac{1}{E-T_i-U_i-h_i+i\eta}U_i\right)\phi_i, \tag{A.12}$$

and then Eq. (A.11) is reduced to

$$\Psi_i^{(+)} = \left[1 + \frac{1}{E-H+i\eta}(V_i - U_i)\right]\chi_i^{(+)}. \tag{A.13}$$

When we operate an operator $(E - H + i\eta)$ on Eq. (A.13) from left,

$$\begin{aligned}(E-H+i\eta)\Psi_i^{(+)} &= [(E-H+i\eta) + (V_i - U_i)]\chi_i^{(+)} \\ &= (E-T_i-U_i-h_i+i\eta)\chi_i^{(+)} \\ &= i\eta\chi_i^{(+)}\end{aligned} \tag{A.14}$$

is obtained. Eq. (A.5) is used in the last equal sign. Operating another operator $(E - T_f - U_f - h_f + i\eta)^{-1}$ on Eq. (A.14) from left, the left-hand-side and right-hand-side of the equation become

$$\begin{aligned}(\text{l.h.s.}) &= \frac{1}{E-T_f-U_f-h_f+i\eta}(E-H+i\eta)\Psi_i^{(+)} \\ &= \frac{1}{E-T_f-U_f-h_f+i\eta}[E-T_f-U_f-h_f+i\eta-(V_f-U_f)]\Psi_i^{(+)} \\ &= \Psi_i^{(+)} - \frac{1}{E-T_f-U_f-h_f+i\eta}(V_f-U_f)\Psi_i^{(+)}\end{aligned} \tag{A.15}$$

and

$$(\text{r.h.s.}) = \frac{1}{E-T_f-U_f-h_f+i\eta}i\eta\chi_i^{(+)}, \tag{A.16}$$

respectively, and then we obtained

$$\Psi_i^{(+)} = \frac{1}{E-T_f-U_f-h_f+i\eta}i\eta\chi_i^{(+)} + \frac{1}{E-T_f-U_f-h_f+i\eta}(V_f-U_f)\Psi_i^{(+)}. \tag{A.17}$$

Only in the case of the label i being equal to f, the first term of this equation becomes

$$\frac{1}{E-T_f-U_f-h_f+i\eta}i\eta\chi_i^{(+)} = \frac{1}{E-T_f-U_f-h_f+i\eta}(E-T_i-U_i-h_i+i\eta)\chi_i^{(+)} = \chi_i^{(+)} \tag{A.18}$$

because of Eq. (A.5), otherwise it vanishes in the $\eta \to 0$ limit. Then Eq. (A.17) can be represented as

$$\Psi_i^{(+)} = \chi_i^{(+)}\delta_{fi} + \frac{1}{E - T_f - U_f - h_f + i\eta}(V_f - U_f)\Psi_i^{(+)} \tag{A.19}$$

and it leads

$$\begin{aligned} V_f\Psi_i^{(+)} &= (U_f + V_f - U_f)\Psi_i^{(+)} \\ &= U_f\left[\chi_i^{(+)}\delta_{fi} + \frac{1}{E - T_f - U_f - h_f + i\eta}(V_f - U_f)\Psi_i^{(+)}\right] + (V_f - U_f)\Psi_i^{(+)} \\ &= U_f\chi_i^{(+)}\delta_{fi} + \left(1 + U_f\frac{1}{E - T_f - U_f - h_f + i\eta}\right)(V_f - U_f)\Psi_i^{(+)}. \end{aligned} \tag{A.20}$$

Finally, the transition matrix (A.2) is reduced to

$$\begin{aligned} T_{fi} &= \left\langle \phi_f \middle| U_f \middle| \chi_i^{(+)} \right\rangle \delta_{fi} + \left\langle \phi_f \middle| \left(1 + U_f\frac{1}{E - T_f - U_f - h_f + i\eta}\right)(V_f - U_f) \middle| \Psi_i^{(+)} \right\rangle \\ &= \left\langle \phi_f \middle| U_f \middle| \chi_i^{(+)} \right\rangle \delta_{fi} + \left\langle \left(1 + U_f\frac{1}{E - T_f - U_f - h_f + i\eta}\right)^{\dagger}\phi_f \middle| V_f - U_f \middle| \Psi_i^{(+)} \right\rangle \\ &= \left\langle \phi_f \middle| U_f \middle| \chi_i^{(+)} \right\rangle \delta_{fi} + \left\langle \chi_f^{(-)} \middle| V_f - U_f \middle| \Psi_i^{(+)} \right\rangle \end{aligned} \tag{A.21}$$

with the use of Eq. (A.12), and Eq. (A.3) has been shown. This is called the Gell-Mann-Goldberger transformation.

Appendix B

Derivation of Equation (2.16)

In this appendix, I show the derivation of Equation (2.16) as demonstrated in Ref. [104]. An arbitrary set of coordinate vectors $\{\boldsymbol{x}_1, \boldsymbol{x}_2, \cdots\}$ is obtained from that of position vectors $\{\boldsymbol{r}_1, \boldsymbol{r}_2, \cdots\}$ in the laboratory system by a linear combination with a suitable coefficients A_{jk}:

$$\boldsymbol{x}_j = \sum_k A_{jk} \boldsymbol{r}_k, \tag{B.1}$$

or in matrix notation:

$$[\boldsymbol{x}] = [A][\boldsymbol{r}]. \tag{B.2}$$

We represent the canonically conjugate momentum of $[\boldsymbol{x}]$ by $[\boldsymbol{q}]$ and that of $[\boldsymbol{r}]$ by $[\boldsymbol{p}]$, then the action function for free paticles S is calculated by

$$S = \sum_j \boldsymbol{q}_j \cdot \boldsymbol{x}_j = \sum_k \boldsymbol{p}_k \cdot \boldsymbol{r}_k \quad \text{or} \quad S = [\boldsymbol{q}]^{\mathrm{t}}[\boldsymbol{x}] = [\boldsymbol{p}]^{\mathrm{t}}[\boldsymbol{r}], \tag{B.3}$$

because S is invariant under the canonical transformation. The superscript t denotes the transpose of a matrix. Using the inverse relation of Eq. (B.2), we obtain

$$[\boldsymbol{q}]^{\mathrm{t}}[\boldsymbol{x}] = [\boldsymbol{p}]^{\mathrm{t}}[A]^{-1}[\boldsymbol{x}], \tag{B.4}$$

and it is reduced to

$$[\boldsymbol{p}]^{\mathrm{t}} = [\boldsymbol{q}]^{\mathrm{t}}[A] \tag{B.5}$$

because $[\boldsymbol{x}]$ is arbitrary. Eq. (B.5) shows that we can write down $[\boldsymbol{p}]$ in terms of $[\boldsymbol{q}]$.

If we set $[\boldsymbol{r}]^{\mathrm{t}} = [\boldsymbol{r}_1, \boldsymbol{r}_2, \boldsymbol{r}_{\mathrm{B}}]^{\mathrm{t}}$ and $[\boldsymbol{x}]^{\mathrm{t}} = [\boldsymbol{R}_1, \boldsymbol{R}_2, \boldsymbol{R}_{\mathrm{c.m.}}]^{\mathrm{t}}$, the coefficitent matrix $[A]$ is

$$[A] = \begin{bmatrix} 1 & 0 & -1 \\ 0 & 1 & -1 \\ \frac{m_1}{m_{\mathrm{tot}}} & \frac{m_2}{m_{\mathrm{tot}}} & \frac{m_{\mathrm{B}}}{m_{\mathrm{tot}}} \end{bmatrix} \tag{B.6}$$

from Eq. (2.15). Using the relation that a momentum operator is given by $-i\hbar$ times grandient in the quantum mechanics, Eq. (B.6) becomes

$$[\nabla_{\boldsymbol{r}_1}, \nabla_{\boldsymbol{r}_2}, \nabla_{\boldsymbol{r}_{\mathrm{B}}}] = [\nabla_{\boldsymbol{R}_1}, \nabla_{\boldsymbol{R}_2}, \nabla_{\boldsymbol{R}_{\mathrm{c.m.}}}] \begin{bmatrix} 1 & 0 & -1 \\ 0 & 1 & -1 \\ \frac{m_1}{m_{\mathrm{tot}}} & \frac{m_2}{m_{\mathrm{tot}}} & \frac{m_{\mathrm{B}}}{m_{\mathrm{tot}}} \end{bmatrix}. \tag{B.7}$$

It is none other than matrix notation of Eq. (2.16).

Appendix C

Detailed calculation of transition matrix of reaction between a nucleon and two-nucleon system

In this appendix, I present the detailed calculation of the transition matrix Eqs. (2.109)-(2.111). The same notation used in Section 2.3 is employed.

C.1 Spin and isospin rearrangement

We rearrange the spin and isospin parts of Eqs. (2.109)-(2.111) in order to the system of particles N_1 and N_2 having the total spin S_{12} and the total isospin T_{12} as

$$\begin{aligned}
&\eta^{(1)}_{\frac{1}{2}\mu_1}\left[\eta^{(2)}_{\frac{1}{2}}\otimes\eta^{(3)}_{\frac{1}{2}}\right]_{I_\mathrm{x}\mu_\mathrm{x}} \\
&\quad=\sum_{SM_S}\left(I_\mathrm{x}\mu_\mathrm{x}\frac{1}{2}\mu_1\middle|SM_S\right)\left[\left[\eta^{(2)}_{\frac{1}{2}}\otimes\eta^{(3)}_{\frac{1}{2}}\right]_{I_\mathrm{x}}\otimes\eta^{(1)}_{\frac{1}{2}}\right]_{SM_S} \\
&\quad=\sum_{SM_S}\left(I_\mathrm{x}\mu_\mathrm{x}\frac{1}{2}\mu_1\middle|SM_S\right)\sum_{S_{12}}(-)^{1+I_\mathrm{x}+S_{12}}\hat{s}_\mathrm{x}\hat{S}_{12}\begin{Bmatrix}1/2 & 1/2 & S_{12}\\ S & 1/2 & I_\mathrm{x}\end{Bmatrix}\left[\left[\eta^{(2)}_{\frac{1}{2}}\otimes\eta^{(1)}_{\frac{1}{2}}\right]_{S_{12}}\otimes\eta^{(3)}_{\frac{1}{2}}\right]_{SM_S},
\end{aligned}\tag{C.1}$$

$$\begin{aligned}
&\zeta^{(1)}_{\frac{1}{2}\nu_1}\left[\zeta^{(2)}_{\frac{1}{2}}\otimes\zeta^{(3)}_{\frac{1}{2}}\right]_{t_\mathrm{x}\nu_\mathrm{x}} \\
&\quad=\sum_{TM_T}\left(t_\mathrm{x}\nu_\mathrm{x}\frac{1}{2}\nu_1\middle|TM_T\right)\left[\left[\zeta^{(2)}_{\frac{1}{2}}\otimes\zeta^{(3)}_{\frac{1}{2}}\right]_{t_\mathrm{x}}\otimes\zeta^{(1)}_{\frac{1}{2}}\right]_{TM_T} \\
&\quad=\sum_{TM_T}\left(t_\mathrm{x}\nu_\mathrm{x}\frac{1}{2}\nu_1\middle|TM_T\right)\sum_{T_{12}}(-)^{1+t_\mathrm{x}+T_{12}}\hat{t}_\mathrm{x}\hat{T}_{12}\begin{Bmatrix}1/2 & 1/2 & T_{12}\\ T & 1/2 & t_\mathrm{x}\end{Bmatrix}\left[\left[\zeta^{(2)}_{\frac{1}{2}}\otimes\zeta^{(1)}_{\frac{1}{2}}\right]_{T_{12}}\otimes\zeta^{(3)}_{\frac{1}{2}}\right]_{TM_T},
\end{aligned}\tag{C.2}$$

$$\begin{aligned}
&\eta^{(2)}_{\frac{1}{2}\mu_1}\left[\eta^{(1)}_{\frac{1}{2}}\otimes\eta^{(3)}_{\frac{1}{2}}\right]_{I_\mathrm{x}\mu_\mathrm{x}} \\
&\quad=\sum_{SM_S}\left(I_\mathrm{x}\mu_\mathrm{x}\frac{1}{2}\mu_1\middle|SM_S\right)\left[\left[\eta^{(1)}_{\frac{1}{2}}\otimes\eta^{(3)}_{\frac{1}{2}}\right]_{I_\mathrm{x}}\otimes\eta^{(2)}_{\frac{1}{2}}\right]_{SM_S} \\
&\quad=\sum_{SM_S}\left(I_\mathrm{x}\mu_\mathrm{x}\frac{1}{2}\mu_1\middle|SM_S\right)\sum_{S_{12}}(-)^{1+I_\mathrm{x}+S_{12}}\hat{s}_\mathrm{x}\hat{S}_{12}\begin{Bmatrix}1/2 & 1/2 & S_{12}\\ S & 1/2 & I_\mathrm{x}\end{Bmatrix}\left[\left[\eta^{(1)}_{\frac{1}{2}}\otimes\eta^{(2)}_{\frac{1}{2}}\right]_{S_{12}}\otimes\eta^{(3)}_{\frac{1}{2}}\right]_{SM_S}
\end{aligned}$$

$$= \sum_{SM_S} \left(I_x\mu_x \frac{1}{2}\mu_1 \middle| SM_S \right) \sum_{S_{12}} (-)^{I_x} \hat{s}_x \hat{S}_{12} \begin{Bmatrix} 1/2 & 1/2 & S_{12} \\ S & 1/2 & I_x \end{Bmatrix} \left[\left[\eta^{(2)}_{\frac{1}{2}} \otimes \eta^{(1)}_{\frac{1}{2}} \right]_{S_{12}} \otimes \eta^{(3)}_{\frac{1}{2}} \right]_{SM_S}, \tag{C.3}$$

$$\begin{aligned} &\zeta^{(2)}_{\frac{1}{2}\nu_1} \left[\zeta^{(1)}_{\frac{1}{2}} \otimes \zeta^{(3)}_{\frac{1}{2}} \right]_{t_x\nu_x} \\ &= \sum_{TM_T} \left(t_x\nu_x \frac{1}{2}\nu_1 \middle| TM_T \right) \left[\left[\zeta^{(1)}_{\frac{1}{2}} \otimes \zeta^{(3)}_{\frac{1}{2}} \right]_{t_x} \otimes \zeta^{(2)}_{\frac{1}{2}} \right]_{TM_T} \\ &= \sum_{TM_T} \left(t_x\nu_x \frac{1}{2}\nu_1 \middle| TM_T \right) \sum_{T_{12}} (-)^{1+t_x+T_{12}} \hat{t}_x \hat{T}_{12} \begin{Bmatrix} 1/2 & 1/2 & T_{12} \\ T & 1/2 & t_x \end{Bmatrix} \left[\left[\zeta^{(1)}_{\frac{1}{2}} \otimes \zeta^{(2)}_{\frac{1}{2}} \right]_{T_{12}} \otimes \zeta^{(3)}_{\frac{1}{2}} \right]_{TM_T} \\ &= \sum_{TM_T} \left(t_x\nu_x \frac{1}{2}\nu_1 \middle| TM_T \right) \sum_{T_{12}} (-)^{t_x} \hat{t}_x \hat{T}_{12} \begin{Bmatrix} 1/2 & 1/2 & T_{12} \\ T & 1/2 & t_x \end{Bmatrix} \left[\left[\zeta^{(2)}_{\frac{1}{2}} \otimes \zeta^{(1)}_{\frac{1}{2}} \right]_{T_{12}} \otimes \zeta^{(3)}_{\frac{1}{2}} \right]_{TM_T}, \end{aligned} \tag{C.4}$$

$$\eta^{(3)}_{\frac{1}{2}\mu_1} \left[\eta^{(2)}_{\frac{1}{2}} \otimes \eta^{(1)}_{\frac{1}{2}} \right]_{I_x\mu_x} = \sum_{SM_S} \left(I_x\mu_x \frac{1}{2}\mu_1 \middle| SM_S \right) \left[\left[\eta^{(2)}_{\frac{1}{2}} \otimes \eta^{(1)}_{\frac{1}{2}} \right]_{I_x} \otimes \eta^{(3)}_{\frac{1}{2}} \right]_{SM_S}, \tag{C.5}$$

$$\zeta^{(3)}_{\frac{1}{2}\nu_1} \left[\zeta^{(2)}_{\frac{1}{2}} \otimes \zeta^{(1)}_{\frac{1}{2}} \right]_{t_x\nu_x} = \sum_{TM_T} \left(t_x\nu_x \frac{1}{2}\nu_1 \middle| TM_T \right) \left[\left[\zeta^{(2)}_{\frac{1}{2}} \otimes \zeta^{(1)}_{\frac{1}{2}} \right]_{t_x} \otimes \zeta^{(3)}_{\frac{1}{2}} \right]_{TM_T}. \tag{C.6}$$

The total spin and isospin of the three-nucleon system are denoted by S and T, respectively. It should be noted that in Eqs. (C.5) and (C.6), S_{12} is equal to I_x and T_{12} is t_x. In the same way, we obtain

$$\begin{aligned} &\eta^{(1)}_{\frac{1}{2}\mu_1} \left[\eta^{(2)}_{\frac{1}{2}} \otimes \eta^{(3)}_{\frac{1}{2}} \right]_{I_x\mu_x} \\ &= \sum_{SM_S} \left(I_x\mu_x \frac{1}{2}\mu_1 \middle| SM_S \right) \left[\left[\eta^{(2)}_{\frac{1}{2}} \otimes \eta^{(3)}_{\frac{1}{2}} \right]_{I_x} \otimes \eta^{(1)}_{\frac{1}{2}} \right]_{SM_S} \\ &= \sum_{SM_S} \left(I_x\mu_x \frac{1}{2}\mu_1 \middle| SM_S \right) \left[(-)^{1-I_x} \left[\eta^{(3)}_{\frac{1}{2}} \otimes \eta^{(2)}_{\frac{1}{2}} \right]_{I_x} \otimes \eta^{(1)}_{\frac{1}{2}} \right]_{SM_S} \\ &= \sum_{SM_S} \left(I_x\mu_x \frac{1}{2}\mu_1 \middle| SM_S \right) \sum_{S_{13}} (-)^{S_{13}} \hat{s}_x \hat{S}_{13} \begin{Bmatrix} 1/2 & 1/2 & S_{13} \\ S & 1/2 & I_x \end{Bmatrix} \left[\left[\eta^{(3)}_{\frac{1}{2}} \otimes \eta^{(1)}_{\frac{1}{2}} \right]_{S_{13}} \otimes \eta^{(2)}_{\frac{1}{2}} \right]_{SM_S}, \end{aligned} \tag{C.7}$$

$$\begin{aligned} &\zeta^{(1)}_{\frac{1}{2}\nu_1} \left[\zeta^{(2)}_{\frac{1}{2}} \otimes \zeta^{(3)}_{\frac{1}{2}} \right]_{t_x\nu_x} \\ &= \sum_{TM_T} \left(t_x\nu_x \frac{1}{2}\nu_1 \middle| TM_T \right) \left[\left[\zeta^{(2)}_{\frac{1}{2}} \otimes \zeta^{(3)}_{\frac{1}{2}} \right]_{t_x} \otimes \zeta^{(1)}_{\frac{1}{2}} \right]_{TM_T} \\ &= \sum_{TM_T} \left(t_x\nu_x \frac{1}{2}\nu_1 \middle| TM_T \right) \left[(-)^{1-t_x} \left[\zeta^{(3)}_{\frac{1}{2}} \otimes \zeta^{(2)}_{\frac{1}{2}} \right]_{t_x} \otimes \zeta^{(1)}_{\frac{1}{2}} \right]_{TM_T} \\ &= \sum_{TM_T} \left(t_x\nu_x \frac{1}{2}\nu_1 \middle| TM_T \right) \sum_{T_{13}} (-)^{T_{13}} \hat{t}_x \hat{T}_{13} \begin{Bmatrix} 1/2 & 1/2 & T_{13} \\ T & 1/2 & t_x \end{Bmatrix} \left[\left[\zeta^{(3)}_{\frac{1}{2}} \otimes \zeta^{(1)}_{\frac{1}{2}} \right]_{T_{13}} \otimes \zeta^{(2)}_{\frac{1}{2}} \right]_{TM_T}, \end{aligned} \tag{C.8}$$

$$\eta^{(2)}_{\frac{1}{2}\mu_1}\left[\eta^{(1)}_{\frac{1}{2}}\otimes\eta^{(3)}_{\frac{1}{2}}\right]_{I_x\mu_x} = (-)^{1-I_x}\sum_{SM_S}\left(I_x\mu_x\frac{1}{2}\mu_1\middle|SM_S\right)\left[\left[\eta^{(3)}_{\frac{1}{2}}\otimes\eta^{(1)}_{\frac{1}{2}}\right]_{I_x}\otimes\eta^{(2)}_{\frac{1}{2}}\right]_{SM_S}, \tag{C.9}$$

$$\zeta^{(2)}_{\frac{1}{2}\nu_1}\left[\zeta^{(1)}_{\frac{1}{2}}\otimes\zeta^{(3)}_{\frac{1}{2}}\right]_{t_x\nu_x} = (-)^{1-t_x}\sum_{TM_T}\left(t_x\nu_x\frac{1}{2}\nu_1\middle|TM_T\right)\left[\left[\zeta^{(3)}_{\frac{1}{2}}\otimes\zeta^{(1)}_{\frac{1}{2}}\right]_{t_x}\otimes\zeta^{(2)}_{\frac{1}{2}}\right]_{TM_T}, \tag{C.10}$$

$$\begin{aligned}
&\eta^{(3)}_{\frac{1}{2}\mu_1}\left[\eta^{(2)}_{\frac{1}{2}}\otimes\eta^{(1)}_{\frac{1}{2}}\right]_{I_x\mu_x}\\
&=\sum_{SM_S}\left(I_x\mu_x\frac{1}{2}\mu_1\middle|SM_S\right)\left[\left[\eta^{(2)}_{\frac{1}{2}}\otimes\eta^{(1)}_{\frac{1}{2}}\right]_{I_x}\otimes\eta^{(3)}_{\frac{1}{2}}\right]_{SM_S}\\
&=\sum_{SM_S}\left(I_x\mu_x\frac{1}{2}\mu_1\middle|SM_S\right)\left[(-)^{1-I_x}\left[\eta^{(1)}_{\frac{1}{2}}\otimes\eta^{(2)}_{\frac{1}{2}}\right]_{I_x}\otimes\eta^{(3)}_{\frac{1}{2}}\right]_{SM_S}\\
&=\sum_{SM_S}\left(I_x\mu_x\frac{1}{2}\mu_1\middle|SM_S\right)\sum_{S_{13}}(-)^{S_{13}}\hat{s}_x\hat{S}_{13}\begin{Bmatrix}1/2 & 1/2 & S_{13}\\ S & 1/2 & I_x\end{Bmatrix}\left[\left[\eta^{(1)}_{\frac{1}{2}}\otimes\eta^{(3)}_{\frac{1}{2}}\right]_{S_{13}}\otimes\eta^{(2)}_{\frac{1}{2}}\right]_{SM_S}\\
&=\sum_{SM_S}\left(I_x\mu_x\frac{1}{2}\mu_1\middle|SM_S\right)\sum_{S_{13}}(-)\hat{s}_x\hat{S}_{13}\begin{Bmatrix}1/2 & 1/2 & S_{13}\\ S & 1/2 & I_x\end{Bmatrix}\left[\left[\eta^{(3)}_{\frac{1}{2}}\otimes\eta^{(1)}_{\frac{1}{2}}\right]_{S_{13}}\otimes\eta^{(2)}_{\frac{1}{2}}\right]_{SM_S},
\end{aligned} \tag{C.11}$$

$$\begin{aligned}
&\zeta^{(3)}_{\frac{1}{2}\nu_1}\left[\zeta^{(2)}_{\frac{1}{2}}\otimes\zeta^{(1)}_{\frac{1}{2}}\right]_{t_x\nu_x}\\
&=\sum_{TM_T}\left(t_x\nu_x\frac{1}{2}\nu_1\middle|TM_T\right)\left[\left[\zeta^{(2)}_{\frac{1}{2}}\otimes\zeta^{(1)}_{\frac{1}{2}}\right]_{t_x}\otimes\zeta^{(3)}_{\frac{1}{2}}\right]_{TM_T}\\
&=\sum_{TM_T}\left(t_x\nu_x\frac{1}{2}\nu_1\middle|TM_T\right)\left[(-)^{1-t_x}\left[\zeta^{(1)}_{\frac{1}{2}}\otimes\zeta^{(2)}_{\frac{1}{2}}\right]_{t_x}\otimes\zeta^{(3)}_{\frac{1}{2}}\right]_{TM_T}\\
&=\sum_{TM_T}\left(t_x\nu_x\frac{1}{2}\nu_1\middle|TM_T\right)\sum_{T_{13}}(-)^{T_{13}}\hat{t}_x\hat{T}_{13}\begin{Bmatrix}1/2 & 1/2 & T_{13}\\ T & 1/2 & t_x\end{Bmatrix}\left[\left[\zeta^{(1)}_{\frac{1}{2}}\otimes\zeta^{(3)}_{\frac{1}{2}}\right]_{T_{13}}\otimes\zeta^{(2)}_{\frac{1}{2}}\right]_{TM_T}\\
&=\sum_{TM_T}\left(t_x\nu_x\frac{1}{2}\nu_1\middle|TM_T\right)\sum_{T_{13}}(-)\hat{t}_x\hat{T}_{13}\begin{Bmatrix}1/2 & 1/2 & T_{13}\\ T & 1/2 & t_x\end{Bmatrix}\left[\left[\zeta^{(3)}_{\frac{1}{2}}\otimes\zeta^{(1)}_{\frac{1}{2}}\right]_{T_{13}}\otimes\zeta^{(2)}_{\frac{1}{2}}\right]_{TM_T}.
\end{aligned} \tag{C.12}$$

Similarly in Eqs. (C.5) and (C.6), the total spin S_{13} and isospin T_{13} of the system of paricle N_1 and N_3 are are I_x and t_x in Eqs. (C.9) and (C.10), respectively.

Utilizing these equations, the isospin parts in Eqs. (2.109)-(2.111) are calculated as

$$\begin{aligned}
&Z^{t_x,S_{12}}_{12:123}(\nu_1'\nu_x'|\nu_1\nu_x)\\
&\equiv\left\langle\zeta^{(1)}_{\frac{1}{2}\nu_1'}\left[\zeta^{(2)}_{\frac{1}{2}}\otimes\zeta^{(3)}_{\frac{1}{2}}\right]_{t_x\nu_x'}\middle|\sum_{T_{12}}t_{12}^{S_{12}T_{12}}\hat{P}_{12}^{T_{12}}\middle|\zeta^{(1)}_{\frac{1}{2}\nu_1}\left[\zeta^{(2)}_{\frac{1}{2}}\otimes\zeta^{(3)}_{\frac{1}{2}}\right]_{t_x\nu_x}\right\rangle\\
&=\hat{t}_x^2\sum_{T'M_T'}\sum_{TM_T}\left(t_x\nu_x'\frac{1}{2}\nu_1'\middle|T'M_T'\right)\left(t_x\nu_x\frac{1}{2}\nu_1\middle|TM_T\right)\\
&\quad\times\sum_{T_{12}'T_{12}}(-)^{T_{12}'+T_{12}}t_{12}^{S_{12}T_{12}}\hat{T}_{12}'\hat{T}_{12}\begin{Bmatrix}1/2 & 1/2 & T_{12}'\\ T' & 1/2 & t_x\end{Bmatrix}\begin{Bmatrix}1/2 & 1/2 & T_{12}\\ T & 1/2 & t_x\end{Bmatrix}
\end{aligned}$$

$$
\begin{aligned}
&\times\left\langle\left[\left[\zeta^{(2)}_{\frac{1}{2}}\otimes\zeta^{(1)}_{\frac{1}{2}}\right]_{T'_{12}}\otimes\zeta^{(3)}_{\frac{1}{2}}\right]_{T'M'_T}\middle|\left[\left[\zeta^{(2)}_{\frac{1}{2}}\otimes\zeta^{(1)}_{\frac{1}{2}}\right]_{T_{12}}\otimes\zeta^{(3)}_{\frac{1}{2}}\right]_{TM_T}\right\rangle\\
&=\hat{t}_{\mathrm{x}}^2\sum_{TM_T}\left(t_{\mathrm{x}}\nu'_{\mathrm{x}}\frac{1}{2}\nu'_1\middle|TM_T\right)\left(t_{\mathrm{x}}\nu_{\mathrm{x}}\frac{1}{2}\nu_1\middle|TM_T\right)\sum_{T_{12}}t_{12}^{S_{12}T_{12}}\hat{T}_{12}^2\begin{Bmatrix}1/2 & 1/2 & T_{12}\\ T & 1/2 & t_{\mathrm{x}}\end{Bmatrix}^2,
\end{aligned}
\tag{C.13}
$$

$$
\begin{aligned}
&Z^{t_{\mathrm{x}},S_{13}}_{13:123}(\nu'_1\nu'_{\mathrm{x}}|\nu_1\nu_{\mathrm{x}})\\
&\equiv\left\langle\zeta^{(1)}_{\frac{1}{2}\nu'_1}\left[\zeta^{(2)}_{\frac{1}{2}}\otimes\zeta^{(3)}_{\frac{1}{2}}\right]_{t_{\mathrm{x}}\nu'_{\mathrm{x}}}\middle|\sum_{T_{13}}t_{13}^{S_{13}T_{13}}\hat{P}_{13}^{T_{13}}\middle|\zeta^{(1)}_{\frac{1}{2}\nu_1}\left[\zeta^{(2)}_{\frac{1}{2}}\otimes\zeta^{(3)}_{\frac{1}{2}}\right]_{t_{\mathrm{x}}\nu_{\mathrm{x}}}\right\rangle\\
&=\hat{t}_{\mathrm{x}}^2\sum_{T'M'_T}\sum_{TM_T}\left(t_{\mathrm{x}}\nu'_{\mathrm{x}}\frac{1}{2}\nu'_1\middle|T'M'_T\right)\left(t_{\mathrm{x}}\nu_{\mathrm{x}}\frac{1}{2}\nu_1\middle|TM_T\right)\\
&\quad\times\sum_{T'_{13}T_{13}}(-)^{T'_{13}+T_{13}}t_{13}^{S_{13}T_{13}}\hat{T}'_{13}\hat{T}_{13}\begin{Bmatrix}1/2 & 1/2 & T'_{13}\\ T' & 1/2 & t_{\mathrm{x}}\end{Bmatrix}\begin{Bmatrix}1/2 & 1/2 & T_{13}\\ T & 1/2 & t_{\mathrm{x}}\end{Bmatrix}\\
&\qquad\times\left\langle\left[\left[\zeta^{(3)}_{\frac{1}{2}}\otimes\zeta^{(1)}_{\frac{1}{2}}\right]_{T'_{13}}\otimes\zeta^{(2)}_{\frac{1}{2}}\right]_{T'M'_T}\middle|\left[\left[\zeta^{(3)}_{\frac{1}{2}}\otimes\zeta^{(1)}_{\frac{1}{2}}\right]_{T_{13}}\otimes\zeta^{(2)}_{\frac{1}{2}}\right]_{TM_T}\right\rangle\\
&=\hat{t}_{\mathrm{x}}^2\sum_{TM_T}\left(t_{\mathrm{x}}\nu'_{\mathrm{x}}\frac{1}{2}\nu'_1\middle|TM_T\right)\left(t_{\mathrm{x}}\nu_{\mathrm{x}}\frac{1}{2}\nu_1\middle|TM_T\right)\sum_{T_{13}}t_{13}^{S_{13}T_{13}}\hat{T}_{13}^2\begin{Bmatrix}1/2 & 1/2 & T_{13}\\ T & 1/2 & t_{\mathrm{x}}\end{Bmatrix}^2,
\end{aligned}
\tag{C.14}
$$

$$
\begin{aligned}
&Z^{t_{\mathrm{x}},S_{12}}_{12:213}(\nu'_1\nu'_{\mathrm{x}}|\nu_1\nu_{\mathrm{x}})\\
&\equiv\left\langle\zeta^{(1)}_{\frac{1}{2}\nu'_1}\left[\zeta^{(2)}_{\frac{1}{2}}\otimes\zeta^{(3)}_{\frac{1}{2}}\right]_{t_{\mathrm{x}}\nu'_{\mathrm{x}}}\middle|\sum_{T_{12}}t_{12}^{S_{12}T_{12}}\hat{P}_{12}^{T_{12}}\middle|\zeta^{(2)}_{\frac{1}{2}\nu_1}\left[\zeta^{(1)}_{\frac{1}{2}}\otimes\zeta^{(3)}_{\frac{1}{2}}\right]_{t_{\mathrm{x}}\nu_{\mathrm{x}}}\right\rangle\\
&=\hat{t}_{\mathrm{x}}^2\sum_{T'M'_T}\sum_{TM_T}\left(t_{\mathrm{x}}\nu'_{\mathrm{x}}\frac{1}{2}\nu'_1\middle|T'M'_T\right)\left(t_{\mathrm{x}}\nu_{\mathrm{x}}\frac{1}{2}\nu_1\middle|TM_T\right)\\
&\quad\times\sum_{T'_{12}T_{12}}(-)^{1+T'_{12}}t_{12}^{S_{12}T_{12}}\hat{T}'_{12}\hat{T}_{12}\begin{Bmatrix}1/2 & 1/2 & T'_{12}\\ T' & 1/2 & t_{\mathrm{x}}\end{Bmatrix}\begin{Bmatrix}1/2 & 1/2 & T_{12}\\ T & 1/2 & t_{\mathrm{x}}\end{Bmatrix}\\
&\qquad\times\left\langle\left[\left[\zeta^{(2)}_{\frac{1}{2}}\otimes\zeta^{(1)}_{\frac{1}{2}}\right]_{T'_{12}}\otimes\zeta^{(3)}_{\frac{1}{2}}\right]_{T'M'_T}\middle|\left[\left[\zeta^{(2)}_{\frac{1}{2}}\otimes\zeta^{(1)}_{\frac{1}{2}}\right]_{T_{12}}\otimes\zeta^{(3)}_{\frac{1}{2}}\right]_{TM_T}\right\rangle\\
&=\hat{t}_{\mathrm{x}}^2\sum_{TM_T}\left(t_{\mathrm{x}}\nu'_{\mathrm{x}}\frac{1}{2}\nu'_1\middle|TM_T\right)\left(t_{\mathrm{x}}\nu_{\mathrm{x}}\frac{1}{2}\nu_1\middle|TM_T\right)\sum_{T_{12}}(-)^{1+T_{12}}t_{12}^{S_{12}T_{12}}\hat{T}_{12}^2\begin{Bmatrix}1/2 & 1/2 & T_{12}\\ T & 1/2 & t_{\mathrm{x}}\end{Bmatrix}^2,
\end{aligned}
\tag{C.15}
$$

$$
\begin{aligned}
&Z^{t_{\mathrm{x}},S_{13}}_{13:321}(\nu'_1\nu'_{\mathrm{x}}|\nu_1\nu_{\mathrm{x}})\\
&\equiv\left\langle\zeta^{(1)}_{\frac{1}{2}\nu'_1}\left[\zeta^{(2)}_{\frac{1}{2}}\otimes\zeta^{(3)}_{\frac{1}{2}}\right]_{t_{\mathrm{x}}\nu'_{\mathrm{x}}}\middle|\sum_{T_{13}}t_{13}^{S_{13}T_{13}}\hat{P}_{13}^{T_{13}}\middle|\zeta^{(3)}_{\frac{1}{2}\nu_1}\left[\zeta^{(2)}_{\frac{1}{2}}\otimes\zeta^{(1)}_{\frac{1}{2}}\right]_{t_{\mathrm{x}}\nu_{\mathrm{x}}}\right\rangle\\
&=\hat{t}_{\mathrm{x}}^2\sum_{T'M'_T}\sum_{TM_T}\left(t_{\mathrm{x}}\nu'_{\mathrm{x}}\frac{1}{2}\nu'_1\middle|T'M'_T\right)\left(t_{\mathrm{x}}\nu_{\mathrm{x}}\frac{1}{2}\nu_1\middle|TM_T\right)
\end{aligned}
$$

$$
\begin{aligned}
&\times \sum_{T'_{13}T_{13}} (-)^{1+T'_{13}} t_{13}^{S_{13}T_{13}} \hat{T}'_{13}\hat{T}_{13} \begin{Bmatrix} 1/2 & 1/2 & T'_{13} \\ T' & 1/2 & t_\mathrm{x} \end{Bmatrix} \begin{Bmatrix} 1/2 & 1/2 & T_{13} \\ T & 1/2 & t_\mathrm{x} \end{Bmatrix} \\
&\quad \times \left\langle \left[\left[\zeta_{\frac{1}{2}}^{(3)} \otimes \zeta_{\frac{1}{2}}^{(1)} \right]_{T'_{13}} \otimes \zeta_{\frac{1}{2}}^{(2)} \right]_{T'M'_T} \middle| \left[\left[\zeta_{\frac{1}{2}}^{(3)} \otimes \zeta_{\frac{1}{2}}^{(1)} \right]_{T_{13}} \otimes \zeta_{\frac{1}{2}}^{(2)} \right]_{TM_T} \right\rangle \\
&= \hat{t}_\mathrm{x}^2 \sum_{TM_T} \left(t_\mathrm{x}\nu'_\mathrm{x}\frac{1}{2}\nu'_1 \middle| TM_T \right) \left(t_\mathrm{x}\nu_\mathrm{x}\frac{1}{2}\nu_1 \middle| TM_T \right) \sum_{T_{13}} (-)^{1+T_{13}} t_{13}^{S_{13}T_{13}} \hat{T}_{13}^2 \begin{Bmatrix} 1/2 & 1/2 & T_{13} \\ T & 1/2 & t_\mathrm{x} \end{Bmatrix}^2,
\end{aligned}
\tag{C.16}
$$

$$
\begin{aligned}
&Z_{12:321}^{t_\mathrm{x},S_{12}}(\nu'_1\nu'_\mathrm{x}|\nu_1\nu_\mathrm{x}) \\
&\equiv \left\langle \zeta_{\frac{1}{2}\nu'_1}^{(1)} \left[\zeta_{\frac{1}{2}}^{(2)} \otimes \zeta_{\frac{1}{2}}^{(3)} \right]_{t_\mathrm{x}\nu'_\mathrm{x}} \middle| \sum_{T_{12}} t_{12}^{S_{12}T_{12}} \hat{P}_{12}^{T_{12}} \middle| \zeta_{\frac{1}{2}\nu_1}^{(3)} \left[\zeta_{\frac{1}{2}}^{(2)} \otimes \zeta_{\frac{1}{2}}^{(1)} \right]_{t_\mathrm{x}\nu_\mathrm{x}} \right\rangle \\
&= \hat{t}_\mathrm{x} \sum_{T'M'_T} \sum_{TM_T} \left(t_\mathrm{x}\nu'_\mathrm{x}\frac{1}{2}\nu'_1 \middle| T'M'_T \right) \left(t_\mathrm{x}\nu_\mathrm{x}\frac{1}{2}\nu_1 \middle| TM_T \right) \sum_{T'_{12}} (-)^{1+t_\mathrm{x}+T'_{12}} t_{12}^{S_{12}t_\mathrm{x}} \hat{T}'_{12} \\
&\quad \times \begin{Bmatrix} 1/2 & 1/2 & T'_{12} \\ T' & 1/2 & t_\mathrm{x} \end{Bmatrix} \left\langle \left[\left[\zeta_{\frac{1}{2}}^{(2)} \otimes \zeta_{\frac{1}{2}}^{(1)} \right]_{T'_{12}} \otimes \zeta_{\frac{1}{2}}^{(3)} \right]_{T'M'_T} \middle| \left[\left[\zeta_{\frac{1}{2}}^{(2)} \otimes \zeta_{\frac{1}{2}}^{(1)} \right]_{t_\mathrm{x}} \otimes \zeta_{\frac{1}{2}}^{(3)} \right]_{TM_T} \right\rangle \\
&= -\hat{t}_\mathrm{x}^2 \sum_{TM_T} \left(t_\mathrm{x}\nu'_\mathrm{x}\frac{1}{2}\nu'_1 \middle| TM_T \right) \left(t_\mathrm{x}\nu_\mathrm{x}\frac{1}{2}\nu_1 \middle| TM_T \right) t_{12}^{S_{12}t_\mathrm{x}} \begin{Bmatrix} 1/2 & 1/2 & t_\mathrm{x} \\ T & 1/2 & t_\mathrm{x} \end{Bmatrix},
\end{aligned}
\tag{C.17}
$$

$$
\begin{aligned}
&Z_{13:213}^{t_\mathrm{x},S_{13}}(\nu'_1\nu'_\mathrm{x}|\nu_1\nu_\mathrm{x}) \\
&\equiv \left\langle \zeta_{\frac{1}{2}\nu'_1}^{(1)} \left[\zeta_{\frac{1}{2}}^{(2)} \otimes \zeta_{\frac{1}{2}}^{(3)} \right]_{t_\mathrm{x}\nu'_\mathrm{x}} \middle| \sum_{T_{13}} t_{13}^{S_{13}T_{13}} \hat{P}_{13}^{T_{13}} \middle| \zeta_{\frac{1}{2}\nu_1}^{(2)} \left[\zeta_{\frac{1}{2}}^{(1)} \otimes \zeta_{\frac{1}{2}}^{(3)} \right]_{t_\mathrm{x}\nu_\mathrm{x}} \right\rangle \\
&= \hat{t}_\mathrm{x} \sum_{T'M'_T} \sum_{TM_T} \left(t_\mathrm{x}\nu'_\mathrm{x}\frac{1}{2}\nu'_1 \middle| T'M'_T \right) \left(t_\mathrm{x}\nu_\mathrm{x}\frac{1}{2}\nu_1 \middle| TM_T \right) \sum_{T'_{13}} (-)^{1-t_\mathrm{x}+T'_{13}} t_{13}^{S_{13}t_\mathrm{x}} \hat{T}'_{13} \\
&\quad \times \begin{Bmatrix} 1/2 & 1/2 & T'_{13} \\ T' & 1/2 & t_\mathrm{x} \end{Bmatrix} \left\langle \left[\left[\zeta_{\frac{1}{2}}^{(3)} \otimes \zeta_{\frac{1}{2}}^{(1)} \right]_{T'_{13}} \otimes \zeta_{\frac{1}{2}}^{(2)} \right]_{T'M'_T} \middle| \left[\left[\zeta_{\frac{1}{2}}^{(3)} \otimes \zeta_{\frac{1}{2}}^{(1)} \right]_{t_\mathrm{x}} \otimes \zeta_{\frac{1}{2}}^{(2)} \right]_{TM_T} \right\rangle \\
&= -\hat{t}_\mathrm{x}^2 \sum_{TM_T} \left(t_\mathrm{x}\nu'_\mathrm{x}\frac{1}{2}\nu'_1 \middle| TM_T \right) \left(t_\mathrm{x}\nu_\mathrm{x}\frac{1}{2}\nu_1 \middle| TM_T \right) t_{13}^{S_{13}t_\mathrm{x}} \begin{Bmatrix} 1/2 & 1/2 & t_\mathrm{x} \\ T & 1/2 & t_\mathrm{x} \end{Bmatrix}.
\end{aligned}
\tag{C.18}
$$

Here, we have used the three properties that (i) the effective interaction $t_{1j}^{S_{1j}T_{1j}}$ does not change the isospins, that (ii) the isospin functions have the orthonormality, and that (iii) t_x and T_{1j} are zero or unity.

Similarly, the spin parts in Eqs. (2.109)-(2.111) are calculated as

$$
\begin{aligned}
&E_{12:123}^{I_\mathrm{x}t_\mathrm{x}}(\mu'_1\nu'_1\mu'_\mathrm{x}\nu'_\mathrm{x}|\mu_1\nu_1\mu_\mathrm{x}\nu_\mathrm{x}) \\
&\equiv \left\langle \eta_{\frac{1}{2}\mu'_1}^{(1)} \left[\eta_{\frac{1}{2}}^{(2)} \otimes \eta_{\frac{1}{2}}^{(3)} \right]_{I_\mathrm{x}\mu'_\mathrm{x}} \middle| \sum_{S_{12}} Z_{12:123}^{t_\mathrm{x},S_{12}}(\nu'_1\nu'_\mathrm{x}|\nu_1\nu_\mathrm{x}) \hat{P}_{12}^{S_{12}} \middle| \eta_{\frac{1}{2}\mu_1}^{(1)} \left[\eta_{\frac{1}{2}}^{(2)} \otimes \eta_{\frac{1}{2}}^{(3)} \right]_{I_\mathrm{x}\mu_\mathrm{x}} \right\rangle \\
&= \hat{s}_\mathrm{x}^2 \sum_{S'M'_S} \sum_{SM_S} \left(I_\mathrm{x}\mu'_\mathrm{x}\frac{1}{2}\mu'_1 \middle| S'M'_S \right) \left(I_\mathrm{x}\mu_\mathrm{x}\frac{1}{2}\mu_1 \middle| SM_S \right) \sum_{S_{12}} \hat{S}_{12}^2 \begin{Bmatrix} 1/2 & 1/2 & S_{12} \\ S' & 1/2 & I_\mathrm{x} \end{Bmatrix} \begin{Bmatrix} 1/2 & 1/2 & S_{12} \\ S & 1/2 & I_\mathrm{x} \end{Bmatrix}
\end{aligned}
$$

$$\times \left\langle \left[\left[\eta^{(2)}_{\frac{1}{2}} \otimes \eta^{(1)}_{\frac{1}{2}} \right]_{S_{12}} \otimes \eta^{(3)}_{\frac{1}{2}} \right]_{S' M_S'} \middle| Z^{t_\mathrm{x},S_{12}}_{12:123}(\nu_1' \nu_\mathrm{x}' | \nu_1 \nu_\mathrm{x}) \middle| \left[\left[\eta^{(2)}_{\frac{1}{2}} \otimes \eta^{(1)}_{\frac{1}{2}} \right]_{S_{12}} \otimes \eta^{(3)}_{\frac{1}{2}} \right]_{S M_S} \right\rangle, \tag{C.19}$$

$$\begin{aligned}
&E^{I_\mathrm{x} t_\mathrm{x}}_{13:123}(\mu_1' \nu_1' \mu_\mathrm{x}' \nu_\mathrm{x}' | \mu_1 \nu_1 \mu_\mathrm{x} \nu_\mathrm{x}) \\
&\equiv \left\langle \eta^{(1)}_{\frac{1}{2}\mu_1'} \left[\eta^{(2)}_{\frac{1}{2}} \otimes \eta^{(3)}_{\frac{1}{2}} \right]_{I_\mathrm{x} \mu_\mathrm{x}'} \middle| \sum_{S_{13}} Z^{t_\mathrm{x},S_{13}}_{13:123}(\nu_1' \nu_\mathrm{x}' | \nu_1 \nu_\mathrm{x}) \hat{P}^{S_{13}}_{13} \middle| \eta^{(1)}_{\frac{1}{2}\mu_1} \left[\eta^{(2)}_{\frac{1}{2}} \otimes \eta^{(3)}_{\frac{1}{2}} \right]_{I_\mathrm{x} \mu_\mathrm{x}} \right\rangle \\
&= \hat{s}_\mathrm{x}^2 \sum_{S' M_S'} \sum_{S M_S} \left(I_\mathrm{x} \mu_\mathrm{x}' \frac{1}{2} \mu_1' \middle| S' M_S' \right) \left(I_\mathrm{x} \mu_\mathrm{x} \frac{1}{2} \mu_1 \middle| S M_S \right) \sum_{S_{13}} \hat{S}_{13}^2 \begin{Bmatrix} 1/2 & 1/2 & S_{13} \\ S' & 1/2 & I_\mathrm{x} \end{Bmatrix} \begin{Bmatrix} 1/2 & 1/2 & S_{13} \\ S & 1/2 & I_\mathrm{x} \end{Bmatrix} \\
&\quad \times \left\langle \left[\left[\eta^{(3)}_{\frac{1}{2}} \otimes \eta^{(1)}_{\frac{1}{2}} \right]_{S_{13}} \otimes \eta^{(2)}_{\frac{1}{2}} \right]_{S' M_S'} \middle| Z^{t_\mathrm{x},S_{13}}_{13:123}(\nu_1' \nu_\mathrm{x}' | \nu_1 \nu_\mathrm{x}) \middle| \left[\left[\eta^{(3)}_{\frac{1}{2}} \otimes \eta^{(1)}_{\frac{1}{2}} \right]_{S_{13}} \otimes \eta^{(2)}_{\frac{1}{2}} \right]_{S M_S} \right\rangle,
\end{aligned} \tag{C.20}$$

$$\begin{aligned}
&E^{I_\mathrm{x} t_\mathrm{x}}_{12:213}(\mu_1' \nu_1' \mu_\mathrm{x}' \nu_\mathrm{x}' | \mu_1 \nu_1 \mu_\mathrm{x} \nu_\mathrm{x}) \\
&\equiv \left\langle \eta^{(1)}_{\frac{1}{2}\mu_1'} \left[\eta^{(2)}_{\frac{1}{2}} \otimes \eta^{(3)}_{\frac{1}{2}} \right]_{I_\mathrm{x} \mu_\mathrm{x}'} \middle| \sum_{S_{12}} Z^{t_\mathrm{x},S_{12}}_{12:213}(\nu_1' \nu_\mathrm{x}' | \nu_1 \nu_\mathrm{x}) \hat{P}^{S_{12}}_{12} \middle| \eta^{(2)}_{\frac{1}{2}\mu_1} \left[\eta^{(1)}_{\frac{1}{2}} \otimes \eta^{(3)}_{\frac{1}{2}} \right]_{I_\mathrm{x} \mu_\mathrm{x}} \right\rangle \\
&= \hat{s}_\mathrm{x}^2 \sum_{S' M_S'} \sum_{S M_S} \left(I_\mathrm{x} \mu_\mathrm{x}' \frac{1}{2} \mu_1' \middle| S' M_S' \right) \left(I_\mathrm{x} \mu_\mathrm{x} \frac{1}{2} \mu_1 \middle| S M_S \right) \\
&\quad \times \sum_{S_{12}} (-)^{1+S_{12}} \hat{S}_{12}^2 \begin{Bmatrix} 1/2 & 1/2 & S_{12} \\ S' & 1/2 & I_\mathrm{x} \end{Bmatrix} \begin{Bmatrix} 1/2 & 1/2 & S_{12} \\ S & 1/2 & I_\mathrm{x} \end{Bmatrix} \\
&\qquad \times \left\langle \left[\left[\eta^{(2)}_{\frac{1}{2}} \otimes \eta^{(1)}_{\frac{1}{2}} \right]_{S_{12}} \otimes \eta^{(3)}_{\frac{1}{2}} \right]_{S' M_S'} \middle| Z^{t_\mathrm{x},S_{12}}_{12:213}(\nu_1' \nu_\mathrm{x}' | \nu_1 \nu_\mathrm{x}) \middle| \left[\left[\eta^{(2)}_{\frac{1}{2}} \otimes \eta^{(1)}_{\frac{1}{2}} \right]_{S_{12}} \otimes \eta^{(3)}_{\frac{1}{2}} \right]_{S M_S} \right\rangle,
\end{aligned} \tag{C.21}$$

$$\begin{aligned}
&E^{I_\mathrm{x} t_\mathrm{x}}_{13:321}(\mu_1' \nu_1' \mu_\mathrm{x}' \nu_\mathrm{x}' | \mu_1 \nu_1 \mu_\mathrm{x} \nu_\mathrm{x}) \\
&\equiv \left\langle \eta^{(1)}_{\frac{1}{2}\mu_1'} \left[\eta^{(2)}_{\frac{1}{2}} \otimes \eta^{(3)}_{\frac{1}{2}} \right]_{I_\mathrm{x} \mu_\mathrm{x}'} \middle| \sum_{S_{13}} Z^{t_\mathrm{x},S_{13}}_{13:321}(\nu_1' \nu_\mathrm{x}' | \nu_1 \nu_\mathrm{x}) \hat{P}^{S_{13}}_{13} \middle| \eta^{(3)}_{\frac{1}{2}\mu_1} \left[\eta^{(2)}_{\frac{1}{2}} \otimes \eta^{(1)}_{\frac{1}{2}} \right]_{I_\mathrm{x} \mu_\mathrm{x}} \right\rangle \\
&= \hat{s}_\mathrm{x}^2 \sum_{S' M_S'} \sum_{S M_S} \left(I_\mathrm{x} \mu_\mathrm{x}' \frac{1}{2} \mu_1' \middle| S' M_S' \right) \left(I_\mathrm{x} \mu_\mathrm{x} \frac{1}{2} \mu_1 \middle| S M_S \right) \\
&\quad \times \sum_{S_{13}} (-)^{1+S_{13}} \hat{S}_{13}^2 \begin{Bmatrix} 1/2 & 1/2 & S_{13} \\ S' & 1/2 & I_\mathrm{x} \end{Bmatrix} \begin{Bmatrix} 1/2 & 1/2 & S_{13} \\ S & 1/2 & I_\mathrm{x} \end{Bmatrix} \\
&\qquad \times \left\langle \left[\left[\eta^{(3)}_{\frac{1}{2}} \otimes \eta^{(1)}_{\frac{1}{2}} \right]_{S_{13}} \otimes \eta^{(2)}_{\frac{1}{2}} \right]_{S' M_S'} \middle| Z^{t_\mathrm{x},S_{13}}_{13:321}(\nu_1' \nu_\mathrm{x}' | \nu_1 \nu_\mathrm{x}) \middle| \left[\left[\eta^{(3)}_{\frac{1}{2}} \otimes \eta^{(1)}_{\frac{1}{2}} \right]_{S_{13}} \otimes \eta^{(2)}_{\frac{1}{2}} \right]_{S M_S} \right\rangle,
\end{aligned} \tag{C.22}$$

$$\begin{aligned}
&E^{I_\mathrm{x} t_\mathrm{x}}_{12:321}(\mu_1' \nu_1' \mu_\mathrm{x}' \nu_\mathrm{x}' | \mu_1 \nu_1 \mu_\mathrm{x} \nu_\mathrm{x}) \\
&\equiv \left\langle \eta^{(1)}_{\frac{1}{2}\mu_1'} \left[\eta^{(2)}_{\frac{1}{2}} \otimes \eta^{(3)}_{\frac{1}{2}} \right]_{I_\mathrm{x} \mu_\mathrm{x}'} \middle| \sum_{S_{12}} Z^{t_\mathrm{x},S_{12}}_{12:321}(\nu_1' \nu_\mathrm{x}' | \nu_1 \nu_\mathrm{x}) \hat{P}^{S_{12}}_{12} \middle| \eta^{(3)}_{\frac{1}{2}\mu_1} \left[\eta^{(2)}_{\frac{1}{2}} \otimes \eta^{(1)}_{\frac{1}{2}} \right]_{I_\mathrm{x} \mu_\mathrm{x}} \right\rangle \\
&= -\hat{s}_\mathrm{x}^2 \sum_{S' M_S'} \sum_{S M_S} \left(I_\mathrm{x} \mu_\mathrm{x}' \frac{1}{2} \mu_1' \middle| S' M_S' \right) \left(I_\mathrm{x} \mu_\mathrm{x} \frac{1}{2} \mu_1 \middle| S M_S \right) \begin{Bmatrix} 1/2 & 1/2 & I_\mathrm{x} \\ S' & 1/2 & I_\mathrm{x} \end{Bmatrix}
\end{aligned}$$

$$\times \left\langle \left[\left[\eta^{(2)}_{\frac{1}{2}} \otimes \eta^{(1)}_{\frac{1}{2}} \right]_{I_\mathrm{x}} \otimes \eta^{(3)}_{\frac{1}{2}} \right]_{S'M'_S} \middle| Z^{t_\mathrm{x},I_\mathrm{x}}_{12:321}(\nu'_1\nu'_\mathrm{x}|\nu_1\nu_\mathrm{x}) \middle| \left[\left[\eta^{(2)}_{\frac{1}{2}} \otimes \eta^{(1)}_{\frac{1}{2}} \right]_{I_\mathrm{x}} \otimes \eta^{(3)}_{\frac{1}{2}} \right]_{SM_S} \right\rangle, \tag{C.23}$$

$$\begin{aligned}
&E^{I_\mathrm{x}t_\mathrm{x}}_{13:213}(\mu'_1\nu'_1\mu'_\mathrm{x}\nu'_\mathrm{x}|\mu_1\nu_1\mu_\mathrm{x}\nu_\mathrm{x}) \\
&\quad \equiv \left\langle \eta^{(1)}_{\frac{1}{2}\mu'_1} \left[\eta^{(2)}_{\frac{1}{2}} \otimes \eta^{(3)}_{\frac{1}{2}} \right]_{I_\mathrm{x}\mu'_\mathrm{x}} \middle| \sum_{S_{13}} Z^{t_\mathrm{x},S_{13}}_{13:213}(\nu'_1\nu'_\mathrm{x}|\nu_1\nu_\mathrm{x}) \hat{P}^{S_{13}}_{13} \middle| \eta^{(2)}_{\frac{1}{2}\mu_1} \left[\eta^{(1)}_{\frac{1}{2}} \otimes \eta^{(3)}_{\frac{1}{2}} \right]_{I_\mathrm{x}\mu_\mathrm{x}} \right\rangle \\
&\quad = -\hat{s}^2_\mathrm{x} \sum_{S'M'_S} \sum_{SM_S} \left(I_\mathrm{x}\mu'_\mathrm{x}\frac{1}{2}\mu'_1 \middle| S'M'_S \right) \left(I_\mathrm{x}\mu_\mathrm{x}\frac{1}{2}\mu_1 \middle| SM_S \right) \begin{Bmatrix} 1/2 & 1/2 & I_\mathrm{x} \\ S' & 1/2 & I_\mathrm{x} \end{Bmatrix} \\
&\qquad \times \left\langle \left[\left[\eta^{(3)}_{\frac{1}{2}} \otimes \eta^{(1)}_{\frac{1}{2}} \right]_{I_\mathrm{x}} \otimes \eta^{(2)}_{\frac{1}{2}} \right]_{S'M'_S} \middle| Z^{t_\mathrm{x},I_\mathrm{x}}_{13:213}(\nu'_1\nu'_\mathrm{x}|\nu_1\nu_\mathrm{x}) \middle| \left[\left[\eta^{(3)}_{\frac{1}{2}} \otimes \eta^{(1)}_{\frac{1}{2}} \right]_{I_\mathrm{x}} \otimes \eta^{(2)}_{\frac{1}{2}} \right]_{SM_S} \right\rangle.
\end{aligned} \tag{C.24}$$

Here, we have also used the two properties that (i) S_{1j} is conserved in general and that (ii) I_x and S_{1j} are zero or unity.

Therefore, the transition matrices (2.109)-(2.111) become

$$\begin{aligned}
&\bar{T}^{I_\mathrm{x}t_\mathrm{x}}_{12:123}(\boldsymbol{\kappa}', \mu'_1\nu'_1\mu'_\mathrm{x}\nu'_\mathrm{x}|\boldsymbol{\kappa}, \mu_1\nu_1\mu_\mathrm{x}\nu_\mathrm{x}) \\
&\quad = \left\langle \phi'_\mathrm{x}(\boldsymbol{r}_1)\mathrm{e}^{i\boldsymbol{\kappa}'\cdot\boldsymbol{s}_1} \middle| E^{I_\mathrm{x}t_\mathrm{x}}_{12:123}(\mu'_1\nu'_1\mu'_\mathrm{x}\nu'_\mathrm{x}|\mu_1\nu_1\mu_\mathrm{x}\nu_\mathrm{x}) \middle| \phi_\mathrm{x}(\boldsymbol{r}_1)\mathrm{e}^{i\boldsymbol{\kappa}\cdot\boldsymbol{s}_1} \right\rangle \\
&\quad = \hat{s}^2_\mathrm{x}\hat{t}^2_\mathrm{x} \sum_{S'M'_S} \sum_{SM_S} \sum_{TM_T} \left(I_\mathrm{x}\mu'_\mathrm{x}\frac{1}{2}\mu'_1 \middle| S'M'_S \right) \left(I_\mathrm{x}\mu_\mathrm{x}\frac{1}{2}\mu_1 \middle| SM_S \right) \left(t_\mathrm{x}\nu'_\mathrm{x}\frac{1}{2}\nu'_1 \middle| TM_T \right) \left(t_\mathrm{x}\nu_\mathrm{x}\frac{1}{2}\nu_1 \middle| TM_T \right) \\
&\qquad \times \sum_{S_{12}T_{12}} \hat{S}^2_{12}\hat{T}^2_{12} \begin{Bmatrix} 1/2 & 1/2 & S_{12} \\ S' & 1/2 & I_\mathrm{x} \end{Bmatrix} \begin{Bmatrix} 1/2 & 1/2 & S_{12} \\ S & 1/2 & I_\mathrm{x} \end{Bmatrix} \begin{Bmatrix} 1/2 & 1/2 & T_{12} \\ T & 1/2 & t_\mathrm{x} \end{Bmatrix}^2 \\
&\qquad \times \left\langle \phi'_\mathrm{x}(\boldsymbol{r}_1)\mathrm{e}^{i\boldsymbol{\kappa}'\cdot\boldsymbol{s}_1} \left[\left[\eta^{(2)}_{\frac{1}{2}} \otimes \eta^{(1)}_{\frac{1}{2}} \right]_{S_{12}} \otimes \eta^{(3)}_{\frac{1}{2}} \right]_{S'M'_S} \right| \\
&\qquad\qquad \times t^{S_{12}T_{12}}_{12} \left| \phi_\mathrm{x}(\boldsymbol{r}_1)\mathrm{e}^{i\boldsymbol{\kappa}\cdot\boldsymbol{s}_1} \left[\left[\eta^{(2)}_{\frac{1}{2}} \otimes \eta^{(1)}_{\frac{1}{2}} \right]_{S_{12}} \otimes \eta^{(3)}_{\frac{1}{2}} \right]_{SM_S} \right\rangle,
\end{aligned} \tag{C.25}$$

$$\begin{aligned}
&\bar{T}^{I_\mathrm{x}t_\mathrm{x}}_{13:123}(\boldsymbol{\kappa}', \mu'_1\nu'_1\mu'_\mathrm{x}\nu'_\mathrm{x}|\boldsymbol{\kappa}, \mu_1\nu_1\mu_\mathrm{x}\nu_\mathrm{x}) \\
&\quad = \left\langle \phi'_\mathrm{x}(\boldsymbol{r}_1)\mathrm{e}^{i\boldsymbol{\kappa}'\cdot\boldsymbol{s}_1} \middle| E^{I_\mathrm{x}t_\mathrm{x}}_{13:123}(\mu'_1\nu'_1\mu'_\mathrm{x}\nu'_\mathrm{x}|\mu_1\nu_1\mu_\mathrm{x}\nu_\mathrm{x}) \middle| \phi_\mathrm{x}(\boldsymbol{r}_1)\mathrm{e}^{i\boldsymbol{\kappa}\cdot\boldsymbol{s}_1} \right\rangle \\
&\quad = \hat{s}^2_\mathrm{x}\hat{t}^2_\mathrm{x} \sum_{S'M'_S} \sum_{SM_S} \sum_{TM_T} \left(I_\mathrm{x}\mu'_\mathrm{x}\frac{1}{2}\mu'_1 \middle| S'M'_S \right) \left(I_\mathrm{x}\mu_\mathrm{x}\frac{1}{2}\mu_1 \middle| SM_S \right) \left(t_\mathrm{x}\nu'_\mathrm{x}\frac{1}{2}\nu'_1 \middle| TM_T \right) \left(t_\mathrm{x}\nu_\mathrm{x}\frac{1}{2}\nu_1 \middle| TM_T \right) \\
&\qquad \times \sum_{S_{13}T_{13}} \hat{S}^2_{13}\hat{T}^2_{13} \begin{Bmatrix} 1/2 & 1/2 & S_{13} \\ S' & 1/2 & I_\mathrm{x} \end{Bmatrix} \begin{Bmatrix} 1/2 & 1/2 & S_{13} \\ S & 1/2 & I_\mathrm{x} \end{Bmatrix} \begin{Bmatrix} 1/2 & 1/2 & T_{13} \\ T & 1/2 & t_\mathrm{x} \end{Bmatrix}^2 \\
&\qquad \times \left\langle \phi'_\mathrm{x}(\boldsymbol{r}_1)\mathrm{e}^{i\boldsymbol{\kappa}'\cdot\boldsymbol{s}_1} \left[\left[\eta^{(3)}_{\frac{1}{2}} \otimes \eta^{(1)}_{\frac{1}{2}} \right]_{S_{13}} \otimes \eta^{(2)}_{\frac{1}{2}} \right]_{S'M'_S} \right| \\
&\qquad\qquad \times t^{S_{13}T_{13}}_{13} \left| \phi_\mathrm{x}(\boldsymbol{r}_1)\mathrm{e}^{i\boldsymbol{\kappa}\cdot\boldsymbol{s}_1} \left[\left[\eta^{(3)}_{\frac{1}{2}} \otimes \eta^{(1)}_{\frac{1}{2}} \right]_{S_{13}} \otimes \eta^{(2)}_{\frac{1}{2}} \right]_{SM_S} \right\rangle,
\end{aligned} \tag{C.26}$$

$$\bar{T}^{I_\mathrm{x}t_\mathrm{x}}_{12:213}(\boldsymbol{\kappa}', \mu'_1\nu'_1\mu'_\mathrm{x}\nu'_\mathrm{x}|\boldsymbol{\kappa}, \mu_1\nu_1\mu_\mathrm{x}\nu_\mathrm{x})$$

$$
\begin{aligned}
&= \left\langle \phi'_{\mathrm{x}}(\boldsymbol{r}_1)\mathrm{e}^{i\boldsymbol{\kappa}'\cdot\boldsymbol{s}_1} \middle| E^{I_{\mathrm{x}}t_{\mathrm{x}}}_{12:213}(\mu'_1\nu'_1\mu'_{\mathrm{x}}\nu'_{\mathrm{x}}|\mu_1\nu_1\mu_{\mathrm{x}}\nu_{\mathrm{x}}) \middle| \phi_{\mathrm{x}}(\boldsymbol{r}_2)\mathrm{e}^{i\boldsymbol{\kappa}\cdot\boldsymbol{s}_2} \right\rangle \\
&= \hat{s}^2_{\mathrm{x}}\hat{t}^2_{\mathrm{x}} \sum_{S'M'_S}\sum_{SM_S}\sum_{TM_T} \left(I_{\mathrm{x}}\mu'_{\mathrm{x}}\frac{1}{2}\mu'_1 \middle| S'M'_S \right)\left(I_{\mathrm{x}}\mu_{\mathrm{x}}\frac{1}{2}\mu_1 \middle| SM_S \right)\left(t_{\mathrm{x}}\nu'_{\mathrm{x}}\frac{1}{2}\nu'_1 \middle| TM_T \right)\left(t_{\mathrm{x}}\nu_{\mathrm{x}}\frac{1}{2}\nu_1 \middle| TM_T \right) \\
&\quad \times \sum_{S_{12}T_{12}} (-)^{S_{12}+T_{12}} \hat{S}^2_{12}\hat{T}^2_{12} \begin{Bmatrix} 1/2 & 1/2 & S_{12} \\ S' & 1/2 & I_{\mathrm{x}} \end{Bmatrix}\begin{Bmatrix} 1/2 & 1/2 & S_{12} \\ S & 1/2 & I_{\mathrm{x}} \end{Bmatrix}\begin{Bmatrix} 1/2 & 1/2 & T_{12} \\ T & 1/2 & t_{\mathrm{x}} \end{Bmatrix}^2 \\
&\qquad \times \left\langle \phi'_{\mathrm{x}}(\boldsymbol{r}_1)\mathrm{e}^{i\boldsymbol{\kappa}'\cdot\boldsymbol{s}_1} \left[\left[\eta^{(2)}_{\frac{1}{2}}\otimes\eta^{(1)}_{\frac{1}{2}}\right]_{S_{12}}\otimes\eta^{(3)}_{\frac{1}{2}}\right]_{S'M'_S} \right| \\
&\qquad\qquad \times t^{S_{12}T_{12}}_{12} \left| \phi_{\mathrm{x}}(\boldsymbol{r}_2)\mathrm{e}^{i\boldsymbol{\kappa}\cdot\boldsymbol{s}_2} \left[\left[\eta^{(2)}_{\frac{1}{2}}\otimes\eta^{(1)}_{\frac{1}{2}}\right]_{S_{12}}\otimes\eta^{(3)}_{\frac{1}{2}}\right]_{SM_S} \right\rangle,
\end{aligned} \tag{C.27}
$$

$$
\begin{aligned}
&\bar{T}^{I_{\mathrm{x}}t_{\mathrm{x}}}_{13:321}(\boldsymbol{\kappa}',\mu'_1\nu'_1\mu'_{\mathrm{x}}\nu'_{\mathrm{x}}|\boldsymbol{\kappa},\mu_1\nu_1\mu_{\mathrm{x}}\nu_{\mathrm{x}}) \\
&= \left\langle \phi'_{\mathrm{x}}(\boldsymbol{r}_1)\mathrm{e}^{i\boldsymbol{\kappa}'\cdot\boldsymbol{s}_1} \middle| E^{I_{\mathrm{x}}t_{\mathrm{x}}}_{13:321}(\mu'_1\nu'_1\mu'_{\mathrm{x}}\nu'_{\mathrm{x}}|\mu_1\nu_1\mu_{\mathrm{x}}\nu_{\mathrm{x}}) \middle| \phi_{\mathrm{x}}(\boldsymbol{r}_3)\mathrm{e}^{i\boldsymbol{\kappa}\cdot\boldsymbol{s}_3} \right\rangle \\
&= \hat{s}^2_{\mathrm{x}}\hat{t}^2_{\mathrm{x}} \sum_{S'M'_S}\sum_{SM_S}\sum_{TM_T} \left(I_{\mathrm{x}}\mu'_{\mathrm{x}}\frac{1}{2}\mu'_1 \middle| S'M'_S \right)\left(I_{\mathrm{x}}\mu_{\mathrm{x}}\frac{1}{2}\mu_1 \middle| SM_S \right)\left(t_{\mathrm{x}}\nu'_{\mathrm{x}}\frac{1}{2}\nu'_1 \middle| TM_T \right)\left(t_{\mathrm{x}}\nu_{\mathrm{x}}\frac{1}{2}\nu_1 \middle| TM_T \right) \\
&\quad \times \sum_{S_{13}T_{13}} (-)^{S_{13}+T_{13}} \hat{S}^2_{13}\hat{T}^2_{13} \begin{Bmatrix} 1/2 & 1/2 & S_{13} \\ S' & 1/2 & I_{\mathrm{x}} \end{Bmatrix}\begin{Bmatrix} 1/2 & 1/2 & S_{13} \\ S & 1/2 & I_{\mathrm{x}} \end{Bmatrix}\begin{Bmatrix} 1/2 & 1/2 & T_{13} \\ T & 1/2 & t_{\mathrm{x}} \end{Bmatrix}^2 \\
&\qquad \times \left\langle \phi'_{\mathrm{x}}(\boldsymbol{r}_1)\mathrm{e}^{i\boldsymbol{\kappa}'\cdot\boldsymbol{s}_1} \left[\left[\eta^{(3)}_{\frac{1}{2}}\otimes\eta^{(1)}_{\frac{1}{2}}\right]_{S_{13}}\otimes\eta^{(2)}_{\frac{1}{2}}\right]_{S'M'_S} \right| \\
&\qquad\qquad \times t^{S_{13}T_{13}}_{13} \left| \phi_{\mathrm{x}}(\boldsymbol{r}_3)\mathrm{e}^{i\boldsymbol{\kappa}\cdot\boldsymbol{s}_3} \left[\left[\eta^{(3)}_{\frac{1}{2}}\otimes\eta^{(1)}_{\frac{1}{2}}\right]_{S_{13}}\otimes\eta^{(2)}_{\frac{1}{2}}\right]_{SM_S} \right\rangle,
\end{aligned} \tag{C.28}
$$

$$
\begin{aligned}
&\bar{T}^{I_{\mathrm{x}}t_{\mathrm{x}}}_{12:321}(\boldsymbol{\kappa}',\mu'_1\nu'_1\mu'_{\mathrm{x}}\nu'_{\mathrm{x}}|\boldsymbol{\kappa},\mu_1\nu_1\mu_{\mathrm{x}}\nu_{\mathrm{x}}) \\
&= \left\langle \phi'_{\mathrm{x}}(\boldsymbol{r}_1)\mathrm{e}^{i\boldsymbol{\kappa}'\cdot\boldsymbol{s}_1} \middle| E^{I_{\mathrm{x}}t_{\mathrm{x}}}_{12:321}(\mu'_1\nu'_1\mu'_{\mathrm{x}}\nu'_{\mathrm{x}}|\mu_1\nu_1\mu_{\mathrm{x}}\nu_{\mathrm{x}}) \middle| \phi_{\mathrm{x}}(\boldsymbol{r}_3)\mathrm{e}^{i\boldsymbol{\kappa}\cdot\boldsymbol{s}_3} \right\rangle \\
&= \hat{s}^2_{\mathrm{x}}\hat{t}^2_{\mathrm{x}} \sum_{S'M'_S}\sum_{SM_S}\sum_{TM_T} \left(I_{\mathrm{x}}\mu'_{\mathrm{x}}\frac{1}{2}\mu'_1 \middle| S'M'_S \right)\left(I_{\mathrm{x}}\mu_{\mathrm{x}}\frac{1}{2}\mu_1 \middle| SM_S \right) \\
&\quad \times \left(t_{\mathrm{x}}\nu'_{\mathrm{x}}\frac{1}{2}\nu'_1 \middle| TM_T \right)\left(t_{\mathrm{x}}\nu_{\mathrm{x}}\frac{1}{2}\nu_1 \middle| TM_T \right)\begin{Bmatrix} 1/2 & 1/2 & I_{\mathrm{x}} \\ S' & 1/2 & I_{\mathrm{x}} \end{Bmatrix}\begin{Bmatrix} 1/2 & 1/2 & t_{\mathrm{x}} \\ T & 1/2 & t_{\mathrm{x}} \end{Bmatrix} \\
&\qquad \times \left\langle \phi'_{\mathrm{x}}(\boldsymbol{r}_1)\mathrm{e}^{i\boldsymbol{\kappa}'\cdot\boldsymbol{s}_1} \left[\left[\eta^{(2)}_{\frac{1}{2}}\otimes\eta^{(1)}_{\frac{1}{2}}\right]_{I_{\mathrm{x}}}\otimes\eta^{(3)}_{\frac{1}{2}}\right]_{S'M'_S} \right| \\
&\qquad\qquad \times t^{I_{\mathrm{x}}t_{\mathrm{x}}}_{12} \left| \phi_{\mathrm{x}}(\boldsymbol{r}_3)\mathrm{e}^{i\boldsymbol{\kappa}\cdot\boldsymbol{s}_3} \left[\left[\eta^{(2)}_{\frac{1}{2}}\otimes\eta^{(1)}_{\frac{1}{2}}\right]_{I_{\mathrm{x}}}\otimes\eta^{(3)}_{\frac{1}{2}}\right]_{SM_S} \right\rangle,
\end{aligned} \tag{C.29}
$$

$$
\begin{aligned}
&\bar{T}^{I_{\mathrm{x}}t_{\mathrm{x}}}_{13:213}(\boldsymbol{\kappa}',\mu'_1\nu'_1\mu'_{\mathrm{x}}\nu'_{\mathrm{x}}|\boldsymbol{\kappa},\mu_1\nu_1\mu_{\mathrm{x}}\nu_{\mathrm{x}}) \\
&= \left\langle \phi'_{\mathrm{x}}(\boldsymbol{r}_1)\mathrm{e}^{i\boldsymbol{\kappa}'\cdot\boldsymbol{s}_1} \middle| E^{I_{\mathrm{x}}t_{\mathrm{x}}}_{13:213}(\mu'_1\nu'_1\mu'_{\mathrm{x}}\nu'_{\mathrm{x}}|\mu_1\nu_1\mu_{\mathrm{x}}\nu_{\mathrm{x}}) \middle| \phi_{\mathrm{x}}(\boldsymbol{r}_2)\mathrm{e}^{i\boldsymbol{\kappa}\cdot\boldsymbol{s}_2} \right\rangle
\end{aligned}
$$

$$
\begin{aligned}
&= \hat{s}_{\mathrm{x}}^2 \hat{t}_{\mathrm{x}}^2 \sum_{S' M_S'} \sum_{S M_S} \sum_{T M_T} \left(I_{\mathrm{x}} \mu_{\mathrm{x}}' \frac{1}{2} \mu_1' \middle| S' M_S' \right) \left(I_{\mathrm{x}} \mu_{\mathrm{x}} \frac{1}{2} \mu_1 \middle| S M_S \right) \\
&\times \left(t_{\mathrm{x}} \nu_{\mathrm{x}}' \frac{1}{2} \nu_1' \middle| T M_T \right) \left(t_{\mathrm{x}} \nu_{\mathrm{x}} \frac{1}{2} \nu_1 \middle| T M_T \right) \begin{Bmatrix} 1/2 & 1/2 & I_{\mathrm{x}} \\ S' & 1/2 & I_{\mathrm{x}} \end{Bmatrix} \begin{Bmatrix} 1/2 & 1/2 & t_{\mathrm{x}} \\ T & 1/2 & t_{\mathrm{x}} \end{Bmatrix} \\
&\times \left\langle \phi_{\mathrm{x}}'(\boldsymbol{r}_1) \mathrm{e}^{i\boldsymbol{\kappa}' \cdot \boldsymbol{s}_1} \left[\left[\eta_{\frac{1}{2}}^{(3)} \otimes \eta_{\frac{1}{2}}^{(1)} \right]_{I_{\mathrm{x}}} \otimes \eta_{\frac{1}{2}}^{(2)} \right]_{S' M_S'} \right| \\
&\times t_{13}^{I_{\mathrm{x}} t_{\mathrm{x}}} \left| \phi_{\mathrm{x}}(\boldsymbol{r}_2) \mathrm{e}^{i\boldsymbol{\kappa} \cdot \boldsymbol{s}_2} \left[\left[\eta_{\frac{1}{2}}^{(3)} \otimes \eta_{\frac{1}{2}}^{(1)} \right]_{I_{\mathrm{x}}} \otimes \eta_{\frac{1}{2}}^{(2)} \right]_{S M_S} \right\rangle .
\end{aligned}
\tag{C.30}
$$

We can find from Eqs. (C.25)-(C.30) that the correspodence of Eqs. (2.112)-(2.114) holds. In the following, we calculate the central (Section C.2), tensor (Section C.3), and spin-orbit (Section C.4) components of these matrices.

C.2 Components of central interactions

The components of the central interactions of the transition matrices (C.25) and (C.26) are given by

$$
\bar{T}_{12:123}^{S_{12}T_{12}(\mathrm{C})}(\boldsymbol{\kappa}', S'M_S'|\boldsymbol{\kappa}, SM_S) \equiv \left\langle \phi_{\mathrm{x}}'(\boldsymbol{r}_1)\mathrm{e}^{i\boldsymbol{\kappa}'\cdot\boldsymbol{s}_1} \middle| t_{12}^{S_{12}T_{12}(\mathrm{C})}(r_3) \middle| \phi_{\mathrm{x}}(\boldsymbol{r}_1)\mathrm{e}^{i\boldsymbol{\kappa}\cdot\boldsymbol{s}_1} \right\rangle \delta_{S'S}\delta_{M_S'M_S}, \tag{C.31}
$$

$$
\bar{T}_{13:123}^{S_{13}T_{13}(\mathrm{C})}(\boldsymbol{\kappa}', S'M_S'|\boldsymbol{\kappa}, SM_S) \equiv \left\langle \phi_{\mathrm{x}}'(\boldsymbol{r}_1)\mathrm{e}^{i\boldsymbol{\kappa}'\cdot\boldsymbol{s}_1} \middle| t_{13}^{S_{13}T_{13}(\mathrm{C})}(r_2) \middle| \phi_{\mathrm{x}}(\boldsymbol{r}_1)\mathrm{e}^{i\boldsymbol{\kappa}\cdot\boldsymbol{s}_1} \right\rangle \delta_{S'S}\delta_{M_S'M_S}, \tag{C.32}
$$

in which we have used the property of $t_{1j}^{S_{1j}T_{1j}}$ which does not affect the spin functions. Now we make two assumptions that (i) particle x can be described only by the S wave and that (ii) ϕ_{x} and ϕ_{x}' are constructed by the superposition of the Gaussians as

$$
\phi_{\mathrm{x}}(\boldsymbol{r}) = \frac{1}{\sqrt{4\pi}} \sum_n c_n \exp\left(-\alpha_n r^2\right), \quad \phi_{\mathrm{x}}'(\boldsymbol{r}) = \frac{1}{\sqrt{4\pi}} \sum_{n'} c_{n'} \exp\left(-\alpha_{n'} r^2\right), \tag{C.33}
$$

in which α_n ($\alpha_{n'}$) and c_n ($c_{n'}$) are the range of the Gaussian and the expansion coefficient, respectively. Taking $\boldsymbol{r}_3$ and $\boldsymbol{s}_3$ as the independent coordinates in Eq. (C.31), we can find from Fig. 2.3

$$
\boldsymbol{r}_1 = \frac{1}{2}\boldsymbol{r}_3 + \boldsymbol{s}_3, \quad \boldsymbol{s}_1 = \frac{3}{4}\boldsymbol{r}_3 - \frac{1}{2}\boldsymbol{s}_3, \tag{C.34}
$$

$$
\boldsymbol{r}_2 = -\frac{1}{2}\boldsymbol{r}_3 + \boldsymbol{s}_3, \quad \boldsymbol{s}_2 = -\frac{3}{4}\boldsymbol{r}_3 - \frac{1}{2}\boldsymbol{s}_3. \tag{C.35}
$$

In addition, taking $\boldsymbol{r}_2$ and $\boldsymbol{s}_2$ as the independent coordinates in Eq. (C.32), the other coordinates are written by

$$
\boldsymbol{r}_1 = \frac{1}{2}\boldsymbol{r}_2 - \boldsymbol{s}_2, \quad \boldsymbol{s}_1 = -\frac{3}{4}\boldsymbol{r}_2 - \frac{1}{2}\boldsymbol{s}_2, \tag{C.36}
$$

$$
\boldsymbol{r}_3 = -\frac{1}{2}\boldsymbol{r}_2 - \boldsymbol{s}_2, \quad \boldsymbol{s}_3 = \frac{3}{4}\boldsymbol{r}_2 - \frac{1}{2}\boldsymbol{s}_2. \tag{C.37}
$$

Then Eqs. (C.31) and (C.32) become

$$
\bar{T}_{12:123}^{S_{12}T_{12}(\mathrm{C})}(\boldsymbol{\kappa}', S'M_S'|\boldsymbol{\kappa}, SM_S) = \delta_{S'S}\delta_{M_S'M_S} \sum_{n'n} c_{n'} c_n I_{12:123,n'n}^{S_{12}T_{12}(\mathrm{C})}, \tag{C.38}
$$

$$
\bar{T}_{13:123}^{S_{13}T_{13}(\mathrm{C})}(\boldsymbol{\kappa}', S'M_S'|\boldsymbol{\kappa}, SM_S) = \delta_{S'S}\delta_{M_S'M_S} \sum_{n'n} c_{n'} c_n I_{13:123,n'n}^{S_{13}T_{13}(\mathrm{C})}, \tag{C.39}
$$

$$\begin{aligned}
I^{S_{12}T_{12}(\mathrm{C})}_{12:123,n'n} \equiv{}& \frac{1}{4\pi}\int \mathrm{d}\boldsymbol{r}_3 \int \mathrm{d}\boldsymbol{s}_3 \exp\left[-\alpha_{n'}\left(\frac{1}{2}\boldsymbol{r}_3+\boldsymbol{s}_3\right)^2\right]\exp\left[-i\boldsymbol{\kappa}'\cdot\left(\frac{3}{4}\boldsymbol{r}_3-\frac{1}{2}\boldsymbol{s}_3\right)\right] \\
&\times t^{S_{12}T_{12}(\mathrm{C})}_{12}(r_3)\exp\left[-\alpha_{n}\left(\frac{1}{2}\boldsymbol{r}_3+\boldsymbol{s}_3\right)^2\right]\exp\left[i\boldsymbol{\kappa}\cdot\left(\frac{3}{4}\boldsymbol{r}_3-\frac{1}{2}\boldsymbol{s}_3\right)\right] \\
={}& \frac{1}{4\pi}\int \mathrm{d}\boldsymbol{r}_3 \int \mathrm{d}\boldsymbol{s}_3\, t^{S_{12}T_{12}(\mathrm{C})}_{12}(r_3)\exp\left[-\alpha_{n'n}\left(\frac{1}{2}\boldsymbol{r}_3+\boldsymbol{s}_3\right)^2\right]\exp\left[i\boldsymbol{q}\cdot\left(\frac{3}{4}\boldsymbol{r}_3-\frac{1}{2}\boldsymbol{s}_3\right)\right] \\
={}& \frac{1}{4\pi}\int \mathrm{d}\boldsymbol{r}_3\, t^{S_{12}T_{12}(\mathrm{C})}_{12}(r_3)\exp\left(-\frac{1}{4}\alpha_{n'n}r_3^2\right)\exp\left(\frac{3}{4}i\boldsymbol{q}\cdot\boldsymbol{r}_3\right) \\
&\times\int \mathrm{d}\boldsymbol{s}_3 \exp(-\alpha_{n'n}s_3^2)\exp\left[-\left(\alpha_{n'n}\boldsymbol{r}_3+\frac{i}{2}\boldsymbol{q}\right)\cdot\boldsymbol{s}_3\right],
\end{aligned} \tag{C.40}$$

$$\begin{aligned}
I^{S_{13}T_{13}(\mathrm{C})}_{13:123,n'n} \equiv{}& \frac{1}{4\pi}\int \mathrm{d}\boldsymbol{r}_2 \int \mathrm{d}\boldsymbol{s}_2 \exp\left[-\alpha_{n'}\left(\frac{1}{2}\boldsymbol{r}_2-\boldsymbol{s}_2\right)^2\right]\exp\left[-i\boldsymbol{\kappa}'\cdot\left(-\frac{3}{4}\boldsymbol{r}_2-\frac{1}{2}\boldsymbol{s}_2\right)\right] \\
&\times t^{S_{13}T_{13}(\mathrm{C})}_{13}(r_2)\exp\left[-\alpha_{n}\left(\frac{1}{2}\boldsymbol{r}_2-\boldsymbol{s}_2\right)^2\right]\exp\left[i\boldsymbol{\kappa}\cdot\left(-\frac{3}{4}\boldsymbol{r}_2-\frac{1}{2}\boldsymbol{s}_2\right)\right] \\
={}& \frac{1}{4\pi}\int \mathrm{d}\boldsymbol{r}_2 \int \mathrm{d}\boldsymbol{s}_2\, t^{S_{13}T_{13}(\mathrm{C})}_{13}(r_2)\exp\left[-\alpha_{n'n}\left(\frac{1}{2}\boldsymbol{r}_2-\boldsymbol{s}_2\right)^2\right]\exp\left[i\boldsymbol{q}\cdot\left(-\frac{3}{4}\boldsymbol{r}_2-\frac{1}{2}\boldsymbol{s}_2\right)\right] \\
={}& \frac{1}{4\pi}\int \mathrm{d}\boldsymbol{r}_2\, t^{S_{13}T_{13}(\mathrm{C})}_{13}(r_2)\exp\left(-\frac{1}{4}\alpha_{n'n}r_2^2\right)\exp\left(-\frac{3}{4}i\boldsymbol{q}\cdot\boldsymbol{r}_2\right) \\
&\times\int \mathrm{d}\boldsymbol{s}_2 \exp(-\alpha_{n'n}s_2^2)\exp\left[-\left(-\alpha_{n'n}\boldsymbol{r}_2+\frac{i}{2}\boldsymbol{q}\right)\cdot\boldsymbol{s}_2\right],
\end{aligned} \tag{C.41}$$

with defining $\alpha_{n'n}$ and $\boldsymbol{q}$ as

$$\alpha_{n'n} \equiv \alpha_{n'} + \alpha_n, \quad \boldsymbol{q} \equiv \boldsymbol{\kappa} - \boldsymbol{\kappa}'. \tag{C.42}$$

Replacing α, $\boldsymbol{\beta}$, and $\boldsymbol{\gamma}$ in Eq. (C.184) as

$$\alpha \to \alpha_{n'n}, \quad \boldsymbol{\beta} \to \pm\alpha_{n'n}\boldsymbol{r}, \quad \boldsymbol{\gamma} \to \frac{\boldsymbol{q}}{2}, \tag{C.43}$$

we obtain

$$\begin{aligned}
&\int \mathrm{d}\boldsymbol{s} \exp(-\alpha_{n'n}s^2)\exp\left[-\left(\pm\alpha_{n'n}\boldsymbol{r}+\frac{i}{2}\boldsymbol{q}\right)\cdot\boldsymbol{s}\right] \\
&\quad= \frac{\pi^{3/2}}{\alpha_{n'n}^{3/2}}\exp\left(\frac{1}{4}\alpha_{n'n}r^2\right)\exp\left(-\frac{q^2}{16\alpha_{n'n}}\right)\exp\left(\pm\frac{i}{4}\boldsymbol{q}\cdot\boldsymbol{r}\right),
\end{aligned} \tag{C.44}$$

and Eqs. (C.40) and (C.41) are reduced to

$$\begin{aligned}
I^{S_{12}T_{12}(\mathrm{C})}_{12:123,n'n} &= \frac{1}{4\pi}\frac{\pi^{3/2}}{\alpha_{n'n}^{3/2}}\exp\left(-\frac{q^2}{16\alpha_{n'n}}\right)\int \mathrm{d}\boldsymbol{r}_3\, t^{S_{12}T_{12}(\mathrm{C})}_{12}(r_3)\mathrm{e}^{i\boldsymbol{q}\cdot\boldsymbol{r}_3} \\
&= \frac{\pi^{3/2}}{\alpha_{n'n}^{3/2}}\exp\left(-\frac{q^2}{16\alpha_{n'n}}\right)\int_0^\infty \mathrm{d}r_3\, r_3^2 t^{S_{12}T_{12}(\mathrm{C})}_{12}(r_3)j_0(qr_3),
\end{aligned} \tag{C.45}$$

$$I^{S_{13}T_{13}(\mathrm{C})}_{13:123,n'n} = \frac{1}{4\pi}\frac{\pi^{3/2}}{\alpha_{n'n}^{3/2}}\exp\left(-\frac{q^2}{16\alpha_{n'n}}\right)\int \mathrm{d}\boldsymbol{r}_2\, t^{S_{13}T_{13}(\mathrm{C})}_{13}(r_2)\mathrm{e}^{-i\boldsymbol{q}\cdot\boldsymbol{r}_2}$$

$$= \frac{\pi^{3/2}}{\alpha_{n'n}^{3/2}} \exp\left(-\frac{q^2}{16\alpha_{n'n}}\right) \int_0^\infty \mathrm{d}r_2\, r_2^2 t_{13}^{S_{13}T_{13}(\mathrm{C})}(r_2) j_0(qr_2). \tag{C.46}$$

with using Eq. (C.185).

The components of the central interactions of the transition matrices (C.27) and (C.28) are given by

$$\bar{T}_{12:213}^{S_{12}T_{12}(\mathrm{C})}(\boldsymbol{\kappa}', S'M_S'|\boldsymbol{\kappa}, SM_S) \equiv \left\langle \phi_\mathrm{x}'(\boldsymbol{r}_1)\mathrm{e}^{i\boldsymbol{\kappa}'\cdot\boldsymbol{s}_1} \middle| t_{12}^{S_{12}T_{12}(\mathrm{C})}(r_3) \middle| \phi_\mathrm{x}(\boldsymbol{r}_2)\mathrm{e}^{i\boldsymbol{\kappa}\cdot\boldsymbol{s}_2} \right\rangle \delta_{S'S}\delta_{M_S'M_S}, \tag{C.47}$$

$$\bar{T}_{13:321}^{S_{13}T_{13}(\mathrm{C})}(\boldsymbol{\kappa}', S'M_S'|\boldsymbol{\kappa}, SM_S) \equiv \left\langle \phi_\mathrm{x}'(\boldsymbol{r}_1)\mathrm{e}^{i\boldsymbol{\kappa}'\cdot\boldsymbol{s}_1} \middle| t_{13}^{S_{13}T_{13}(\mathrm{C})}(r_2) \middle| \phi_\mathrm{x}(\boldsymbol{r}_3)\mathrm{e}^{i\boldsymbol{\kappa}\cdot\boldsymbol{s}_3} \right\rangle \delta_{S'S}\delta_{M_S'M_S}. \tag{C.48}$$

Similarly to the calculation of Eqs. (C.31) and (C.32),

$$\bar{T}_{12:213}^{S_{12}T_{12}(\mathrm{C})}(\boldsymbol{\kappa}', S'M_S'|\boldsymbol{\kappa}, SM_S) = \delta_{S'S}\delta_{M_S'M_S} \sum_{n'n} c_{n'}c_n I_{12:213,n'n}^{S_{12}T_{12}(\mathrm{C})}, \tag{C.49}$$

$$\bar{T}_{13:321}^{S_{13}T_{13}(\mathrm{C})}(\boldsymbol{\kappa}', S'M_S'|\boldsymbol{\kappa}, SM_S) = \delta_{S'S}\delta_{M_S'M_S} \sum_{n'n} c_{n'}c_n I_{13:321,n'n}^{S_{13}T_{13}(\mathrm{C})}, \tag{C.50}$$

$$\begin{aligned}
I_{12:213,n'n}^{S_{12}T_{12}(\mathrm{C})} \equiv{}& \frac{1}{4\pi}\int \mathrm{d}\boldsymbol{r}_3 \int \mathrm{d}\boldsymbol{s}_3 \exp\left[-\alpha_{n'}\left(\frac{1}{2}\boldsymbol{r}_3 + \boldsymbol{s}_3\right)^2\right] \exp\left[-i\boldsymbol{\kappa}'\cdot\left(\frac{3}{4}\boldsymbol{r}_3 - \frac{1}{2}\boldsymbol{s}_3\right)\right] \\
&\times t_{12}^{S_{12}T_{12}(\mathrm{C})}(r_3) \exp\left[-\alpha_n\left(-\frac{1}{2}\boldsymbol{r}_3 + \boldsymbol{s}_3\right)^2\right] \exp\left[i\boldsymbol{\kappa}\cdot\left(-\frac{3}{4}\boldsymbol{r}_3 - \frac{1}{2}\boldsymbol{s}_3\right)\right] \\
={}& \frac{1}{4\pi}\int \mathrm{d}\boldsymbol{r}_3\, t_{12}^{S_{12}T_{12}(\mathrm{C})}(r_3) \exp\left(-\frac{1}{4}\alpha_{n'n}r_3^2\right) \exp\left(-\frac{3}{4}i\boldsymbol{Q}\cdot\boldsymbol{r}_3\right) \\
&\times \int \mathrm{d}\boldsymbol{s}_3 \exp(-\alpha_{n'n}s_3^2) \exp\left[-\left(\bar{\alpha}_{n'n}\boldsymbol{r}_3 + \frac{i}{2}\boldsymbol{q}\right)\cdot\boldsymbol{s}_3\right],
\end{aligned} \tag{C.51}$$

$$\begin{aligned}
I_{13:321,n'n}^{S_{13}T_{13}(\mathrm{C})} \equiv{}& \frac{1}{4\pi}\int \mathrm{d}\boldsymbol{r}_2 \int \mathrm{d}\boldsymbol{s}_2 \exp\left[-\alpha_{n'}\left(\frac{1}{2}\boldsymbol{r}_2 - \boldsymbol{s}_2\right)^2\right] \exp\left[-i\boldsymbol{\kappa}'\cdot\left(-\frac{3}{4}\boldsymbol{r}_2 - \frac{1}{2}\boldsymbol{s}_2\right)\right] \\
&\times t_{13}^{S_{13}T_{13}(\mathrm{C})}(r_2) \exp\left[-\alpha_n\left(-\frac{1}{2}\boldsymbol{r}_2 - \boldsymbol{s}_2\right)^2\right] \exp\left[i\boldsymbol{\kappa}\cdot\left(\frac{3}{4}\boldsymbol{r}_2 - \frac{1}{2}\boldsymbol{s}_2\right)\right] \\
={}& \frac{1}{4\pi}\int \mathrm{d}\boldsymbol{r}_2\, t_{13}^{S_{13}T_{13}(\mathrm{C})}(r_2) \exp\left(-\frac{1}{4}\alpha_{n'n}r_2^2\right) \exp\left(\frac{3}{4}i\boldsymbol{Q}\cdot\boldsymbol{r}_2\right) \\
&\times \int \mathrm{d}\boldsymbol{s}_2 \exp(-\alpha_{n'n}s_2^2) \exp\left[-\left(-\bar{\alpha}_{n'n}\boldsymbol{r}_2 + \frac{i}{2}\boldsymbol{q}\right)\cdot\boldsymbol{s}_2\right],
\end{aligned} \tag{C.52}$$

in which

$$\bar{\alpha}_{n'n} \equiv \alpha_{n'} - \alpha_n, \quad \boldsymbol{Q} \equiv \boldsymbol{\kappa} + \boldsymbol{\kappa}', \tag{C.53}$$

are obtained. Replacing α, $\boldsymbol{\beta}$, and $\boldsymbol{\gamma}$ in Eq. (C.184) as

$$\alpha \to \alpha_{n'n}, \quad \boldsymbol{\beta} \to \pm\bar{\alpha}_{n'n}\boldsymbol{r}, \quad \boldsymbol{\gamma} \to \frac{\boldsymbol{q}}{2}, \tag{C.54}$$

we get

$$\int \mathrm{d}\boldsymbol{s} \exp(-\alpha_{n'n}s^2) \exp\left[-\left(\pm\bar{\alpha}_{n'n}\boldsymbol{r} + \frac{i}{2}\boldsymbol{q}\right)\cdot\boldsymbol{s}\right]$$

$$= \frac{\pi^{3/2}}{\alpha_{n'n}^{3/2}} \exp\left(\frac{1}{4}\alpha_{n'n} r^2\right) \exp\left(-\frac{\alpha_{n'}\alpha_n}{\alpha_{n'n}} r^2\right) \exp\left(-\frac{q^2}{16\alpha_{n'n}}\right) \exp\left(\pm\frac{\bar{\alpha}_{n'n}}{4\alpha_{n'n}} i\boldsymbol{q}\cdot\boldsymbol{r}\right), \tag{C.55}$$

and Eqs. (C.51) and (C.52) are reduced to

$$\begin{aligned} I_{12:213,n'n}^{S_{12}T_{12}(\mathrm{C})} &= \frac{1}{4\pi}\frac{\pi^{3/2}}{\alpha_{n'n}^{3/2}} \exp\left(-\frac{q^2}{16\alpha_{n'n}}\right) \int \mathrm{d}\boldsymbol{r}_3\, t_{12}^{S_{12}T_{12}(\mathrm{C})}(r_3) \\ &\quad \times \exp\left[i\left(-\frac{3}{4}\boldsymbol{Q} + \frac{\bar{\alpha}_{n'n}}{4\alpha_{n'n}}\boldsymbol{q}\right)\cdot\boldsymbol{r}_3\right] \exp\left(-\frac{\alpha_{n'}\alpha_n}{\alpha_{n'n}} r_3^2\right) \\ &= \frac{\pi^{3/2}}{\alpha_{n'n}^{3/2}} \exp\left(-\frac{q^2}{16\alpha_{n'n}}\right) \int_0^\infty \mathrm{d}r_3\, r_3^2 t_{12}^{S_{12}T_{12}(\mathrm{C})}(r_3) j_0(|\boldsymbol{p}_{n'n}|r_3) \exp\left(-\frac{\alpha_{n'}\alpha_n}{\alpha_{n'n}} r_3^2\right), \end{aligned} \tag{C.56}$$

$$\begin{aligned} I_{13:321,n'n}^{S_{13}T_{13}(\mathrm{C})} &= \frac{1}{4\pi}\frac{\pi^{3/2}}{\alpha_{n'n}^{3/2}} \exp\left(-\frac{q^2}{16\alpha_{n'n}}\right) \int \mathrm{d}\boldsymbol{r}_2\, t_{13}^{S_{13}T_{13}(\mathrm{C})}(r_2) \\ &\quad \times \exp\left[-i\left(-\frac{3}{4}\boldsymbol{Q} + \frac{\bar{\alpha}_{n'n}}{4\alpha_{n'n}}\boldsymbol{q}\right)\cdot\boldsymbol{r}_2\right] \exp\left(-\frac{\alpha_{n'}\alpha_n}{\alpha_{n'n}} r_2^2\right) \\ &= \frac{\pi^{3/2}}{\alpha_{n'n}^{3/2}} \exp\left(-\frac{q^2}{16\alpha_{n'n}}\right) \int_0^\infty \mathrm{d}r_2\, r_2^2 t_{13}^{S_{13}T_{13}(\mathrm{C})}(r_2) j_0(|\boldsymbol{p}_{n'n}|r_2) \exp\left(-\frac{\alpha_{n'}\alpha_n}{\alpha_{n'n}} r_2^2\right), \end{aligned} \tag{C.57}$$

in which we have used Eq. (C.185) and defined

$$\boldsymbol{p}_{n'n} \equiv -\frac{3}{4}\boldsymbol{Q} + \frac{\bar{\alpha}_{n'n}}{4\alpha_{n'n}}\boldsymbol{q}. \tag{C.58}$$

The components of the central interactions of the transition matrices (C.29) and (C.30) are given by

$$\bar{T}_{12:321}^{S_{12}T_{12}(\mathrm{C})}(\boldsymbol{\kappa}', S'M_S'|\boldsymbol{\kappa}, SM_S) \equiv \left\langle \phi_{\mathrm{x}}'(\boldsymbol{r}_1)\mathrm{e}^{i\boldsymbol{\kappa}'\cdot\boldsymbol{s}_1} \middle| t_{12}^{S_{12}T_{12}(\mathrm{C})}(r_3) \middle| \phi_{\mathrm{x}}(\boldsymbol{r}_3)\mathrm{e}^{i\boldsymbol{\kappa}\cdot\boldsymbol{s}_3} \right\rangle \delta_{S'S}\delta_{M_S'M_S}, \tag{C.59}$$

$$\bar{T}_{13:213}^{S_{13}T_{13}(\mathrm{C})}(\boldsymbol{\kappa}', S'M_S'|\boldsymbol{\kappa}, SM_S) \equiv \left\langle \phi_{\mathrm{x}}'(\boldsymbol{r}_1)\mathrm{e}^{i\boldsymbol{\kappa}'\cdot\boldsymbol{s}_1} \middle| t_{13}^{S_{13}T_{13}(\mathrm{C})}(r_2) \middle| \phi_{\mathrm{x}}(\boldsymbol{r}_2)\mathrm{e}^{i\boldsymbol{\kappa}\cdot\boldsymbol{s}_2} \right\rangle \delta_{S'S}\delta_{M_S'M_S}. \tag{C.60}$$

Similarly to the calculation of Eqs. (C.31) and (C.32),

$$\bar{T}_{12:321}^{S_{12}T_{12}(\mathrm{C})}(\boldsymbol{\kappa}', S'M_S'|\boldsymbol{\kappa}, SM_S) = \delta_{S'S}\delta_{M_S'M_S} \sum_{n'n} c_{n'}c_n I_{12:321,n'n}^{S_{12}T_{12}(\mathrm{C})}, \tag{C.61}$$

$$\bar{T}_{13:213}^{S_{13}T_{13}(\mathrm{C})}(\boldsymbol{\kappa}', S'M_S'|\boldsymbol{\kappa}, SM_S) = \delta_{S'S}\delta_{M_S'M_S} \sum_{n'n} c_{n'}c_n I_{13:213,n'n}^{S_{13}T_{13}(\mathrm{C})}, \tag{C.62}$$

$$\begin{aligned} I_{12:321,n'n}^{S_{12}T_{12}(\mathrm{C})} &\equiv \frac{1}{4\pi} \int \mathrm{d}\boldsymbol{r}_3 \int \mathrm{d}\boldsymbol{s}_3 \exp\left[-\alpha_{n'}\left(\frac{1}{2}\boldsymbol{r}_3 + \boldsymbol{s}_3\right)^2\right] \exp\left[-i\boldsymbol{\kappa}'\cdot\left(\frac{3}{4}\boldsymbol{r}_3 - \frac{1}{2}\boldsymbol{s}_3\right)\right] \\ &\quad \times t_{12}^{S_{12}T_{12}(\mathrm{C})}(r_3) \exp\left(-\alpha_n r_3^2\right) \exp\left(i\boldsymbol{\kappa}\cdot\boldsymbol{s}_3\right) \\ &= \frac{1}{4\pi} \int \mathrm{d}\boldsymbol{r}_3\, t_{12}^{S_{12}T_{12}(\mathrm{C})}(r_3) \exp\left(-\beta_{n'n} r_3^2\right) \exp\left(-\frac{3}{4} i\boldsymbol{\kappa}'\cdot\boldsymbol{r}_3\right) \\ &\quad \times \int \mathrm{d}\boldsymbol{s}_3 \exp\left(-\alpha_{n'} s_3^2\right) \exp\left[-\left(\alpha_{n'}\boldsymbol{r}_3 - i\boldsymbol{Q}'\right)\cdot\boldsymbol{s}_3\right], \end{aligned} \tag{C.63}$$

$$
\begin{aligned}
I^{S_{13}T_{13}(\mathrm{C})}_{13:213,n'n} \equiv{}& \frac{1}{4\pi}\int \mathrm{d}\boldsymbol{r}_2 \int \mathrm{d}\boldsymbol{s}_2 \exp\left[-\alpha_{n'}\left(\frac{1}{2}\boldsymbol{r}_2-\boldsymbol{s}_2\right)^2\right]\exp\left[-i\boldsymbol{\kappa}'\cdot\left(-\frac{3}{4}\boldsymbol{r}_2-\frac{1}{2}\boldsymbol{s}_2\right)\right]\\
&\times t^{S_{13}T_{13}(\mathrm{C})}_{13}(r_2)\exp\left(-\alpha_n r_2^2\right)\exp(i\boldsymbol{\kappa}\cdot\boldsymbol{s}_2)\\
={}& \frac{1}{4\pi}\int \mathrm{d}\boldsymbol{r}_2\, t^{S_{13}T_{13}(\mathrm{C})}_{13}(r_2)\exp\left(-\beta_{n'n}r_2^2\right)\exp\left(\frac{3}{4}i\boldsymbol{\kappa}'\cdot\boldsymbol{r}_2\right)\\
&\times\int \mathrm{d}\boldsymbol{s}_2 \exp\left(-\alpha_{n'}s_2^2\right)\exp\left[-(-\alpha_{n'}\boldsymbol{r}_2-i\boldsymbol{Q}')\cdot\boldsymbol{s}_2\right],
\end{aligned}
\tag{C.64}
$$

with defining $\beta_{n'n}$ and $\boldsymbol{Q}'$ as

$$
\beta_{n'n} \equiv \frac{1}{4}\alpha_{n'}+\alpha_n, \quad \boldsymbol{Q}' \equiv \boldsymbol{\kappa}+\frac{1}{2}\boldsymbol{\kappa}'.
\tag{C.65}
$$

Replacing α, $\boldsymbol{\beta}$, and $\boldsymbol{\gamma}$ in Eq. (C.184) as

$$
\alpha \to \alpha_{n'}, \quad \boldsymbol{\beta} \to \pm\alpha_{n'}\boldsymbol{r}, \quad \boldsymbol{\gamma} \to -\boldsymbol{Q}',
\tag{C.66}
$$

the integrals concerning $\boldsymbol{s}_3$ and $\boldsymbol{s}_2$ in Eqs. (C.63) and (C.64) are calculated as

$$
\begin{aligned}
&\int \mathrm{d}\boldsymbol{s} \exp\left(-\alpha_{n'}s^2\right)\exp\left[-(\pm\alpha_{n'}\boldsymbol{r}-i\boldsymbol{Q}')\cdot\boldsymbol{s}\right]\\
&\quad= \frac{\pi^{3/2}}{\alpha_{n'}^{3/2}}\exp\left(\frac{1}{4}\alpha_{n'}r^2\right)\exp\left[-\frac{(Q')^2}{4\alpha_{n'}}\right]\exp\left(\mp\frac{i}{2}\boldsymbol{Q}'\cdot\boldsymbol{r}\right),
\end{aligned}
\tag{C.67}
$$

and

$$
\begin{aligned}
I^{S_{12}T_{12}(\mathrm{C})}_{12:321,n'n} ={}& \frac{1}{4\pi}\frac{\pi^{3/2}}{\alpha_{n'}^{3/2}}\exp\left[-\frac{(Q')^2}{4\alpha_{n'}}\right]\int \mathrm{d}\boldsymbol{r}_3\, t^{S_{12}T_{12}(\mathrm{C})}_{12}(r_3)\\
&\times\exp\left(-\alpha_n r_3^2\right)\exp\left[-i\left(\frac{3}{4}\boldsymbol{\kappa}'+\frac{1}{2}\boldsymbol{Q}'\right)\cdot\boldsymbol{r}_3\right]\\
={}& \frac{\pi^{3/2}}{\alpha_{n'}^{3/2}}\exp\left[-\frac{(Q')^2}{4\alpha_{n'}}\right]\int_0^\infty \mathrm{d}r_3\, r_3^2 t^{S_{12}T_{12}(\mathrm{C})}_{12}(r_3)j_0\left(|\boldsymbol{p}'|r_3\right)\exp\left(-\alpha_n r_3^2\right),
\end{aligned}
\tag{C.68}
$$

$$
\begin{aligned}
I^{S_{13}T_{13}(\mathrm{C})}_{13:213,n'n} ={}& \frac{1}{4\pi}\frac{\pi^{3/2}}{\alpha_{n'}^{3/2}}\exp\left[-\frac{(Q')^2}{4\alpha_{n'}}\right]\int \mathrm{d}\boldsymbol{r}_2\, t^{S_{13}T_{13}(\mathrm{C})}_{13}(r_2)\\
&\times\exp\left(-\alpha_n r_2^2\right)\exp\left[i\left(\frac{3}{4}\boldsymbol{\kappa}'+\frac{1}{2}\boldsymbol{Q}'\right)\cdot\boldsymbol{r}_2\right]\\
={}& \frac{\pi^{3/2}}{\alpha_{n'}^{3/2}}\exp\left[-\frac{(Q')^2}{4\alpha_{n'}}\right]\int_0^\infty \mathrm{d}r_2\, r_2^2 t^{S_{13}T_{13}(\mathrm{C})}_{13}(r_2)j_0\left(|\boldsymbol{p}'|r_2\right)\exp\left(-\alpha_n r_2^2\right),
\end{aligned}
\tag{C.69}
$$

are obtained with making the use of Eq. (C.185). $\boldsymbol{p}'$ is defined by

$$
\boldsymbol{p}' \equiv \frac{3}{4}\boldsymbol{\kappa}'+\frac{1}{2}\boldsymbol{Q}' = \frac{1}{2}\boldsymbol{\kappa}+\boldsymbol{\kappa}'.
\tag{C.70}
$$

C.3 Components of tensor interactions

The components of the tensor interactions of the transition matrices (C.25) and (C.26) are given by

$$\begin{aligned}
&\bar{T}^{S_{12}T_{12}(\mathrm{T})}_{12:123}(\boldsymbol{\kappa}', S'M'_S|\boldsymbol{\kappa}, SM_S) \\
&\quad \equiv \left\langle \phi'_{\mathrm{x}}(\boldsymbol{r}_1)\mathrm{e}^{i\boldsymbol{\kappa}'\cdot\boldsymbol{s}_1}\left[\left[\eta^{(2)}_{\frac{1}{2}}\otimes\eta^{(1)}_{\frac{1}{2}}\right]_{S_{12}}\otimes\eta^{(3)}_{\frac{1}{2}}\right]_{S'M'_S}\right| \\
&\qquad \times t^{S_{12}T_{12}(\mathrm{T})}_{12}(r_3)\hat{S}^{\mathrm{T}}_{12}\left|\phi_{\mathrm{x}}(\boldsymbol{r}_1)\mathrm{e}^{i\boldsymbol{\kappa}\cdot\boldsymbol{s}_1}\left[\left[\eta^{(2)}_{\frac{1}{2}}\otimes\eta^{(1)}_{\frac{1}{2}}\right]_{S_{12}}\otimes\eta^{(3)}_{\frac{1}{2}}\right]_{SM_S}\right\rangle, \qquad \text{(C.71)}
\end{aligned}$$

$$\begin{aligned}
&\bar{T}^{S_{13}T_{13}(\mathrm{T})}_{13:123}(\boldsymbol{\kappa}', S'M'_S|\boldsymbol{\kappa}, SM_S) \\
&\quad \equiv \left\langle \phi'_{\mathrm{x}}(\boldsymbol{r}_1)\mathrm{e}^{i\boldsymbol{\kappa}'\cdot\boldsymbol{s}_1}\left[\left[\eta^{(3)}_{\frac{1}{2}}\otimes\eta^{(1)}_{\frac{1}{2}}\right]_{S_{13}}\otimes\eta^{(2)}_{\frac{1}{2}}\right]_{S'M'_S}\right| \\
&\qquad \times t^{S_{13}T_{13}(\mathrm{T})}_{13}(r_2)\hat{S}^{\mathrm{T}}_{13}\left|\phi_{\mathrm{x}}(\boldsymbol{r}_1)\mathrm{e}^{i\boldsymbol{\kappa}\cdot\boldsymbol{s}_1}\left[\left[\eta^{(3)}_{\frac{1}{2}}\otimes\eta^{(1)}_{\frac{1}{2}}\right]_{S_{13}}\otimes\eta^{(2)}_{\frac{1}{2}}\right]_{SM_S}\right\rangle. \qquad \text{(C.72)}
\end{aligned}$$

We can rewrite the tensor operators (2.101) as

$$S^{\mathrm{T}}_{1a} = \frac{9[\boldsymbol{r}_b\otimes\boldsymbol{\sigma}_1]_{00}[\boldsymbol{r}_b\otimes\boldsymbol{\sigma}_a]_{00}}{r_b^2} + \sqrt{3}[\boldsymbol{\sigma}_1\otimes\boldsymbol{\sigma}_a]_{00} \qquad \text{(C.73)}$$

with using

$$\boldsymbol{\sigma}_1\cdot\boldsymbol{r}_b = -\sqrt{3}[\boldsymbol{r}_b\otimes\boldsymbol{\sigma}_1]_{00}, \quad \boldsymbol{\sigma}_a\cdot\boldsymbol{r}_b = -\sqrt{3}[\boldsymbol{r}_b\otimes\boldsymbol{\sigma}_a]_{00}, \quad \boldsymbol{\sigma}_1\cdot\boldsymbol{\sigma}_a = -\sqrt{3}[\boldsymbol{\sigma}_1\otimes\boldsymbol{\sigma}_a]_{00}, \qquad \text{(C.74)}$$

in which (a, b) begin $(2, 3)$ or $(3, 2)$. In addition, $[\boldsymbol{r}_b\otimes\boldsymbol{\sigma}_1]_{00}[\boldsymbol{r}_b\otimes\boldsymbol{\sigma}_a]_{00}$ in Eq. (C.73) can be calculated as

$$\begin{aligned}
&[\boldsymbol{r}_b\otimes\boldsymbol{\sigma}_1]_{00}[\boldsymbol{r}_b\otimes\boldsymbol{\sigma}_a]_{00} \\
&\quad = [[\boldsymbol{r}_b\otimes\boldsymbol{\sigma}_1]_0\otimes[\boldsymbol{r}_b\otimes\boldsymbol{\sigma}_a]_0]_{00} \\
&\quad = \sum_{j'j}\hat{j}'\hat{j}\begin{Bmatrix} 1 & 1 & 0 \\ 1 & 1 & 0 \\ j' & j & 0 \end{Bmatrix}\left[[\boldsymbol{r}_b\otimes\boldsymbol{r}_b]_{j'}\otimes[\boldsymbol{\sigma}_1\otimes\boldsymbol{\sigma}_a]_j\right]_{00} \\
&\quad = \frac{1}{3}[\boldsymbol{r}_b\otimes\boldsymbol{r}_b]_{00}[\boldsymbol{\sigma}_1\otimes\boldsymbol{\sigma}_a]_{00} + \frac{\sqrt{3}}{3}[[\boldsymbol{r}_b\otimes\boldsymbol{r}_b]_1\otimes[\boldsymbol{\sigma}_1\otimes\boldsymbol{\sigma}_a]_1]_{00} + \frac{\sqrt{5}}{3}[[\boldsymbol{r}_b\otimes\boldsymbol{r}_b]_2\otimes[\boldsymbol{\sigma}_1\otimes\boldsymbol{\sigma}_a]_2]_{00} \\
&\quad = -\frac{\sqrt{3}}{9}r_b^2[\boldsymbol{\sigma}_1\otimes\boldsymbol{\sigma}_a]_{00} + \frac{2\sqrt{6\pi}}{9}r_b^2[Y_2(\hat{\boldsymbol{r}}_b)\otimes[\boldsymbol{\sigma}_1\otimes\boldsymbol{\sigma}_a]_2]_{00} \qquad \text{(C.75)}
\end{aligned}$$

because the followings hold:

$$\begin{aligned}
[\boldsymbol{r}_b\otimes\boldsymbol{r}_b]_{00} &= \frac{4\pi}{3}r_b^2[Y_1(\hat{\boldsymbol{r}}_b)\otimes Y_1(\hat{\boldsymbol{r}}_b)]_{00} \\
&= \frac{4\pi}{3}r_b^2\cdot\frac{3}{\sqrt{4\pi}}(1010|00)Y_{00}(\hat{\boldsymbol{r}}_b) = -\frac{r_b^2}{\sqrt{3}}, \qquad \text{(C.76)}
\end{aligned}$$

$$[\boldsymbol{r}_b\otimes\boldsymbol{r}_b]_{1m} = \frac{i}{\sqrt{2}}(\boldsymbol{r}_b\times\boldsymbol{r}_b)_m = 0, \qquad \text{(C.77)}$$

$$[\boldsymbol{r}_b \otimes \boldsymbol{r}_b]_{2m} = \frac{4\pi}{3} r_b^2 [Y_1(\hat{\boldsymbol{r}}_b) \otimes Y_1(\hat{\boldsymbol{r}}_b)]_{2m}$$
$$= \frac{4\pi}{3} r_b^2 \cdot \frac{1}{\sqrt{4\pi}} \frac{1}{\sqrt{5}} (1010|20) Y_{2m}(\hat{\boldsymbol{r}}_b) = \sqrt{\frac{8\pi}{15}} r_b^2 Y_{2m}(\hat{\boldsymbol{r}}_b). \tag{C.78}$$

Then S_{1a}^{T} becomes

$$\hat{S}_{1a}^{\mathrm{T}} = 2\sqrt{6\pi} [Y_2(\hat{\boldsymbol{r}}_b) \otimes [\boldsymbol{\sigma}_1 \otimes \boldsymbol{\sigma}_b]_2]_{00} = 2\sqrt{\frac{6\pi}{5}} \sum_m (-)^m Y_{2m}(\hat{\boldsymbol{r}}_b) [\boldsymbol{\sigma}_1 \otimes \boldsymbol{\sigma}_a]_{2-m}. \tag{C.79}$$

Inserting this into Eqs. (C.71) and (C.72) and some arrangement,

$$\begin{aligned} &\bar{T}_{12:123}^{S_{12}T_{12}(\mathrm{T})}(\boldsymbol{\kappa}', S' M_S' | \boldsymbol{\kappa}, S M_S) \\ &= 2\sqrt{\frac{6\pi}{5}} \sum_m (-)^m \left\langle \phi_{\mathrm{x}}'(\boldsymbol{r}_1) \mathrm{e}^{i\boldsymbol{\kappa}'\cdot\boldsymbol{s}_1} \middle| t_{12}^{S_{12}T_{12}(\mathrm{T})}(r_3) Y_{2m}(\hat{\boldsymbol{r}}_3) \middle| \phi_{\mathrm{x}}(\boldsymbol{r}_1) \mathrm{e}^{i\boldsymbol{\kappa}\cdot\boldsymbol{s}_1} \right\rangle \\ &\quad \times \left\langle \left[\left[\eta_{\frac{1}{2}}^{(2)} \otimes \eta_{\frac{1}{2}}^{(1)} \right]_{S_{12}} \otimes \eta_{\frac{1}{2}}^{(3)} \right]_{S' M_S'} \middle| [\boldsymbol{\sigma}_1 \otimes \boldsymbol{\sigma}_2]_{2-m} \middle| \left[\left[\eta_{\frac{1}{2}}^{(2)} \otimes \eta_{\frac{1}{2}}^{(1)} \right]_{S_{12}} \otimes \eta_{\frac{1}{2}}^{(3)} \right]_{S M_S} \right\rangle, \end{aligned} \tag{C.80}$$

$$\begin{aligned} &\bar{T}_{13:123}^{S_{13}T_{13}(\mathrm{T})}(\boldsymbol{\kappa}', S' M_S' | \boldsymbol{\kappa}, S M_S) \\ &= 2\sqrt{\frac{6\pi}{5}} \sum_m (-)^m \left\langle \phi_{\mathrm{x}}'(\boldsymbol{r}_1) \mathrm{e}^{i\boldsymbol{\kappa}'\cdot\boldsymbol{s}_1} \middle| t_{13}^{S_{13}T_{13}(\mathrm{T})}(r_2) Y_{2m}(\hat{\boldsymbol{r}}_2) \middle| \phi_{\mathrm{x}}(\boldsymbol{r}_1) \mathrm{e}^{i\boldsymbol{\kappa}\cdot\boldsymbol{s}_1} \right\rangle \\ &\quad \times \left\langle \left[\left[\eta_{\frac{1}{2}}^{(3)} \otimes \eta_{\frac{1}{2}}^{(1)} \right]_{S_{13}} \otimes \eta_{\frac{1}{2}}^{(2)} \right]_{S' M_S'} \middle| [\boldsymbol{\sigma}_1 \otimes \boldsymbol{\sigma}_3]_{2-m} \middle| \left[\left[\eta_{\frac{1}{2}}^{(3)} \otimes \eta_{\frac{1}{2}}^{(1)} \right]_{S_{13}} \otimes \eta_{\frac{1}{2}}^{(2)} \right]_{S M_S} \right\rangle \end{aligned} \tag{C.81}$$

are obtained. The spin parts of Eqs. (C.80) and (C.81) are calculated as

$$\begin{aligned} &\left\langle \left[\left[\eta_{\frac{1}{2}}^{(a)} \otimes \eta_{\frac{1}{2}}^{(1)} \right]_{S_{1a}} \otimes \eta_{\frac{1}{2}}^{(b)} \right]_{S' M_S'} \middle| [\boldsymbol{\sigma}_1 \otimes \boldsymbol{\sigma}_a]_{2-m} \middle| \left[\left[\eta_{\frac{1}{2}}^{(a)} \otimes \eta_{\frac{1}{2}}^{(1)} \right]_{S_{1a}} \otimes \eta_{\frac{1}{2}}^{(b)} \right]_{S M_S} \right\rangle \\ &= \sum_{M_{1a}' M_{1a}} \sum_{\mu_b} \left(S_{1a} M_{1a}' \frac{1}{2} \mu_b \middle| S' M_S' \right) \left(S_{1a} M_{1a} \frac{1}{2} \mu_b \middle| S M_S \right) \\ &\quad \times \left\langle \left[\eta_{\frac{1}{2}}^{(a)} \otimes \eta_{\frac{1}{2}}^{(1)} \right]_{S_{1a} M_{1a}'} \middle| [\boldsymbol{\sigma}_1 \otimes \boldsymbol{\sigma}_a]_{2-m} \middle| \left[\eta_{\frac{1}{2}}^{(a)} \otimes \eta_{\frac{1}{2}}^{(1)} \right]_{S_{1a} M_{1a}} \right\rangle, \end{aligned} \tag{C.82}$$

and from the Wigner-Eckart theorem, the matrix element in the right-hand-side of Eq. (C.82) is reduced to

$$\begin{aligned} &\left\langle \left[\eta_{\frac{1}{2}}^{(a)} \otimes \eta_{\frac{1}{2}}^{(1)} \right]_{S_{1a} M_{1a}'} \middle| [\boldsymbol{\sigma}_1 \otimes \boldsymbol{\sigma}_a]_{2-m} \middle| \left[\eta_{\frac{1}{2}}^{(a)} \otimes \eta_{\frac{1}{2}}^{(1)} \right]_{S_{1a} M_{1a}} \right\rangle \\ &= \frac{1}{\hat{S}_{1a}} (S_{1a} M_{1a} 2 - m | S_{1a} M_{1a}') \left\langle \left[\eta_{\frac{1}{2}}^{(a)} \otimes \eta_{\frac{1}{2}}^{(1)} \right]_{S_{1a}} \middle\| [\boldsymbol{\sigma}_1 \otimes \boldsymbol{\sigma}_a]_2 \middle\| \left[\eta_{\frac{1}{2}}^{(a)} \otimes \eta_{\frac{1}{2}}^{(1)} \right]_{S_{1a}} \right\rangle \\ &= \frac{1}{\hat{S}_{1a}} (S_{1a} M_{1a} 2 - m | S_{1a} M_{1a}') \cdot \sqrt{5} \hat{S}_{1a}^2 \begin{Bmatrix} 1/2 & 1/2 & S_{1a} \\ 1/2 & 1/2 & S_{1a} \\ 1 & 1 & 2 \end{Bmatrix} \left\langle \eta_{\frac{1}{2}}^{(1)} \middle\| \boldsymbol{\sigma}_1 \middle\| \eta_{\frac{1}{2}}^{(1)} \right\rangle \left\langle \eta_{\frac{1}{2}}^{(a)} \middle\| \boldsymbol{\sigma}_a \middle\| \eta_{\frac{1}{2}}^{(a)} \right\rangle \\ &= 2\sqrt{\frac{5}{3}} (1 M_{1a} 2 - m | 1 M_{1a}'). \end{aligned} \tag{C.83}$$

It should be noted that Eq. (C.83) is equal to zero in the case of $S_{1a} = 0$ and that the Pauli matrix is defined by the spin operator multiplied by 2. Then we get

$$\begin{aligned}
&\bar{T}^{S_{12}T_{12}(\mathrm{T})}_{12:123}(\boldsymbol{\kappa}', S'M'_S|\boldsymbol{\kappa}, SM_S) \\
&\quad = 4\sqrt{2\pi}\sum_{m\mu_3}\sum_{M'_{12}M_{12}}(-)^m(1M_{12}2-m|1M'_{12})\left(S_{12}M'_{12}\frac{1}{2}\mu_3\middle|S'M'_S\right)\left(S_{12}M_{12}\frac{1}{2}\mu_3\middle|SM_S\right) \\
&\qquad \times \left\langle \phi'_{\mathrm{x}}(\boldsymbol{r}_1)\mathrm{e}^{i\boldsymbol{\kappa}'\cdot\boldsymbol{s}_1}\middle| t^{S_{12}T_{12}(\mathrm{T})}_{12}(r_3)Y_{2m}(\hat{\boldsymbol{r}}_3)\middle|\phi_{\mathrm{x}}(\boldsymbol{r}_1)\mathrm{e}^{i\boldsymbol{\kappa}\cdot\boldsymbol{s}_1}\right\rangle,
\end{aligned} \tag{C.84}$$

$$\begin{aligned}
&\bar{T}^{S_{13}T_{13}(\mathrm{T})}_{13:123}(\boldsymbol{\kappa}', S'M'_S|\boldsymbol{\kappa}, SM_S) \\
&\quad = 4\sqrt{2\pi}\sum_{m\mu_2}\sum_{M'_{13}M_{13}}(-)^m(1M_{13}2-m|1M'_{13})\left(S_{13}M'_{13}\frac{1}{2}\mu_2\middle|S'M'_S\right)\left(S_{13}M_{13}\frac{1}{2}\mu_2\middle|SM_S\right) \\
&\qquad \times \left\langle \phi'_{\mathrm{x}}(\boldsymbol{r}_1)\mathrm{e}^{i\boldsymbol{\kappa}'\cdot\boldsymbol{s}_1}\middle| t^{S_{13}T_{13}(\mathrm{T})}_{13}(r_2)Y_{2m}(\hat{\boldsymbol{r}}_2)\middle|\phi_{\mathrm{x}}(\boldsymbol{r}_1)\mathrm{e}^{i\boldsymbol{\kappa}\cdot\boldsymbol{s}_1}\right\rangle.
\end{aligned} \tag{C.85}$$

Now we make the same assumptions in Section C.2, that is,

- that particle x can be described only by the S wave,
- that ϕ_{x} and ϕ'_{x} are constructed by the superposition of the Gaussians as in Eq. (C.33).

Taking $\boldsymbol{r}_3$ and $\boldsymbol{s}_3$ in Eq. (C.84) and $\boldsymbol{r}_2$ and $\boldsymbol{s}_2$ in Eq. (C.85), these transition matrices become

$$\begin{aligned}
&\bar{T}^{S_{12}T_{12}(\mathrm{T})}_{12:123}(\boldsymbol{\kappa}', S'M'_S|\boldsymbol{\kappa}, SM_S) \\
&\quad = 4\sqrt{2\pi}\sum_{m\mu_3}\sum_{M'_{12}M_{12}}(-)^m(1M_{12}2-m|1M'_{12}) \\
&\qquad \times \left(S_{12}M'_{12}\frac{1}{2}\mu_3\middle|S'M'_S\right)\left(S_{12}M_{12}\frac{1}{2}\mu_3\middle|SM_S\right)\sum_{n'n}c_{n'}c_n I^{S_{12}T_{12}(\mathrm{T})}_{12:123,m,n'n},
\end{aligned} \tag{C.86}$$

$$\begin{aligned}
&\bar{T}^{S_{13}T_{13}(\mathrm{T})}_{13:123}(\boldsymbol{\kappa}', S'M'_S|\boldsymbol{\kappa}, SM_S) \\
&\quad = 4\sqrt{2\pi}\sum_{m\mu_2}\sum_{M'_{13}M_{13}}(-)^m(1M_{13}2-m|1M'_{13}) \\
&\qquad \times \left(S_{13}M'_{13}\frac{1}{2}\mu_2\middle|S'M'_S\right)\left(S_{13}M_{13}\frac{1}{2}\mu_2\middle|SM_S\right)\sum_{n'n}c_{n'}c_n I^{S_{13}T_{13}(\mathrm{T})}_{13:123,m,n'n},
\end{aligned} \tag{C.87}$$

$$\begin{aligned}
&I^{S_{12}T_{12}(\mathrm{T})}_{12:123,m,n'n} \\
&\quad \equiv \frac{1}{4\pi}\int \mathrm{d}\boldsymbol{r}_3\int \mathrm{d}\boldsymbol{s}_3 \exp\left[-\alpha_{n'}\left(\frac{1}{2}\boldsymbol{r}_3+\boldsymbol{s}_3\right)^2\right]\exp\left[-i\boldsymbol{\kappa}'\cdot\left(\frac{3}{4}\boldsymbol{r}_3-\frac{1}{2}\boldsymbol{s}_3\right)\right] \\
&\qquad \times t^{S_{12}T_{12}(\mathrm{T})}_{12}(r_3)Y_{2m}(\hat{\boldsymbol{r}}_3)\exp\left[-\alpha_n\left(\frac{1}{2}\boldsymbol{r}_3+\boldsymbol{s}_3\right)^2\right]\exp\left[i\boldsymbol{\kappa}\cdot\left(\frac{3}{4}\boldsymbol{r}_3-\frac{1}{2}\boldsymbol{s}_3\right)\right] \\
&\quad = \frac{1}{4\pi}\frac{\pi^{3/2}}{\alpha_{n'n}^{3/2}}\exp\left(-\frac{q^2}{16\alpha_{n'n}}\right)\int \mathrm{d}\boldsymbol{r}_3\, t^{S_{12}T_{12}(\mathrm{T})}_{12}(r_3)Y_{2m}(\hat{\boldsymbol{r}}_3)\mathrm{e}^{i\boldsymbol{q}\cdot\boldsymbol{r}_3} \\
&\quad = -\frac{\pi^{3/2}}{\alpha_{n'n}^{3/2}}\exp\left(-\frac{q^2}{16\alpha_{n'n}}\right)Y_{2m}(\hat{\boldsymbol{q}})\int_0^\infty \mathrm{d}r_3\, r_3^2 t^{S_{12}T_{12}(\mathrm{T})}_{12}(r_3)j_2(qr_3),
\end{aligned} \tag{C.88}$$

$$
\begin{aligned}
& I^{S_{13}T_{13}(\mathrm{T})}_{13:123,m,n'n} \\
& \quad \equiv \frac{1}{4\pi}\int \mathrm{d}\boldsymbol{r}_2 \int \mathrm{d}\boldsymbol{s}_2 \exp\left[-\alpha_{n'}\left(\frac{1}{2}\boldsymbol{r}_2-\boldsymbol{s}_2\right)^2\right]\exp\left[-i\boldsymbol{\kappa}'\cdot\left(-\frac{3}{4}\boldsymbol{r}_2-\frac{1}{2}\boldsymbol{s}_2\right)\right] \\
& \qquad \times t^{S_{13}T_{13}(\mathrm{T})}_{13}(r_2)Y_{2m}(\hat{\boldsymbol{r}}_2)\exp\left[-\alpha_n\left(\frac{1}{2}\boldsymbol{r}_2-\boldsymbol{s}_2\right)^2\right]\exp\left[i\boldsymbol{\kappa}\cdot\left(-\frac{3}{4}\boldsymbol{r}_2-\frac{1}{2}\boldsymbol{s}_2\right)\right] \\
& \quad = \frac{1}{4\pi}\frac{\pi^{3/2}}{\alpha^{3/2}_{n'n}}\exp\left(-\frac{q^2}{16\alpha_{n'n}}\right)\int \mathrm{d}\boldsymbol{r}_2\, t^{S_{13}T_{13}(\mathrm{T})}_{13}(r_2)Y_{2m}(\hat{\boldsymbol{r}}_2)\mathrm{e}^{-i\boldsymbol{q}\cdot\boldsymbol{r}_2} \\
& \quad = -\frac{\pi^{3/2}}{\alpha^{3/2}_{n'n}}\exp\left(-\frac{q^2}{16\alpha_{n'n}}\right)Y_{2m}(\hat{\boldsymbol{q}})\int_0^\infty \mathrm{d}r_2\, r_2^2 t^{S_{13}T_{13}(\mathrm{T})}_{13}(r_2)j_2(qr_2),
\end{aligned}
\tag{C.89}
$$

in which we have used Eqs. (C.44) and (C.185).

The components of the tensor interactions of the transition matrices (C.27) and (C.28) are given by

$$
\begin{aligned}
& \bar{T}^{S_{12}T_{12}(\mathrm{T})}_{12:213}(\boldsymbol{\kappa}', S'M'_S|\boldsymbol{\kappa}, SM_S) \\
& \quad \equiv \left\langle \phi'_{\mathrm{x}}(\boldsymbol{r}_1)\mathrm{e}^{i\boldsymbol{\kappa}'\cdot\boldsymbol{s}_1}\left[\left[\eta^{(2)}_{\frac{1}{2}}\otimes\eta^{(1)}_{\frac{1}{2}}\right]_{S_{12}}\otimes\eta^{(3)}_{\frac{1}{2}}\right]_{S'M'_S}\right| \\
& \qquad \times t^{S_{12}T_{12}(\mathrm{T})}_{12}(r_3)\hat{S}^{\mathrm{T}}_{12}\left|\phi_{\mathrm{x}}(\boldsymbol{r}_2)\mathrm{e}^{i\boldsymbol{\kappa}\cdot\boldsymbol{s}_2}\left[\left[\eta^{(2)}_{\frac{1}{2}}\otimes\eta^{(1)}_{\frac{1}{2}}\right]_{S_{12}}\otimes\eta^{(3)}_{\frac{1}{2}}\right]_{SM_S}\right\rangle,
\end{aligned}
\tag{C.90}
$$

$$
\begin{aligned}
& \bar{T}^{S_{13}T_{13}(\mathrm{T})}_{13:321}(\boldsymbol{\kappa}', S'M'_S|\boldsymbol{\kappa}, SM_S) \\
& \quad \equiv \left\langle \phi'_{\mathrm{x}}(\boldsymbol{r}_1)\mathrm{e}^{i\boldsymbol{\kappa}'\cdot\boldsymbol{s}_1}\left[\left[\eta^{(3)}_{\frac{1}{2}}\otimes\eta^{(1)}_{\frac{1}{2}}\right]_{S_{13}}\otimes\eta^{(2)}_{\frac{1}{2}}\right]_{S'M'_S}\right| \\
& \qquad \times t^{S_{13}T_{13}(\mathrm{T})}_{13}(r_2)\hat{S}^{\mathrm{T}}_{13}\left|\phi_{\mathrm{x}}(\boldsymbol{r}_3)\mathrm{e}^{i\boldsymbol{\kappa}\cdot\boldsymbol{s}_3}\left[\left[\eta^{(3)}_{\frac{1}{2}}\otimes\eta^{(1)}_{\frac{1}{2}}\right]_{S_{13}}\otimes\eta^{(2)}_{\frac{1}{2}}\right]_{SM_S}\right\rangle.
\end{aligned}
\tag{C.91}
$$

We can calculate them in the similar way shown above, and then

$$
\begin{aligned}
& \bar{T}^{S_{12}T_{12}(\mathrm{T})}_{12:213}(\boldsymbol{\kappa}', S'M'_S|\boldsymbol{\kappa}, SM_S) \\
& \quad = 4\sqrt{2\pi}\sum_{m\mu_3}\sum_{M'_{12}M_{12}}(-)^m(1M_{12}2-m|1M'_{12}) \\
& \qquad \times \left(S_{12}M'_{12}\frac{1}{2}\mu_3\middle|S'M'_S\right)\left(S_{12}M_{12}\frac{1}{2}\mu_3\middle|SM_S\right)\sum_{n'n}c_{n'}c_n I^{S_{12}T_{12}(\mathrm{T})}_{12:213,m,n'n},
\end{aligned}
\tag{C.92}
$$

$$
\begin{aligned}
& \bar{T}^{S_{13}T_{13}(\mathrm{T})}_{13:321}(\boldsymbol{\kappa}', S'M'_S|\boldsymbol{\kappa}, SM_S) \\
& \quad = 4\sqrt{2\pi}\sum_{m\mu_2}\sum_{M'_{13}M_{13}}(-)^m(1M_{13}2-m|1M'_{13}) \\
& \qquad \times \left(S_{13}M'_{13}\frac{1}{2}\mu_2\middle|S'M'_S\right)\left(S_{13}M_{13}\frac{1}{2}\mu_2\middle|SM_S\right)\sum_{n'n}c_{n'}c_n I^{S_{13}T_{13}(\mathrm{T})}_{13:321,m,n'n},
\end{aligned}
\tag{C.93}
$$

$$
I^{S_{12}T_{12}(\mathrm{T})}_{12:213,m,n'n}
$$

$$
\begin{aligned}
&\equiv \frac{1}{4\pi}\int \mathrm{d}\boldsymbol{r}_3 \int \mathrm{d}\boldsymbol{s}_3 \exp\left[-\alpha_{n'}\left(\frac{1}{2}\boldsymbol{r}_3+\boldsymbol{s}_3\right)^2\right] \exp\left[-i\boldsymbol{\kappa}'\cdot\left(\frac{3}{4}\boldsymbol{r}_3-\frac{1}{2}\boldsymbol{s}_3\right)\right] \\
&\quad\times t_{12}^{S_{12}T_{12}(\mathrm{T})}(r_3)Y_{2m}(\hat{\boldsymbol{r}}_3)\exp\left[-\alpha_n\left(-\frac{1}{2}\boldsymbol{r}_3+\boldsymbol{s}_3\right)^2\right]\exp\left[i\boldsymbol{\kappa}\cdot\left(-\frac{3}{4}\boldsymbol{r}_3-\frac{1}{2}\boldsymbol{s}_3\right)\right] \\
&= \frac{1}{4\pi}\frac{\pi^{3/2}}{\alpha_{n'n}^{3/2}}\exp\left(-\frac{q^2}{16\alpha_{n'n}}\right)\int \mathrm{d}\boldsymbol{r}_3\, t_{12}^{S_{12}T_{12}(\mathrm{T})}(r_3)Y_{2m}(\hat{\boldsymbol{r}}_3)\mathrm{e}^{i\boldsymbol{p}_{n'n}\cdot\boldsymbol{r}_3}\exp\left(-\frac{\alpha_{n'}\alpha_n}{\alpha_{n'n}}r_3^2\right) \\
&= -\frac{\pi^{3/2}}{\alpha_{n'n}^{3/2}}\exp\left(-\frac{q^2}{16\alpha_{n'n}}\right)Y_{2m}(\hat{\boldsymbol{p}}_{n'n})\int_0^\infty \mathrm{d}r_3\, r_3^2 t_{12}^{S_{12}T_{12}(\mathrm{T})}(r_3)j_2(|\boldsymbol{p}_{n'n}|r_3)\exp\left(-\frac{\alpha_{n'}\alpha_n}{\alpha_{n'n}}r_3^2\right),
\end{aligned}
\tag{C.94}
$$

$$
\begin{aligned}
&I_{13:321,m,n'n}^{S_{13}T_{13}(\mathrm{T})} \\
&\equiv \frac{1}{4\pi}\int \mathrm{d}\boldsymbol{r}_2 \int \mathrm{d}\boldsymbol{s}_2 \exp\left[-\alpha_{n'}\left(\frac{1}{2}\boldsymbol{r}_2-\boldsymbol{s}_2\right)^2\right] \exp\left[-i\boldsymbol{\kappa}'\cdot\left(-\frac{3}{4}\boldsymbol{r}_2-\frac{1}{2}\boldsymbol{s}_2\right)\right] \\
&\quad\times t_{13}^{S_{13}T_{13}(\mathrm{T})}(r_2)Y_{2m}(\hat{\boldsymbol{r}}_2)\exp\left[-\alpha_n\left(-\frac{1}{2}\boldsymbol{r}_2-\boldsymbol{s}_2\right)^2\right]\exp\left[i\boldsymbol{\kappa}\cdot\left(\frac{3}{4}\boldsymbol{r}_2-\frac{1}{2}\boldsymbol{s}_2\right)\right] \\
&= \frac{1}{4\pi}\frac{\pi^{3/2}}{\alpha_{n'n}^{3/2}}\exp\left(-\frac{q^2}{16\alpha_{n'n}}\right)\int \mathrm{d}\boldsymbol{r}_2\, t_{13}^{S_{13}T_{13}(\mathrm{T})}(r_2)Y_{2m}(\hat{\boldsymbol{r}}_2)\mathrm{e}^{-i\boldsymbol{p}_{n'n}\cdot\boldsymbol{r}_2}\exp\left(-\frac{\alpha_{n'}\alpha_n}{\alpha_{n'n}}r_2^2\right) \\
&= -\frac{\pi^{3/2}}{\alpha_{n'n}^{3/2}}\exp\left(-\frac{q^2}{16\alpha_{n'n}}\right)Y_{2m}(\hat{\boldsymbol{p}}_{n'n})\int_0^\infty \mathrm{d}r_2\, r_2^2 t_{13}^{S_{13}T_{13}(\mathrm{T})}(r_2)j_2(|\boldsymbol{p}_{n'n}|r_2)\exp\left(-\frac{\alpha_{n'}\alpha_n}{\alpha_{n'n}}r_2^2\right)
\end{aligned}
\tag{C.95}
$$

are obtain with using Eqs. (C.55) and (C.185).

The components of the tensor interactions of the transition matrices (C.29) and (C.30) are given by

$$
\begin{aligned}
&\bar{T}_{12:321}^{S_{12}T_{12}(\mathrm{T})}(\boldsymbol{\kappa}', S'M_S'|\boldsymbol{\kappa}, SM_S) \\
&\equiv \left\langle \phi_{\mathrm{x}}'(\boldsymbol{r}_1)\mathrm{e}^{i\boldsymbol{\kappa}'\cdot\boldsymbol{s}_1}\left[\left[\eta_{\frac{1}{2}}^{(2)}\otimes\eta_{\frac{1}{2}}^{(1)}\right]_{s_{\mathrm{x}}}\otimes\eta_{\frac{1}{2}}^{(3)}\right]_{S'M_S'}\right| \\
&\qquad\times t_{12}^{S_{12}T_{12}(\mathrm{T})}(r_3)\hat{S}_{12}^{\mathrm{T}}\left|\phi_{\mathrm{x}}(\boldsymbol{r}_3)\mathrm{e}^{i\boldsymbol{\kappa}\cdot\boldsymbol{s}_3}\left[\left[\eta_{\frac{1}{2}}^{(2)}\otimes\eta_{\frac{1}{2}}^{(1)}\right]_{s_{\mathrm{x}}}\otimes\eta_{\frac{1}{2}}^{(3)}\right]_{SM_S}\right\rangle,
\end{aligned}
\tag{C.96}
$$

$$
\begin{aligned}
&\bar{T}_{13:213}^{S_{13}T_{13}(\mathrm{T})}(\boldsymbol{\kappa}', S'M_S'|\boldsymbol{\kappa}, SM_S) \\
&\equiv \left\langle \phi_{\mathrm{x}}'(\boldsymbol{r}_1)\mathrm{e}^{i\boldsymbol{\kappa}'\cdot\boldsymbol{s}_1}\left[\left[\eta_{\frac{1}{2}}^{(3)}\otimes\eta_{\frac{1}{2}}^{(1)}\right]_{s_{\mathrm{x}}}\otimes\eta_{\frac{1}{2}}^{(2)}\right]_{S'M_S'}\right| \\
&\qquad\times t_{13}^{S_{13}T_{13}(\mathrm{T})}(r_2)\hat{S}_{13}^{\mathrm{T}}\left|\phi_{\mathrm{x}}(\boldsymbol{r}_2)\mathrm{e}^{i\boldsymbol{\kappa}\cdot\boldsymbol{s}_2}\left[\left[\eta_{\frac{1}{2}}^{(3)}\otimes\eta_{\frac{1}{2}}^{(1)}\right]_{s_{\mathrm{x}}}\otimes\eta_{\frac{1}{2}}^{(2)}\right]_{SM_S}\right\rangle.
\end{aligned}
\tag{C.97}
$$

Calculating them similarly to Eqs. (C.71) and (C.72), we get

$$
\begin{aligned}
&\bar{T}_{12:321}^{S_{12}T_{12}(\mathrm{T})}(\boldsymbol{\kappa}', S'M_S'|\boldsymbol{\kappa}, SM_S) \\
&= 4\sqrt{2\pi}\sum_{m\mu_3}\sum_{M_{12}'M_{12}}(-)^m(1M_{12}2-m|1M_{12}') \\
&\quad\times\left(s_{\mathrm{x}}M_{12}'\frac{1}{2}\mu_3\middle|S'M_S'\right)\left(s_{\mathrm{x}}M_{12}\frac{1}{2}\mu_3\middle|SM_S\right)\sum_{n'n}c_{n'}c_n I_{12:321,m,n'n}^{S_{12}T_{12}(\mathrm{T})},
\end{aligned}
\tag{C.98}
$$

$$
\begin{aligned}
&\bar{T}^{S_{13}T_{13}(\mathrm{T})}_{13:213}(\boldsymbol{\kappa}', S'M_S'|\boldsymbol{\kappa}, SM_S) \\
&\quad = 4\sqrt{2\pi}\sum_{m\mu_2}\sum_{M_{13}'M_{13}}(-)^m(1M_{13}2-m|1M_{13}') \\
&\qquad \times \left(s_\mathrm{x}M_{13}'\frac{1}{2}\mu_2\middle| S'M_S'\right)\left(s_\mathrm{x}M_{13}\frac{1}{2}\mu_2\middle| SM_S\right)\sum_{n'n}c_{n'}c_n I^{S_{13}T_{13}(\mathrm{T})}_{13:213,m,n'n},
\end{aligned}
\tag{C.99}
$$

$$
\begin{aligned}
&I^{S_{12}T_{12}(\mathrm{T})}_{12:321,m,n'n} \\
&\equiv \frac{1}{4\pi}\int \mathrm{d}\boldsymbol{r}_3\int \mathrm{d}\boldsymbol{s}_3 \exp\left[-\alpha_{n'}\left(\frac{1}{2}\boldsymbol{r}_3+\boldsymbol{s}_3\right)^2\right]\exp\left[-i\boldsymbol{\kappa}'\cdot\left(\frac{3}{4}\boldsymbol{r}_3-\frac{1}{2}\boldsymbol{s}_3\right)\right] \\
&\qquad \times t^{S_{12}T_{12}(\mathrm{T})}_{12}(r_3)Y_{2m}(\hat{\boldsymbol{r}}_3)\exp\left(-\alpha_n r_3^2\right)\exp\left(i\boldsymbol{\kappa}\cdot\boldsymbol{s}_3\right) \\
&= \frac{1}{4\pi}\frac{\pi^{3/2}}{\alpha_{n'}^{3/2}}\exp\left[-\frac{(Q')^2}{4\alpha_{n'}}\right]\int \mathrm{d}\boldsymbol{r}_3\, t^{S_{12}T_{12}(\mathrm{T})}_{12}(r_3)Y_{2m}(\hat{\boldsymbol{r}}_3)\exp\left(-\alpha_n r_3^2\right)\exp\left(-i\boldsymbol{p}'\cdot\boldsymbol{r}_3\right) \\
&= -\frac{\pi^{3/2}}{\alpha_{n'}^{3/2}}\exp\left[-\frac{(Q')^2}{4\alpha_{n'}}\right]Y_{2m}(\hat{\boldsymbol{p}}')\int_0^\infty \mathrm{d}r_3\, r_3^2 t^{S_{12}T_{12}(\mathrm{T})}_{12}(r_3)j_2(|\boldsymbol{p}'|r_3)\exp\left(-\alpha_n r_3^2\right),
\end{aligned}
\tag{C.100}
$$

$$
\begin{aligned}
&I^{S_{13}T_{13}(\mathrm{T})}_{13:213,m,n'n} \\
&\equiv \frac{1}{4\pi}\int \mathrm{d}\boldsymbol{r}_2\int \mathrm{d}\boldsymbol{s}_2 \exp\left[-\alpha_{n'}\left(\frac{1}{2}\boldsymbol{r}_2-\boldsymbol{s}_2\right)^2\right]\exp\left[-i\boldsymbol{\kappa}'\cdot\left(-\frac{3}{4}\boldsymbol{r}_2-\frac{1}{2}\boldsymbol{s}_2\right)\right] \\
&\qquad \times t^{S_{13}T_{13}(\mathrm{T})}_{13}(r_2)Y_{2m}(\hat{\boldsymbol{r}}_2)\exp\left(-\alpha_n r_2^2\right)\exp\left(i\boldsymbol{\kappa}\cdot\boldsymbol{s}_2\right) \\
&= \frac{1}{4\pi}\frac{\pi^{3/2}}{\alpha_{n'}^{3/2}}\exp\left[-\frac{(Q')^2}{4\alpha_{n'}}\right]\int \mathrm{d}\boldsymbol{r}_2\, t^{S_{13}T_{13}(\mathrm{T})}_{13}(r_2)Y_{2m}(\hat{\boldsymbol{r}}_2)\exp\left(-\alpha_n r_2^2\right)\exp\left(i\boldsymbol{p}'\cdot\boldsymbol{r}_2\right) \\
&= -\frac{\pi^{3/2}}{\alpha_{n'}^{3/2}}\exp\left[-\frac{(Q')^2}{4\alpha_{n'}}\right]Y_{2m}(\hat{\boldsymbol{p}}')\int_0^\infty \mathrm{d}r_2\, r_2^2 t^{S_{13}T_{13}(\mathrm{T})}_{13}(r_2)j_2(|\boldsymbol{p}'|r_2)\exp\left(-\alpha_n r_2^2\right)
\end{aligned}
\tag{C.101}
$$

with Eqs. (C.67) and (C.185).

C.4 Components of spin-orbit interactions

The components of the spin-orbit interactions of the transition matrices (C.25) and (C.26) are given by

$$
\begin{aligned}
&\bar{T}^{S_{12}T_{12}(\mathrm{LS})}_{12:123}(\boldsymbol{\kappa}', S'M_S'|\boldsymbol{\kappa}, SM_S) \\
&\equiv \left\langle \phi_\mathrm{x}'(\boldsymbol{r}_1)\mathrm{e}^{i\boldsymbol{\kappa}'\cdot\boldsymbol{s}_1}\left[\left[\eta^{(2)}_{\frac{1}{2}}\otimes\eta^{(1)}_{\frac{1}{2}}\right]_{S_{12}}\otimes\eta^{(3)}_{\frac{1}{2}}\right]_{S'M_S'}\right| \\
&\qquad \times t^{S_{12}T_{12}(\mathrm{LS})}_{12}(r_3)\hat{\boldsymbol{\ell}}_{12}\cdot\boldsymbol{S}_{12}\left|\phi_\mathrm{x}(\boldsymbol{r}_1)\mathrm{e}^{i\boldsymbol{\kappa}\cdot\boldsymbol{s}_1}\left[\left[\eta^{(2)}_{\frac{1}{2}}\otimes\eta^{(1)}_{\frac{1}{2}}\right]_{S_{12}}\otimes\eta^{(3)}_{\frac{1}{2}}\right]_{SM_S}\right\rangle,
\end{aligned}
\tag{C.102}
$$

$$
\begin{aligned}
&\bar{T}^{S_{13}T_{13}(\mathrm{LS})}_{13:123}(\boldsymbol{\kappa}', S'M_S'|\boldsymbol{\kappa}, SM_S) \\
&\equiv \left\langle \phi_\mathrm{x}'(\boldsymbol{r}_1)\mathrm{e}^{i\boldsymbol{\kappa}'\cdot\boldsymbol{s}_1}\left[\left[\eta^{(3)}_{\frac{1}{2}}\otimes\eta^{(1)}_{\frac{1}{2}}\right]_{S_{13}}\otimes\eta^{(2)}_{\frac{1}{2}}\right]_{S'M_S'}\right|
\end{aligned}
$$

$$\times\, t_{13}^{S_{13}T_{13}(\mathrm{LS})}(r_2)\hat{\boldsymbol{\ell}}_{13}\cdot\boldsymbol{S}_{13}\left|\phi_{\mathrm{x}}(\boldsymbol{r}_1)\mathrm{e}^{i\boldsymbol{\kappa}\cdot\boldsymbol{s}_1}\left[\left[\eta_{\frac{1}{2}}^{(3)}\otimes\eta_{\frac{1}{2}}^{(1)}\right]_{S_{13}}\otimes\eta_{\frac{1}{2}}^{(2)}\right]_{SM_S}\right\rangle. \tag{C.103}$$

From the definition of the orbital angular momentum operator, $\hat{\boldsymbol{\ell}}_{12}\cdot\boldsymbol{S}_{12}$ and $\hat{\boldsymbol{\ell}}_{13}\cdot\boldsymbol{S}_{13}$ become

$$\hat{\boldsymbol{\ell}}_{12}\cdot\boldsymbol{S}_{12} = -i(\boldsymbol{r}_3\times\nabla_{\boldsymbol{r}_3})\cdot\boldsymbol{S}_{12},\quad \hat{\boldsymbol{\ell}}_{13}\cdot\boldsymbol{S}_{13} = -i(\boldsymbol{r}_2\times\nabla_{\boldsymbol{r}_2})\cdot\boldsymbol{S}_{13}, \tag{C.104}$$

and they generate

$$\hat{\boldsymbol{\ell}}_{12}\cdot\boldsymbol{S}_{12}\left|\phi_{\mathrm{x}}(\boldsymbol{r}_1)\mathrm{e}^{i\boldsymbol{\kappa}\cdot\boldsymbol{s}_1}\right\rangle = -i\phi_{\mathrm{x}}(\boldsymbol{r}_1)\big(\boldsymbol{r}_3\times\nabla_{\boldsymbol{r}_3}\mathrm{e}^{i\boldsymbol{\kappa}\cdot\boldsymbol{s}_1}\big)\cdot\boldsymbol{S}_{12} - i[\boldsymbol{r}_3\times\nabla_{\boldsymbol{r}_3}\phi_{\mathrm{x}}(\boldsymbol{r}_1)]\cdot\boldsymbol{S}_{12}\mathrm{e}^{i\boldsymbol{\kappa}\cdot\boldsymbol{s}_1}, \tag{C.105}$$

$$\hat{\boldsymbol{\ell}}_{13}\cdot\boldsymbol{S}_{13}\left|\phi_{\mathrm{x}}(\boldsymbol{r}_1)\mathrm{e}^{i\boldsymbol{\kappa}\cdot\boldsymbol{s}_1}\right\rangle = -i\phi_{\mathrm{x}}(\boldsymbol{r}_1)\big(\boldsymbol{r}_2\times\nabla_{\boldsymbol{r}_2}\mathrm{e}^{i\boldsymbol{\kappa}\cdot\boldsymbol{s}_1}\big)\cdot\boldsymbol{S}_{13} - i[\boldsymbol{r}_2\times\nabla_{\boldsymbol{r}_2}\phi_{\mathrm{x}}(\boldsymbol{r}_1)]\cdot\boldsymbol{S}_{13}\mathrm{e}^{i\boldsymbol{\kappa}\cdot\boldsymbol{s}_1}. \tag{C.106}$$

Making the use of the same assumptions in Sections C.2 and C.3, the gradients in Eqs. (C.105) and (C.106) are calculated as

$$\nabla_{\boldsymbol{r}_3}\mathrm{e}^{i\boldsymbol{\kappa}\cdot\boldsymbol{s}_1} = \nabla_{\boldsymbol{r}_3}\exp\left[i\boldsymbol{\kappa}\cdot\left(\frac{3}{4}\boldsymbol{r}_3-\frac{1}{2}\boldsymbol{s}_3\right)\right] = \frac{3}{4}i\boldsymbol{\kappa}\exp\left[i\boldsymbol{\kappa}\cdot\left(\frac{3}{4}\boldsymbol{r}_3-\frac{1}{2}\boldsymbol{s}_3\right)\right], \tag{C.107}$$

$$\nabla_{\boldsymbol{r}_2}\mathrm{e}^{i\boldsymbol{\kappa}\cdot\boldsymbol{s}_1} = \nabla_{\boldsymbol{r}_2}\exp\left[i\boldsymbol{\kappa}\cdot\left(-\frac{3}{4}\boldsymbol{r}_2-\frac{1}{2}\boldsymbol{s}_2\right)\right] = -\frac{3}{4}i\boldsymbol{\kappa}\exp\left[i\boldsymbol{\kappa}\cdot\left(-\frac{3}{4}\boldsymbol{r}_2-\frac{1}{2}\boldsymbol{s}_2\right)\right], \tag{C.108}$$

$$\begin{aligned}\nabla_{\boldsymbol{r}_3}\phi_{\mathrm{x}}(\boldsymbol{r}_1) &= \frac{1}{\sqrt{4\pi}}\sum_n c_n\nabla_{\boldsymbol{r}_3}\exp\left[-\alpha_n\left(\frac{1}{2}\boldsymbol{r}_3+\boldsymbol{s}_3\right)^2\right]\\ &= \frac{1}{\sqrt{4\pi}}\sum_n c_n\left[-\alpha_n\left(\frac{1}{2}\boldsymbol{r}_3+\boldsymbol{s}_3\right)\right]\exp\left[-\alpha_n\left(\frac{1}{2}\boldsymbol{r}_3+\boldsymbol{s}_3\right)^2\right],\end{aligned} \tag{C.109}$$

$$\begin{aligned}\nabla_{\boldsymbol{r}_2}\phi_{\mathrm{x}}(\boldsymbol{r}_1) &= \frac{1}{\sqrt{4\pi}}\sum_n c_n\nabla_{\boldsymbol{r}_2}\exp\left[-\alpha_n\left(\frac{1}{2}\boldsymbol{r}_2-\boldsymbol{s}_2\right)^2\right]\\ &= \frac{1}{\sqrt{4\pi}}\sum_n c_n\left[-\alpha_n\left(\frac{1}{2}\boldsymbol{r}_2-\boldsymbol{s}_2\right)\right]\exp\left[-\alpha_n\left(\frac{1}{2}\boldsymbol{r}_2-\boldsymbol{s}_2\right)^2\right].\end{aligned} \tag{C.110}$$

Then we can separate the transition matrices (C.102) and (C.103), respectively, into the two parts as shown below:

$$\begin{aligned}&\bar{T}_{12:123}^{S_{12}T_{12}(\mathrm{LS})}(\boldsymbol{\kappa}',S'M_S'|\boldsymbol{\kappa},SM_S)\\ &\quad= \bar{T}_{12:123}^{S_{12}T_{12}(\mathrm{LS})(1)}(\boldsymbol{\kappa}',S'M_S'|\boldsymbol{\kappa},SM_S) + \bar{T}_{12:123}^{S_{12}T_{12}(\mathrm{LS})(2)}(\boldsymbol{\kappa}',S'M_S'|\boldsymbol{\kappa},SM_S),\end{aligned} \tag{C.111}$$

$$\begin{aligned}&\bar{T}_{13:123}^{S_{13}T_{13}(\mathrm{LS})}(\boldsymbol{\kappa}',S'M_S'|\boldsymbol{\kappa},SM_S)\\ &\quad= \bar{T}_{13:123}^{S_{13}T_{13}(\mathrm{LS})(1)}(\boldsymbol{\kappa}',S'M_S'|\boldsymbol{\kappa},SM_S) + \bar{T}_{13:123}^{S_{13}T_{13}(\mathrm{LS})(2)}(\boldsymbol{\kappa}',S'M_S'|\boldsymbol{\kappa},SM_S),\end{aligned} \tag{C.112}$$

$$\begin{aligned}&\bar{T}_{12:123}^{S_{12}T_{12}(\mathrm{LS})(1)}(\boldsymbol{\kappa}',S'M_S'|\boldsymbol{\kappa},SM_S)\\ &\quad\equiv \left\langle \phi_{\mathrm{x}}'(\boldsymbol{r}_1)\mathrm{e}^{i\boldsymbol{\kappa}'\cdot\boldsymbol{s}_1}\left[\left[\eta_{\frac{1}{2}}^{(2)}\otimes\eta_{\frac{1}{2}}^{(1)}\right]_{S_{12}}\otimes\eta_{\frac{1}{2}}^{(3)}\right]_{S'M_S'}\right| t_{12}^{S_{12}T_{12}(\mathrm{LS})}(r_3)\end{aligned}$$

$$\times \frac{3}{4}(\boldsymbol{r}_3 \times \boldsymbol{\kappa}) \cdot \boldsymbol{S}_{12} \left| \phi_{\mathrm{x}}(\boldsymbol{r}_1) \mathrm{e}^{i\boldsymbol{\kappa}\cdot\boldsymbol{s}_1} \left[\left[\eta_{\frac{1}{2}}^{(2)} \otimes \eta_{\frac{1}{2}}^{(1)} \right]_{S_{12}} \otimes \eta_{\frac{1}{2}}^{(3)} \right]_{SM_S} \right\rangle, \tag{C.113}$$

$$\begin{aligned}
&\bar{T}_{13:123}^{S_{13}T_{13}(\mathrm{LS})(1)}(\boldsymbol{\kappa}', S'M'_S|\boldsymbol{\kappa}, SM_S) \\
&\equiv -\left\langle \phi'_{\mathrm{x}}(\boldsymbol{r}_1) \mathrm{e}^{i\boldsymbol{\kappa}'\cdot\boldsymbol{s}_1} \left[\left[\eta_{\frac{1}{2}}^{(3)} \otimes \eta_{\frac{1}{2}}^{(1)} \right]_{S_{13}} \otimes \eta_{\frac{1}{2}}^{(2)} \right]_{S'M'_S} \right| t_{13}^{S_{13}T_{13}(\mathrm{LS})}(r_2) \\
&\quad \times \frac{3}{4}(\boldsymbol{r}_2 \times \boldsymbol{\kappa}) \cdot \boldsymbol{S}_{13} \left| \phi_{\mathrm{x}}(\boldsymbol{r}_1) \mathrm{e}^{i\boldsymbol{\kappa}\cdot\boldsymbol{s}_1} \left[\left[\eta_{\frac{1}{2}}^{(3)} \otimes \eta_{\frac{1}{2}}^{(1)} \right]_{S_{13}} \otimes \eta_{\frac{1}{2}}^{(2)} \right]_{SM_S} \right\rangle,
\end{aligned} \tag{C.114}$$

$$\begin{aligned}
&\bar{T}_{12:123}^{S_{12}T_{12}(\mathrm{LS})(2)}(\boldsymbol{\kappa}', S'M'_S|\boldsymbol{\kappa}, SM_S) \\
&\equiv i\left\langle \phi'_{\mathrm{x}}(\boldsymbol{r}_1) \mathrm{e}^{i\boldsymbol{\kappa}'\cdot\boldsymbol{s}_1} \left[\left[\eta_{\frac{1}{2}}^{(2)} \otimes \eta_{\frac{1}{2}}^{(1)} \right]_{S_{12}} \otimes \eta_{\frac{1}{2}}^{(3)} \right]_{S'M'_S} \right| t_{12}^{S_{12}T_{12}(\mathrm{LS})}(r_3) \\
&\quad \times (\boldsymbol{r}_3 \times \boldsymbol{s}_3) \cdot \boldsymbol{S}_{12} \left| \frac{1}{\sqrt{4\pi}} \sum_n c_n \alpha_n \exp\bigl(-\alpha_n r_1^2\bigr) \mathrm{e}^{i\boldsymbol{\kappa}\cdot\boldsymbol{s}_1} \left[\left[\eta_{\frac{1}{2}}^{(2)} \otimes \eta_{\frac{1}{2}}^{(1)} \right]_{S_{12}} \otimes \eta_{\frac{1}{2}}^{(3)} \right]_{SM_S} \right\rangle,
\end{aligned} \tag{C.115}$$

$$\begin{aligned}
&\bar{T}_{13:123}^{S_{13}T_{13}(\mathrm{LS})(2)}(\boldsymbol{\kappa}', S'M'_S|\boldsymbol{\kappa}, SM_S) \\
&\equiv -i\left\langle \phi'_{\mathrm{x}}(\boldsymbol{r}_1) \mathrm{e}^{i\boldsymbol{\kappa}'\cdot\boldsymbol{s}_1} \left[\left[\eta_{\frac{1}{2}}^{(3)} \otimes \eta_{\frac{1}{2}}^{(1)} \right]_{S_{13}} \otimes \eta_{\frac{1}{2}}^{(2)} \right]_{S'M'_S} \right| t_{13}^{S_{13}T_{13}(\mathrm{LS})}(r_2) \\
&\quad \times (\boldsymbol{r}_2 \times \boldsymbol{s}_2) \cdot \boldsymbol{S}_{13} \left| \frac{1}{\sqrt{4\pi}} \sum_n c_n \alpha_n \exp\bigl(-\alpha_n r_1^2\bigr) \mathrm{e}^{i\boldsymbol{\kappa}\cdot\boldsymbol{s}_1} \left[\left[\eta_{\frac{1}{2}}^{(3)} \otimes \eta_{\frac{1}{2}}^{(1)} \right]_{S_{13}} \otimes \eta_{\frac{1}{2}}^{(2)} \right]_{SM_S} \right\rangle.
\end{aligned} \tag{C.116}$$

First, we calculate Eqs. (C.113) and (C.114). The operator $(\boldsymbol{r}_k \times \boldsymbol{\kappa}) \cdot \boldsymbol{S}_{1j}$ can be rewritten by

$$\begin{aligned}
(\boldsymbol{r}_k \times \boldsymbol{\kappa}) \cdot \boldsymbol{S}_{1j} &= \boldsymbol{r}_k \cdot (\boldsymbol{\kappa} \times \boldsymbol{S}_{1j}) \\
&= -\sqrt{3}[\boldsymbol{r}_k \otimes (\boldsymbol{\kappa} \times \boldsymbol{S}_{1j})]_{00} \\
&= -\sqrt{3} \cdot \sqrt{\frac{4\pi}{3}} r_k [Y_1(\hat{\boldsymbol{r}}_k) \otimes (\boldsymbol{\kappa} \times \boldsymbol{S}_{1j})]_{00} \\
&= -\sqrt{3} \cdot \sqrt{\frac{4\pi}{3}} r_k \sum_m (1m1-m|00) Y_{1m}(\hat{\boldsymbol{r}}_k)(\boldsymbol{\kappa} \times \boldsymbol{S}_{1j})_{1-m} \\
&= \sqrt{\frac{4\pi}{3}} r_k \sum_m (-)^m Y_{1m}(\hat{\boldsymbol{r}}_k)(\boldsymbol{\kappa} \times \boldsymbol{S}_{1j})_{1-m},
\end{aligned} \tag{C.117}$$

and

$$\begin{aligned}
(\boldsymbol{\kappa} \times \boldsymbol{S}_{1j})_{1-m} &= -i\sqrt{2}[\boldsymbol{\kappa} \otimes \boldsymbol{S}_{1j}]_{1-m} \\
&= -i\sqrt{2} \cdot \sqrt{\frac{4\pi}{3}} \kappa [Y_1(\hat{\boldsymbol{\kappa}}) \otimes \boldsymbol{S}_{1j}]_{1-m} \\
&= -i\sqrt{\frac{8\pi}{3}} \kappa \sum_{aa'} (1a1a'|1-m) Y_{1a}(\hat{\boldsymbol{\kappa}}) S_{1j}^{(a')},
\end{aligned} \tag{C.118}$$

in which $(j,k)=(2,3)$ or $(3,2)$. Then we obtain

$$(\boldsymbol{r}_k\times\boldsymbol{\kappa})\cdot\boldsymbol{S}_{1j}=-\frac{4\pi\sqrt{2}}{3}i\kappa r_k\sum_m\sum_{aa'}(-)^m(1a1a'|1-m)Y_{1m}(\hat{\boldsymbol{r}}_k)Y_{1a}(\hat{\boldsymbol{\kappa}})S_{1j}^{(a')}. \tag{C.119}$$

Inserting this into Eqs, (C.113) and (C.114), they become

$$\begin{aligned}&\bar{T}^{S_{12}T_{12}(\mathrm{LS})(1)}_{12:123}(\boldsymbol{\kappa}',S'M_S'|\boldsymbol{\kappa},SM_S)\\&\quad=-\pi i\sqrt{2}\sum_m\sum_{aa'}(-)^m(1a1a'|1-m)\kappa Y_{1a}(\hat{\boldsymbol{\kappa}})\\&\qquad\times\left\langle\phi_{\mathrm{x}}'(\boldsymbol{r}_1)\mathrm{e}^{i\boldsymbol{\kappa}'\cdot\boldsymbol{s}_1}\middle|t_{12}^{S_{12}T_{12}(\mathrm{LS})}(r_3)r_3Y_{1m}(\hat{\boldsymbol{r}}_3)\middle|\phi_{\mathrm{x}}(\boldsymbol{r}_1)\mathrm{e}^{i\boldsymbol{\kappa}\cdot\boldsymbol{s}_1}\right\rangle\\&\qquad\times\left\langle\left[\left[\eta_{\frac12}^{(2)}\otimes\eta_{\frac12}^{(1)}\right]_{S_{12}}\otimes\eta_{\frac12}^{(3)}\right]_{S'M_S'}\middle|S_{12}^{(a')}\middle|\left[\left[\eta_{\frac12}^{(2)}\otimes\eta_{\frac12}^{(1)}\right]_{S_{12}}\otimes\eta_{\frac12}^{(3)}\right]_{SM_S}\right\rangle,\end{aligned}\tag{C.120}$$

$$\begin{aligned}&\bar{T}^{S_{13}T_{13}(\mathrm{LS})(1)}_{13:123}(\boldsymbol{\kappa}',S'M_S'|\boldsymbol{\kappa},SM_S)\\&\quad=\pi i\sqrt{2}\sum_m\sum_{aa'}(-)^m(1a1a'|1-m)\kappa Y_{1a}(\hat{\boldsymbol{\kappa}})\\&\qquad\times\left\langle\phi_{\mathrm{x}}'(\boldsymbol{r}_1)\mathrm{e}^{i\boldsymbol{\kappa}'\cdot\boldsymbol{s}_1}\middle|t_{13}^{S_{13}T_{13}(\mathrm{LS})}(r_2)r_2Y_{1m}(\hat{\boldsymbol{r}}_2)\middle|\phi_{\mathrm{x}}(\boldsymbol{r}_1)\mathrm{e}^{i\boldsymbol{\kappa}\cdot\boldsymbol{s}_1}\right\rangle\\&\qquad\times\left\langle\left[\left[\eta_{\frac12}^{(3)}\otimes\eta_{\frac12}^{(1)}\right]_{S_{13}}\otimes\eta_{\frac12}^{(2)}\right]_{S'M_S'}\middle|S_{13}^{(a')}\middle|\left[\left[\eta_{\frac12}^{(3)}\otimes\eta_{\frac12}^{(1)}\right]_{S_{13}}\otimes\eta_{\frac12}^{(2)}\right]_{SM_S}\right\rangle.\end{aligned}\tag{C.121}$$

The matrix elements of the spin parts in Eqs. (C.120) and (C.121) can be calculated as

$$\begin{aligned}&\left\langle\left[\left[\eta_{\frac12}^{(j)}\otimes\eta_{\frac12}^{(1)}\right]_{S_{1j}}\otimes\eta_{\frac12}^{(k)}\right]_{S'M_S'}\middle|S_{1j}^{(a')}\middle|\left[\left[\eta_{\frac12}^{(j)}\otimes\eta_{\frac12}^{(1)}\right]_{S_{1j}}\otimes\eta_{\frac12}^{(k)}\right]_{SM_S}\right\rangle\\&=\sum_{M_{1j}'M_{1j}}\sum_{\mu_k}\left(S_{1j}M_{1j}'\frac12\mu_k\middle|S'M_S'\right)\left(S_{1j}M_{1j}\frac12\mu_k\middle|SM_S\right)\\&\qquad\times\left\langle\left[\eta_{\frac12}^{(j)}\otimes\eta_{\frac12}^{(1)}\right]_{S_{1j}M_{1j}'}\middle|S_{1j}^{(a')}\middle|\left[\eta_{\frac12}^{(j)}\otimes\eta_{\frac12}^{(1)}\right]_{S_{1j}M_{1j}}\right\rangle\\&=\sum_{M_{1j}'M_{1j}}\sum_{\mu_k}\left(S_{1j}M_{1j}'\frac12\mu_k\middle|S'M_S'\right)\left(S_{1j}M_{1j}\frac12\mu_k\middle|SM_S\right)\\&\qquad\times\left(S_{1j}M_{1j}1a'|S_{1j}M_{1j}'\right)\left\langle\left[\eta_{\frac12}^{(j)}\otimes\eta_{\frac12}^{(1)}\right]_{S_{1j}}\middle\|\hat{S}_{1j}\middle\|\left[\eta_{\frac12}^{(j)}\otimes\eta_{\frac12}^{(1)}\right]_{S_{1j}}\right\rangle\\&=\sum_{M_{1j}'M_{1j}}\sum_{\mu_k}\left(S_{1j}M_{1j}'\frac12\mu_k\middle|S'M_S'\right)\left(S_{1j}M_{1j}\frac12\mu_k\middle|SM_S\right)\left(S_{1j}M_{1j}1a'|S_{1j}M_{1j}'\right)\cdot\sqrt{2},\end{aligned}\tag{C.122}$$

and it makes Eqs. (C.120) and (C.121) be

$$\begin{aligned}&\bar{T}^{S_{12}T_{12}(\mathrm{LS})(1)}_{12:123}(\boldsymbol{\kappa}',S'M_S'|\boldsymbol{\kappa},SM_S)\\&\quad=-2\pi i\sum_{\mu_3}\sum_{M_{12}'M_{12}}\left(S_{12}M_{12}'\frac12\mu_3\middle|S'M_S'\right)\left(S_{12}M_{12}\frac12\mu_3\middle|SM_S\right)\\&\qquad\times\sum_m\sum_{aa'}(-)^m\left(S_{12}M_{12}1a'|S_{12}M_{12}'\right)(1a1a'|1-m)\kappa Y_{1a}(\hat{\boldsymbol{\kappa}})\end{aligned}$$

$$\times \left\langle \phi'_{\mathrm{x}}(\boldsymbol{r}_1)\mathrm{e}^{i\boldsymbol{\kappa}'\cdot\boldsymbol{s}_1} \middle| t_{12}^{S_{12}T_{12}(\mathrm{LS})}(r_3) r_3 Y_{1m}(\hat{\boldsymbol{r}}_3) \middle| \phi_{\mathrm{x}}(\boldsymbol{r}_1)\mathrm{e}^{i\boldsymbol{\kappa}\cdot\boldsymbol{s}_1} \right\rangle, \tag{C.123}$$

$$\begin{aligned}
&\bar{T}_{13:123}^{S_{13}T_{13}(\mathrm{LS})(1)}(\boldsymbol{\kappa}', S'M'_S|\boldsymbol{\kappa}, SM_S) \\
&= 2\pi i \sum_{\mu_2} \sum_{M'_{13}M_{13}} \left(S_{13}M'_{13}\frac{1}{2}\mu_2 \middle| S'M'_S \right) \left(S_{13}M_{13}\frac{1}{2}\mu_2 \middle| SM_S \right) \\
&\quad \times \sum_m \sum_{aa'} (-)^m (S_{13}M_{13}1a'|S_{13}M'_{13})(1a1a'|1-m)\kappa Y_{1a}(\hat{\boldsymbol{\kappa}}) \\
&\qquad \times \left\langle \phi'_{\mathrm{x}}(\boldsymbol{r}_1)\mathrm{e}^{i\boldsymbol{\kappa}'\cdot\boldsymbol{s}_1} \middle| t_{13}^{S_{13}T_{13}(\mathrm{LS})}(r_2) r_2 Y_{1m}(\hat{\boldsymbol{r}}_2) \middle| \phi_{\mathrm{x}}(\boldsymbol{r}_1)\mathrm{e}^{i\boldsymbol{\kappa}\cdot\boldsymbol{s}_1} \right\rangle.
\end{aligned} \tag{C.124}$$

It should be noted that we have used the Wigner-Eckart theorem:

$$\left\langle \left[\eta_{\frac{1}{2}}^{(j)} \otimes \eta_{\frac{1}{2}}^{(1)}\right]_{S_{1j}} \middle\| \hat{S}_{1j} \middle\| \left[\eta_{\frac{1}{2}}^{(j)} \otimes \eta_{\frac{1}{2}}^{(1)}\right]_{S_{1j}} \right\rangle = \sqrt{2} \tag{C.125}$$

in the case of $S_{1j} = 1$. Then taking $\boldsymbol{r}_3$ and $\boldsymbol{s}_3$ in Eq. (C.123) and $\boldsymbol{r}_2$ and $\boldsymbol{s}_2$ in Eq. (C.124), these transition matrices become

$$\begin{aligned}
&\bar{T}_{12:123}^{S_{12}T_{12}(\mathrm{LS})(1)}(\boldsymbol{\kappa}', S'M'_S|\boldsymbol{\kappa}, SM_S) \\
&= -2\pi i \sum_{\mu_3} \sum_{M'_{12}M_{12}} \left(S_{12}M'_{12}\frac{1}{2}\mu_3 \middle| S'M'_S \right) \left(S_{12}M_{12}\frac{1}{2}\mu_3 \middle| SM_S \right) \\
&\quad \times \sum_m \sum_{aa'} (-)^m (S_{12}M_{12}1a'|S_{12}M'_{12})(1a1a'|1-m)\kappa Y_{1a}(\hat{\boldsymbol{\kappa}}) \sum_{n'n} c_{n'}c_n I_{12:123,m,n'n}^{S_{12}T_{12}(\mathrm{LS})(1)},
\end{aligned} \tag{C.126}$$

$$\begin{aligned}
&\bar{T}_{13:123}^{S_{13}T_{13}(\mathrm{LS})(1)}(\boldsymbol{\kappa}', S'M'_S|\boldsymbol{\kappa}, SM_S) \\
&= 2\pi i \sum_{\mu_2} \sum_{M'_{13}M_{13}} \left(S_{13}M'_{13}\frac{1}{2}\mu_2 \middle| S'M'_S \right) \left(S_{13}M_{13}\frac{1}{2}\mu_2 \middle| SM_S \right) \\
&\quad \times \sum_m \sum_{aa'} (-)^m (S_{13}M_{13}1a'|S_{13}M'_{13})(1a1a'|1-m)\kappa Y_{1a}(\hat{\boldsymbol{\kappa}}) \sum_{n'n} c_{n'}c_n I_{13:123,m,n'n}^{S_{13}T_{13}(\mathrm{LS})(1)},
\end{aligned} \tag{C.127}$$

$$\begin{aligned}
&I_{12:123,m,n'n}^{S_{12}T_{12}(\mathrm{LS})(1)} \\
&\equiv \frac{1}{4\pi} \int \mathrm{d}\boldsymbol{r}_3 \int \mathrm{d}\boldsymbol{s}_3 \exp\left[-\alpha_{n'}\left(\frac{1}{2}\boldsymbol{r}_3 + \boldsymbol{s}_3\right)^2\right] \exp\left[-i\boldsymbol{\kappa}'\cdot\left(\frac{3}{4}\boldsymbol{r}_3 - \frac{1}{2}\boldsymbol{s}_3\right)\right] \\
&\qquad \times t_{12}^{S_{12}T_{12}(\mathrm{LS})}(r_3) r_3 Y_{1m}(\hat{\boldsymbol{r}}_3) \exp\left[-\alpha_n\left(\frac{1}{2}\boldsymbol{r}_3 + \boldsymbol{s}_3\right)^2\right] \exp\left[i\boldsymbol{\kappa}\cdot\left(\frac{3}{4}\boldsymbol{r}_3 - \frac{1}{2}\boldsymbol{s}_3\right)\right] \\
&= \frac{1}{4\pi}\frac{\pi^{3/2}}{\alpha_{n'n}^{3/2}} \exp\left(-\frac{q^2}{16\alpha_{n'n}}\right) \int \mathrm{d}\boldsymbol{r}_3\, r_3 t_{12}^{S_{12}T_{12}(\mathrm{LS})}(r_3) Y_{1m}(\hat{\boldsymbol{r}}_3)\mathrm{e}^{i\boldsymbol{q}\cdot\boldsymbol{r}_3} \\
&= i\frac{\pi^{3/2}}{\alpha_{n'n}^{3/2}} \exp\left(-\frac{q^2}{16\alpha_{n'n}}\right) Y_{1m}(\hat{\boldsymbol{q}}) \int \mathrm{d}r_3\, r_3^3 t_{12}^{S_{12}T_{12}(\mathrm{LS})}(r_3) j_1(qr_3),
\end{aligned} \tag{C.128}$$

$$\begin{aligned}
&I_{13:123,m,n'n}^{S_{13}T_{13}(\mathrm{LS})(1)} \\
&\equiv \frac{1}{4\pi} \int \mathrm{d}\boldsymbol{r}_2 \int \mathrm{d}\boldsymbol{s}_2 \exp\left[-\alpha_{n'}\left(\frac{1}{2}\boldsymbol{r}_2 - \boldsymbol{s}_2\right)^2\right] \exp\left[-i\boldsymbol{\kappa}'\cdot\left(-\frac{3}{4}\boldsymbol{r}_2 - \frac{1}{2}\boldsymbol{s}_2\right)\right]
\end{aligned}$$

$$
\begin{aligned}
&\times t_{13}^{S_{13}T_{13}(\mathrm{LS})}(r_2) r_2 Y_{1m}(\hat{\boldsymbol{r}}_2) \exp\left[-\alpha_n\left(\frac{1}{2}\boldsymbol{r}_2-\boldsymbol{s}_2\right)^2\right] \exp\left[i\boldsymbol{\kappa}\cdot\left(-\frac{3}{4}\boldsymbol{r}_2-\frac{1}{2}\boldsymbol{s}_2\right)\right] \\
&= \frac{1}{4\pi}\frac{\pi^{3/2}}{\alpha_{n'n}^{3/2}} \exp\left(-\frac{q^2}{16\alpha_{n'n}}\right) \int \mathrm{d}\boldsymbol{r}_2\, r_2 t_{13}^{S_{13}T_{13}(\mathrm{LS})}(r_2) Y_{1m}(\hat{\boldsymbol{r}}_2) \mathrm{e}^{-i\boldsymbol{q}\cdot\boldsymbol{r}_2} \\
&= -i\frac{\pi^{3/2}}{\alpha_{n'n}^{3/2}} \exp\left(-\frac{q^2}{16\alpha_{n'n}}\right) Y_{1m}(\hat{\boldsymbol{q}}) \int \mathrm{d}r_2\, r_2^3 t_{13}^{S_{13}T_{13}(\mathrm{LS})}(r_2) j_1(qr_2),
\end{aligned}
\tag{C.129}
$$

in which we have used Eqs. (C.44) and (C.185).

Next, we calculate Eqs. (C.115) and (C.116). The operator $(\boldsymbol{r}_3 \times \boldsymbol{s}_3) \cdot \boldsymbol{S}_{1j}$ can be rewritten by

$$
\begin{aligned}
(\boldsymbol{r}_k \times \boldsymbol{s}_k) \cdot \boldsymbol{S}_{1j} &= \boldsymbol{S}_{1j} \cdot (\boldsymbol{r}_k \times \boldsymbol{s}_k) \\
&= -\sqrt{3}[\boldsymbol{S}_{1j} \otimes (\boldsymbol{r}_k \times \boldsymbol{s}_k)]_{00} \\
&= -\sqrt{3}\sum_a (1a1-a|00) S_{1j}^{(a)} (\boldsymbol{r}_k \times \boldsymbol{s}_k)_{1-a} \\
&= \sum_a (-)^a S_{1j}^{(a)} (\boldsymbol{r}_k \times \boldsymbol{s}_k)_{1-a},
\end{aligned}
\tag{C.130}
$$

and

$$
\begin{aligned}
(\boldsymbol{r}_k \times \boldsymbol{s}_k)_{1-a} &= -i\sqrt{2}[\boldsymbol{r}_k \otimes \boldsymbol{s}_k]_{1-a} \\
&= -i\sqrt{2}\cdot\frac{4\pi}{3} r_k s_k [Y_1(\hat{\boldsymbol{r}}_k) \otimes Y_1(\hat{\boldsymbol{s}}_k)]_{1-a} \\
&= -\frac{4\pi\sqrt{2}}{3} i r_k s_k \sum_{mm'} (1m1m'|1-a) Y_{1m}(\hat{\boldsymbol{r}}_k) Y_{1m'}(\hat{\boldsymbol{s}}_k),
\end{aligned}
\tag{C.131}
$$

in which $(j,k) = (2,3)$ or $(3,2)$. Then we obtain

$$
(\boldsymbol{r}_k \times \boldsymbol{s}_k) \cdot \boldsymbol{S}_{1j} = -\frac{4\pi\sqrt{2}}{3} i r_k s_k \sum_{mm'}\sum_a (-)^a (1m1m'|1-a) Y_{1m}(\hat{\boldsymbol{r}}_k) Y_{1m'}(\hat{\boldsymbol{s}}_k) S_{1j}^{(a)}.
\tag{C.132}
$$

Inserting this into Eqs. (C.115) and (C.116), they become

$$
\begin{aligned}
&\bar{T}_{12:123}^{S_{12}T_{12}(\mathrm{LS})(2)}(\boldsymbol{\kappa}', S'M_S'|\boldsymbol{\kappa}, SM_S) \\
&= \frac{8\pi}{3} \sum_{M_{12}'M_{12}} \sum_{\mu_3} \left(S_{12}M_{12}'\frac{1}{2}\mu_3\middle| S'M_S'\right)\left(S_{12}M_{12}\frac{1}{2}\mu_3\middle| SM_S\right) \\
&\quad \times \sum_{mm'}\sum_a (-)^a (S_{12}M_{12}1a|S_{12}M_{12}')(1m1m'|1-a) \\
&\quad \times \left\langle \phi_{\mathrm{x}}'(\boldsymbol{r}_1)\mathrm{e}^{i\boldsymbol{\kappa}'\cdot\boldsymbol{s}_1}\middle| t_{12}^{S_{12}T_{12}(\mathrm{LS})}(r_3) r_3 Y_{1m}(\hat{\boldsymbol{r}}_3)\right. \\
&\quad \left.\times s_3 Y_{1m'}(\hat{\boldsymbol{s}}_3) \middle| \frac{1}{\sqrt{4\pi}}\sum_n c_n\alpha_n \exp(-\alpha_n r_1^2)\mathrm{e}^{i\boldsymbol{\kappa}\cdot\boldsymbol{s}_1}\right\rangle,
\end{aligned}
\tag{C.133}
$$

$$
\begin{aligned}
&\bar{T}_{13:123}^{S_{13}T_{13}(\mathrm{LS})(2)}(\boldsymbol{\kappa}', S'M_S'|\boldsymbol{\kappa}, SM_S) \\
&= -\frac{8\pi}{3} \sum_{M_{13}'M_{13}} \sum_{\mu_2} \left(S_{13}M_{13}'\frac{1}{2}\mu_2\middle| S'M_S'\right)\left(S_{13}M_{13}\frac{1}{2}\mu_2\middle| SM_S\right) \\
&\quad \times \sum_{mm'}\sum_a (-)^a (S_{13}M_{13}1a|S_{13}M_{13}')(1m1m'|1-a)
\end{aligned}
$$

$$\times \left\langle \phi_{\rm x}'(\boldsymbol{r}_1)\mathrm{e}^{i\boldsymbol{\kappa}'\cdot\boldsymbol{s}_1} \middle| t_{13}^{S_{13}T_{13}(\mathrm{LS})}(r_2) r_2 Y_{1m}(\hat{\boldsymbol{r}}_2) \right.$$
$$\left. \times s_2 Y_{1m'}(\hat{\boldsymbol{s}}_2) \middle| \frac{1}{\sqrt{4\pi}} \sum_n c_n \alpha_n \exp\left(-\alpha_n r_1^2\right) \mathrm{e}^{i\boldsymbol{\kappa}\cdot\boldsymbol{s}_1} \right\rangle, \tag{C.134}$$

in which we have used Eq. (C.125). Taking $\boldsymbol{r}_3$ and $\boldsymbol{s}_3$ in Eq. (C.133) and $\boldsymbol{r}_2$ and $\boldsymbol{s}_2$ in Eq. (C.134), these transition matrices become

$$\begin{aligned}
&\bar{T}_{12:123}^{S_{12}T_{12}(\mathrm{LS})(2)}(\boldsymbol{\kappa}', S'M_S'|\boldsymbol{\kappa}, SM_S) \\
&= \frac{8\pi}{3} \sum_{\mu_3} \sum_{M_{12}'M_{12}} \left(S_{12}M_{12}'\frac{1}{2}\mu_3 \middle| S'M_S'\right) \left(S_{12}M_{12}\frac{1}{2}\mu_3 \middle| SM_S\right) \\
&\quad \times \sum_{mm'} \sum_a (-)^a \left(S_{12}M_{12}1a|S_{12}M_{12}'\right)\left(1m1m'|1-a\right) \sum_{n'n} c_{n'}c_n\alpha_n I_{12:123,mm',n'n}^{S_{12}T_{12}(\mathrm{LS})(2)},
\end{aligned} \tag{C.135}$$

$$\begin{aligned}
&\bar{T}_{13:123}^{S_{13}T_{13}(\mathrm{LS})(2)}(\boldsymbol{\kappa}', S'M_S'|\boldsymbol{\kappa}, SM_S) \\
&= -\frac{8\pi}{3} \sum_{\mu_2} \sum_{M_{13}'M_{13}} \left(S_{13}M_{13}'\frac{1}{2}\mu_2 \middle| S'M_S'\right) \left(S_{13}M_{13}\frac{1}{2}\mu_2 \middle| SM_S\right) \\
&\quad \times \sum_{mm'} \sum_a (-)^a \left(S_{13}M_{13}1a|S_{13}M_{13}'\right)\left(1m1m'|1-a\right) \sum_{n'n} c_{n'}c_n\alpha_n I_{13:123,mm',n'n}^{S_{13}T_{13}(\mathrm{LS})(2)},
\end{aligned} \tag{C.136}$$

$$\begin{aligned}
&I_{12:123,mm',n'n}^{S_{12}T_{12}(\mathrm{LS})(2)} \\
&\equiv \frac{1}{4\pi} \int \mathrm{d}\boldsymbol{r}_3 \int \mathrm{d}\boldsymbol{s}_3 \exp\left[-\alpha_{n'}\left(\frac{1}{2}\boldsymbol{r}_3 + \boldsymbol{s}_3\right)^2\right] \exp\left[-i\boldsymbol{\kappa}'\cdot\left(\frac{3}{4}\boldsymbol{r}_3 - \frac{1}{2}\boldsymbol{s}_3\right)\right] \\
&\quad \times t_{12}^{S_{12}T_{12}(\mathrm{LS})}(r_3) r_3 Y_{1m}(\hat{\boldsymbol{r}}_3) s_3 Y_{1m}(\hat{\boldsymbol{s}}_3) \exp\left[-\alpha_n\left(\frac{1}{2}\boldsymbol{r}_3 + \boldsymbol{s}_3\right)^2\right] \exp\left[i\boldsymbol{\kappa}\cdot\left(\frac{3}{4}\boldsymbol{r}_3 - \frac{1}{2}\boldsymbol{s}_3\right)\right] \\
&= \frac{1}{4\pi} \int \mathrm{d}\boldsymbol{r}_3\, r_3 t_{12}^{S_{12}T_{12}(\mathrm{LS})}(r_3) Y_{1m}(\hat{\boldsymbol{r}}_3) \exp\left(-\frac{1}{4}\alpha_{n'n}r_3^2\right) \exp\left(\frac{3}{4}i\boldsymbol{q}\cdot\boldsymbol{r}_3\right) \\
&\quad \times \int \mathrm{d}\boldsymbol{s}_3\, s_3 Y_{1m'}(\hat{\boldsymbol{s}}_3) \exp\left(-\alpha_{n'n}s_3^2\right) \exp\left[-\left(\alpha_{n'n}\boldsymbol{r}_3 + \frac{i}{2}\boldsymbol{q}\right)\cdot\boldsymbol{s}_3\right],
\end{aligned} \tag{C.137}$$

$$\begin{aligned}
&I_{13:123,mm',n'n}^{S_{13}T_{13}(\mathrm{LS})(2)} \\
&\equiv \frac{1}{4\pi} \int \mathrm{d}\boldsymbol{r}_2 \int \mathrm{d}\boldsymbol{s}_2 \exp\left[-\alpha_{n'}\left(\frac{1}{2}\boldsymbol{r}_2 - \boldsymbol{s}_2\right)^2\right] \exp\left[-i\boldsymbol{\kappa}'\cdot\left(-\frac{3}{4}\boldsymbol{r}_2 - \frac{1}{2}\boldsymbol{s}_2\right)\right] \\
&\quad \times t_{13}^{S_{13}T_{13}(\mathrm{LS})}(r_2) r_2 Y_{1m}(\hat{\boldsymbol{r}}_2) s_2 Y_{1m}(\hat{\boldsymbol{s}}_2) \exp\left[-\alpha_n\left(\frac{1}{2}\boldsymbol{r}_2 - \boldsymbol{s}_2\right)^2\right] \exp\left[i\boldsymbol{\kappa}\cdot\left(-\frac{3}{4}\boldsymbol{r}_2 - \frac{1}{2}\boldsymbol{s}_2\right)\right] \\
&= \frac{1}{4\pi} \int \mathrm{d}\boldsymbol{r}_2\, r_2 t_{13}^{S_{13}T_{13}(\mathrm{LS})}(r_2) Y_{1m}(\hat{\boldsymbol{r}}_2) \exp\left(-\frac{1}{4}\alpha_{n'n}r_2^2\right) \exp\left(-\frac{3}{4}i\boldsymbol{q}\cdot\boldsymbol{r}_2\right) \\
&\quad \times \int \mathrm{d}\boldsymbol{s}_2\, s_2 Y_{1m'}(\hat{\boldsymbol{s}}_2) \exp\left(-\alpha_{n'n}s_2^2\right) \exp\left[-\left(-\alpha_{n'n}\boldsymbol{r}_2 + \frac{i}{2}\boldsymbol{q}\right)\cdot\boldsymbol{s}_2\right].
\end{aligned} \tag{C.138}$$

Here, we consider the integrals regarding $\boldsymbol{s}_3$ in Eq. (C.137) and $\boldsymbol{s}_2$ in Eq. (C.138) in the general form:

$$I_{m'} \equiv \int \mathrm{d}\boldsymbol{s}\, s Y_{1m'}(\hat{\boldsymbol{s}}) \exp\left(-\alpha s^2\right) \exp[-(\boldsymbol{\beta} + i\boldsymbol{\gamma})\cdot\boldsymbol{s}], \tag{C.139}$$

in which α is a positive real number and $\boldsymbol{\beta}$ and $\boldsymbol{\gamma}$ are real vectors. In the Cartesian coordinate system, the spherical harmonics has the form:

$$Y_{10}(\hat{\boldsymbol{s}}) = \sqrt{\frac{3}{4\pi}}\cos\theta = \sqrt{\frac{3}{4\pi}}\frac{X_3}{s}, \quad Y_{1\pm1}(\theta,\varphi) = \mp\sqrt{\frac{3}{8\pi}}\sin\theta\,\mathrm{e}^{\pm i\varphi} = \mp\sqrt{\frac{3}{8\pi}}\frac{X_1 \pm iX_2}{s}, \tag{C.140}$$

and then it makes Eq. (C.139) be

$$\begin{aligned} I_0 = \sqrt{\frac{3}{4\pi}} &\int_{-\infty}^{\infty} \mathrm{d}X_1 \exp\left(-\alpha X_1^2\right) \exp[-(\beta_1 + i\gamma_1)X_1] \\ &\times \int_{-\infty}^{\infty} \mathrm{d}X_2 \exp\left(-\alpha X_2^2\right) \exp[-(\beta_2 + i\gamma_2)X_2] \\ &\quad\times \int_{-\infty}^{\infty} \mathrm{d}X_3\, X_3 \exp\left(-\alpha X_3^2\right) \exp[-(\beta_3 + i\gamma_3)X_3], \end{aligned} \tag{C.141}$$

$$\begin{aligned} I_{\pm1} = \mp\sqrt{\frac{3}{8\pi}} &\int_{-\infty}^{\infty} \mathrm{d}X_1\, X_1 \exp\left(-\alpha X_1^2\right) \exp[-(\beta_1 + i\gamma_1)X_1] \\ &\times \int_{-\infty}^{\infty} \mathrm{d}X_2 \exp\left(-\alpha X_2^2\right) \exp[-(\beta_2 + i\gamma_2)X_2] \\ &\quad\times \int_{-\infty}^{\infty} \mathrm{d}X_3 \exp\left(-\alpha X_3^2\right) \exp[-(\beta_3 + i\gamma_3)X_3] \\ &\qquad - i\sqrt{\frac{3}{8\pi}} \int_{-\infty}^{\infty} \mathrm{d}X_1 \exp\left(-\alpha X_1^2\right) \exp[-(\beta_1 + i\gamma_1)X_1] \\ &\qquad\quad\times \int_{-\infty}^{\infty} \mathrm{d}X_2\, X_2 \exp\left(-\alpha X_2^2\right) \exp[-(\beta_2 + i\gamma_2)X_2] \\ &\qquad\qquad\times \int_{-\infty}^{\infty} \mathrm{d}X_3 \exp\left(-\alpha X_3^2\right) \exp[-(\beta_3 + i\gamma_3)X_3]. \end{aligned} \tag{C.142}$$

Utilizing Eqs. (C.182) and (C.183), these integrals are calculated as

$$\begin{aligned} I_0 &= -\sqrt{\frac{3}{4\pi}}\frac{\pi^{3/2}}{\alpha^{3/2}}\frac{\beta_3 + i\gamma_3}{2\alpha}\prod_{j=1}^{3}\exp\left[\frac{(\beta_j + i\gamma_j)^2}{4\alpha}\right] \\ &= -\frac{1}{2\alpha}\frac{\pi^{3/2}}{\alpha^{3/2}}\left[\beta Y_{10}\left(\hat{\boldsymbol{\beta}}\right) + i\gamma Y_{10}(\hat{\boldsymbol{\gamma}})\right]\exp\left[\frac{(\boldsymbol{\beta} + i\boldsymbol{\gamma})^2}{4\alpha}\right], \end{aligned} \tag{C.143}$$

$$\begin{aligned} I_{\pm1} &= \pm\sqrt{\frac{3}{8\pi}}\frac{\pi^{3/2}}{\alpha^{3/2}}\frac{\beta_1 + i\gamma_1}{2\alpha}\prod_{j=1}^{3}\exp\left[\frac{(\beta_j + i\gamma_j)^2}{4\alpha}\right] \\ &\quad + i\sqrt{\frac{3}{8\pi}}\frac{\pi^{3/2}}{\alpha^{3/2}}\frac{\beta_2 + i\gamma_2}{2\alpha}\prod_{j=1}^{3}\exp\left[\frac{(\beta_j + i\gamma_j)^2}{4\alpha}\right] \\ &= \pm\sqrt{\frac{3}{8\pi}}\frac{\pi^{3/2}}{\alpha^{3/2}}\frac{(\beta_1 \pm i\beta_2) + i(\gamma_1 \pm i\gamma_2)}{2\alpha}\exp\left[\frac{(\boldsymbol{\beta} + i\boldsymbol{\gamma})^2}{4\alpha}\right] \\ &= -\frac{1}{2\alpha}\frac{\pi^{3/2}}{\alpha^{3/2}}\left[\beta Y_{1\pm1}\left(\hat{\boldsymbol{\beta}}\right) + i\gamma Y_{1\pm1}(\hat{\boldsymbol{\gamma}})\right]\exp\left[\frac{(\boldsymbol{\beta} + i\boldsymbol{\gamma})^2}{4\alpha}\right], \end{aligned} \tag{C.144}$$

and we can write them in the single form:

$$I_{m'} = -\frac{1}{2\alpha}\frac{\pi^{3/2}}{\alpha^{3/2}}\left[\beta Y_{1m'}\left(\hat{\boldsymbol{\beta}}\right) + i\gamma Y_{1m'}(\hat{\boldsymbol{\gamma}})\right]\exp\left[\frac{(\boldsymbol{\beta} + i\boldsymbol{\gamma})^2}{4\alpha}\right]$$

$$= -\frac{1}{2\alpha}\frac{\pi^{3/2}}{\alpha^{3/2}}\left[\beta Y_{1m'}\left(\hat{\boldsymbol{\beta}}\right) + i\gamma Y_{1m'}(\hat{\boldsymbol{\gamma}})\right]\exp\left(\frac{\beta^2}{4\alpha}\right)\exp\left(-\frac{\gamma^2}{4\alpha}\right)\exp\left(\frac{i}{2\alpha}\boldsymbol{\beta}\cdot\boldsymbol{\gamma}\right). \tag{C.145}$$

Replacing α, $\boldsymbol{\beta}$, and $\boldsymbol{\gamma}$ in Eq. (C.145) as

$$\alpha \to \alpha_{n'n}, \quad \boldsymbol{\beta} \to \pm\alpha_{n'n}\boldsymbol{r}, \quad \boldsymbol{\gamma} \to \frac{\boldsymbol{q}}{2}, \tag{C.146}$$

we get

$$\begin{aligned}&\int \mathrm{d}\boldsymbol{s}\, sY_{1m'}(\hat{\boldsymbol{s}})\exp\left(-\alpha_{n'n}s^2\right)\exp\left[-\left(\pm\alpha_{n'n}\boldsymbol{r} + \frac{i}{2}\boldsymbol{q}\right)\cdot\boldsymbol{s}\right]\\ &= \mp\frac{1}{2\alpha_{n'n}}\frac{\pi^{3/2}}{\alpha_{n'n}^{3/2}}\left[\alpha_{n'n}rY_{1m'}(\hat{\boldsymbol{r}}) \pm \frac{i}{2}qY_{1m'}(\hat{\boldsymbol{q}})\right]\exp\left(\frac{1}{4}\alpha_{n'n}r^2\right)\exp\left(-\frac{q^2}{16\alpha_{n'n}}\right)\exp\left(\pm\frac{i}{4}\boldsymbol{q}\cdot\boldsymbol{r}\right),\end{aligned} \tag{C.147}$$

in which Eq. (C.184) have been used. Finally,

$$\begin{aligned}&I^{S_{12}T_{12}(\mathrm{LS})(2)}_{12:123,mm',n'n}\\ &= -\frac{1}{4\pi}\frac{1}{2\alpha_{n'n}}\frac{\pi^{3/2}}{\alpha_{n'n}^{3/2}}\exp\left(-\frac{q^2}{16\alpha_{n'n}}\right)\int \mathrm{d}\boldsymbol{r}_3\, r_3 t^{S_{12}T_{12}(\mathrm{LS})}_{12}(r_3)\\ &\quad\times Y_{1m}(\hat{\boldsymbol{r}}_3)\left[\alpha_{n'n}r_3Y_{1m'}(\hat{\boldsymbol{r}}_3) + \frac{i}{2}qY_{1m'}(\hat{\boldsymbol{q}})\right]\mathrm{e}^{i\boldsymbol{q}\cdot\boldsymbol{r}_3}\\ &= -\frac{3}{\sqrt{4\pi}}\frac{\pi^{3/2}}{2\alpha_{n'n}^{3/2}}\exp\left(-\frac{q^2}{16\alpha_{n'n}}\right)\sum_{LM}\bar{Y}^{(+)}_{LM}(1m1m',\hat{\boldsymbol{q}})\int_0^\infty \mathrm{d}r_3\, r_3^4 t^{S_{12}T_{12}(\mathrm{LS})}_{12}(r_3)j_L(qr_3)\\ &\quad + \frac{1}{4\alpha_{n'n}}\frac{\pi^{3/2}}{\alpha_{n'n}^{3/2}}q\exp\left(-\frac{q^2}{16\alpha_{n'n}}\right)Y_{1m}(\hat{\boldsymbol{q}})Y_{1m'}(\hat{\boldsymbol{q}})\int_0^\infty \mathrm{d}r_3\, r_3^3 t^{S_{12}T_{12}(\mathrm{LS})}_{12}(r_3)j_1(qr_3),\end{aligned} \tag{C.148}$$

$$\begin{aligned}&I^{S_{13}T_{13}(\mathrm{LS})(2)}_{13:123,mm',n'n}\\ &= \frac{1}{4\pi}\frac{1}{2\alpha_{n'n}}\frac{\pi^{3/2}}{\alpha_{n'n}^{3/2}}\exp\left(-\frac{q^2}{16\alpha_{n'n}}\right)\int \mathrm{d}\boldsymbol{r}_2\, r_2 t^{S_{13}T_{13}(\mathrm{LS})}_{13}(r_2)\\ &\quad\times Y_{1m}(\hat{\boldsymbol{r}}_2)\left[\alpha_{n'n}r_2Y_{1m'}(\hat{\boldsymbol{r}}_2) - \frac{i}{2}qY_{1m'}(\hat{\boldsymbol{q}})\right]\mathrm{e}^{-i\boldsymbol{q}\cdot\boldsymbol{r}_2}\\ &= \frac{3}{\sqrt{4\pi}}\frac{\pi^{3/2}}{2\alpha_{n'n}^{3/2}}\exp\left(-\frac{q^2}{16\alpha_{n'n}}\right)\sum_{LM}\bar{Y}^{(-)}_{LM}(1m1m',\hat{\boldsymbol{q}})\int_0^\infty \mathrm{d}r_2\, r_2^4 t^{S_{13}T_{13}(\mathrm{LS})}_{13}(r_2)j_L(qr_2)\\ &\quad - \frac{1}{4\alpha_{n'n}}\frac{\pi^{3/2}}{\alpha_{n'n}^{3/2}}q\exp\left(-\frac{q^2}{16\alpha_{n'n}}\right)Y_{1m}(\hat{\boldsymbol{q}})Y_{1m'}(\hat{\boldsymbol{q}})\int_0^\infty \mathrm{d}r_2\, r_2^3 t^{S_{13}T_{13}(\mathrm{LS})}_{13}(r_2)j_1(qr_2),\end{aligned} \tag{C.149}$$

$$\bar{Y}^{(\pm)}_{LM}(1m1m',\hat{\boldsymbol{q}}) \equiv \frac{(\pm i)^L}{\hat{L}}(1m1m'|LM)(1010|L0)Y_{LM}(\hat{\boldsymbol{q}}) \tag{C.150}$$

are obtained with using Eqs. (C.185) and (C.187).

The components of the spin-orbit interactions of the transition matrices (C.27) and (C.28) are given by

$$\begin{aligned}&\bar{T}^{S_{12}T_{12}(\mathrm{LS})}_{12:213}(\boldsymbol{\kappa}', S'M'_S|\boldsymbol{\kappa}, SM_S)\\ &\equiv \left\langle \phi'_{\mathrm{x}}(\boldsymbol{r}_1)\mathrm{e}^{i\boldsymbol{\kappa}'\cdot\boldsymbol{s}_1}\left[\left[\eta^{(2)}_{\frac{1}{2}}\otimes\eta^{(1)}_{\frac{1}{2}}\right]_{S_{12}}\otimes\eta^{(3)}_{\frac{1}{2}}\right]_{S'M'_S}\right|\end{aligned}$$

$$\times t_{12}^{S_{12}T_{12}(\mathrm{LS})}(r_3)\hat{\boldsymbol{\ell}}_{12}\cdot\boldsymbol{S}_{12}\left|\phi_{\mathrm{x}}(\boldsymbol{r}_2)\mathrm{e}^{i\boldsymbol{\kappa}\cdot\boldsymbol{s}_2}\left[\left[\eta_{\frac{1}{2}}^{(2)}\otimes\eta_{\frac{1}{2}}^{(1)}\right]_{S_{12}}\otimes\eta_{\frac{1}{2}}^{(3)}\right]_{SM_S}\right\rangle, \tag{C.151}$$

$$\begin{aligned}&\bar{T}_{13:321}^{S_{13}T_{13}(\mathrm{LS})}(\boldsymbol{\kappa}',S'M_S'|\boldsymbol{\kappa},SM_S)\\&\equiv\left\langle\phi_{\mathrm{x}}'(\boldsymbol{r}_1)\mathrm{e}^{i\boldsymbol{\kappa}'\cdot\boldsymbol{s}_1}\left[\left[\eta_{\frac{1}{2}}^{(3)}\otimes\eta_{\frac{1}{2}}^{(1)}\right]_{S_{13}}\otimes\eta_{\frac{1}{2}}^{(2)}\right]_{S'M_S'}\right|\\&\qquad\times t_{13}^{S_{13}T_{13}(\mathrm{LS})}(r_2)\hat{\boldsymbol{\ell}}_{13}\cdot\boldsymbol{S}_{13}\left|\phi_{\mathrm{x}}(\boldsymbol{r}_3)\mathrm{e}^{i\boldsymbol{\kappa}\cdot\boldsymbol{s}_3}\left[\left[\eta_{\frac{1}{2}}^{(3)}\otimes\eta_{\frac{1}{2}}^{(1)}\right]_{S_{13}}\otimes\eta_{\frac{1}{2}}^{(2)}\right]_{SM_S}\right\rangle.\end{aligned} \tag{C.152}$$

Calculating them similarly to Eqs. (C.105) and (C.106), we obtain

$$\hat{\boldsymbol{\ell}}_{12}\cdot\boldsymbol{S}_{12}\left|\phi_{\mathrm{x}}(\boldsymbol{r}_2)\mathrm{e}^{i\boldsymbol{\kappa}\cdot\boldsymbol{s}_2}\right\rangle=-i\phi_{\mathrm{x}}(\boldsymbol{r}_2)\left(\boldsymbol{r}_3\times\nabla_{\boldsymbol{r}_3}\mathrm{e}^{i\boldsymbol{\kappa}\cdot\boldsymbol{s}_2}\right)\cdot\boldsymbol{S}_{12}-i[\boldsymbol{r}_3\times\nabla_{\boldsymbol{r}_3}\phi_{\mathrm{x}}(\boldsymbol{r}_2)]\cdot\boldsymbol{S}_{12}\mathrm{e}^{i\boldsymbol{\kappa}\cdot\boldsymbol{s}_2}, \tag{C.153}$$

$$\hat{\boldsymbol{\ell}}_{13}\cdot\boldsymbol{S}_{13}\left|\phi_{\mathrm{x}}(\boldsymbol{r}_3)\mathrm{e}^{i\boldsymbol{\kappa}\cdot\boldsymbol{s}_3}\right\rangle=-i\phi_{\mathrm{x}}(\boldsymbol{r}_3)\left(\boldsymbol{r}_2\times\nabla_{\boldsymbol{r}_2}\mathrm{e}^{i\boldsymbol{\kappa}\cdot\boldsymbol{s}_3}\right)\cdot\boldsymbol{S}_{13}-i[\boldsymbol{r}_2\times\nabla_{\boldsymbol{r}_2}\phi_{\mathrm{x}}(\boldsymbol{r}_3)]\cdot\boldsymbol{S}_{13}\mathrm{e}^{i\boldsymbol{\kappa}\cdot\boldsymbol{s}_3}, \tag{C.154}$$

and

$$\nabla_{\boldsymbol{r}_3}\mathrm{e}^{i\boldsymbol{\kappa}\cdot\boldsymbol{s}_2}=\nabla_{\boldsymbol{r}_3}\exp\left[i\boldsymbol{\kappa}\cdot\left(-\frac{3}{4}\boldsymbol{r}_3-\frac{1}{2}\boldsymbol{s}_3\right)\right]=-\frac{3}{4}i\boldsymbol{\kappa}\exp\left[i\boldsymbol{\kappa}\cdot\left(-\frac{3}{4}\boldsymbol{r}_3-\frac{1}{2}\boldsymbol{s}_3\right)\right], \tag{C.155}$$

$$\nabla_{\boldsymbol{r}_2}\mathrm{e}^{i\boldsymbol{\kappa}\cdot\boldsymbol{s}_3}=\nabla_{\boldsymbol{r}_2}\exp\left[i\boldsymbol{\kappa}\cdot\left(\frac{3}{4}\boldsymbol{r}_2-\frac{1}{2}\boldsymbol{s}_2\right)\right]=\frac{3}{4}i\boldsymbol{\kappa}\exp\left[i\boldsymbol{\kappa}\cdot\left(\frac{3}{4}\boldsymbol{r}_2-\frac{1}{2}\boldsymbol{s}_2\right)\right], \tag{C.156}$$

$$\begin{aligned}\nabla_{\boldsymbol{r}_3}\phi_{\mathrm{x}}(\boldsymbol{r}_2)&=\frac{1}{\sqrt{4\pi}}\sum_n c_n\nabla_{\boldsymbol{r}_3}\exp\left[-\alpha_n\left(-\frac{1}{2}\boldsymbol{r}_3+\boldsymbol{s}_3\right)^2\right]\\&=-\frac{1}{\sqrt{4\pi}}\sum_n c_n\left[-\alpha_n\left(-\frac{1}{2}\boldsymbol{r}_3+\boldsymbol{s}_3\right)\right]\exp\left[-\alpha_n\left(-\frac{1}{2}\boldsymbol{r}_3+\boldsymbol{s}_3\right)^2\right],\end{aligned} \tag{C.157}$$

$$\begin{aligned}\nabla_{\boldsymbol{r}_2}\phi_{\mathrm{x}}(\boldsymbol{r}_3)&=\frac{1}{\sqrt{4\pi}}\sum_n c_n\nabla_{\boldsymbol{r}_2}\exp\left[-\alpha_n\left(-\frac{1}{2}\boldsymbol{r}_2-\boldsymbol{s}_2\right)^2\right]\\&=-\frac{1}{\sqrt{4\pi}}\sum_n c_n\left[-\alpha_n\left(-\frac{1}{2}\boldsymbol{r}_2-\boldsymbol{s}_2\right)\right]\exp\left[-\alpha_n\left(-\frac{1}{2}\boldsymbol{r}_2-\boldsymbol{s}_3\right)^2\right].\end{aligned} \tag{C.158}$$

Making the use of them, we can separate the transition matrices (C.151) and (C.152), respectively, into the two parts as shown below:

$$\begin{aligned}&\bar{T}_{12:213}^{S_{12}T_{12}(\mathrm{LS})}(\boldsymbol{\kappa}',S'M_S'|\boldsymbol{\kappa},SM_S)\\&=\bar{T}_{12:213}^{S_{12}T_{12}(\mathrm{LS})(1)}(\boldsymbol{\kappa}',S'M_S'|\boldsymbol{\kappa},SM_S)+\bar{T}_{12:213}^{S_{12}T_{12}(\mathrm{LS})(2)}(\boldsymbol{\kappa}',S'M_S'|\boldsymbol{\kappa},SM_S),\end{aligned} \tag{C.159}$$

$$\begin{aligned}&\bar{T}_{13:321}^{S_{13}T_{13}(\mathrm{LS})}(\boldsymbol{\kappa}',S'M_S'|\boldsymbol{\kappa},SM_S)\\&=\bar{T}_{13:321}^{S_{13}T_{13}(\mathrm{LS})(1)}(\boldsymbol{\kappa}',S'M_S'|\boldsymbol{\kappa},SM_S)+\bar{T}_{13:321}^{S_{13}T_{13}(\mathrm{LS})(2)}(\boldsymbol{\kappa}',S'M_S'|\boldsymbol{\kappa},SM_S),\end{aligned} \tag{C.160}$$

$$\bar{T}_{12:213}^{S_{12}T_{12}(\mathrm{LS})(1)}(\boldsymbol{\kappa}',S'M_S'|\boldsymbol{\kappa},SM_S)$$

$$\equiv -\left\langle \phi'_{\rm x}(\boldsymbol{r}_1)\mathrm{e}^{i\boldsymbol{\kappa}'\cdot\boldsymbol{s}_1}\left[\left[\eta^{(2)}_{\frac{1}{2}}\otimes\eta^{(1)}_{\frac{1}{2}}\right]_{S_{12}}\otimes\eta^{(3)}_{\frac{1}{2}}\right]_{S'M'_S}\right| t^{S_{12}T_{12}(\mathrm{LS})}_{12}(r_3)$$
$$\times\frac{3}{4}(\boldsymbol{r}_3\times\boldsymbol{\kappa})\cdot\boldsymbol{S}_{12}\left|\phi_{\rm x}(\boldsymbol{r}_2)\mathrm{e}^{i\boldsymbol{\kappa}\cdot\boldsymbol{s}_2}\left[\left[\eta^{(2)}_{\frac{1}{2}}\otimes\eta^{(1)}_{\frac{1}{2}}\right]_{S_{12}}\otimes\eta^{(3)}_{\frac{1}{2}}\right]_{SM_S}\right\rangle, \tag{C.161}$$

$$\bar{T}^{S_{13}T_{13}(\mathrm{LS})(1)}_{13:321}(\boldsymbol{\kappa}',S'M'_S|\boldsymbol{\kappa},SM_S)$$
$$\equiv \left\langle \phi'_{\rm x}(\boldsymbol{r}_1)\mathrm{e}^{i\boldsymbol{\kappa}'\cdot\boldsymbol{s}_1}\left[\left[\eta^{(3)}_{\frac{1}{2}}\otimes\eta^{(1)}_{\frac{1}{2}}\right]_{S_{13}}\otimes\eta^{(2)}_{\frac{1}{2}}\right]_{S'M'_S}\right| t^{S_{13}T_{13}(\mathrm{LS})}_{13}(r_2)$$
$$\times\frac{3}{4}(\boldsymbol{r}_2\times\boldsymbol{\kappa})\cdot\boldsymbol{S}_{13}\left|\phi_{\rm x}(\boldsymbol{r}_3)\mathrm{e}^{i\boldsymbol{\kappa}\cdot\boldsymbol{s}_3}\left[\left[\eta^{(3)}_{\frac{1}{2}}\otimes\eta^{(1)}_{\frac{1}{2}}\right]_{S_{13}}\otimes\eta^{(2)}_{\frac{1}{2}}\right]_{SM_S}\right\rangle, \tag{C.162}$$

$$\bar{T}^{S_{12}T_{12}(\mathrm{LS})(2)}_{12:213}(\boldsymbol{\kappa}',S'M'_S|\boldsymbol{\kappa},SM_S)$$
$$\equiv -i\left\langle \phi'_{\rm x}(\boldsymbol{r}_1)\mathrm{e}^{i\boldsymbol{\kappa}'\cdot\boldsymbol{s}_1}\left[\left[\eta^{(2)}_{\frac{1}{2}}\otimes\eta^{(1)}_{\frac{1}{2}}\right]_{S_{12}}\otimes\eta^{(3)}_{\frac{1}{2}}\right]_{S'M'_S}\right| t^{S_{12}T_{12}(\mathrm{LS})}_{12}(r_3)$$
$$\times(\boldsymbol{r}_3\times\boldsymbol{s}_3)\cdot\boldsymbol{S}_{12}\left|\frac{1}{\sqrt{4\pi}}\sum_n c_n\alpha_n\exp\!\left(-\alpha_n r_2^2\right)\mathrm{e}^{i\boldsymbol{\kappa}\cdot\boldsymbol{s}_2}\left[\left[\eta^{(2)}_{\frac{1}{2}}\otimes\eta^{(1)}_{\frac{1}{2}}\right]_{S_{12}}\otimes\eta^{(3)}_{\frac{1}{2}}\right]_{SM_S}\right\rangle, \tag{C.163}$$

$$\bar{T}^{S_{13}T_{13}(\mathrm{LS})(2)}_{13:321}(\boldsymbol{\kappa}',S'M'_S|\boldsymbol{\kappa},SM_S)$$
$$\equiv i\left\langle \phi'_{\rm x}(\boldsymbol{r}_1)\mathrm{e}^{i\boldsymbol{\kappa}'\cdot\boldsymbol{s}_1}\left[\left[\eta^{(3)}_{\frac{1}{2}}\otimes\eta^{(1)}_{\frac{1}{2}}\right]_{S_{13}}\otimes\eta^{(2)}_{\frac{1}{2}}\right]_{S'M'_S}\right| t^{S_{13}T_{13}(\mathrm{LS})}_{13}(r_2)$$
$$\times(\boldsymbol{r}_2\times\boldsymbol{s}_2)\cdot\boldsymbol{S}_{13}\left|\frac{1}{\sqrt{4\pi}}\sum_n c_n\alpha_n\exp\!\left(-\alpha_n r_3^2\right)\mathrm{e}^{i\boldsymbol{\kappa}\cdot\boldsymbol{s}_3}\left[\left[\eta^{(3)}_{\frac{1}{2}}\otimes\eta^{(1)}_{\frac{1}{2}}\right]_{S_{13}}\otimes\eta^{(2)}_{\frac{1}{2}}\right]_{SM_S}\right\rangle. \tag{C.164}$$

We can calculate these matrices as shown from Eq. (C.117) to Eq. (C.150). Then the transition matrices (C.161) and (C.162) become

$$\bar{T}^{S_{12}T_{12}(\mathrm{LS})(1)}_{12:213}(\boldsymbol{\kappa}',S'M'_S|\boldsymbol{\kappa},SM_S)$$
$$=2\pi i\sum_{\mu_3}\sum_{M'_{12}M_{12}}\left(S_{12}M'_{12}\frac{1}{2}\mu_3\middle|S'M'_S\right)\left(S_{12}M_{12}\frac{1}{2}\mu_3\middle|SM_S\right)$$
$$\times\sum_m\sum_{aa'}(-)^m\left(S_{12}M_{12}1a'|S_{12}M'_{12}\right)(1a1a'|1-m)\kappa Y_{1a}(\hat{\boldsymbol{\kappa}})\sum_{n'n}c_{n'}c_n I^{S_{12}T_{12}(\mathrm{LS})(1)}_{12:213,m,n'n}, \tag{C.165}$$

$$\bar{T}^{S_{13}T_{13}(\mathrm{LS})(1)}_{13:321}(\boldsymbol{\kappa}',S'M'_S|\boldsymbol{\kappa},SM_S)$$
$$=-2\pi i\sum_{\mu_2}\sum_{M'_{13}M_{13}}\left(S_{13}M'_{13}\frac{1}{2}\mu_2\middle|S'M'_S\right)\left(S_{13}M_{13}\frac{1}{2}\mu_2\middle|SM_S\right)$$
$$\times\sum_m\sum_{aa'}(-)^m\left(S_{13}M_{13}1a'|S_{13}M'_{13}\right)(1a1a'|1-m)\kappa Y_{1a}(\hat{\boldsymbol{\kappa}})\sum_{n'n}c_{n'}c_n I^{S_{13}T_{13}(\mathrm{LS})(1)}_{13:321,m,n'n}, \tag{C.166}$$

$$\begin{aligned}
&I^{S_{12}T_{12}(\mathrm{LS})(1)}_{12:213,m,n'n} \\
&\equiv \frac{1}{4\pi}\int \mathrm{d}\boldsymbol{r}_3 \int \mathrm{d}\boldsymbol{s}_3 \exp\left[-\alpha_{n'}\left(\frac{1}{2}\boldsymbol{r}_3+\boldsymbol{s}_3\right)^2\right]\exp\left[-i\boldsymbol{\kappa}'\cdot\left(\frac{3}{4}\boldsymbol{r}_3-\frac{1}{2}\boldsymbol{s}_3\right)\right] \\
&\qquad\times t^{S_{12}T_{12}(\mathrm{LS})}_{12}(r_3)r_3Y_{1m}(\hat{\boldsymbol{r}}_3)\exp\left[-\alpha_n\left(-\frac{1}{2}\boldsymbol{r}_3+\boldsymbol{s}_3\right)^2\right]\exp\left[i\boldsymbol{\kappa}\cdot\left(-\frac{3}{4}\boldsymbol{r}_3-\frac{1}{2}\boldsymbol{s}_3\right)\right] \\
&=\frac{1}{4\pi}\frac{\pi^{3/2}}{\alpha^{3/2}_{n'n}}\exp\left(-\frac{q^2}{16\alpha_{n'n}}\right)\int \mathrm{d}\boldsymbol{r}_3\, r_3 t^{S_{12}T_{12}(\mathrm{LS})}_{12}(r_3)Y_{1m}(\hat{\boldsymbol{r}}_3)\mathrm{e}^{i\boldsymbol{p}_{n'n}\cdot\boldsymbol{r}_3}\exp\left(-\frac{\alpha_{n'}\alpha_n}{\alpha_{n'n}}r_3^2\right) \\
&=i\frac{\pi^{3/2}}{\alpha^{3/2}_{n'n}}\exp\left(-\frac{q^2}{16\alpha_{n'n}}\right)Y_{1m}(\hat{\boldsymbol{p}}_{n'n})\int_0^\infty \mathrm{d}r_3\, r_3^3 t^{S_{12}T_{12}(\mathrm{LS})}_{12}(r_3)j_1(|\boldsymbol{p}_{n'n}|r_3)\exp\left(-\frac{\alpha_{n'}\alpha_n}{\alpha_{n'n}}r_3^2\right),
\end{aligned}\tag{C.167}$$

$$\begin{aligned}
&I^{S_{13}T_{13}(\mathrm{LS})(1)}_{13:321,m,n'n} \\
&\equiv \frac{1}{4\pi}\int \mathrm{d}\boldsymbol{r}_2 \int \mathrm{d}\boldsymbol{s}_2 \exp\left[-\alpha_{n'}\left(\frac{1}{2}\boldsymbol{r}_2-\boldsymbol{s}_2\right)^2\right]\exp\left[-i\boldsymbol{\kappa}'\cdot\left(-\frac{3}{4}\boldsymbol{r}_2-\frac{1}{2}\boldsymbol{s}_2\right)\right] \\
&\qquad\times t^{S_{13}T_{13}(\mathrm{LS})}_{13}(r_2)r_2Y_{1m}(\hat{\boldsymbol{r}}_2)\exp\left[-\alpha_n\left(-\frac{1}{2}\boldsymbol{r}_2-\boldsymbol{s}_2\right)^2\right]\exp\left[i\boldsymbol{\kappa}\cdot\left(\frac{3}{4}\boldsymbol{r}_2-\frac{1}{2}\boldsymbol{s}_2\right)\right] \\
&=\frac{1}{4\pi}\frac{\pi^{3/2}}{\alpha^{3/2}_{n'n}}\exp\left(-\frac{q^2}{16\alpha_{n'n}}\right)\int \mathrm{d}\boldsymbol{r}_2\, r_2 t^{S_{13}T_{13}(\mathrm{LS})}_{13}(r_2)Y_{1m}(\hat{\boldsymbol{r}}_2)\mathrm{e}^{-i\boldsymbol{p}_{n'n}\cdot\boldsymbol{r}_2}\exp\left(-\frac{\alpha_{n'}\alpha_n}{\alpha_{n'n}}r_2^2\right) \\
&=-i\frac{\pi^{3/2}}{\alpha^{3/2}_{n'n}}\exp\left(-\frac{q^2}{16\alpha_{n'n}}\right)Y_{1m}(\hat{\boldsymbol{p}}_{n'n})\int_0^\infty \mathrm{d}r_2\, r_2^3 t^{S_{13}T_{13}(\mathrm{LS})}_{13}(r_2)j_1(|\boldsymbol{p}_{n'n}|r_2)\exp\left(-\frac{\alpha_{n'}\alpha_n}{\alpha_{n'n}}r_2^2\right),
\end{aligned}\tag{C.168}$$

in which Eqs. (C.55) and (C.185), and the others (C.163) and (C.164) do

$$\begin{aligned}
&\bar{T}^{S_{12}T_{12}(\mathrm{LS})(2)}_{12:213}(\boldsymbol{\kappa}',S'M_S'|\boldsymbol{\kappa},SM_S) \\
&\quad=-\frac{8\pi}{3}\sum_{\mu_3}\sum_{M_{12}'M_{12}}\left(S_{12}M_{12}'\frac{1}{2}\mu_3\middle|S'M_S'\right)\left(S_{12}M_{12}\frac{1}{2}\mu_3\middle|SM_S\right) \\
&\qquad\times\sum_{mm'}\sum_a(-)^a\big(S_{12}M_{12}1a|S_{12}M_{12}'\big)\big(1m1m'|1-a\big)\sum_{n'n}c_{n'}c_n\alpha_n I^{S_{12}T_{12}(\mathrm{LS})(2)}_{12:213,mm',n'n},
\end{aligned}\tag{C.169}$$

$$\begin{aligned}
&\bar{T}^{S_{13}T_{13}(\mathrm{LS})(2)}_{13:321}(\boldsymbol{\kappa}',S'M_S'|\boldsymbol{\kappa},SM_S) \\
&\quad=\frac{8\pi}{3}\sum_{\mu_2}\sum_{M_{13}'M_{13}}\left(S_{13}M_{13}'\frac{1}{2}\mu_2\middle|S'M_S'\right)\left(S_{13}M_{13}\frac{1}{2}\mu_2\middle|SM_S\right) \\
&\qquad\times\sum_{mm'}\sum_a(-)^a\big(S_{13}M_{13}1a|S_{13}M_{13}'\big)\big(1m1m'|1-a\big)\sum_{n'n}c_{n'}c_n\alpha_n I^{S_{13}T_{13}(\mathrm{LS})(2)}_{13:321,mm',n'n},
\end{aligned}\tag{C.170}$$

$$\begin{aligned}
&I^{S_{12}T_{12}(\mathrm{LS})(2)}_{12:213,mm',n'n} \\
&\equiv -\frac{1}{4\pi}\frac{1}{2\alpha_{n'n}}\frac{\pi^{3/2}}{\alpha^{3/2}_{n'n}}\exp\left(-\frac{q^2}{16\alpha_{n'n}}\right)\int \mathrm{d}\boldsymbol{r}_3\, r_3 t^{S_{12}T_{12}(\mathrm{LS})}_{12}(r_3) \\
&\qquad\times Y_{1m}(\hat{\boldsymbol{r}}_3)\left[\bar{\alpha}_{n'n}r_3Y_{1m'}(\hat{\boldsymbol{r}}_3)+\frac{i}{2}qY_{1m'}(\hat{\boldsymbol{q}})\right]\mathrm{e}^{i\boldsymbol{p}_{n'n}\cdot\boldsymbol{r}_3}\exp\left(-\frac{\alpha_{n'}\alpha_n}{\alpha_{n'n}}r_3^2\right) \\
&=-\frac{3}{\sqrt{4\pi}}\frac{\bar{\alpha}_{n'n}}{2\alpha_{n'n}}\frac{\pi^{3/2}}{\alpha^{3/2}_{n'n}}\exp\left(-\frac{q^2}{16\alpha_{n'n}}\right)\sum_{LM}\bar{Y}^{(+)}_{LM}(1m1m',\hat{\boldsymbol{p}}_{n'n})
\end{aligned}$$

$$\times \int_0^\infty \mathrm{d}r_3\, r_3^4 t_{12}^{S_{12}T_{12}(\mathrm{LS})}(r_3) j_L(|\boldsymbol{p}_{n'n}|r_3) \exp\left(-\frac{\alpha_{n'}\alpha_n}{\alpha_{n'n}} r_3^2\right)$$

$$+ \frac{1}{4\alpha_{n'n}} \frac{\pi^{3/2}}{\alpha_{n'n}^{3/2}} q \exp\left(-\frac{q^2}{16\alpha_{n'n}}\right) Y_{1m}(\hat{\boldsymbol{q}}) Y_{1m'}(\hat{\boldsymbol{p}}_{n'n})$$

$$\times \int_0^\infty \mathrm{d}r_3\, r_3^3 t_{12}^{S_{12}T_{12}(\mathrm{LS})}(r_3) j_1(|\boldsymbol{p}|_{n'n} r_3) \exp\left(-\frac{\alpha_{n'}\alpha_n}{\alpha_{n'n}} r_3^2\right), \tag{C.171}$$

$$I_{13:321,mm',n'n}^{S_{13}T_{13}(\mathrm{LS})(2)}$$

$$\equiv \frac{1}{4\pi} \frac{1}{2\alpha_{n'n}} \frac{\pi^{3/2}}{\alpha_{n'n}^{3/2}} \exp\left(-\frac{q^2}{16\alpha_{n'n}}\right) \int \mathrm{d}\boldsymbol{r}_2\, r_2 t_{13}^{S_{13}T_{13}(\mathrm{LS})}(r_2)$$

$$\times Y_{1m}(\hat{\boldsymbol{r}}_2) \left[\bar{\alpha}_{n'n} r_2 Y_{1m'}(\hat{\boldsymbol{r}}_2) - \frac{i}{2} q Y_{1m'}(\hat{\boldsymbol{q}})\right] \mathrm{e}^{-i\boldsymbol{p}_{n'n}\cdot\boldsymbol{r}_2} \exp\left(-\frac{\alpha_{n'}\alpha_n}{\alpha_{n'n}} r_2^2\right)$$

$$= \frac{3}{\sqrt{4\pi}} \frac{\bar{\alpha}_{n'n}}{2\alpha_{n'n}} \frac{\pi^{3/2}}{\alpha_{n'n}^{3/2}} \exp\left(-\frac{q^2}{16\alpha_{n'n}}\right) \sum_{LM} \bar{Y}_{LM}^{(-)}(1m1m', \hat{\boldsymbol{p}}_{n'n})$$

$$\times \int_0^\infty \mathrm{d}r_2\, r_2^4 t_{13}^{S_{13}T_{13}(\mathrm{LS})}(r_2) j_L(|\boldsymbol{p}_{n'n}|r_2) \exp\left(-\frac{\alpha_{n'}\alpha_n}{\alpha_{n'n}} r_2^2\right)$$

$$- \frac{1}{4\alpha_{n'n}} \frac{\pi^{3/2}}{\alpha_{n'n}^{3/2}} q \exp\left(-\frac{q^2}{16\alpha_{n'n}}\right) Y_{1m}(\hat{\boldsymbol{q}}) Y_{1m'}(\hat{\boldsymbol{p}}_{n'n})$$

$$\times \int_0^\infty \mathrm{d}r_2\, r_2^3 t_{13}^{S_{13}T_{13}(\mathrm{LS})}(r_2) j_1(|\boldsymbol{p}|_{n'n} r_2) \exp\left(-\frac{\alpha_{n'}\alpha_n}{\alpha_{n'n}} r_2^2\right), \tag{C.172}$$

$$\bar{Y}_{LM}^{(\pm)}(1m1m', \hat{\boldsymbol{p}}_{n'n}) \equiv \frac{(\pm i)^L}{\hat{L}} (1m1m'|LM)(1010|L0) Y_{LM}(\hat{\boldsymbol{p}}_{n'n}), \tag{C.173}$$

in which we have used Eq. (C.145) with replacing α, $\boldsymbol{\beta}$, and $\boldsymbol{\gamma}$ as

$$\alpha \to \alpha_{n'n}, \quad \boldsymbol{\beta} \to \pm\bar{\alpha}_{n'n}\boldsymbol{r}, \quad \boldsymbol{\gamma} \to \frac{\boldsymbol{q}}{2}, \tag{C.174}$$

respectively, and have used Eqs. (C.185) and (C.187).

The components of the spin-orbit interactions of the transition matrices (C.29) and (C.30) are given by

$$\bar{T}_{12:321}^{S_{12}T_{12}(\mathrm{LS})}(\boldsymbol{\kappa}', S'M_S'|\boldsymbol{\kappa}, SM_S)$$

$$\equiv \left\langle \phi_{\mathrm{x}}'(\boldsymbol{r}_1)\mathrm{e}^{i\boldsymbol{\kappa}'\cdot\boldsymbol{s}_1} \left[\left[\eta_{\frac{1}{2}}^{(2)} \otimes \eta_{\frac{1}{2}}^{(1)}\right]_{S_{12}} \otimes \eta_{\frac{1}{2}}^{(3)}\right]_{S'M_S'} \right|$$

$$\times\, t_{12}^{S_{12}T_{12}(\mathrm{LS})}(r_3) \hat{\boldsymbol{\ell}}_{12}\cdot\boldsymbol{S}_{12} \left| \phi_{\mathrm{x}}(\boldsymbol{r}_3)\mathrm{e}^{i\boldsymbol{\kappa}\cdot\boldsymbol{s}_3} \left[\left[\eta_{\frac{1}{2}}^{(2)} \otimes \eta_{\frac{1}{2}}^{(1)}\right]_{S_{12}} \otimes \eta_{\frac{1}{2}}^{(3)}\right]_{SM_S} \right\rangle, \tag{C.175}$$

$$\bar{T}_{13:213}^{S_{13}T_{13}(\mathrm{LS})}(\boldsymbol{\kappa}', S'M_S'|\boldsymbol{\kappa}, SM_S)$$

$$\equiv \left\langle \phi_{\mathrm{x}}'(\boldsymbol{r}_1)\mathrm{e}^{i\boldsymbol{\kappa}'\cdot\boldsymbol{s}_1} \left[\left[\eta_{\frac{1}{2}}^{(3)} \otimes \eta_{\frac{1}{2}}^{(1)}\right]_{S_{13}} \otimes \eta_{\frac{1}{2}}^{(2)}\right]_{S'M_S'} \right|$$

$$\times\, t_{13}^{S_{13}T_{13}(\mathrm{LS})}(r_2) \hat{\boldsymbol{\ell}}_{13}\cdot\boldsymbol{S}_{13} \left| \phi_{\mathrm{x}}(\boldsymbol{r}_2)\mathrm{e}^{i\boldsymbol{\kappa}\cdot\boldsymbol{s}_2} \left[\left[\eta_{\frac{1}{2}}^{(3)} \otimes \eta_{\frac{1}{2}}^{(1)}\right]_{S_{13}} \otimes \eta_{\frac{1}{2}}^{(2)}\right]_{SM_S} \right\rangle. \tag{C.176}$$

Calculating them similarly to Eqs. (C.105) and (C.106), we obtain

$$\begin{aligned}\hat{\boldsymbol{\ell}}_{12}\cdot\boldsymbol{S}_{12}\left|\phi_{\mathrm{x}}(\boldsymbol{r}_3)\mathrm{e}^{i\boldsymbol{\kappa}\cdot\boldsymbol{s}_3}\right\rangle &= -i\phi_{\mathrm{x}}(\boldsymbol{r}_3)\big(\boldsymbol{r}_3\times\nabla_{\boldsymbol{r}_3}\mathrm{e}^{i\boldsymbol{\kappa}\cdot\boldsymbol{s}_3}\big)\cdot\boldsymbol{S}_{12} - i[\boldsymbol{r}_3\times\nabla_{\boldsymbol{r}_3}\phi_{\mathrm{x}}(\boldsymbol{r}_3)]\cdot\boldsymbol{S}_{12}\mathrm{e}^{i\boldsymbol{\kappa}\cdot\boldsymbol{s}_3}\\ &= -i[\boldsymbol{r}_3\times\nabla_{\boldsymbol{r}_3}\phi_{\mathrm{x}}(\boldsymbol{r}_3)]\cdot\boldsymbol{S}_{12}\mathrm{e}^{i\boldsymbol{\kappa}\cdot\boldsymbol{s}_3},\end{aligned} \tag{C.177}$$

$$\begin{aligned}\hat{\boldsymbol{\ell}}_{13}\cdot\boldsymbol{S}_{13}\left|\phi_{\mathrm{x}}(\boldsymbol{r}_2)\mathrm{e}^{i\boldsymbol{\kappa}\cdot\boldsymbol{s}_2}\right\rangle &= -i\phi_{\mathrm{x}}(\boldsymbol{r}_2)\big(\boldsymbol{r}_2\times\nabla_{\boldsymbol{r}_2}\mathrm{e}^{i\boldsymbol{\kappa}\cdot\boldsymbol{s}_2}\big)\cdot\boldsymbol{S}_{13} - i[\boldsymbol{r}_2\times\nabla_{\boldsymbol{r}_2}\phi_{\mathrm{x}}(\boldsymbol{r}_2)]\cdot\boldsymbol{S}_{13}\mathrm{e}^{i\boldsymbol{\kappa}\cdot\boldsymbol{s}_2}\\ &= -i[\boldsymbol{r}_2\times\nabla_{\boldsymbol{r}_2}\phi_{\mathrm{x}}(\boldsymbol{r}_2)]\cdot\boldsymbol{S}_{13}\mathrm{e}^{i\boldsymbol{\kappa}\cdot\boldsymbol{s}_2},\end{aligned} \tag{C.178}$$

and

$$\nabla_{\boldsymbol{r}_3}\phi_{\mathrm{x}}(\boldsymbol{r}_3) = \frac{1}{\sqrt{4\pi}}\sum_n c_n\nabla_{\boldsymbol{r}_3}\exp\big(-\alpha_n r_3^2\big) = \frac{1}{\sqrt{4\pi}}\sum_n c_n(-2\alpha_n\boldsymbol{r}_3)\exp\big(-\alpha_n r_3^2\big), \tag{C.179}$$

$$\nabla_{\boldsymbol{r}_2}\phi_{\mathrm{x}}(\boldsymbol{r}_2) = \frac{1}{\sqrt{4\pi}}\sum_n c_n\nabla_{\boldsymbol{r}_2}\exp\big(-\alpha_n r_2^2\big) = \frac{1}{\sqrt{4\pi}}\sum_n c_n(-2\alpha_n\boldsymbol{r}_2)\exp\big(-\alpha_n r_2^2\big). \tag{C.180}$$

Due to the property of the vector product between the same two vactors, that is, $\boldsymbol{r}\times\boldsymbol{r}=\boldsymbol{0}$, the transition matrices (C.175) and (C.176) are zero:

$$\bar{T}^{S_{12}T_{12}(\mathrm{LS})}_{12:321}(\boldsymbol{\kappa}', S'M_S'|\boldsymbol{\kappa}, SM_S) = \bar{T}^{S_{13}T_{13}(\mathrm{LS})}_{13:213}(\boldsymbol{\kappa}', S'M_S'|\boldsymbol{\kappa}, SM_S) = 0. \tag{C.181}$$

The assumption that particle x can be described only by the S wave causes this result. So Eqs. (C.175) and (C.176) can have finite values when finite orbital angular momentum are included.

C.5 List of mathmatical formula

In this section, the mathematical formulas used in this appendix are listed. Unless otherwise stated, α is a positive real number, $\boldsymbol{\beta}$ and γ are real vectors whose jth components are β_j and γ_j, respectively.

$$\begin{aligned}&\int_{-\infty}^{\infty}\mathrm{d}x_j\exp\big(-\alpha x_j^2\big)\exp[-(\beta_j+i\gamma_j)x_j]\\ &\quad=\exp\left[\frac{(\beta_j+i\gamma_j)^2}{4\alpha}\right]\int_{-\infty}^{\infty}\mathrm{d}x_j\exp\left[-\alpha\left(x_j+\frac{\beta_j+i\gamma_j}{2\alpha}\right)^2\right]\\ &\quad=\sqrt{\frac{\pi}{\alpha}}\exp\left[\frac{(\beta_j+i\gamma_j)^2}{4\alpha}\right].\end{aligned} \tag{C.182}$$

$$\begin{aligned}&\int_{-\infty}^{\infty}\mathrm{d}x_j\,x_j\exp\big(-\alpha x_j^2\big)\exp[-(\beta_j+i\gamma_j)x_j]\\ &\quad=\exp\left[\frac{(\beta_j+i\gamma_j)^2}{4\alpha}\right]\int_{-\infty}^{\infty}\mathrm{d}x_j\,x_j\exp\left[-\alpha\left(x_j+\frac{\beta_j+i\gamma_j}{2\alpha}\right)^2\right]\\ &\quad=-\sqrt{\frac{\pi}{\alpha}}\frac{\beta_j+i\gamma_j}{2\alpha}\exp\left[\frac{(\beta_j+i\gamma_j)^2}{4\alpha}\right].\end{aligned} \tag{C.183}$$

$$\begin{aligned}&\int\mathrm{d}\boldsymbol{R}\exp\big(-\alpha R^2\big)\exp[-(\boldsymbol{\beta}+i\boldsymbol{\gamma})\cdot\boldsymbol{R}]\\ &\quad=\prod_{j=1,2,3}\int_{-\infty}^{\infty}\mathrm{d}x_j\exp\big(-\alpha x_j^2\big)\exp[-(\beta_j+i\gamma_j)x_j]\end{aligned}$$

$$
\begin{aligned}
&= \frac{\pi^{3/2}}{\alpha^{3/2}} \exp\left[\frac{(\boldsymbol{\beta} + i\boldsymbol{\gamma})^2}{4\alpha}\right] \\
&= \frac{\pi^{3/2}}{\alpha^{3/2}} \exp\left(\frac{\beta^2}{4\alpha}\right) \exp\left(-\frac{\gamma^2}{4\alpha}\right) \exp\left(\frac{i}{2\alpha}\boldsymbol{\beta}\cdot\boldsymbol{\gamma}\right).
\end{aligned}
\tag{C.184}
$$

$$
\begin{aligned}
\int \mathrm{d}\hat{\boldsymbol{R}}\, Y_{LM}\left(\hat{\boldsymbol{R}}\right) \mathrm{e}^{\pm i\boldsymbol{K}\cdot\boldsymbol{R}} &= \int \mathrm{d}\hat{\boldsymbol{R}}\, Y_{LM}\left(\hat{\boldsymbol{R}}\right) \cdot 4\pi \sum_{L'M'} (\pm i)^{L'} j_{L'}(KR) Y_{L'M'}\left(\hat{\boldsymbol{K}}\right) Y^*_{L'M'}\left(\hat{\boldsymbol{R}}\right) \\
&= 4\pi \sum_{L'M'} (\pm i)^{L'} j_{L'}(KR) Y_{L'M'}(hat\boldsymbol{K}) \int \mathrm{d}\hat{\boldsymbol{R}}\, Y_{LM}\left(\hat{\boldsymbol{R}}\right) Y^*_{L'M'}\left(\hat{\boldsymbol{R}}\right) \\
&= 4\pi \sum_{L'M'} (\pm i)^{L'} j_{L'}(KR) Y_{L'M'}\left(\hat{\boldsymbol{K}}\right) \delta_{L'L}\delta_{M'M} \\
&= 4\pi (\pm i)^{L} j_{L}(KR) Y_{LM}\left(\hat{\boldsymbol{K}}\right).
\end{aligned}
\tag{C.185}
$$

$$
\int \mathrm{d}\hat{\boldsymbol{R}}\, Y_{L_1M_1}\left(\hat{\boldsymbol{R}}\right) Y_{L_2M_2}\left(\hat{\boldsymbol{R}}\right) Y^*_{LM}\left(\hat{\boldsymbol{R}}\right) = \frac{1}{\sqrt{4\pi}} \frac{\hat{L}_1\hat{L}_2}{\hat{L}} (L_1M_1L_2M_2|LM)(L_10L_20|L0).
\tag{C.186}
$$

$$
\begin{aligned}
&\int \mathrm{d}\hat{\boldsymbol{R}}\, Y_{L_1M_1}\left(\hat{\boldsymbol{R}}\right) Y_{L_2M_2}\left(\hat{\boldsymbol{R}}\right) \mathrm{e}^{\pm i\boldsymbol{K}\cdot\boldsymbol{R}} \\
&= \int \mathrm{d}\hat{\boldsymbol{R}}\, Y_{L_1M_1}\left(\hat{\boldsymbol{R}}\right) Y_{L_2M_2}\left(\hat{\boldsymbol{R}}\right) \cdot 4\pi \sum_{LM} (\pm i)^{L} j_{L}(KR) Y_{LM}\left(\hat{\boldsymbol{K}}\right) Y^*_{LM}\left(\hat{\boldsymbol{R}}\right) \\
&= 4\pi \sum_{LM} (\pm i)^{L} j_{L}(KR) Y_{LM}\left(\hat{\boldsymbol{K}}\right) \int \mathrm{d}\hat{\boldsymbol{R}}\, Y_{L_1M_1}\left(\hat{\boldsymbol{R}}\right) Y_{L_2M_2}\left(\hat{\boldsymbol{R}}\right) Y^*_{LM}\left(\hat{\boldsymbol{R}}\right) \\
&= 4\pi \sum_{LM} (\pm i)^{L} j_{L}(KR) Y_{LM}\left(\hat{\boldsymbol{K}}\right) \cdot \frac{1}{\sqrt{4\pi}} \frac{\hat{L}_1\hat{L}_2}{\hat{L}} (L_1M_1L_2M_2|LM)(L_10L_20|L0).
\end{aligned}
\tag{C.187}
$$

$$
Y_{LM}\left(\widehat{\pm\alpha\boldsymbol{K}}\right) = Y_{LM}\left(\widehat{\pm\boldsymbol{K}}\right) = (\pm)^{L} Y_{LM}\left(\hat{\boldsymbol{K}}\right)
\tag{C.188}
$$

$$
\hat{\boldsymbol{K}} = (\theta_{\boldsymbol{K}}, \varphi_{\boldsymbol{K}}), \quad \widehat{-\boldsymbol{K}} = (\pi - \theta_{\boldsymbol{K}}, \pi + \varphi_{\boldsymbol{K}})
\tag{C.189}
$$

Reference

[1] C. F. v. Weizsäcker, Zeitschrift für Physik **96**, 431 (1935).

[2] H. A. Bethe and R. F. Bacher, Rev. Mod. Phys. **8**, 82 (1936).

[3] M. G. Mayer, Phys. Rev. **74**, 235 (1948).

[4] M. G. Mayer, Phys. Rev. **75**, 1969 (1949).

[5] M. G. Mayer, Phys. Rev. **78**, 16 (1950).

[6] M. G. Mayer, Phys. Rev. **78**, 22 (1950).

[7] O. Haxel, J. H. D. Jensen, and H. E. Suess, Phys. Rev. **75**, 1766 (1949).

[8] A. Bohr, Mat. Fys. Medd. Dan. Vid. Selsk. **26**, No. 14 (1952).

[9] A. Bohr and B. R. Mottelson, Mat. Fys. Medd. Dan. Vid. Selsk. **27**, No. 16 (1953).

[10] A. Bohr and B. R. Mottelson, *Nuclear Structure*, Vol. I (World Scientific 1998).

[11] A. Bohr and B. R. Mottelson, *Nuclear Structure*, Vol. II (World Scientific 1998).

[12] T. Wakasa, K. Ogata, and T. Noro, Prog. Part. Nucl. Phys. **96**, 32 (2017).

[13] T. Noro, T. Wakasa, T. Ishida, H. P. Yoshida, M. Dozono, H. Fujimura, K. Fujita, K. Hatanaka, T. Ishikawa, M. Itoh, J. Kamiya, T. Kawabata, Y. Maeda, H. Matsubara, M. Nakamura, H. Sakaguchi, Y. Sakemi, Y. Shimizu, H. Takeda, Y. Tameshige, A. Tamii, K. Tamura, S. Terashima, M. Uchida, Y. Yasuda, and M. Yosoi, Prog. Theor. Exp. Phys. **2020**, 093D02 (2020).

[14] G. F. Bertsch, in *Fifty Years of Nuclear BCS*, edited by R. A. Broglia and V. Zelevinsky (World Scientific, Singapore, 2013).

[15] D. M. Brink and R. A. Broglia, *Nuclear Superfluidity: Pairing in Finite Systems* (Cambridge University Press, Cambridge, 2005).

[16] K. S. Egiyan, N. Dashyan, M. Sargsian, S. Stepanyan, L. B. Weinstein, G. Adams, P. Ambrozewicz, E. Anciant, M. Anghinolfi, B. Asavapibhop, G. Asryan, G. Audit, T. Auger, H. Avakian, H. Bagdasaryan, J. P. Ball, S. Barrow, M. Battaglieri, K. Beard, I. Bedlinski, M. Bektasoglu, M. Bellis, N. Benmouna, N. Bianchi, A. S. Biselli, S. Boiarinov, B. E. Bonner, S. Bouchigny, R. Bradford, D. Branford, W. J. Briscoe, W. K. Brooks, V. D. Burkert, C. Butuceanu, J. R. Calarco, D. S. Carman, B. Carnahan, C. Cetina, L. Ciciani, P. L. Cole, A. Coleman, D. Cords, J. Connelly, P. Corvisiero, D. Crabb, H. Crannell, J. P. Cummings, E. DeSanctis, R. DeVita, P. V. Degtyarenko, R. Demirchyan, H. Denizli, L. Dennis, K. V. Dharmawardane, K. S. Dhuga, C. Djalali, G. E. Dodge, D. Doughty, P. Dragovitsch, M. Dugger, S. Dytman, O. P. Dzyubak, M. Eckhause, H. Egiyan, L. Elouadrhiri, A. Empl, P. Eugenio, R. Fatemi, R. J. Feuerbach, J. Ficenec, T. A. Forest, H. Funsten, M. Gai, G. Gavalian, S. Gilad, G. P. Gilfoyle, K. L. Giovanetti, P. Girard, C. I. O. Gordon, K. Griffioen, M. Guidal, M. Guillo, L. Guo, V. Gyurjyan, C. Hadjidakis, R. S. Hakobyan, J. Hardie, D. Heddle, P. Heimberg, F. W. Hersman, K. Hicks, R. S. Hicks, M. Holtrop, J. Hu, C. E. Hyde-Wright, Y. Ilieva, M. M. Ito, D. Jenkins, K. Joo, J. H. Kelley, M. Khandaker, D. H. Kim, K. Y. Kim, K. Kim, M. S. Kim, W. Kim, A. Klein, F. J. Klein, A. Klimenko, M. Klusman, M. Kossov, L. H. Kramer, Y. Kuang, S. E. Kuhn, J. Kuhn, J. Lachniet, J. M. Laget, D. Lawrence, J. Li, K. Lukashin, J. J. Manak, C. Marchand, L. C. Maximon, S. McAleer, J. McCarthy, J. W. C. McNabb, B. A. Mecking, S. Mehrabyan, J. J. Melone, M. D. Mestayer, C. A. Meyer, K. Mikhailov, R. Minehart, M. Mirazita, R. Miskimen, L. Morand, S. A. Morrow, M. U. Mozer, V. Muccifora, J. Mueller, L. Y. Murphy, G. S. Mutchler, J. Napolitano, R. Nasseripour, S. O. Nelson, S. Niccolai, G. Niculescu, I. Niculescu, B. B. Niczyporuk, R. A. Niyazov, M. Nozar, G. V. O'Rielly, A. K. Opper, M. Osipenko, K. Park, E. Pasyuk, G. Peterson, S. A. Philips, N. Pivnyuk, D. Pocanic, O. Pogorelko, E. Polli, S. Pozdniakov, B. M. Preedom, J. W. Price, Y. Prok, D. Protopopescu, L. M. Qin, B. A. Raue, G. Riccardi, G. Ricco, M. Ripani,

B. G. Ritchie, F. Ronchetti, P. Rossi, D. Rowntree, P. D. Rubin, F. Sabatié, K. Sabourov, C. Salgado, J. P. Santoro, V. Sapunenko, R. A. Schumacher, V. S. Serov, Y. G. Sharabian, J. Shaw, S. Simionatto, A. V. Skabelin, E. S. Smith, L. C. Smith, D. I. Sober, M. Spraker, A. Stavinsky, P. Stoler, I. Strakovsky, S. Strauch, M. Strikman, M. Taiuti, S. Taylor, D. J. Tedeschi, U. Thoma, R. Thompson, L. Todor, C. Tur, M. Ungaro, M. F. Vineyard, A. V. Vlassov, K. Wang, A. Weisberg, H. Weller, D. P. Weygand, C. S. Whisnant, E. Wolin, M. H. Wood, A. Yegneswaran, J. Yun, B. Zhang, J. Zhao, and Z. Zhou, Phys. Rev. C **68**, 014313 (2003).

[17] K. S. Egiyan, N. B. Dashyan, M. M. Sargsian, M. I. Strikman, L. B. Weinstein, G. Adams, P. Ambrozewicz, M. Anghinolfi, B. Asavapibhop, G. Asryan, H. Avakian, H. Baghdasaryan, N. Baillie, J. P. Ball, N. A. Baltzell, V. Batourine, M. Battaglieri, I. Bedlinskiy, M. Bektasoglu, M. Bellis, N. Benmouna, A. S. Biselli, B. E. Bonner, S. Bouchigny, S. Boiarinov, R. Bradford, D. Branford, W. K. Brooks, S. Bültmann, V. D. Burkert, C. Bultuceanu, J. R. Calarco, S. L. Careccia, D. S. Carman, B. Carnahan, S. Chen, P. L. Cole, P. Coltharp, P. Corvisiero, D. Crabb, H. Crannell, J. P. Cummings, E. D. Sanctis, R. DeVita, P. V. Degtyarenko, H. Denizli, L. Dennis, K. V. Dharmawardane, C. Djalali, G. E. Dodge, J. Donnelly, D. Doughty, P. Dragovitsch, M. Dugger, S. Dytman, O. P. Dzyubak, H. Egiyan, L. Elouadrhiri, A. Empl, P. Eugenio, R. Fatemi, G. Fedotov, R. J. Feuerbach, T. A. Forest, H. Funsten, G. Gavalian, N. G. Gevorgyan, G. P. Gilfoyle, K. L. Giovanetti, F. X. Girod, J. T. Goetz, E. Golovatch, R. W. Gothe, K. A. Griffioen, M. Guidal, M. Guillo, N. Guler, L. Guo, V. Gyurjyan, C. Hadjidakis, J. Hardie, F. W. Hersman, K. Hicks, I. Hleiqawi, M. Holtrop, J. Hu, M. Huertas, C. E. Hyde-Wright, Y. Ilieva, D. G. Ireland, B. S. Ishkhanov, M. M. Ito, D. Jenkins, H. S. Jo, K. Joo, H. G. Juengst, J. D. Kellie, M. Khandaker, K. Y. Kim, K. Kim, W. Kim, A. Klein, F. J. Klein, A. Klimenko, M. Klusman, L. H. Kramer, V. Kubarovsky, J. Kuhn, S. E. Kuhn, S. Kuleshov, J. Lachniet, J. M. Laget, J. Langheinrich, D. Lawrence, T. Lee, K. Livingston, L. C. Maximon, S. McAleer, B. McKinnon, J. W. C. McNabb, B. A. Mecking, M. D. Mestayer, C. A. Meyer, T. Mibe, K. Mikhailov, R. Minehart, M. Mirazita, R. Miskimen, V. Mokeev, S. A. Morrow, J. Mueller, G. S. Mutchler, P. Nadel-Turonski, J. Napolitano, R. Nasseripour, S. Niccolai, G. Niculescu, I. Niculescu, B. B. Niczyporuk, R. A. Niyazov, G. V. O'Rielly, M. Osipenko, A. I. Ostrovidov, K. Park, E. Pasyuk, C. Peterson, J. Pierce, N. Pivnyuk, D. Pocanic, O. Pogorelko, E. Polli, S. Pozdniakov, B. M. Preedom, J. W. Price, Y. Prok, D. Protopopescu, L. M. Qin, B. A. Raue, G. Riccardi, G. Ricco, M. Ripani, B. G. Ritchie, F. Ronchetti, G. Rosner, P. Rossi, D. Rowntree, P. D. Rubin, F. Sabatié, C. Salgado, J. P. Santoro, V. Sapunenko, R. A. Schumacher, V. S. Serov, Y. G. Sharabian, J. Shaw, E. S. Smith, L. C. Smith, D. I. Sober, A. Stavinsky, S. Stepanyan, B. E. Stokes, P. Stoler, S. Strauch, R. Suleiman, M. Taiuti, S. Taylor, D. J. Tedeschi, R. Thompson, A. Tkabladze, S. Tkachenko, L. Todor, C. Tur, M. Ungaro, M. F. Vineyard, A. V. Vlassov, D. P. Weygand, M. Williams, E. Wolin, M. H. Wood, A. Yegneswaran, J. Yun, L. Zana, and J. Zhang, Phys. Rev. Lett. **96**, 082501 (2006).

[18] R. Subedi, R. Shneor, P. Monaghan, B. D. Anderson, K. Aniol, J. Annand, J. Arrington, H. Benaoum, F. Benmokhtar, W. Boeglin, J. P. Chen, S. Choi, E. Cisbani, B. Craver, S. Frullani, F. Garibaldi, S. Gilad, R. Gilman, O. Glamazdin, J. O. Hansen, D. W. Higinbotham, T. Holmstrom, H. Ibrahim, R. Igarashi, C. W. de Jager, E. Jans, X. Jiang, L. J. Kaufman, A. Kelleher, A. Kolarkar, G. Kumbartzki, J. J. LeRose, R. Lindgren, N. Liyanage, D. J. Margaziotis, P. Markowitz, S. Marrone, M. Mazouz, D. Meekins, R. Michaels, B. Moffit, C. F. Perdrisat, E. Piasetzky, M. Potokar, V. Punjabi, Y. Qiang, J. Reinhold, G. Ron, G. Rosner, A. Saha, B. Sawatzky, A. Shahinyan, S. Širca, K. Slifer, P. Solvignon, V. Sulkosky, G. M. Urciuoli, E. Voutier, J. W. Watson, L. B. Weinstein, B. Wojtsekhowski, S. Wood, X. C. Zheng, and L. Zhu, Science **320**, 1476 (2008).

[19] R. Shneor, P. Monaghan, R. Subedi, B. D. Anderson, K. Aniol, J. Annand, J. Arrington, H. Benaoum, F. Benmokhtar, P. Bertin, W. Bertozzi, W. Boeglin, J. P. Chen, S. Choi, E. Chudakov, E. Cisbani, B. Craver, C. W. de Jager, R. J. Feuerbach, S. Frullani, F. Garibaldi, O. Gayou, S. Gilad, R. Gilman, O. Glamazdin, J. Gomez, J.-O. Hansen, D. W. Higinbotham, T. Holmstrom, H. Ibrahim, R. Igarashi, E. Jans, X. Jiang, Y. Jiang, L. Kaufman, A. Kelleher, A. Kolarkar, E. Kuchina, G. Kumbartzki, J. J. LeRose, R. Lindgren, N. Liyanage, D. J. Margaziotis, P. Markowitz, S. Marrone, M. Mazouz, D. Meekins, R. Michaels, B. Moffit, S. Nanda, C. F. Perdrisat, E. Piasetzky, M. Potokar, V. Punjabi, Y. Qiang, J. Reinhold, B. Reitz, G. Ron, G. Rosner, A. Saha, B. Sawatzky, A. Shahinyan, S. Širca, K. Slifer, P. Solvignon, V. Sulkosky, N. Thompson, P. E. Ulmer, G. M. Urciuoli, E. Voutier, K. Wang, J. W. Watson, L. B. Weinstein, B. Wojtsekhowski, S. Wood, H. Yao, X. Zheng, and L. Zhu, Phys. Rev. Lett. **99**, 072501 (2007).

[20] M. M. Sargsian, T. V. Abrahamyan, M. I. Strikman, and L. L. Frankfurt, Phys. Rev. C **71**, 044615 (2005).

[21] R. Schiavilla, R. B. Wiringa, S. C. Pieper, and J. Carlson, Phys. Rev. Lett. **98**, 132501 (2007).

[22] K. Ikeda, N. Takigawa, and H. Horiuchi, Prog. Theor. Phys. Suppl. **E68**, 464 (1968).

[23] F. Hoyle, Astrophys. J. Suppl. **1**, 121 (1954).

[24] J. Tanaka, Z. Yang, Z. Typel, S. Adachi, S. Bai, P. van Beek, D. Beaumel, Y. Fujikawa, J. Han, S. Heil, S. Huang, A. Inoue, Y. Jiang, M. Knösel, N. Kobayashi, Y. Kubota, W. Liu, J. Lou, Y. Maeda, Y. Matsuda, K. Miki, S. Nakamura, K. Ogata, V. Panin, G. Scheit, F. Schindler, P. Schrock, D. Symochko, A. Tamii, T. Uesaka, V. Wagner, K. Yoshida, J. Zenihiro, and T. Aumann, Science **371**, 260 (2021).

[25] M. Baldo, U. Lombardo, and P. Schuck, Phys. Rev. C **52**, 975 (1995).

[26] E. Garrido, P. Sarriguren, E. Moya de Guerra, and P. Schuck, Phys. Rev. C **60**, 064312 (1999).

[27] E. Garrido, P. Sarriguren, E. Moya de Guerra, U. Lombardo, P. Schuck, and H. J. Schulze, Phys. Rev. C **63**, 037304 (2001).

[28] A. L. Goodman, Phys. Rev. C **58**, R3051 (1998).

[29] S. Frauendorf and A. O. Macchiavelli, Prog. Part. Nucl. Phys. **78**, 24 (2014).

[30] K. Yoshida, Phys. Rev. C **90**, 031303(R) (2014).

[31] E. Litvinova, C. Robin, and I. A. Egorova, Phys. Lett. B **776**, 72 (2018).

[32] H. Masui and M. Kimura, Progress of Theoretical and Experimental Physics **2016**, 053D01 (2016).

[33] T. Kammuri, T. Motobayashi, I. Kohno, S. Nakajima, M. Yoshie, K. Katori, T. Mikumo, and H. Kamitsubo, Journal of Physics G: Nuclear Physics **4**, L93 (1978).

[34] U. Götz, M. Ichimura, R. A. Broglia, and A. Winther, Physics Reports **16**, 115 (1975).

[35] S. Kikuchi, Phys. Rev. **80**, 492 (1950).

[36] D. Walker, Phys. Rev. **81**, 634 (1951).

[37] C. Levinthal and A. Silverman, Phys. Rev. **82**, 822 (1951).

[38] J. S. Levinger, Phys. Rev. **84**, 43 (1951).

[39] J. S. Levinger, Nuclear Physics A **699**, 3rd Int. Conf. on Perspectives in Hadronic Physics, 255 (2002).

[40] S. Terashima, L. Yu, H. J. Ong, I. Tanihata, S. Adachi, N. Aoi, P. Y. Chan, H. Fujioka, M. Fukuda, H. Geissel, G. Gey, J. Golak, E. Haettner, C. Iwamoto, T. Kawabata, H. Kamada, X. Y. Le, H. Sakaguchi, A. Sakaue, C. Scheidenberger, B. H. Sun, A. Tamii, T. L. Tang, D. T. Tran, K. Topolnicki, T. F. Wang, Y. N. Watanabe, H. Weick, H. Witała, G. X. Zhang, and L. H. Zhu, Phys. Rev. Lett. **121**, 242501 (2018).

[41] G. Jacob and T. A. J. Maris, Rev. Mod. Phys. **38**, 121 (1966).

[42] G. Jacob and T. A. J. Maris, Rev. Mod. Phys. **45**, 6 (1973).

[43] P. Kitching, C. A. Miller, D. A. Hutcheon, A. N. James, W. J. McDonald, J. M. Cameron, W. C. Olsen, and G. Roy, Phys. Rev. Lett. **37**, 1600 (1976).

[44] N. S. Chant and P. G. Roos, Phys. Rev. C **15**, 57 (1977).

[45] N. S. Chant and P. G. Roos, Phys. Rev. C **27**, 1060 (1983).

[46] C. Samanta, N. S. Chant, P. G. Roos, A. Nadasen, J. Wesick, and A. A. Cowley, Phys. Rev. C **34**, 1610 (1986).

[47] A. A. Cowley, J. J. Lawrie, G. C. Hillhouse, D. M. Whittal, S. V. Förtsch, J. V. Pilcher, F. D. Smit, and P. G. Roos, Phys. Rev. C **44**, 329 (1991).

[48] D. S. Carman, L. C. Bland, N. S. Chant, T. Gu, G. M. Huber, J. Huffman, A. Klyachko, B. C. Markham, P. G. Roos, P. Schwandt, and K. Solberg, Phys. Rev. C **59**, 1869 (1999).

[49] K. Ogata, K. Yoshida, and K. Minomo, Phys. Rev. C **92**, 034616 (2015).

[50] K. Minomo, M. Kohno, K. Yoshida, and K. Ogata, Phys. Rev. C **96**, 024609 (2017).

[51] S. Chen, J. Lee, P. Doornenbal, A. Obertelli, C. Barbieri, Y. Chazono, P. Navrátil, K. Ogata, T. Otsuka, F. Raimondi, V. Somá, Y. Utsuno, K. Yoshida, H. Baba, F. Browne, D. Calvet, F. Château, N. Chiga, A. Corsi, M. L. Cortés, A. Delbart, J.-M. Gheller, A. Giganon, A. Gillibert, C. Hilaire, T. Isobe, J. Kahlbow, T. Kobayashi, Y. Kubota, V. Lapoux, H. N. Liu, T. Motobayashi, I. Murray, H. Otsu, V. Panin, N. Paul, W. Rodriguez, H. Sakurai, M. Sasano, D. Steppenbeck, L. Stuhl, Y. L. Sun, Y. Togano, T. Uesaka, K. Wimmer, K. Yoneda, N. Achouri, O. Aktas, T. Aumann, L. X. Chung, F. Flavigny, S. Franchoo, I. Gašparić, R.-B. Gerst, J. Gibelin, K. I. Hahn, D. Kim, T. Koiwai, Y. Kondo, P. Koseoglou, C. Lehr, B. D. Linh, T. Lokotko, M. MacCormick, K. Moschner, T. Nakamura, S. Y. Park, D. Rossi, E. Sahin, D. Sohler, P.-A. Söderström, S. Takeuchi, H. Törnqvist, V. Vaquero, V. Wagner, S. Wang, V. Werner, X. Xu, H. Yamada, D. Yan, Z. Yang, M. Yasuda, and L. Zanetti, Phys. Rev. Lett. **123**, 142501 (2019).

[52] K. Yoshida, K. Minomo, and K. Ogata, Phys. Rev. C **94**, 044604 (2016).

[53] M. Lyu, K. Yoshida, Y. Kanada-En'yo, and K. Ogata, Phys. Rev. C **97**, 044612 (2018).

[54] K. Yoshida, K. Ogata, and Y. Kanada-En'yo, Phys. Rev. C **98**, 024614 (2018).

[55] P. G. Roos, H. Him, M. Jain, and H. D. Holmgren, Phys. Rev. Lett. **22**, 242 (1969).

[56] P. G. Roos, N. S. Chant, A. A. Cowley, D. A. Goldberg, H. D. Holmgren, and R. Woody, Phys. Rev. C **15**, 69 (1977).

[57] A. Nadasen, N. S. Chant, P. G. Roos, T. A. Carey, R. Cowen, C. Samanta, and J. Wesick, Phys. Rev. C **22**, 1394 (1980).

[58] T. A. Carey, P. G. Roos, N. S. Chant, A. Nadasen, and H. L. Chen, Phys. Rev. C **29**, 1273 (1984).

[59] C. W. Wang, P. G. Roos, N. S. Chant, G. Ciangaru, F. Khazaie, D. J. Mack, A. Nadasen, S. J. Mills, R. E. Warner, E. Norbeck, F. D. Becchetti, J. W. Janecke, and P. M. Lister, Phys. Rev. C **31**, 1662 (1985).

[60] A. Nadasen, P. G. Roos, N. S. Chant, C. C. Chang, G. Ciangaru, H. F. Breuer, J. Wesick, and E. Norbeck, Phys. Rev. C **40**, 1130 (1989).

[61] J. Mabiala, A. A. Cowley, S. V. Förtsch, E. Z. Buthelezi, R. Neveling, F. D. Smit, G. F. Steyn, and J. J. Van Zyl, Phys. Rev. C **79**, 054612 (2009).

[62] C. Samanta, N. S. Chant, P. G. Roos, A. Nadasen, and A. A. Cowley, Phys. Rev. C **26**, 1379 (1982).

[63] L. D. Faddeev, Zh. Eksp. Theor. Fiz. **39**, 1459 (1960).

[64] L. D. Faddeev, Sov. Phys. JETP **12**, 1014 (1961).

[65] E. O. Alt, P. Grassberger, and W. Sandhas, Nucl. Phys. B **2**, 167 (1967).

[66] K. L. Lim and I. E. McCarthy, Phys. Rev. **133**, 1006 (1964).

[67] Y. L. Luo and M. Kawai, Phys. Rev. C **43**, 2367 (1991).

[68] Y. Watanabe, R. Kuwata, S. Weili, M. Higashi, H. Shinohara, M. Kohno, K. Ogata, and M. Kawai, Phys. Rev. C **59**, 2136 (1999).

[69] K. Minomo, K. Ogata, M. Kohno, Y. R. Shimizu, and M. Yahiro, J. Phys. G **37**, 085011 (2010).

[70] M. Kamimura, M. Yahiro, Y. Iseri, Y. Sakuragi, H. Kameyama, and M. Kawai, Prog. Theor. Phys. Suppl. **89**, 1 (1986).

[71] N. Austern, Y. Iseri, M. Kamimura, M. Kawai, G. Rawitscher, and M. Yahiro, Phys. Rep. **154**, 125 (1987).

[72] M. Yahiro, K. Ogata, T. Matsumoto, and K. Minomo, Prog. Theor. Exp. Phys. **2012**, 01A206, 242501 (2012).

[73] R. Ent, B. L. Berman, H. P. Blok, J. F. J. van den Brand, W. J. Briscoe, M. N. Harakeh, E. Jans, P. D. Kunz, and L. Lapikás, Nucl. Phys. A **578**, 93 (1994).

[74] W. G. Love and M. A. Franey, Phys. Rev. C **24**, 1073 (1981).

[75] W. G. Love and M. A. Franey, Phys. Rev. C **27**, 438 (1983).

[76] M. A. Franey and W. G. Love, Phys. Rev. C **31**, 488 (1985).

[77] Y. Chazono, K. Yoshida, K. Yoshida, and K. Ogata, Phys. Rev. C **103**, 024609 (2021).

[78] S. Hama, B. C. Clark, E. D. Cooper, H. S. Sherif, and R. L. Mercer, Phys. Rev. C **41**, 2737 (1990).

[79] E. D. Cooper, S. Hama, B. C. Clark, and R. L. Mercer, Phys. Rev. C **47**, 297 (1993).

[80] E. D. Cooper, S. Hama, and B. C. Clark, Phys. Rev. C **80**, 034605 (2009).

[81] H. An and C. Cai, Phys. Rev. C **73**, 054605 (2006).

[82] F. Perey and B. Buck, Nucl. Phys. **32**, 353 (1962).

[83] L. G. Arnold, B. C. Clark, R. L. Mercer, and P. Schwandt, Phys. Rev. C **23**, 1949 (1981).

[84] K. Sagara, H. Oguri, S. Shimizu, K. Maeda, H. Nakamura, T. Nakashima, and S. Morinobu, Phys. Rev. C **50**, 576 (1994).

[85] T. A. Cahill, J. Greenwood, H. Willmes, and D. J. Shadoan, Phys. Rev. C **4**, 1499 (1971).

[86] S. N. Bunker, J. M. Cameron, R. Carlson, J. R. Richardson, P. Tomaš, W. T. H. Van Oers, and J. W. Verba, Nucl. Phys. A **113**, 461 (1968).

[87] K. Sekiguchi, H. Sakai, H. Witała, W. Glöckle, J. Golak, M. Hatano, H. Kamada, H. Kato, Y. Maeda, J. Nishikawa, A. Nogga, T. Ohnishi, H. Okamura, N. Sakamoto, S. Sakoda, Y. Satou, K. Suda, A. Tamii, T. Uesaka, T. Wakasa, and K. Yako, Phys. Rev. C **65**, 034003 (2002).

[88] K. Ermisch, H. R. Amir-Ahmadi, A. M. van den Berg, R. Castelijns, B. Davids, A. Deltuva, E. Epelbaum, W. Glöckle, J. Golak, M. N. Harakeh, M. Hunyadi, M. A. d. Huu, N. Kalantar-Nayestanaki, H. Kamada, M. Kiš, M. Mahjour-Shafiei, A. Nogga, P. U. Sauer, H. Witała, and H. J. Wörtche, Phys. Rev. C **71**, 064004 (2005).

[89] K. Kuroda, A. Michalowicz, and M. Poulet, Phys. Lett. **13**, 67 (1964).

[90] K. Hatanaka, Y. Shimizu, D. Hirooka, J. Kamiya, Y. Kitamura, Y. Maeda, T. Noro, E. Obayashi, K. Sagara, T. Saito, H. Sakai, Y. Sakemi, K. Sekiguchi, A. Tamii, T. Wakasa, T. Yagita, K. Yako, H. P. Yoshida, V. P. Ladygin, H. Kamada, W. Glöckle, J. Golak, A. Nogga, and H. Witała, Phys. Rev. C **66**, 044002 (2002).

[91] N. E. Booth, C. Dolnick, R. J. Esterling, J. Parry, J. Scheid, and D. Sherden, Phys. Rev. D **4**, 1261 (1971).

[92] E. T. Boschitz, W. K. Roberts, J. S. Vincent, M. Blecher, K. Gotow, P. C. Gugelot, C. F. Perdrisat, L. W. Swenson, and J. R. Priest, Phys. Rev. C **6**, 457 (1972).

[93] E. Winkelmann, P. R. Bevington, M. W. McNaughton, H. B. Willard, F. H. Cverna, E. P. Chamberlin, and N. S. P. King, Phys. Rev. C **21**, 2535 (1980).

[94] K. Yoshida, Prog. Theor. Exp. Phys. **2013**, 113D02, 064004 (2013).

[95] K. Yoshida, Prog. Theor. Exp. Phys. **2021**, 019201, 064004 (2021).

[96] N. Van Giai and H. Sagawa, Phys. Lett. B **106**, 379 (1981).

[97] Y. Taniguchi, K. Yoshida, Y. Chiba, Y. Kanada-En'yo, M. Kimura, and K. Ogata, Phys. Rev. C **103**, L031305 (2021).

[98] K. Hatanaka, M. Kawabata, N. Matsuoka, Y. Mizuno, S. Morinobu, M. Nakamura, T. Noro, A. Okihana, K. Sagara, K. Takahisa, H. Takeda, K. Tamura, M. Tanaka, S. Toyama, H. Yamazaki, and Y. Yuasa, Phys. Rev. Lett. **78**, 1014 (1997).

[99] T. Matsumoto, T. Kamizato, K. Ogata, Y. Iseri, E. Hiyama, M. Kamimura, and M. Yahiro, Phys. Rev. C **68**, 064607 (2003).

[100] H. Witała, W. Glöckle, D. Hüber, J. Golak, and H. Kamada, Phys. Rev. Lett. **81**, 1183 (1998).

[101] S. Nemoto, K. Chmielewski, S. Oryu, and P. U. Sauer, Phys. Rev. C **58**, 2599 (1998).

[102] W. P. Abfalterer, F. B. Bateman, F. S. Dietrich, C. Elster, R. W. Finlay, W. Glöckle, J. Golak, R. C. Haight, D. Hüber, G. L. Morgan, and H. Witala, Phys. Rev. Lett. **81**, 57 (1998).

[103] H. Witała, H. Kamada, A. Nogga, W. Glöckle, C. Elster, and D. Hüber, Phys. Rev. C **59**, 3035 (1999).

[104] D. F. Jackson and T. Berggren, Nucl. Phys. **62**, 353 (1965).